Investigating the endothelial PI3 kinase signalling pathway in vascular repair

by

Maikel Farhan

A thesis submitted in partial fulfillment of the requirements for the degree of

Doctor of Philosophy

in

Experimental Medicine

Department of Medicine

University of Alberta

Abstract

Thrombotic microangiopathy (TMA) is a broad term for a range of diseases that usually manifest with rapid failure of the affected organ. Although different in etiology, these diseases share a common pattern of injury originating in the vascular endothelium. In turn, the injured vasculature elicits a physiological response in a trial to repair the damage. Accumulating evidence support the significance of vascular repair but the key regulators, and the underlying mechanism are still elusive. We have shown before that key aspects of the genetic programming involved in angiogenesis are required for vascular repair. In this thesis: **First, we characterized the PI3K/AKT pathway**, the main angiogenic pathway, outputs in the endothelial cell (EC). We approached the pathway at three different levels; upstream (mTORC2), midstream (Akt) and downstream (mTORC1). Our results indicate sustained inactivation of mTORC1 activity, up-regulated mTORC2-dependent Akt1 activation. In turn, ECs exposed to mTORC1-inhibition were resistant to apoptosis and hyper-responsive to renal cell carcinoma (RCC)-stimulated angiogenesis after relief of the inhibition. Conversely, mTORC1/2 dual inhibition or selective mTORC2 inactivation inhibited angiogenesis in response to RCC cells and vascular endothelial growth factor (VEGF). mTORC2-inactivation decreased EC migration more than Akt1- or mTORC1-inactivation. Mechanistically, mTORC2 inactivation robustly suppressed VEGF-stimulated EC actin polymerization, and inhibited focal adhesion formation and activation of focal adhesion kinase, independent of Akt. We concluded mTORC2 may have a superior role to Akt and mTORC1 in angiogenesis and vascular repair.

Second, we identified the role of Facio-genital dysplasia-5 (FGD5) in regulation of the PI3K/AKT pathway. FGD5 is selectively expressed in EC and was reported to regulate angiogenesis. FGD5 deficiency reduced the number of angiogenic sprouts and their filopodia.

These defects were accompanied by down regulation of tip cell-specific markers. FGD5 inactivation led to a decrease in EC migration and early protrusion (lamellipodia) formation. In resting, as well as VEGF-stimulated, EC, FGD5 formed a complex with VEGFR2 and was enriched at the leading edge of the cells and among endosomes. Further, FGD5 loss decreased endosomal VEGFR2 coupling to PI3K and diverted VEGFR2 to lysosomal degradation. This indicates FGD5 regulates VEGFR2 retention in recycling endosomes and coupling to PI3K/mTORC2-dependent cytoskeletal remodeling.

Third, we investigated the role of FGD5 in regulation of G protein-coupled receptors (GPCRs) signaling. GPCRs operate in conjunction with VEGFR2 to activate PI3K pathway. We showed dual stimulation of GPCRs and VEGFR2 had synergic effect on angiogenesis. FGD5-loss abolished the GPCRs angiogenic effect and signaling to PI3K. Cdc42 inhibition, a RHO GEF required for PI3K activity, recapitulated the same signaling defects of FGD5 deficiency indicating that FGD5 may control PI3K activity through Cdc42. Subcellular localization of PI3K and its downstream Akt showed no change in PI3K localization to the early endosomes in case of FGD5 deficiency. However, failure of recruitment of active Akt to the PI3K positive endosomes suggests a defect in PI3K activity after FGD5 loss. This study investigated a novel role of FGD5 in regulating GPCRs signaling to PI3K, and suggests FGD5 as a convergence node regulating multiple angiogenic pathways that can spark hope for novel anti-angiogenic therapy.

Finally, we studied vascular injury in animal model of chronic allograft vasculopathy (CAV). We showed that deficiency of Apelin, a peptide involved in angiogenesis that signals through PI3K in the endothelium, accelerated the vascular lesions in CAV and markedly affected

the function of the transplanted grafts. This indicated that apelin may protect against the vascular injury produced in CAV.

In summary, this work identifies potential targets that can regulate angiogenesis and vascular repair; and expands our understanding of the underlying mechanisms involved in angiogenesis. Further, it suggests novel candidates for antiangiogenic therapy to regulate pathological angiogenesis.

Preface

Some of the research conducted for this thesis forms part of existing publication and a submitted manuscript. The third chapter is published in *PLoS one* journal as "Farhan, M. A., Carmine-Simmen, K., Lewis, J. D., Moore, R. B., & Murray, A. G. (2015). Endothelial cell mTOR complex-2 regulates sprouting angiogenesis" with a doi number (10.1371/journal.pone.0135245). The fourth chapter is submitted to the *ATVB* journal with an ID (ATVB/2016/307495) as "Farhan M., Azad A., Nicolas T. and Allan G. Murray. Facio-genital dysplasia-5 (FGD5) regulates VEGF receptor-2 coupling to PI3 kinase and trafficking" and is currently under revision at the time of writing. The animals used in this project were maintained according to the Canadian Council for Animal Care (CCAC) guidelines under a protocol approved by the Animal Care and Use Committee of the University of Alberta.

Acknowledgement

This work would have never finish without the tremendous support of my wife Sylvia Kalainy. You were always next to me when I needed you. No word can describe your dedication and love.

To my beloved family, my father Adel Aziz Farhan, my mother Sonia Kromer Zakhary, and my brother Mina Farhan. Each one of you has a print in my life that changed me to what I am now. I learned from my father how to take care of my family and how to work hard to achieve my goals. My mother was the first person to show me how to study and she made me love knowledge. My brother was the voice of wisdom that convinced me to seek graduate studies and he was the first to believe in me that I can finish a PhD degree.

To my supervisor Dr Allan Murray. You were a friend before being a supervisor. Your guidance and support helped me not only through my PhD but also at the career level. You are a good leader and a great scientist. I hope I can be like you one day. I will never forget how you helped me and my wife and I hope I can pay you back a small part of what you did for me.

To my committee members, Dr Nicolas Touret and Dr Sean McMurtry. Thank you for your mindful thoughts and your wonderful advice and feedback that helped me to improve myself.

A special thanks to Dr Evangelos Michelakis who taught me critical thinking, and saw something special in me. He encouraged me to apply for residency in the University of Alberta to be a clinician scientist, and he offered me a great support.

I would like also to thank all my lab members who were good listeners and wonderful preceptors.

Table of Contents

List of figures

List of abbreviations

2-D: Two dimension

3-D: Three dimension

ADAMTS: A Disintegrin And Metalloproteinase with Thrombospondin Motifs

ADMA: Asymmetric dimethyl arginine

AKI: Acute kidney injury

Akt: Protein kinase B

ALK: Activin receptor-like kinase

AMP: Adenosine monophosphate

AMR: Antibody-mediated rejection

ANOVA: Analysis of variance

BAEC: Bovine aortic endothelial cells

BSA: Bovine serum albumin

bFGF: Basic fibroblast growth factor

BM: Basement membrane

BMDC: Bone marrow-derived cells

BUN: Blood urea nitrogen

CAC: Circulating angiogenic cells

CAD: Coronary artery disease

CAM: Chorioallantoic membrane assay

CAV: Cardiac allograft vasculopathy

CCR5: C-C chemokine receptor type 5

Cdc-42: Cell division control protein 42 homolog

CFU: Colony forming unit

CRP: C-reactive protein

CXCR4: C-X-C chemokine receptor type 4

DAF-2 DA: Diaminofluorescein diacetate

Dll4: Delta-like 4

DMEM: Dulbecco's modified Eagle's medium

DMSO: Dimethyl sulfoxide

DNA: Deoxyribonucleic acid

DTT: Dithiothreitol

ECD: Extracellular domain

EC: Endothelial cells

ECG: Electrocardiogram

ECM: Extra cellular matrix

ECFC: Endothelial colony forming cells

E. coli: Escherichia coli

EdU: 5-ethynyl-2'-deoxyuridine

EGF: Epidermal growth factor

ELISA: Enzyme-linked immunosorbent assay

eNOS: Endothelial nitric oxide synthase

eEPCs: Embryonic endothelial progenitor cells

EPC: Endothelial progenitor cells

ERK: Extracellular signal-regulated kinase

ESAM: Endothelial cell selective adhesion molecule

ESM1: Endothelial-specific molecule 1

ESRD: End-stage renal disease

FAK: Focal adhesion kinase

FBS: Fetal bovine serum

FGD5: Faciogenital dysplasia 5 protein

FGF: Fibroblast growth factor

FLT1: FMS-like tyrosine kinase

FOXO: Forkhead transcription factor

GEC: Glomerular endothelial cells

GEFs: Guanine nucleotide exchange factors

GFP: Green fluorescent protein

GPCR: G-protein coupled receptors

H & E: Hematoxylin & Eosin

HA: Hyaluronic acid

HAEC: Human heart aorta endothelial cells

HBSS: Hank's balanced salt solution

HDL: High-density lipoprotein

HDMEC: Human dermal microvascular endothelial cells

HIF1: Hypoxia inducible factor 1

HMEC-1: Human microvascular endothelial cells

HSPG: Heparan sulphate proteoglycans

HSV: Habu snake venom

HUS: Hemolytic uremic syndrome

HUVEC: Human umbilical vein endothelial cells

ICAM: Intercellular adhesion molecule

IGF2: Insulin-like growth factor 2

IGF2R: Insulin-like growth factor 2 receptor

IGFBP3: Insulin-like growth factor binding protein 3

ILK: Integrin-linked kinase

IQGAP1: Ras GTPase-activating-like protein IQGAP1

IV: intravenous

kDa: kilo dalton

KDR: kinase insert domain receptor

MAPK: Mitogen activated protein kinase

MAPKAP-2: Mitogen activated protein kinase activated kinase 2

MHC-II: Major histocompatibility class II

MMP-9: Matrix metalloproteinase-9

MNC: Mononuclear cells

MOA: Marasmius oreades agglutinin

mRNA: Messenger ribonucleic acid

mSin1: Mammalian stress-activated protein kinase-interacting protein 1

mTOR: Mammalian target of rapamycin

mTORC1: mTOR complex 1

mTORC2: mTOR complex 2

NICD: Notch intracellular domain

NK: Natural killer

Nrarp: Notch-regulated ankyrin-repeat protein

NRPs: Neuropilin receptors

NO: Nitric oxide

NOS: Nitric oxide synthase

OCT: Optimal cutting temperature

PAK: Serine/threonine-protein kinase

PAR: Protease activated receptor

PBST: Phosphate buffered saline with tween-20

PECAM: Platelet endothelial cell adhesion molecule

PCNA: Proliferating cell nuclear antigen

PCR: Polymerase chain reaction

PDGF: Platelet-derived growth factor

PDGFR: Platelet-derived growth factor receptor

PDK: Phosphoinositide-dependent kinase

PDG2: Prostaglandin D2

PDGE2: Prostaglandin E2

PGF2α: Prostaglandin F2α

PGH2: Prostaglandin H2

PGI2: Prostacyclin

PH: Pulmonary hypertension

PI: Phosphoinositide

PI3K: Phosphotidylinositide-3 kinase

PIP2: Phosphotidylinositol (4,5) bisphosphate

PIP3: Phosphatidylinositol (3,4,5) triphosphate

PlGF: Placental growth factor

PKC: Protein kinase C

PRAS40: Proline-rich Akt substrate 40 kDa

Ptdlns: Phosphotidylinositol

PTEN: Phosphatase and tensin homologue deleted on chromosome 10

qPCR: Quantitative polymerase chain reaction

Rac1: Ras-related C3 botulinum toxin substrate 1

Raptor: Regulatory associated protein of mTOR

Rictor: Rapamycin-insensitive companion of mTOR

ROS: Reactive oxygen species

RTK: Receptor tyrosine kinases

S1P: Sphingosine 1-phosphate

SDF1: Stromal cell-derived factor 1

SH2: src homology

SHP: SH2 protein-tyrosine phosphatases

siRNA: Small interfering RNA

TGF-β: Transforming growth factor β

TGF-βR: Transforming growth factor β receptor

Tie-2: Tyrosine kinase with immunoglobulin-like and EGF like domains 2

TMA: Thrombotic microangiopathy

TNFα: Tumor necrosis factor α

TTP: Thrombotic thrombocytopenic purpura

TUNEL: Terminal deoxynucleotidyl transferase nick-end labeling

TxA2: Thromboxane A2

VCAM: Vascular cell adhesion molecule

VE-Cad: Vascular endothelial cadherin

VEGF: Vascular endothelial growth factor

VEGFR2: Vascular endothelial growth factor receptor 2

vWF: von Willebrand factor

Chapter I: Introduction

1 Thesis outline

This thesis investigates novel targets to regulate angiogenesis and contributes to our understanding of the mechanisms underlying the formation of new blood vessels. **The first chapter** provides a comprehensive background regarding physiological and pathological angiogenesis. **The second chapter** explains the materials and methods used to carry out the research project. **The third chapter** evaluates the significance of different molecules on the VEGF-receptor-2/PI3Kinase pathway, the key pathway regulating angiogenesis. This chapter also investigates the impact of regulating molecules upstream and downstream of the pathway on angiogenesis. In addition, it investigates the crosstalk and overlap of different targets on the pathway. **The fourth chapter** investigates the role of a novel endothelial restricted-protein (Facio-genital dysplasia 5; FGD5) in angiogenesis. Further, this work explains the involvement of FGD5 in the VEGFR2/PI3Kinase pathway, and provides insights on the trafficking of VEGFR2 in endothelial cells (EC). **The fifth chapter** is a further study of FGD5 and its implication in regulating other angiogenesis pathways. In this study we elaborate on a novel role of FGD5 in regulating the G protein-coupled receptors (GPCRs). **The sixth chapter** is a translational project that applies some of our in vitro findings into an animal model of vascular injury. In this observational study we illustrate the requirement of one of the angiogenic cues to hamper vascular injury.

1.1 Objectives

1- Characterization of the PI3K/AKT pathway outputs in the EC

Aims: Regulating the VEGFR2/PI3Kinase pathway early before the signal reach the downstream effector Akt has a privilege in controlling angiogenesis. In primary EC, mTORC1 regulates Akt through a negative feedback loop.

2- Identification of the mechanism of FGD5 in regulation of the VEGFR2-stimulated PI3K/AKT pathway signalling

Aims: FGD5-loss inhibits the VEGF-mediated angiogenesis. TO study the subcellular localization of FGD5 in EC and its association with VEGFR2.

3- Characterization of the role of FGD5 in regulation of GPCR signaling

Aims: Comparing the potency of VEGF to stromal cell-derived factor 1 (SDF1), a GPCR ligand, in inducing angiogenesis. FGD5 regulates GPCR signaling to PI3K and the GPCR-mediated angiogenesis.

4-Characterization of vascular repair of Apelin-deficient hearts in a model of chronic allograft vasculopathy (CAV) in mice.

Aims: Apelin loss exacerbates the vascular injury in CAV. The vascular injury in Apelin deficient mice is not due to immunological hyper-reactivity.

1.2 Contribution to knowledge

First, sustained mTORC1 inhibition activates maladaptive PI3kinase signaling to Akt and responsiveness to proangiogenic growth factors in primary human ECs. In contrast, mTORC2 inactivation prevents Akt and downstream FOXO1/3, or S6 kinase hyper-stimulation. Moreover, mTORC2 regulates EC matrix adhesion, motility, and angiogenesis in vitro independent of downstream Akt-regulated events. These findings indicate that mTORC2 in the endothelium is an attractive target to inhibit pathologic neoangiogenesis.

Second, our work identifies the function of FGD5 in regulation of tip cell-cytoskeletal remodelling in VEGF-guided sprouting angiogenesis. Moreover, we identify FGD5 to be an upstream regulator of mTORC2, and describe a novel role for FGD5 to regulate the coupling of PI3K to active VEGFR2 in the early endosome compartment, and to retain VEGFR2 in the recycling endosome compartment. These data indicate that FGD5 is a potential target to regulate pathological angiogenesis.

Third, in this study we investigate a novel role of FGD5 in regulating GPCRs signaling to PI3Kinaseβ; propose Cdc42 to mediate the cross talk between FGD5 and PI3Kinaseβ; and suggest FGD5 as a convergence node regulating multiple angiogenic pathways that can serve as a potential candidate for anti-angiogenic therapy.

Finally, we demonstrate the significance of Apelin in development of vascular injury in a model of chronic graft rejection in transplanted hearts of mice; and propose Apelin as a candidate to protect against endothelial damage and promote vascular repair.

2 Developmental angiogenesis

Angiogenesis is the process of formation of new blood vessels from already existing ones. It occurs during embryonic development to support tissue growth and provide organs with nourishment. In adults, angiogenesis occurs in many physiological processes as inflammation and wound healing, as well as varoius pathologies as tumors and diabetic retinopathy [1]. Thus, understanding the signaling molecules that regulate angiogenesis could ultimately inhibit vessel growth to tumors or enrich the vasculature of an ischemic area.

Judah Folkman was the first to refer to the therapeutic implications of angiogenesis in the modern history when he hypothesized that tumor growth is angiogenesis-dependent[2]. Since then, angiogenesis has been a matter of intensive research.

The process starts as early as the development of the cardiovascular system during embryogenesis [3]. The lumen of blood vessels in contact with blood is lined with a thin and smooth layer of endothelial cells (EC), which originate from mesoderm. Mesoderm differentiates to hemangioblasts that further give rise to hematopoietic stem cells and angioblasts [4]. Angioblasts are EC progenitor cells with commitment to the EC lineage but have not acquired all characteristic markers of EC yet [5]. Vasculogenesis is the initial formation of blood vessels from angioblasts [5,6]. The process involves multiple steps of mesoderm differentiation to angioblasts and growth factor-mediated angioblasts migration to form blood islands, where EC full differentiation takes place [6,7]. The primordial vessels expand by sprouting of new capillaries to form more developed vascular network in a process termed angiogenesis.

Angiogenesis can be initiated by sprouting or intussusception in utero as well as in adults. Sprouting angiogenesis is characterized by budding of EC towards angiogenic cues like the vascular endothelial growth factor (VEGF). Therefore, Sprouting angiogenesis commonly occurs

to supply blood to tissues that were devoid of vasculature. Whereas, intussusceptive angiogenesis involves the invasion of existing blood vessels by interstitial tissue to split the lumen and form transvascular tissue pillars. These two mechanisms can occur simultaneously or independently.

2.1 Sprouting Angiogenesis

Sprouting angiogenesis is initiated when hypoxia induces the secretion of angiogenic cues from poorly perfused tissue. The key proangiogenic growth factor is VEGF-A [8,9]. The first EC to lead the way of the sprouting capillary through the extra cellular matrix (ECM) is designated "tip cell" [10,11]. Finger like filopodia extending from tip cells differentiate it from the quiescent EC. Filopodia secret proteolytic enzymes to digest the ECM and facilitate tip cell's migration. In addition, filopodia are enriched with VEGFR2 that can sense the environment and direct the migration towards the VEGF gradient [12,13]. Then filopodia anchor the leading edge of the migrating tip cell to the ECM stimulating focal adhesions and integrins to polymerize actin filaments within the cell. Contraction of Actin filaments will eventually pull the cell towards the angiogenic cue. Following tip cells in the sprout, are the stalk cells, which proliferate to elongate the newly formed capillary. Vacuoles within the stalk cells start to develop and fuse together forming the future lumen of the capillary. When the hypoxic tissue starts to receive blood supply, it stops secreting angiogenic cues to prevent further angiogenesis. Finally, maturation and stabilization of the blood vessel require incorporation of pericytes and ECM to envelope the EC [14]. Tip cells and stalk cells have distinct molecular signatures, whereas tip cells express high levels of VEGFR2, CXCR4, platelet-derived growth factor (PDGF), delta-like ligand-4 (DLL4), neuropilin-1 (NRP1) [15-18]; stalk cells express Notch receptor, Nrarp and VEGFR1 [19-21].

Delta-Notch signaling is a key regulator of Tip cell/stalk cell differentiation. The transmembrane ligand DLL4 binds to its notch receptor on the adjacent cell through cell-cell interaction [19]. VEGF induces the expression of DLL4 which stimulates Notch receptor in the adjacent cells (the future stalk cells). After ligand binding, Notch is cleaved intracellularly, producing the Notch intracellular domain (NICD) that reduces the transcription of VEGFR2 resulting in stalk cells that are less responsive to VEGF stimulation. On the other hand, DDL4 will upregulate the expression of VEGFR2 resulting in tip cells that are more sensitive to VEGF. This allows the stalk cells to maintain their position behind the leading tip cells [22]. Therefore, only EC receiving highest level of VEGF will successfully differentiate to tip cells [11]. Accumulating evidence supports that the formation of vasculature is dependent on VEGF concentration. VEGF reduction by 50% was embryonically lethal in mice due to vascular defects [8,23]. Moreover, the excessive production of VEGF in tumors led to hypervascularity [24]. It's worth noting that, ectopic VEGFR2 agonists inhibited EC migration, but dramatically increased the density of vasculature attributed to propagation in EC proliferation. In transgenic mice overexpressing VEGF, and after injection of VEGF-A or VEGF-E in mice retina, the number of EC in blood vessels, the size of the vessels, and the density of the vascular network were increased. These observations demonstrate that in the mice retina tip cells and stalk cells respond differently to VEGF stimulation. Whereas tip cell migrates in response to extracellular VEGF gradient and distribution, stalk cell appears to proliferate depending on the total VEGF concentration [15].

2.2 Intussusceptive Angiogenesis

Intussusceptive angiogenesis is referred to as "splitting angiogenesis" because the wall of the vessel invaginates into the lumen splitting it into halves. In this way blood vessels can branch and expand faster than the sprouting angiogenesis because it requires only reorganization of the EC. However, intussusceptive angiogenesis plays a minor role in adults because it is mainly significant during embryogenesis, where growth is fast and resources are limited. In addition, intussusception mainly develops new capillaries where vasculature already exist [25-27]. This type of angiogenesis was first identified in postnatal lungs of rats and humans [28,29], and is known to occur in vascular networks surrounding an epithelial surface like the intestinal mucosa [30,31]. It also occurs in many other organs like skeletal muscles and heart. Although the mechanism of sprouting angiogenesis is clearly described, intussusceptive angiogenesis is poorly understood. Researchers studying intussusceptive angiogenesis were hampered by the difficult techniques required to monitor its progress. To date, the only method available is determining tissue pillars from scanning electron micrographs of vascular casts. However, studies in the chick chorioallantoic membrane (CAM) have shown the intussusceptive angiogenesis can be stimulated with VEGF, and that the many growth factors' interactions and signaling pathways required for sprouting [26] angiogenesis are rarely involved [25,30]. Moreover, in some high flow regions of the circulation, mechanical shear stress can be enough to stimulate intussusceptive growth [25].

3 Pathological angiogenesis (Tumor angiogenesis)

In tumors, angiogenesis is not only stimulated, but the blood vessels formed are also abnormal in structure and function [32,33]. Tumor vessels are tortuous, connect to one another randomly, branch

irregularly and not fully differentiated into arterioles and venuoles [33-35]. Similarly, EC in the tumor vasculature lose their polarity, migrate away from the basement membrane with leading tip cells penetrating deep into the tissue, and do not form a smooth unilayer [34-36]. In addition, tumor EC are often leaky, separated by wide gaps and have multiple fenestrations, resulting in hemorrhage and increased interstitial fluid pressure, which limits tumor's perfusion and induces hypoxia [34,37-39].The decrease in perfusion limits the delivery of drugs to tumor tissue, whereas hypoxia reduces the efficacy of irradiation and certain chemotherapeutics by decreasing the formation of reactive oxygen species. These result in resistance to conventional anticancer treatments [40]. Further, because tumors have high metabolic demands, they produce a plethora of pro-angiogenic factors [41]. These factors render tumor vessels even more abnormal, which therefore creates a vicious cycle. The key angiogeneic factor is vascular endothelial growth factor (VEGF) that stimulates EC growth, migration, permeability, lumen formation and survival [8,9,42]; and studies have shown that high levels of VEGF correlate with vessel abnormalities in tumors [24,43,44]. These have led to the notion that targeting tumor angiogenesis by VEGF pathway inhibition may break the tumors-resistance vicious circle.

4 The role of VEGFR2/PI3Kinase pathway in angiogenesis

4.1 VEGFR2/PI3Kinase

The VEGF family has five members, VEGF-A (also known as VEGF), placenta growth factor (PlGF), VEGF-B, VEGF-C and VEGF-D, which regulate angiogenesis and lymphangiogenesis

[45-48]. Among these, VEGF-A plays a major role in blood vessel formation. Not only, the VEGF-A homozygous knockout mice were embryonically lethal, but also loss of one VEGF allele led to severe vascular malformation and intrauterine death [8,49]. Many isoforms of VEGF are produced by alternative splicing. Of these, VEGF-A (also known as VEGF) has the highest biological activity as it binds to the co-receptor neuropilin-1 (Nrp1). The other isoforms are VEGF-B, VEGF-C and VEGF-D. VEGF-B binds only to VEGFR1 and exerts a very mild stimulatory effect on angiogenesis because the kinase activity of VEGFR1 is lower than that of VEGFR2 [50]. However, VEGF-B was reported to have a role in stimulation and maintenance of the coronary artery system [51]. On the other hand VEGF-D and VEGF-C have a high affinity for VEGFR3, and they stimulate lymphangiogenesis. VEGF-C expression was detected during embryogenesis, and its loss exhibits a lethal phenotype at the prenatal stage due to mal-lymphangiogenesis and lymphedema [52].

VEGF receptors (VEGFRs) are structurally related to the platelet derived growth factor (PDGF) receptor family. They have seven Ig domains in the extracellular region, a single transmembrane region, and a tyrosine kinase (TK) domain with a long kinase insert sequence in the intracellular region. Despite the structural similarity with PDGF, VEGFRs do not have a Y-xx-M motif to bind to the SH2 domain in the p85 subunit of PI3Kinase [47,53]. The major autophosphorylation site on VEGFR-2 is Y1175 [54]. The 1175-phenylalanine (F) mutation of VEGFR-2 or the intracellular injection of anti-Y1175 specific antibody dramatically inhibited VEGF-dependent cell proliferation [54]. Mice that express a mutated Y1173F VEGFR2 die at E8.5-9.5 because of vascular defects that resemble the defects of VEGFR2 deficient mice [55].

Only a few SH2 domain-containing molecules have been shown to interact directly with VEGFR2. PLCγ binds to phosphorylated Y1175 and activates the mitogen-activated protein

kinase (MAPK)/extracellular-signal-regulated kinase-1/2 (ERK1/2) pathway in EC [54]. The adaptor Shb binds to Y1175 [56] and genetically targeting Shb was reported to inhibit VEGF-mediated migration and activation of PI3Kinase [56]. Another adaptor that binds to Y1175 is Sck/ShcB [57], which plays a dispensable role in development [58]. Finally, there is a debate whether VEGFR2 binds to ShcA and Grb2 to recruit the Ras-activating nucleotide-exchange factor son of sevenless to the receptor [57,59].

VEGFR2 activates the Ras/Raf/MAPK pathway but studies reported a limited mitogen activity after VEGF stimulation. Therefore, the significance of the Ras/MAPK pathway downstream of VEGFR2 is unclear. Of note, Ras activation has been coupled to an angiogenic phenotype in previous reports [59,60].

Another important phosphorylation site in VEGFR2 is Tyr951, which is a binding site for the T-cell-specific adaptor TSAd (also known as VEGF receptor-associated protein (VRAP)) [61]. TSAd has been shown to regulate EC migration [61,62], and its deficiency inhibited tumor neovascularization in mice [61]. Moreover, VEGF induced the interaction between TSAd and Src [61]. This indicates that TSAd may regulate Src activity and in turn vascular permeability downstream of VEGFR2. A recent study has shown that TSAd-mediated activation of Src family kinases (SFKs), triggers autophosphorylation of a pair of tyrosine residues, Y773 and Y815, in the Y-xx-M motif of the tyrosine kinase receptor Axl [63]. Subsequently, Axl forms a high affinity binding site for p85 and results in PI3K activation. Other molecules that have colocalize with the phosphorylated VEGFR2 and regulated VEGFR2-induced EC migration are: focal-adhesion kinase (FAK) [64,65] and IQGAP1, which binds Rac1 [66,67].

Although, VEGFR-1 has a high affinity for VEGF [68], its kinase activity is less than that of VEGFR-2. This suggests that VEGFR-1 may serve as a decoy receptor and negatively regulate angiogenesis under certain conditions. Indeed, VEGFR-1 knockout mice die at E8.5-9.0, due to overgrowth of endothelial cells and uncontrolled formation of disorganized blood vessels [69]. Moreover, the VEGFR-1 TK-deficient mice were healthy with normal angiogenesis [70]. This confirms that VEGFR-1 traps VEGF and decreases the pro-angiogenic signals from VEGFR-2.

VEGFR2 is expressed in EC, hematopoietic stem cells and megakaryocytes [71,72]. VEGFR2 expression is higher in endothelial progenitor cells than in adult quiescent EC [73]. Mice deficient in VEFGR2 died in utero at embryonic day 8.5 due to vascular defects [74]. Binding of VEGFR2 to its ligand VEGF is followed by dimerization and auto phosphorylation of the kinase domain. Phosphorylation of the tyrosine residue Y1175/1173 activates the phosphatidylinositide 3-kinase (PI3K) [75]. PI3Ks are divided into three classes according to their structural and substrate specificity [76]. Of these, the most commonly studied is class I PI3K that is further divided into: class IA, which are activated by RTKs, G protein coupled receptors (GPCRs) and the small GTPase Ras; and class IB, which is only activated by GPCRs and plays a minor role in EC compared to Class IA [77,78]. Class IA PI3K consists of a p110 catalytic subunit and a p85 regulatory subunit. In mammals, there are three isoforms of the class IA PI3K catalytic p110 subunits: α, β; and δ whose role is mainly confined to leukocytes [79,80]. The lipid kinase activity of p110α is regulated by RTKs and Ras, which binds directly to the Ras-binding domain (RBD) on p110α [81,82]. In contrast, p110β is activated by RTKs such as VEGFR2[83], but it is an important downstream of GPCRs [84,85]. Instead of Ras, Rac and Cdc42 from the Rho subfamily of small GTPases bind and activate p110β via their RBD [86]. In response to VEGF binding to VEGFR2, PI3K is recruited to the plasma membrane by direct interaction of its p85 subunit with tyrosine

phosphate motifs on activated receptors. The activated p110 catalytic subunit forms a docking site on the plasma membrane and endosomes by generating phosphatidylinositol-3, 4, 5-trisphosphate (PIP3), which activates multiple downstream signaling pathways. PI3Kinase activation is terminated by the phosphatase and tensin homologue deleted on chromosome 10 (PTEN) (Figure 1). PTEN hydrolyses PIP3 to PIP2 and is considered a tumor suppressor gene. Mutations in PTEN were detected in many cancers [87,88] and its loss causes a disease of hypervascularity designated Cowden syndrome [89]. Of note, p110α and p110β are highly expressed in immortalized mouse cardiac EC and HUVECs, and studies have shown an essential function of class I PI3Ks in vascular development and angiogenesis [90,91]. Global deletion of *the gene* encoding p110α in mice is embryonically lethal due to vascular abnormalities [92,93] as well as the EC-restricted deletion of p110α [91]. In contrast, EC-restricted knockout of p110 β was tolerable unless the mice were challenged with vascular injury [91,94]. Thus, PI3K could be a potential candidate for regulating VEGF-mediated angiogenesis.

4.2 AKT (Protein kinase B)

PI3Kinase phosphorylates phosphatidylinositol 4,5-bisphosphate (PIP2) to phosphatidylinositol-3,4,5-triphosphate (PIP3), which forms high affinity binding sites for the pleckstrin homology (PH) domains of phosphoinositide-dependent kinase 1 (PDK1) and Akt [95]. Akt is a serine threonine kinase, which presents in three isoforms Akt1, Akt2, Akt3. It worth noting, that the three isoforms have distinct functions. Akt1 is responsible for cell survival and growth, Akt2 is implicated in insulin signaling pathway and Akt3 is expressed mainly in the brain. However, all isoforms share a similar structure: an N-terminal pleckstrin homology domain (PH), a central serine–threonine catalytic domain, and C-terminal domain necessary for the induction and

maintenance of kinase activity. After localization of inactive Akt to PIP3, it is phosphorylated by PDK1 on the amino acid threonine T308 residue in the kinase domain. Similarly, the mammalian target of rapamycin complex 2 (mTORC2) phosphorylates the amino acid serine S473 residue in the C-terminal of Akt. Once AKT has been phosphorylated and activated, it phosphorylates many other proteins as glycogen synthase kinase 3 and the forkhead box family of transcription factors (FOXOs). Thereby, regulating a wide range of cellular processes. Regarding angiogenesis, AKT activates endothelial nitric oxide (NO) synthase (eNOS), HIF1α, HIF2α and inhibits Tuberous sclerosis protein 2 (TSC2) which is a known inhibitor of angiogenesis [96]. Of note, Akt1 is the predominant isoform in EC [97], Akt1-loss in mice led to defects in placental development, vascular maturation and permeability [97], and dual Akt1 and Akt2 deletion in mice was lethal shortly after birth [98].

4.3 Mammalian target of rapamycin (mTOR)

mTOR is a member of the phosphatidylinositol 3 (PI3)-kinase-related kinase superfamily [99, 100]. In mammalian cells, mTOR is assembled in two distinct signaling complexes: mTOR complex-1 (mTORC1), inhibited by rapamycin and derivative rapalog drugs; and mTOR complex-2 (mTORC2). In addition to the mTOR catalytic subunit, mTORC1 consists of raptor (regulatory associated protein of mTOR), mLST8 (also termed G-protein β-subunit-like protein, GβL, a yeast homolog of LST8), and PRAS40 (proline-rich Akt substrate 40 kDa) [101,102]. mTORC2 similarly includes mTOR and mLST8, but raptor is replaced by two mTORC2-specific subunits: rictor (rapamycin-insensitive companion of mTOR) and mSin1(mammalian stress-activated protein kinase-interacting protein 1) [103,104]. Each complex also includes other structural and

regulatory components. Although the inhibitory effect of rapalogs on mTORC1 is established, the effect of rapalogs on mTORC2 is controversial [105].

The signal transduction pathway is mediated by PI3kinase activation, then direct and indirect stimulation of the downstream effectors: mTORC2, Akt, and mTORC1. Embryonic loss of mTORC1 activity is lethal early in gestation, before development of the vasculature. In contrast, loss of mTORC2 activity, either by knockout of mLST8 or rictor, results in abnormal vascular development and death at embryonic day 10.5 [106]. In many cancer cells, the pathway is hyper activated as a result of mutated expression of upstream components including PI3 kinase-alpha or the counter-regulatory phosphatase PTEN. These data suggest that agents acting against mTOR might optimally achieve control of tumor neovascularization. Recent work has identified complex feedback regulation between mTOR and PI3kinase activity in cancer cells, which modulated the responses to both receptor tyrosine kinase and androgen receptor stimulation [107,108]. This prompts the need to validate the feedback mechanism in primary human EC and to compare the involvement of mTORC1 versus mTORC2 in this mechanism.

5 VEGFR2 beyond ligand binding (receptor trafficking)

A sequence of events occurs following PI3K/Akt activation, which modulates the activation's duration and strength. Upon ligand binding, VEGFR2 is internalized by endocytosis and either degraded by lysosomes or recycled to the plasma membrane. VEGFR2 endocytosis is clathrin-mediated, whereas its transport is controlled by a group of Rab GTPases. Rab 5 facilitates formation of early endosomes carrying VEGFR2 [109]. Later Rab4 and Rab11 will drive VEGFR2 to fast or slow recycling vesicles, respectively [110]. On the contrary, Rab7 will direct VEGFR2 to late endosomes and subsequently to degradation (Figure 2) [109]. VEGFR2 continues to signal

from within the endosomes, and the receptor trafficking among these endosome compartments can affect signal output from the receptor [111-113]. The VEGFR2/PI3K coupling is found in Rab5-endosomes, and is extinguished by the time VEGFR2 traffics to the Rab11-endosome [111]. Perturbation of endocytic trafficking of VEGFR2 is associated with altered signaling. For example, retention of VEGFR2 to the plasma membrane, by association with VE-cadherin, promotes receptor de-phosphorylation [114]. Moreover, delayed endocytosis induced by loss of Numb activity is also associated with decreased Akt phosphorylation despite VEGF receptor activation [115]. Few regulators of this VEGF receptor sorting are known. NRP1, a co-receptor for VEGFA, interacts with VEGFR2 and favours VEGFR2 transfer to recycling Rab11 endosomes [111]. Further, VEGFR2 de-ubiquitinylation by USP8, promotes VEGFR2 recycling and signaling [116]. Conversely, serine phosphorylation of the PEST domain of VEGFR2, and recruitment of PDCL3 are implicated to guide receptor trafficking toward the degradation pathway [117,118]. This dephosphorylation and recycling of the activated VEGFR2 from the early endosome to the plasma membrane is a feature of VEGFR2 distinct from the degradation typical of other activated receptor tyrosine kinases in EC [111].

6 Therapeutics of angiogenesis

Therapeutic proangiogenic drugs are candidates for treatment of the diseases associated with defect in agiogenesis. Preclinical studies in rats showed that oral administration of bFGF can induce angiogenesis in duodenal ulcers, which accelerated the healing process [119]. As a result, phase I clinical trials were performed to test the efficacy of bFGF compared to the conventional duodenal and gastric ulcer therapy. Interestingly, bFGF had a superior effect to the conventional therapy in healing the nonsteroidal anti-inflammatory drug (NSAD)-induced gastric ulcer [120].

Another clinical trial investigating the safety and feasibility of bFGF administration in patients with coronary artery disease, who were not candidates for thrombolytic therapy, suggested bFGF as a novel therapy for cardiovascular diseases [121]. Currently, it is well established in the literature that angiogenic stimulants can induce cardiac tissue repair and regeneration in ischemic heart diseases through the induction of angiogenesis, improvement of perfusion, delivery of survival factors to sites of tissue repair, and mobilization of regenerative stem cells [122-125]. However, there are no FDA approved angiogenic drugs to treat ischemic cardiovascular disease. Of note, the only available method approved by FDA to promote angiogenesis in myocardial ischemia the transmyocardial laser revascularization (TMR).

6.1 Cancer

Tumors are highly demanding tissue, so they recruit the surrounding vasculature by secreting proangiogenic cues to supply it with nourishment. The newly formed blood vessels will support tumor growth and metastasis. Therefore, several antiangiogenic agents have been studied to prevent tumor progression. The prototype of VEGF inhibitors, Bevacizumab (Avastin), was approved by FDA to treat glioblastoma, colorectal cancer, some lung cancers, and metastatic renal cell carcinoma [126,127]. Bevacizumab is a monoclonal antibody that binds specifically to VEGF and prevents VEGFR2 activation [128]. Sorafenib and Sunitinib, are other FDA-approved angiogenic inhibitors that bind to VEGFRs and PDGFRs on the EC (Sorafinib also inhibits Raf kinases) to block their activities [129].

6.2 Ocular neovascularization

Angiogenic therapy is currently being investigated in ophthalmic conditions associated with pathological neovascularization like age-related macular degeneration (AMD), proliferative diabetic retinopathy (PDR), diabetic macular edema (DME), neovascular glaucoma, corneal neovascularization (trachoma), and pterygium. The first FDA-approved blood vessel therapy for macular degeneration was the photodynamic therapy Visudyne [130,131]. Shortly after, the anti-VEGF aptamer (pegaptanib, Macugen), and the anti-VEGF monoclonal antibody (ranibizumab, Lucentis) were approved for AMD and DME [132,133].

6.3 Interferon alpha-2a to treat hemangiomas

Hemangiomas occur in 1 out of 100 neonates and in 1 out of 5 premature infants [134]. Most hemangiomas are self-limited and they regress by the age of 10-15 years. However, about 10% of hemangiomas can have fatal outcomes by involving vital organs, obstructing an airway, or causing Kasabach-Merritt syndrome. Of note, Kasabach-Merritt syndrome -a disease characterized by thrombocytopenia, coagulopathy, and hepatic hemangiomas- has a high mortality rate reaching up to 50% of cases [135]. Corticosteroid therapy is effective in nearly 30% of hemangiomas [136]. Interferon alpha-2a (IFNα-2a) is an antiangiogenic agent that dramatically reduced the size of pulmonary hemangioma in a 7-year-old child [137]. In another study, IFNα-2a induced hemangioma regression in 18 out of 20 patients [138]. IFNα-2a suppresses the production of FGFs in human tumor cells, and inhibits EC proliferation and migration, which makes it a good candidate to treat hemangiomas because bFGF is overexpressed in hemangiomas.

6.4 Rheumatoid arthritis

Rheumatoid arthritis (RA) is a chronic disease in which angiogenesis is induced resulting in delivery of more inflammatory cells to the affected site. Tissue infiltration with inflammatory cells will lead to synovial hyperplasia and progressive bone and cartilage destruction in the affected joints [139,140]. In RA, the hyperangiogenic environment results from excessive pro-angiogenic factors secretion that exceeds and counteracts the effect of the angiogenic inhibitors. Hence, inhibition of joint neovascularization can alleviate synovitis and pannus formation [141,142].

Minocycline and TNP-470 (also known as AGM-470) have shown efficacy as potent inhibitors of the vascular pannus in experimental arthritis [143,144]. However, data from clinical trials investigating antangiogenic agents in arthritis is not yet available.

7 Tumor resistance to antiangiogenic therapy (Tumor escape)

Although, introducing bevacizumab, sunitinib and sorafenib to clinics elicited tumor stasis or shrinkage and in some cases increased survival, the results were transient and followed by tumor regrowth and disease progression [145-148]. The recurrence of tumors, designated tumor escape, is attributed to activation of alternative pathways to sustain tumor growth despite the inhibition of the antiangiogenic drug's targets [149-152]. For example, initially breast cancer requires only VEGF for angiogenesis, but at later stages, additional angiogenic cues like fibroblast growth factor 1 (FGF-1), FGF-2, transforming growth factor–β (TGF-β), platelet-derived endothelial cell growth factor (PD-ECGF), and placental growth factor (PlGF) will drive angiogenesis in these tumors [153]. Thus Relf et al hypothesized that a late-stage breast tumor may escape anti-VEGF treatment

by releasing alternative angiogenic factors [153]. The activation or upregulation of alternative pro-angiogenic signaling pathways within the tumor was observed during preclinical trials in a genetically engineered tumor mouse model [149]. When the mice were treated with a monoclonal antibody that specifically blocked VEGFR signaling (in particular VEGFR2), there was a transient response (10-14 days), indicated by tumor stasis and reductions in tumor vascularity, followed by tumor regrowth and restoration of tumor vasculature. Interestingly, the relapsing tumors expressed higher levels of the pro-angiogenic factors fibroblast growth factor 1 (FGF1) and FGF2, and angiopoietin 1 than did the untreated mice models. Consistently, study of glioblastoma patients being treated with the VEGFR inhibitor cediranib (Recentin, Astra Zeneca) showed a transient response phase, and then a relapse or progression phase. Also, levels of FGF2 were found to be higher in the blood of relapsing patients than in that of the same patients during the response phase [154]. In fact, the evidence that tyrosine kinase inhibitors (TKIs) can transiently increase plasma levels of pro-angiogenic factors has been documented in the clinic before, and was proposed as a predictive biomarker for tumor response [155-157].

Another proangiogenic factor being upregulated as a result of antiangiogenic therapy is the stromal-derived factor 1 (SDF1) as the plasma levels of SDF1 correlate with metastasis in bevacizumab-treated patients with advanced rectal cancer [158], and in cediranib-treated patients with glioblastoma [154,159]. Further, SDF1 expression was also detected in various cancer cells [160,161] and its receptor CXC receptor 4 (CXCR4) was also found on tumor-associated endothelial cells [162]. It is now clear that tumors in different organs exploit the SDF1/CXCR4 pathway to escape from the current antiangiogenic therapy [163]. Nevertheless, whether anti-VEGF/SDF1 dual therapy will be more effective than anti-VEGF monotherapy is still to be determined.

Alternatively, investigating molecules that represent a convergence node for multiple angiogenic pathways could prevent tumor escape.

8 Potential candidates to efficiently regulate angiogenesis

8.1 SDF1/CXCR4

SDF1 is highly conserved between human and mouse and was identified as a chemokine that induces the chemotaxis of lymphocytes [164-167] and hematopoietic progenitor cells [168,169]. SDF1 deletion in mice was lethal shortly after birth [170]. SDF1 binds specifically to the GPCR CXCR4, which is expressed on lymphocytes, monocytes, neutrophils, and epithelial cells [171,172] and was recently found on various human EC [173-175]. Furthermore, SDF1 induces angiogenesis *in vitro* and *in vivo* [176,177].

In mice embryos, CXCR4 is specifically expressed in arteries of the mesentery and its expression is significantly reduced in SDF1-deficient mice. SDF1 or CXCR4 global deletion in mice produces defects in tip cell filopodia extension and angiogenesis in mesentery [178]. EC-restricted deletion of CXCR4 results in the same defects noticed in the CXR4-deficient mice [178]. Similar results were obtained in mice retina after treatment with antibodies against SDF1 or the CXCR4 antagonist (AMD3100) [177,179].

Recently, the notion that either VEGF or FGF induced surface expression of CXCR4 only on EC, and increased EC migration and angiogenesis in response to SDF1 [176,180], have drawn the attention towards SDF1/CXCR4 as a target to prevent tumor escape. Moreover, SDF1/CXCR4 pathway also affects tumor angiogenesis independently of the VEGF pathway [181,182]. On the basis of these findings, multiple agents are currently being developed to target the SDF1 pathway

in cancer. However, blockade of the SDF1 pathway had minor tumor suppression effects on established tumors. Moreover, CXCR4 antagonists inhibited tumor growth in some cases [183,184], but were ineffective in others [185-187]. Interpretation of these studies is complicated by the effect of the CXCR4 inhibitor on pro-angiogenic leukocyte trafficking to tumors. Thus, these preclinical studies suggest that blocking the SDF1 pathway solely may not be sufficient, except for certain solid tumors. Further, a therapeutic strategy to selectively inhibit CXCR4 in the endothelium is needed.

8.2 Apelin

8.2.1 Background

The cloning of the human apelin GPCR (APJ) after it was detected in the human genome facilitated the understanding of apelin signaling [188,189]. Investigating the structure of APJ revealed that the protein sequence is very close to the angiotensin receptors [189]. More extensive analysis of the protein sequence revealed that APJ belongs to rhodopsin class of GPCRs which includes angiotensin II receptor and the two chemokine receptors, CXCR4 and CXCR7 [190]. This structure suggested that apelin might have chemotactic properties and hemodynamic function. The receptor's ligand was identified later by the discovery of the gene encoding apelin. Apelin can be present in different isoforms of different lengths produced by proteolytic cleavage of the 77 amino acid propeptide [191]. The detection of APJ in the mesoderm of mice [188], and zebrafish [192] embryos suggested a role in the cell lineages originating from mesoderm, such as hemopoietic, myocardial, and ECs [193,194]. Apelin loss in zebrafish induced embryonic vascular malformation [195]. In vivo angiogenesis assays in normal and tumor mouse models [195-197] confirmed the role of apelin in physiological and pathological angiogenesis. In addition to angiogenesis, apelin has an

inotropic and vasodilator effect by inducing EC secretion of nitric oxide (NO) [198-200]. Apelin-deficient mice are viable but have smaller blood vessels and defects in retinal vascularization [201]. Similarly, APJ deficiency also decreases the development of the retinal network [202]. Interestingly, the apelin gene was not expressed in the whole retinal vasculature, but was restricted to the leading edge of vessels, which corresponds to the tip cell [196]. In line with this observation, separate isolation of tip or stalk cells by laser capture microdissection identified apelin as a tip cell marker [202].

8.2.2 Apelin in vascular repair

Apelin is proposed to promote angiogenesis. In mice, adipose tissue transplantation is characterized by graft hypoxia due to lack of blood supply. After 2 days of transplantation, apelin expression significantly increased and graft revascularization started to occur [203]. Administration of apelin in rats was protective against lung vascular injury induced by hyperoxia. Further, administration of apelin after the injury had occurred promoted recovery by inducing angiogenesis and alveolarization [204].

Another evidence is the marked reduction of angiogenesis in the retina of apelin-deficient mice after oxygen-induced retinopathy [205]. Whereas, injection of apelin in the vitreous induces the sprouting and the proliferation of EC in the retina [206].

Finally, treatment with apelin promoted angiogenesis in the infarcted myocardium and improved cardiac function [207], while its deficiency increased the myocardial ischemia reperfusion injury [208].

9 Rho GTPases

Rho GTPases are members of the Ras superfamily of GTPases and they regulate many cellular functions including cell division, adhesion, survival, and cell motility [209,210]. The GTPases are molecular switches that bounce between GTP- and GDP-bound forms [211]. The GTP-bound form is active and can bind to specific downstream effectors, but once the GTP is hydrolysed to GDP they lose activity [211]. This "on" and "off" state is controlled by the activator Guanine nucleotide exchange factors (GEFs) and the counter regulator GTPase activating proteins (GAPs) [212,213]. To date, twenty members of the Rho family proteins have been identified in humans; among them, RhoA, Rac1 and Cdc42 are the best-characterized members and they all control cell motility by regulating cytoskeleton reorganization. Studies showed that Rac1 controls lamellipodia formation, Cdc42 regulates filopodia extension, and RhoA promotes myosin contractility [209] . Consistently, they were found to be active at the leading edge of migrating fibroblasts [214,215].

9.1 Guanine nucleotide exchange factors (RhoGEFs)

There are 83 genes encoding for different Rho GEFs in human [216]. RhoGEFs exert their activity by substituting GDP with GTP on the RhoGTPases [216]. One family of RhoGEFs is the diffuse B cell lymphoma (dbl)-family [216]. Members of dbl family have a dbl homology (DH) domain, which is responsible for the RhoGEF activity, and a pleckstrin homology (PH) domain which mediates localization and binding to membranous phospholipids [217,218]. Interestingly, studies suggested that spatial dynamics of Rho GEFs could shape their activity [217,219]. Indeed, serum-activated Rac1 requires Tiam-1, a Rac1 upstream RhoGEF, localization to the plasma membrane [220]. Phosphorylation of the RhoGEFs can also regulate their activity as phosphorylation of

specific tyrosine residues was observed to induce conformational changes and expose the DH domain [221]. In line with this observation, only phosphorylated Vav-1, a Rho GEF, can induce Rac activation in vitro and in COS-7 cells [222]. Another interesting mechanism of regulation that is observed in GEFs is regulation by the Gα subunit of heterotrimeric G proteins. G proteins transfer signals from a wide range of transcellular heptahelical receptors to many intracellular effectors. Investigations revealed that the GTPase activity of two G protein α subunits, Gα12 and Gα13, were stimulated by the Rho guanine nucleotide exchange factor p115 RhoGEF. Further, activated Gα13 bound to p115 RhoGEF and stimulated its capacity to catalyze nucleotide exchange on Rho [223,224].

9.2 Rho GTPase activating proteins (RhoGAPs)

RhoGAPs are a large family of molecules that regulate Rho GTPases by inducing their intrinsic GTPase activity, which in turn causes inactivation of RhoGTPases [213]. The significance of RhoGAP in regulating Rho GTPase was demonstrated in EC deficient in p73, a RhoGAP specifically expressed in vascular smooth muscles and EC [225]. p73 loss resulted in increased Rho activity and extensive stress fiber formation due to release of Rho from the p73 inhibitory effect. Further, inhibition of p73 resulted in defective angiogenesis due to defects in proliferation and migration [225]. RhoGAPs also have a significant role in terminating receptors' activity. G proteins play a crucial role in signaling downstream of RTKs and GPCRs. For instance, the GTP-bound form of Ras and of the Gα subunits mediate signals from these receptors until binding of RhoGAPs to the GTP-bound Ras or Gα. Studies showed that this binding increased Ras and Gα intrinsic GTPase activity by two to four folds, promoted the hydrolysis of bound GTP to GDP

and converted the G proteins to their inactive state within a range of 50–200 ms [226,227].

9.3 Facio-genital dysplasia 5 (FGD5)

Facio-genital dysplasia-5 (FGD5) is a member of zinc-finger (FYVE), Rho guanine exchange factor (Rho GEF) and pleckstrin homology (PH) domain containing family (Figure 3). Although, the family consists of 7 members (FGD1-6 and FRG), only FGD5 is robustly expressed in highly vascularized organs and especially in EC [228,229]. The Rho GEF domain induces Rho GTPases activity by exchanging GDP for GTP and may explains the observed FGD5-mediated Cdc42 activity [228]. The PH domain precedes the Rho GEF domain to catalyze its enzymatic activity. In addition, in Rho GEFs the PH domain plays a crucial role in recruiting the protein to the cell membrane [230]. The FYVE domain increases the binding specificity as it usually mediates interactions with phosphatidylinositol- 3´-phosphate [231], which suggests that FGD5 function is associated with endosomal trafficking [232-234]. FGD5 is named after the X-linked developmental facio-genital dysplasia syndrome or the Aarskog-Scott syndrome, which result from mutations in the gene encoding FGD1, the prototype of FGD protein family [235].

Recently, FGD5 has been investigated to elucidate its physiological significance in EC. In a previous report we showed that FGD5-loss negatively regulates VEGF/PI3K pathway, and angiogenesis in 3 dimensional (3D) angiogenesis assay and *in vivo* [229]. In contrast, another group had shown that FGD5 promotes apoptosis and is involved in vascular remodelling [236]. The inconsistent results can be attributed to differences in experimental techniques. While, the latter group relied on overexpression of FGD5 in mice retina, we and others performed selective loss of function experiments [228,229] Overexpression of FGD5 in cells where it is not normally present,

like mural cells, may confound the results. Further, the evidences that FGD5 null mice did not survive beyond embryonic day 12 (E12) [237] and the robust expression of FGD5 in aorta-gonad mesonephros of mice embryos, which is the origin of the aorta [237], suggest that FGD5 may have a pivotal role in vascular development and angiogenesis. However, a mechanistic understanding of the role FGD5 plays in VEGF-mediated angiogenesis, and how it regulates the VEGF/ PI3 kinase/ Akt pathway are still to be determined.

10 Endothelial injury-induced diseases

10.1 Microvessl Injury: Thrombotic microangiopathies (TMA)

TMA is diverse; it could be hereditary or acquired and can occur in any age. However, TMA syndromes share the same clinical and pathological features. The presentation includes microangiopathic hemolytic anemia, thrombocytopenia, and organ injury [238]. Microscopically, they typically show vascular damage, arteriolar and capillary thrombosis, and abnormal EC [239].

10.1.1 Thrombotic thrombocytopenic purpura TTP (Acquired and Hereditary)

In 1924, Moschcowitz was the first to describe thrombotic thrombocytopenic purpura (TTP), when he discovered hyaline thrombi in terminal arterioles and capillaries throughout most organs in an autopsy of one of his patients who died with multiple organ failure [240]. TTP is also known as ADAMTS13 deficiency–mediated TMA.

Cause: Under normal physiological conditions, ADAMTS13 cleaves and deactivates von Willebrand factor multimers secreted by EC [238]. When ADAMTS13 is deficient, von Willebrand factor will form long multimers and predispose to platelet deposition on EC and thrombus formation [238]. TTP can be hereditary due to genetic mutations in ADAMTS13 [241], or acquired due to an autoimmune disorder caused by autoantibody inhibition of ADAMTS1 3 [238].

Presentation: Hereditary TTP rarely cause severe acute kidney injury. However, it commonly presents with recurrent episodes of microangiopathic hemolytic anemia, thrombocytopenia, and other signs of organ damage.

Diagnosis: Deficiency in ADAMTS13, absence of antibodies against ADAMTS13, and documentation of mutations in ADAMTS13 are features of hereditary TTP [242]. Heterogeneity in siblings with hereditary TTP and in ADAMTS13-deficient mice suggests the involvement of other genetic or environmental factors [243].

On the other hand, acquired TTP can present with minimal abnormalities or critical signs of organ failure [244]. Weakness, gastrointestinal symptoms, purpura, and transient focal neurologic abnormalities are common. Diagnostic criteria are microangiopathic hemolytic anemia and thrombocytopenia without another apparent cause [245].

Treatment: The treatment is usually chronic and includes plasma infusion [246], or plasma-derived factor VIII concentrate that contains ADAMTS13 [247]. Before proposing plasma infusion, only 10% of TTP patients had survived [248] compared to 78% after plasma transfusion [249].

10.1.2 Complement-Mediated TMA (Acquired and Hereditary)

Complement-mediated TMA is characterized primarily by renal failure and was first recognized in 1975 as a familial disorder [250,251] until 1998 when the association between TMA and mutations

in the gene encoding complement factor H (CFH) was established [252]. Then, another mutations inducing complement activation have been identified in patients with TMA.

Cause: hyperactivation of the complement alternative pathway is the lead cause. Unopposed hydrolysis of C3 to C3b leads to deposition of C3b on tissues, which initiates the assembly of the C5b-9 terminal complement complex (the membrane-attack complex) and injury of normal tissue. Although, the exact mechanism is still elusive, there is evidence supporting the involvement of EC injury and complement dysregulation on the platelets [253]. In addition to genetic mutations, antibodies against CFH can result in acquired TMA. CFH antibodies account for about 10% of complement-mediated TMA.

Presentation: hypertension and acute kidney failure are common in complement-mediated TMA. Severe kidney injury without any apparent underlying cause is usually a distinguishing feature.

Diagnosis: is made after excluding Shiga toxin–producing infection and includes microangiopathic hemolytic anemia, high serum creatinine, thrombocytopenia, and preserved ADAMTS13 activity [254]. Of note, normal plasma levels of C3, C4, and complement factor H do not exclude complement-mediated TMA.

Treatment: Anticomplement therapy is used as an adjuvant to plasma therapy. Eculizumab is currently the only available anticomplement agent. However, it has limited effect in patients with C5 mutations [255]. Using immunosuppressant to reduce the antibody titer against CFH is also considered.

10.1.3 Shiga Toxin–Mediated hemolytic–Uremic syndrome (ST-HUS)

ST-HUS was first described in 1962 in patients with renal failure preceeded by diarrhea [256]. Twenty years later, during an outbreak of hemorrhagic colitis, Escherichia coli (E. coli) O157:H7

was identified as the causative organism [257] and the association between ST-HUS and Shiga toxin– producing E. coli was confirmed [258]. Of note, E. coli O157:H7 is the most common strain producing shiga toxin but not the only one [259]. ST-HUS is much more common in young age and has a 3% mortality rate [260].

Cause: infection occurs through contaminated water, beef products, vegetables, and other foods [261-263]. Shiga toxin binds to globotriaosylceramide (Gb3) on EC [264], and renal mesangial [265] and epithelial cells [266,267], which induces cell apoptosis. Shiga toxin is also a mediator of inflammation and thrombosis [268] and by inducing von Willebrand factor secretion from EC [264].

Presentation: history of contaminated food ingestion, acute abdomen, and bloody diarrhea followed by thrombocytopenia and renal failure [259].

Diagnosis: Shiga toxin can be detected by stool analyses but could be absent from stool in later stages [269].

Treatment: mainly supportive by hydration and renal dialysis [260]. Despite the lack of specific treatment, end stage renal disease is a rare complication [270].

10.1.4 Drug-Mediated TMA (immune reaction)

Drug-mediated TMA can be caused by secondary immunologic reactions or direct toxic effects [271]. Immune reaction in drug-mediated TMA was first recognized with quinine, a drug used for treatment of malaria [272]. Further studies identified quinine dependent antibodies that were reactive against multiple cell types [273,274]. Many other drugs have been reported to be associated with TMA as Quetiapine, an antipsychotic, and gemcitabine, a chemotherapeutic [275,276].

Cause: The mechanism is not fully understood, but one hypothesis is that drugs may facilitate the binding of specific antibodies to the cells by providing a binding-complementary structure

for both the antibody and the epitope [277]. There is evidence that the Quinine-dependent antibodies may mediate TMA, by activating EC [278].

Presentation: sudden onset of severe systemic symptoms, acute kidney injury and recent history of drug exposure are features of drug-mediated TMA.

Diagnosis: In addition to the clinical diagnosis, drug-dependent antibodies should be detected in serum. Of note, false negative results are common but do not exclude a drug-mediated TMA [278].

Treatment: Drug discontinuation, supportive care and plasma exchange are the only recommended treatment. Chronic kidney disease is common.

10.1.5 Drug-Mediated TMA (toxic dose–related reaction)

Drugs like VEGF inhibitors, immunosuppressants, and chemotherapy were reported to cause a dose-dependent TMA.

Cause: The mechanism depends mainly on the causative drug. Cyclosporine and tacrolimus were found to cause EC dysfunction, stimulate platelet aggregation and thrombus formation, through the inhibition of prostacyclin. Another example is the development of glomerular TMA after VEGF restricted inhibition in renal EC and podocytes [279,280].

Presentation: typically presents with hypertension and gradual loss of kidney function of unknown etiology [280]. With treatment, thrombosis, thrombocytopenia, and microangiopathy often resolve but renal failure tend to persist.

Treatment: similar to the drug-mediated immune reaction, drug discontinuation, supportive care and plasma exchange are the only recommended treatment. For some drugs, such as cyclo-sporine and tacrolimus, dose reduction -rather than drug avoidance- may be sufficient.

10.1.6 Metabolism-Mediated TMA

Hereditary disorder of vitamin B12 metabolism, designated cobalamin C disease, was reported to cause TMA and multiple organ failure in infants [281,282].

Cause: homozygous or heterozygous mutations in the gene encoding the methylmalonic aciduria and homocystinuria type C protein (MMACHC) can lead to deficiency in methylcobalamin, which cause hyperhomocysteinemia, decreased plasma methionine, and aciduria. Abnormal vitamin B12 metabolism is associated with platelet aggregation, EC dysfunction, and coagulation activation [283].

Presentation: usually presents in infancy with multiple developmental abnormalities, anemia, thrombocytopenia, and acute kidney injury. Forty percent of the patients will develop chronic kidney disease.

Diagnosis: routine lab work showing hyperhomocysteinemia, decreased plasma methionine, methylmalonic aciduria, and normal plasma vitamin B12 levels indicates an intracellular defect of vitamin B12 metabolism [283].

Treatment: infants with metabolism-mediated TMA improve with intravenous administration of hydroxycobalamin.

10.2 Large Vessel Injury: Allograft vasculopathy (AV)

Acute graft rejection can be controlled by potent immunosuppressants, such as cyclosporine or tacrolimus. However, immunosuppressive therapy does not prevent late failure of transplants. Thus, late or chronic graft failure has emerged as a major problem in clinical heart

transplantation [284]. The most common injury associated with chronic cardiac graft failure is allograft vasculopathy (AV) [285]. Of note, cardiac allograft vasculopathy (CAV) is one of the major causes of death after 3 years of transplantation [284].

10.2.1 Histo pathological features

AV starts with EC lesion in the coronary arteries that progress to become occlusive over time [285]. This occlusive intimal lesion consists of EC, smooth muscle-like cells and infiltrating leukocytes [286]. These features were documented in both human cardiac allografts and animal models such as aortic allografts [285,287]. The classic microscopic picture of CAV shows fibromuscular hyperplasia in the intima and media of large and small epicardial coronary arteries, occlusion of the small vessels, and myocardial infarction [288,289]. CAV can develop in the proximal arteries as early as 6 months post-surgery [290]. CAV can manifest differently according to the affected vessels. Intramyocardial arteries show mainly intimal fibromuscular hyperplasia and inflammation, whereas epicardial coronary arteries show intimal fibromuscular hyperplasia, lymphocyte and macrophage infiltration, and secondary atheromatous changes [291]. The inflammatory infiltrate is usually severe in the intima and adventitia but the internal elastic lamina stays intact. CAV can be differentiated easily from atherosclerosis [292,293] because CAV injury lacks atheroma formation or calcification, is more concentric, and involves all sizes of epicardial and intramyocardial coronaries. In contrast, atherosclerosis is eccentric, affects proximal vessels, and spares the intramyocardial coronaries. Further, atheromatous plaques frequently calcify, and rarely show signs of inflammation [292]. Nevertheless, both pathologies may co-exist in human donor arteries. To date, the mechanism of the AV and the role that the various vascular elements play in its generation are still to be determined.

10.2.2 Mechanism

Studies have shown an association between chronic rejection of transplanted hearts and the development of donor-specific antibodies to human leukocyte antigens (HLA). The induced immune response usually involves allorecognition of donor antigens by recipient T lymphocytes as presented by recipient antigen presenting cells [294,295]. Then, activated lymphocytes adhere to graft EC, invade the vessel wall, inflict injury, stimulate the release of growth factors, cytokines/chemokines, and cellular adhesion molecules, and the development of alloantibodies. This sequela results in the proliferation of vascular smooth muscle cells and the subsequent occlusion of the lumen [294,296]. There is evidence that the severity of CAV positively correlates with inflammation and with HLA mismatch [294]. Nonimmunologic factors, such as ischemia-reperfusion injury, hyperglycemia, and hyperlipidemia, and cytomegalovirus infection, can also lead to the development chronic inflammation and eventually CAV [284,297,298].

10.2.3 The role of EC in development of CAV

EC regulates many physiological functions like thrombus formation, vascular tone, and inflammation [299]. The endothelium also has a thrombolytic effect by secreting many antithrombotic factors as tissue plasminogen activator, heparans, thrombomodulin, and nitric oxide (NO) [299]. NO is produced from arterial EC in response to flow and shear forces, which activate endothelial nitric oxide synthase (eNOS) [299]. In addition to its vasodilator effect, NO plays an anti-inflammatory role by inhibiting the adhesion of leukocytes, the aggregation of thrombocytes, the production of proinflammatory cytokines, and the proliferation of SMC [300,301].

Therefore, EC dysfunction can lead to intimal thickening, plaque formation, and ultimately serious clinical events [302].

In CAV, coronary EC serve as potent stimulators as well as targets of allogeneic lymphocyte reactivity [303]. EC injury in CAV can be denuding or nondenuding injury. In nondenuding injury, EC proliferate rapidly trying to compensate for injury, which leads to EC dysfunction. Both immune-related and nonimmune-related factors contribute to nondenuding injury. In contrast, denuding injury is caused by peritransplant ischemia-reperfusion injury or in acute cellular rejection. Denuding injury may be so severe that the underlying basement membrane, intimal SMCs and extra cellular matrix (ECM) get exposed to blood components.

Heterotopic cardiac transplantation in rats has shown relatively normal EC, similar to that in the arteries of the native heart in syngrafts and CsA-treated allografts [304]. However, saline-treated allografts underwent cell-mediated rejection and showed progressive EC injury characterized by areas devoid of cells and bare ECM. The injured sites were covered by platelets and leukocytes, which transmigrated to the subendothelial space too. Taken together, early EC damage can represent the trigger that initiate CAV [304].

Acetylcholine stimulates the release of NO from EC. However, paradoxical coronary vasoconstriction to acetylcholine in allograft recipients with or without CAV has been observed [305]. This indicates that EC dysfunction is a common finding in cardiac transplant recipients and can represent an early marker for the development of CAV. Of note, EC dysfunction is not diffuse after cardiac transplantation [306]. Normal functional EC is also present in coronaries of CAV denoting that there is a process of EC repair and that endothelial function may not be irreversibly damaged [306]. In line with this evidence, intravenous administration of L-arginine was reported to improve EC vasodilator function of coronary arteries if given at an early stage of

CAV [307]. Another evidence that EC plays a significant role in development of CAV is the association between the coronary EC dysfunction in humans and myocardial perfusion defects [308]. Moreover, early epicardial EC dysfunction predicts the development of vasculopathy 1 year after transplantation in transplant and non-transplant patients [309,310].

In animal models of AV, NO deficiency accelerates AV pathogenesis. The inducible form of NOS (iNOS) is expressed in the vessel wall of the aortic allograft and its inhibition significantly increases intimal hyperplasia [311]. Furthermore, early overexpression of iNOS completely prevents the development of structural changes in CAV [311]. The notion that eNOS has a vascular protective role was first described in murine AV model, when injury was accelerated in aortic allografts of eNOS-deficient mice [312]. Additionally, Iwata et al demonstrated that liposome-mediated gene delivery of eNOS to transplanted hearts in rabbits can effectively reduce EC injury and enhance graft survival [313]. Clinical evidences that eNOS function is gradually impaired after human heart transplantation [314], and reduced myocardial eNOS gene expression in coronary endothelial dysfunction [315] also support the significance of eNOS in the pathogenesis of AV.

10.2.4 Animal models of CAV

Most CAV models have used heterotopic cardiac transplantation or orthotopic artery transplantation into both mice and rats. Heterotopic cardiac transplantation is performed by the interposition of a donor heart into a nonphysiological position, such as the abdomen, in the recipient. In the abdomen, the donor pulmonary artery and aorta are anastomosed to the recipient ascending vena cava and descending aorta, respectively [316]. Although there is limited blood flow into the ventricles of this transplanted heart in spite of maintained cardiac contractions, the

myocardium is adequately perfused with recipient blood. Hence, the vasculature and myocardium are exposed to the host immune system similar to clinical heart transplantation. There are numerous studies using the heterotopic heart transplant model that advanced the understanding of CAV. Wilhelm et al used a rat heterotopic heart transplant model to demonstrate that an upregulation of transforming growth factor (TGF)-β is observed only in brain-dead donor rats, which may lead to increased graft fibrosis [317]. The rat heterotopic heart transplant model has also shown an association between CMV infections and the development of CAV [318]. Recently, study investigating mouse heterotopic models showed that EC apoptosis contributes to the development of CAV [319].

In the orthotopic arterial transplant model [320], blood flows through the artery under more or less normal physiological conditions. Arteries transplanted in this manner consistently develop intimal thickening and are used extensively to investigate AV [320]. To further mimic clinical scenarios of transplantation, complete and minor MHC mismatched strains of mice are used to investigate acute rejection [321] and CAV, respectively; and the efficacy of immunosuppressive agents [322].

11 Vascular repair

The integrity of the vascular endothelium is required for normal physiological functions, and is determined by the balance between endothelial turnover and repair. For instance, in inflammation EC is damaged and shed of the vascular wall leaving it naked and vulnerable to platelet aggregation and thrombus formation. EC replacement by proliferation of neighbouring residing EC, and/or by the recruitment of EPC from the circulation, and/or angiogenesis prevents further vascular damage and repairs the insult.

Studies have shown that angiogenesis and EC turnover are important defense mechanisms in renal inflammatory diseases and allograft rejection. Therefore, understanding vascular repair may have therapeutic implications to protect against EC injury and chronic disease progression.

11.1 Vascular repair by EC proliferation

Although the rate of tissue turnover for many somatic cells like blood, skin and gut is known, little information is available regarding EC turn over or what's the baseline level of EC turn over required for vascular repair [323].

For example, circulating blood cells are replaced and replenished on hourly basis without any noticeable change in blood cell count. Blood cells are derived from hematopoietic stem cells and hematopoietic progenitor cells in bone marrow [324]. In the intestine, about 100 billion epithelial cells are renewed daily [325]. Moreover, the epidermis of the skin is completely renewed every 28 days, roughly [326]. These processes of tissue turnover that are required to maintain the normal physiological functions of different organs, indicate that the EC of the cardiovascular system that feed all the other systems must also have a repair capacity. Despite the detection of necrotic EC circulating in the blood stream reflecting an EC replacement, the full mechanism of vascular repair is not fully understood.

EC were thought to divide only during embryogenesis and stay quiescent in the vasculature thereafter [327]. More thorough investigations have revealed that EC proliferate by mitosis from adjacent cells as a method of repair [328-332]. Later, some factors that could stimulate EC proliferation in the aorta were identified like metabolic disorders, infections and endotoxins. Other studies also showed that not all endothelial cells lining the aorta have the same proliferative potential [333-336]. Specially, in rodents, some EC in the aorta proliferated slowly

while others had a very high rate of replication reaching 60% [337]. Induction of vascular injury by inserting a cannula and vascular scraping of femoral and carotid arteries in rodents [334,338,339] showed that minor vascular injuries can be repaired by spreading of remaining healthly EC, while larger defects were repaired by migration of adjacent EC [340].

Moreover, tritiated thymidine infusion studies into mice suggested high variability in EC turnover in normal tissues ranging from a few months [341] to a hundred days [342]. Recently, EC proliferation was reported in lung vasculature after pneumonectomy. EC proliferation resulted in release of specific angiocrine factors that induce alveologenesis. This endothelial–epithelial interaction led to compensatory lung growth in adult mice [343]. However, questions remained about whether circulating primary cells contribute to vascular repair in conjunction with the residing EC [344,345].

11.2 Vascular repair by EPCs

EPCs are being heavily investigated since their discovery by Asahara and colleagues [346] who reported that a subset of human circulating blood cells expressing CD34 (15 % of peripheral blood cells) and VEGFR2 displayed the ability to form tube-like structures and to home to sites of ischemia and neoangiogenesis [346]. There is a paradigm concerning the involvement of EPCs in vascular repair. Some investigators suggest that EPCs are recruited to the site of vessel injury and provide paracrine support for residing EC. In turn, EC migrate and proliferate to initiate vascular repair. Others suggest that EPCs can reprogram to mature EC and provide a long term reparative potential to the endothelial intima.

The indirect role of EPCs in vascular repair:

Fluorescent-labeled bone marrow cells demonstrate that no bone-marrow-derived endothelial or EPCs incorporated into the site of tumor neovascularization. However, bone marrow-labeled cells were detected in the perivascular area of endothelial repair [347]. Another evidence, atherosclerosis animal models showed that no bone-marrow-derived circulating cells were incorporated in the endothelium covering the site of vascular plaque [348]. Similarly, re-endothelialization of an injured carotid artery did not occur through recruitment of circulating bone-marrow-derived cells [349], but rather through migration and proliferation of resident EC in the healthy arterial segments [350-352].

The direct role of EPCs in vascular repair:

EPCs isolated from the blood stream of animals, and human subjects can form an endothelial monolayer to line the lumen of implanted Dacron materials or intravascular devices [353]. Further, EPCs can form perfused blood vessels that form a network with the host circulation upon transplantation into immunodeficient mice [354-356].

Whether EPCs function directly or indirectly, there is no doubt that EPCs represent a main pillar for vascular repair since the presence of the concentrations of circulating EPCs is inversely proportional to microvascular obstruction after acute myocardial infarction [357]. The circulating concentration of EPCs has also been documented to increase tenfold after acute myocardial infarction in human [358] indicating vascular repair.

11.3 Vascular repair by angiogenesis

Angiogenesis is a key component of inflammation and has shown to be significant in ischemic and chronic inflammatory diseases, including diabetes, retinopathy, atherosclerosis, allograft rejection, coronary artery disease, myocardial infarction, and heart failure [359-371]. Moreover, several acute and chronic renal diseases, including ischemic nephropathy, glomerulonephritis, and interstitial nephritis, were found to be associated with angiogenesis. Therefore, angiogenesis regulation has been proposed to control the progression of many diseases [367,372,373]. In diseases like glomerulonephritis and ischemic nephropathy, accelerated vascular injury occurs in response to reduction of proangiogenic factors and/or EPCs [367,374-376]. Interestingly, delivery of proangiogenic factors to induce angiogenesis can promote recovery. More evidences from literature supporting the role of angiogenesis in repair include; the lead EC at the edge of a wound in the monolayer share transcriptional features of the angiogenic tip cell, EC tip cell morphologic differentiation plays a significant role in repair of injury to the established microvasculature, and EC tip cell genes are required for vascular repair in models of glomerular microvascular injury [94,377-379].

When rats were injected with anti-Thy-1.1 antibody and Habu-snake venom they developed acute glomerulonephritis characterized by severe mesangiolysis and marked destruction of capillary network on day 2 [375]. Administration of VEGF for 9 days, significantly enhanced EC proliferation and glomerular capillary repair. The repair process showed capillary regeneration from the remaining EC and new capillary growth from the existing glomerular vascular network [375,380]. After 8 weeks, a new glomerular capillary pole developed [375].

On the other hand, angiogenesis can facilitate the recruitment of inflammatory cells in chronic diseases like atherosclerosis, which in turn will sustain the angiogenesis reaction [361,363,366,381,382]. Therefore, it has been proposed that antiangiogenesis therapy can attenuate chronic inflammatory diseases.

12 Angiogenesis assays

The development of angiogenesis assays has been essential to the discovery of proangiogenic and antiangiogenic drugs. In vitro assays are more suitable to study a single step in blood vessel development or to isolate the effect of specific angiogenic stimulus or pathway. In addition, in vitro assays are high throughput and quantitative but usually need to be confirmed in vivo. In vivo experiments are more laborious and difficult to quantitate, but because angiogenesis is a complex process involving many growth factors and different cell types, in vivo experiments represents more genuine techniques to study the bigger picture of angiogenesis.

12.1 In vitro angiogenesis assays

12.1.1 Commonly used cell models to study in vitro angiogenesis

Human umbilical vein endothelial cells (HUVECs): HUVECs were first isolated from freshly obtained human umbilical cords by Jaffe et al. Transmission electron microscopy showed cultured EC contained cytoplasmic inclusions (Weibel-Palade bodies) similar to *in situ* endothelial cells. Consistently, these inclusions were also found in EC lining the umbilical veins, but were not seen in smooth muscle cells or fibroblasts in culture or *in situ* [383]. HUVECs

are widely used in angiogenesis research because they are easily cultured and isolated from human umbilical veins [383]. Moreover, HUVECs in combination with mouse myoblast cells (C_2C_{12}) and mouse embryonic fibroblasts (MEFs) can form a three dimensional prevascular network [384,385]. Thus, HUVECs are being investigated in the field of tissue engineering and in vitro prevascularization [384]. Interestingly, HUVECs and 10T1/2 mesenchymal precursor cells interacted in a three-dimensional fibronectin–type I collagen gel to form engineered vascular networks. When these vascular networks were implanted in mice, they formed long tubes that, subsequently, connected to the mouse circulation and became perfused [385].

Bovine aortic endothelial cells (BAECs): are obtained from arterial ECs of bovine aortae by collagenase. The cultured ECs consist of a homogeneous population of tightly packed, polygonal cells that can be serially subcultured for up to 30 passages without any apparent change in morphology or loss of growth potential. The isolated bovine endothelial cells were identified by the presence of Weibel-Palade bodies, pinocytotic vesicles. Further, they express the EC specific factor VIII antigen [386]. The BAECs are easily isolated from the aorta of cattle and could be cultured easily. However, the aortic ECs form tight junctions between each other so they do not sprout easily and they are not the best models to study angiogenesis. In addition the cells are not human in origin so the genetic differences between humans and cattle may interfere with the results [386,387].

Endothelial progenitor cells (EPCs): the evidence for circulating stem cells was demonstrated by the fact that HSCs from peripheral blood can provide sustained hematopoietic recovery [388]. Angioblasts and EPCs share certain genetic signature including Flk-1, Tie-2, and CD34.

Therefore, these progenitor cells may originate from a common precursor [389,390]. Recently endothelial progenitor cells have been detected in the circulation and isolated by magnetic bead selection on the basis of cell surface CD34 expression. However, it's very difficult to isolate EPCs from peripheral blood because they constitute about 0.5% of the circulating cells [346]. Studies have shown that these cells contribute largely to vascular repair. In vitro, these cells could differentiate into ECs expressing CD31. In animal models of ischemia, EPCs were detected in sites of active angiogenesis [94,346]. As a result EPCs are being heavily investigated to induce angiogenesis in ischemic tissues and for delivering anti- or pro-angiogenic agents, to sites of pathological angiogenesis. In cancer, inhibition of EPCs mobilization from the bone marrow has shown clinical significance, as tumors were not able to grow in animals that lack functional EPCs [169,391]. Hence, EPCs mobilization inhibitors have been proposed for cancer therapy [392,393].

Human dermal microvascular endothelial cells (HDMECs): are easily isolated and represent a good model to study angiogenesis of microvessels and capillaries [394]. HDMECs are isolated from neonatal foreskins by magnetic beads coupled with anti-E-selectin antibodies after transient induction of E-selectin by the tumor necrosis factor-α (TNF-α), a phenomenon known to be EC-specific [395]. In culture, HDMECs showed typical cobblestone appearance, expressed CD31 and von Willebrand factor, and formed capillary-like tubes in a three-dimensional angiogenesis assay [396].

Immortalized human microvascular endothelial cell line (HMEC-1): The study of human vascular EC is limited by difficulties to isolate and culture primary cells. Therefore, an immortalized EC cell line was created by transfecting HDMECS with the large T antigen of the simian virus 40 [397]. These cells can be subcultured up to 95 passages, show the cobble stone

appearance, express von Willebrand's factor and CD31 [398], and form microtubules resembling capillaries in a two dimensional angiogenesis assay [397]. Interestingly, HMEC-1 was able to seed vascular grafts and coronary stents indicating a potential application in antithrombotic and antiproliferative therapy [399]. HMEC-1 can survive in very low serum media, while primary EC require at least 20% serum supplementation. However, some immortalized cell lines showed tumorgenicity, chromosomal abnormality or loss of primary EC features [400]. Therefore, primary EC is considered superior to immortalized cell lines.

12.1.2 Two dimensional (2D) tube formation assay

Method: EC are grown between two layers of matrix (Matrigel®, collagen, or fibrin). Subsequently, the cells connect with each other and form a tubule-like network [401]. The tubule formation can be monitored under microscope and quantified as average tubules' length and number of tubules either manually or using specific softwares.

Advantages: easy to perform and takes only 24 hours. Being embedded in matrix, the cells grow under relative hypoxia (lack of oxygen), which mimics the in vivo angiogenic condition [402,403].

Disadvantages: does not simulate the three dimensional (3D) in vivo structure [404]. Affected by both the type of matrix and density of cells [405].

12.1.3 Three dimensional (3D) angiogenesis assay

3D assays simulate the in vivo angiogenesis and are good representative to EC tip cell differentiation and tubule formation. Recently, these assays were used extensively to study novel pro- or anti-angiogenic agents. The assay involves the EC attachment, migration and

differentiation of EC into tip cells and finally to tubules in a manner that simulates the in vivo situation [401,406].

Method: microcarrier beads are coated with EC and embedded in Matrigel® or fibrin gel. After 5-7 days tubules will start to form. Quantification is based on two variables: number of sprouts/bead and average length of sprouts [407].

Advantages: resembles the 3D in vivo structure. Being embedded in matrix, the cells grow under relative hypoxia, which mimics the in vivo angiogenic environment. In addition, it can mimic different in vivo situations depending on the used matrix e.g. fibrin would be the most appropriate for wound healing and revascularization, where endothelial cells migrate into a fibrin clot as part of the repair process. This assay recapitulates the in vivo angiogenesis events and gene expression. It involves basement membrane degradation, tip cell formation, sprout elongation, lumen formation, branching, and anastomosis; and is regulated by notch signaling. A major advantage of growing cells in vitro is the ability to isolate tip cells or stalk cells by laser capture microdissection to examine gene expression in different cell populations. Therefore, the 3D angiogenesis assay provides a definite asset to in vivo studies [407].

Disadvantages: time consuming, difficult technique, and difficult to analyze the results in 3D structure, as some tubules will not be visible by the regular microscopes [408].

12.2 Ex vivo angiogenesis assays

Angiogenesis in vivo is complex and involves EC, mural cells, and the surrounding microenvironment. This led to the development of organ culture methods to precisely evaluate

this complex process. The ex vivo assays are based on implanting parts of specific tissue in a 3D matrix in vitro, and monitoring any microvessel outgrowths from these implants.

12.2.1 Rat and mouse aortic ring assay

Method: being large in size, patent and easily to dissect, the aorta is cut into rings and embedded in Matrigel® or collagen. Angiogenesis starts after 5-7 days. Quantification is achieved by measurement of the length and prevalence of vessel-like extensions from the explant [409].

Advantages: this assay is considered to essentially recapitulate the in vivo angiogenesis environment because the system includes the surrounding mural cells (e.g. pericytes), 3D structure, and the cells are not manipulated with subcultures as the in vitro models [409].

Disadvantages: the cells are not genetically modifiable (e.g. Knock down, or over expression), difficult technique, difficult to analyze [410]. In addition, angiogenesis typically originates from the venous side [411] and from smaller vessels suggesting a minor role of the aorta in adult angiogenesis. However, veins lack the wall- muscular-support and are smaller than the aorta [412], these favor against the dissection and preserving the vein's lumen patency.

12.2.2 Vena cava-aorta model

Method: rings of aorta and vena cava from the same animal are embedded together in Matrigel® or collagen [412].

Advantages: avoids the lack of venous vessels in the aortic ring assay. Although angiogenesis occurs mainly from the venous side, the aorta is still needed to emphasize the anastomoses between the venous and the arterial vessels.

Disadvantages: in addition to the aortic ring disadvantages, it's difficult to obtain the vena cava and the venous vessels tend to collapse as it lacks the muscular lining compared to arteries [412].

12.3 In vivo angiogenesis assays

12.3.1 Corneal angiogenesis assay

Not only transparent, but the cornea is also the only avascular tissue in the body. Therefore, any newly-formed blood vessels emerging from the limbus into the cornea indicate neoangiogenesis. Given the nature of the cornea, angiogenesis can be easily identified and quantified [413,414].

Method: a sustained-release polymer pellet or sponge, containing a proangiogenic molecule, is implanted in cornea of rabbits, rats, or mice. Angiogenesis-formation starts after 3 days. Then, the agent to be tested can be administered topically or systemically. In turn, the effect on angiogenesis can be observed in the cornea throughout the course of the experiment. This requires a slit lamp for rabbits and stereomicroscope for mice. Definitive visualization of the mouse corneal vasculature can be achieved by injecting India ink intravenously. Lately, use of fluorochrome-labeled high-molecular weight dextran has replaced the India ink.

Advantages: the results produced are reliable. The cornea is avascular organ so the implants rarely cause edema or inflammation, which typically occurs by extravasation of inflammatory mediators from the surrounding vasculature [413].

Disadvantages: expensive, difficult to perform and time consuming. Taking into consideration the avascular nature of the cornea, it is not the best model to study angiogenesis [403].

12.3.2 Chick embryo chorioallantoic membrane (CAM) assay

The CAM of the chick is accessible system because it lies outside the embryo making it suitable to study complex angiogenesis *in vivo*. This model provides a physiological system for analysis of cells, cross-species xenografts, mammalian tissue explants, tumors and pharmacological reagents because the chick embryo is relatively immunotolerant [415-417].

Method: CAM, corresponds to placenta in mammals, is easily accessible by cutting a window in the egg shell or the whole embryo can be transferred to a culture dish. The test molecule could be delivered by gelatinous sponge or slow release polymer pellets. Angiogenesis is observed after 3 days and measured by removal of the area of CAM around the implant, then use of a dissecting microscope to count the number of formed vessels [402].

Advantages: simple, inexpensive and the test molecules can be preserved in the CAM circulation for a long time due to the lack of excretion out of the egg shell.

Disadvantages: difficult to differentiate between the newly formed and the already existing vessels. As vasculogenesis occurs in CAM up to 11 days, results obtained from embryos earlier than 11 days may be affected by endogenous factors. Therefore, in most cases it is preferable to wait until day 11. Moreover, the window in the eggshell can stimulate an inflammatory response [418].

12.3.3 Matrigel® plug assay

The Matrigel plug assay is considered the method of choice for studying in vivo angiogenesis [419,420]. Cold liquid Matrigel can be pre-mixed with angiogenesis-inducing agents such as VEGF

or tumor cells, which will solidify rapidly in room temperature or after subcutaneous injection in mice. Subsequently, the implants will be invaded by new blood vessels extending from the host vasculature [421].

Method: Matrigel®, a protein mixture enriched with growth factors, containing the test molecule, is injected subcutaneously in immune-deficient mice to avoid graft rejection. After 7 days the plug can be retrieved and examined for angiogenesis. Quantification is done either by sectioning the Matrigel® and assessing the extent of the vessel growth into the plug microscopically or by measuring the hemoglobin content of the plug [419].

Advantages: the assay is simple, reliable and quantitative [419].

Disadvantages: not a representative of the physiological or tumor-mediated angiogenesis sites. It's preferable to inject the plug intraperitoneal rather than subcutaneously. However, retrieving the plug after intraperitoneal injection is challenging. Another drawback is mice heterogeneity making the results more difficult to be replicable. To overcome this problem, both the control and the treated plugs should be injected into the same mouse [402].

12.3.4 Zebrafish

The zebrafish is a significant system to study developmental angiogenesis because it shares many genes and mechanisms of angiogenesis regulation with mammals [422].

Method: depends on the characteristics of the agent being tested. Lipophilic agents can be directly added to the water and will be absorbed by the zebrafish, but peptides must be injected into the yolksacs of the embryos. The embryos develop outside the mother and are transparent, so the blood vessel formation can be easily monitored using dissecting microscopes [423].

Transgenic zebrafish expressing fluorescent dyes under the control of EC-specific promoters are available (eg. mTie2-GFP) [423-425].

Advantage: inexpensive, high yield, and easy technique. It is also possible to specifically knock down a gene using antisense morpholino oligonucleotides, to isolate the effect of single targets on angiogenesis [426].

Disadvantage: the assay evaluates vasculogenesis more than angiogenesis. However, these processes are not completely separated in the developing embryo [427]

13 Rab GTPases

The Rab (Ras-related in brain) [428] family, which belongs to the Ras superfamily of small GTPases, consists of at least 60 different members [429]. The different Rab GTPases are present in special intracellular membranes within the cytoplasm, where they regulat distinct steps in membrane trafficking [430].

The Rab GTPases bounce between a GTP- and a GDP-bound form. The GTP-bound Rabs are active [431] and can recruit specific sets of effector proteins onto the cell membranes. These effector proteins facilitate vesicle formation, actin- and tubulin-dependent vesicle movement, and membrane fusion [430].

In eukaryotic cells, lipids and proteins regularly shuttle between distinct membrane-bounded organelles through transport vesicles. These vesicles originate from a donor compartment and fuse with a distinct acceptor compartment. The budding, motility and fusion of the vesicles are regulated by the Rab GTPases [432].

The reversible membrane localization of the Rab GTPases depends on the post-translational modification of a cysteine motif at the carboxyl terminus with highly hydrophobic geranylgeranyl groups [433]. This post-translational modification is regulated by a Rab escort protein (REP), which presents the Rab protein to the geranylgeranyl transferase. REP then delivers the hydrophobic geranylgeranylated Rabs to the appropriate membrane [433]. The target specificity of the Rab GTPases relies on membrane receptors that recognize the complex between REP and specific Rabs [434].

Figures

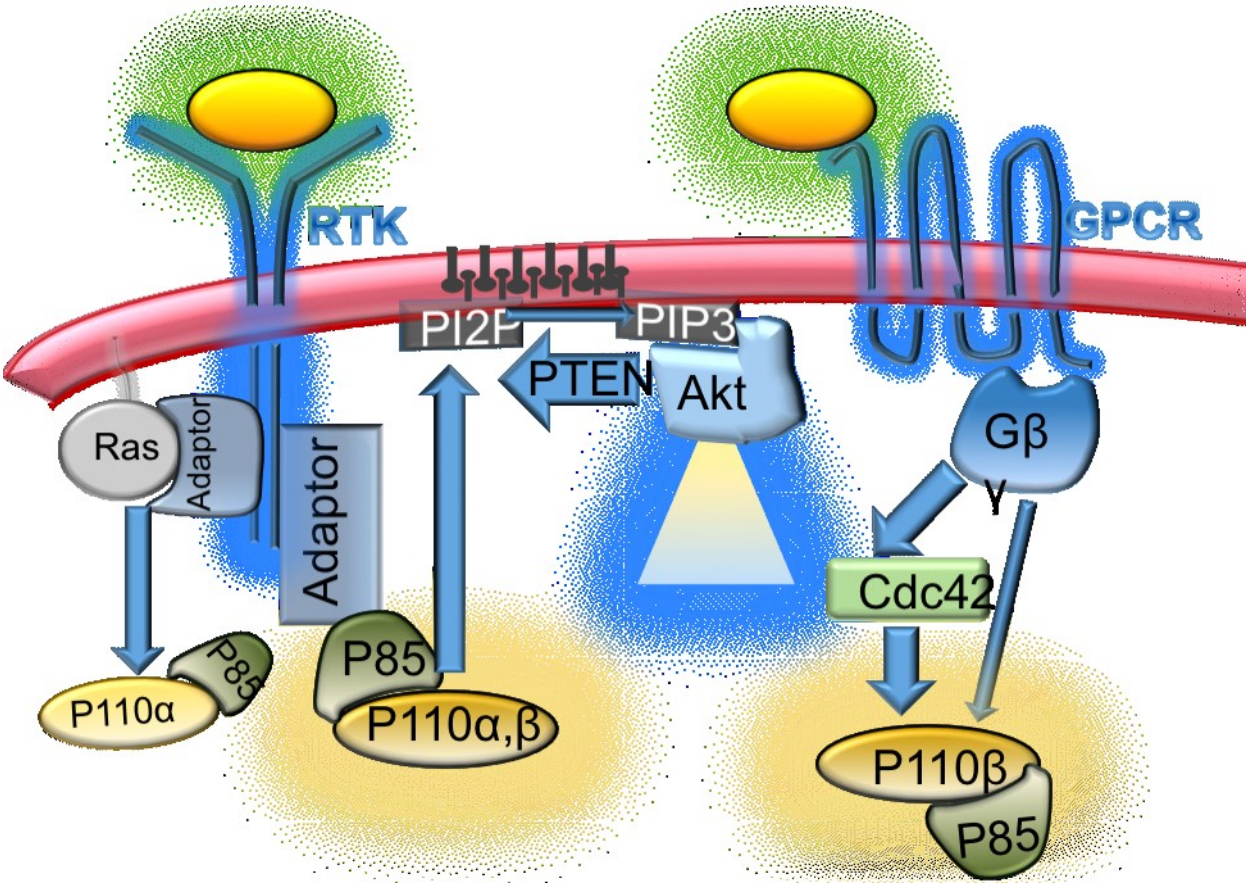

Figure 1. The PI3K/AKT pathway. Receptor tyrosine kinase (RTK) and G-protein coupled receptor (GPCR) activate PI3K, which transfers PIP2 to PIP3. PIP3 forms docking sites for Akt.

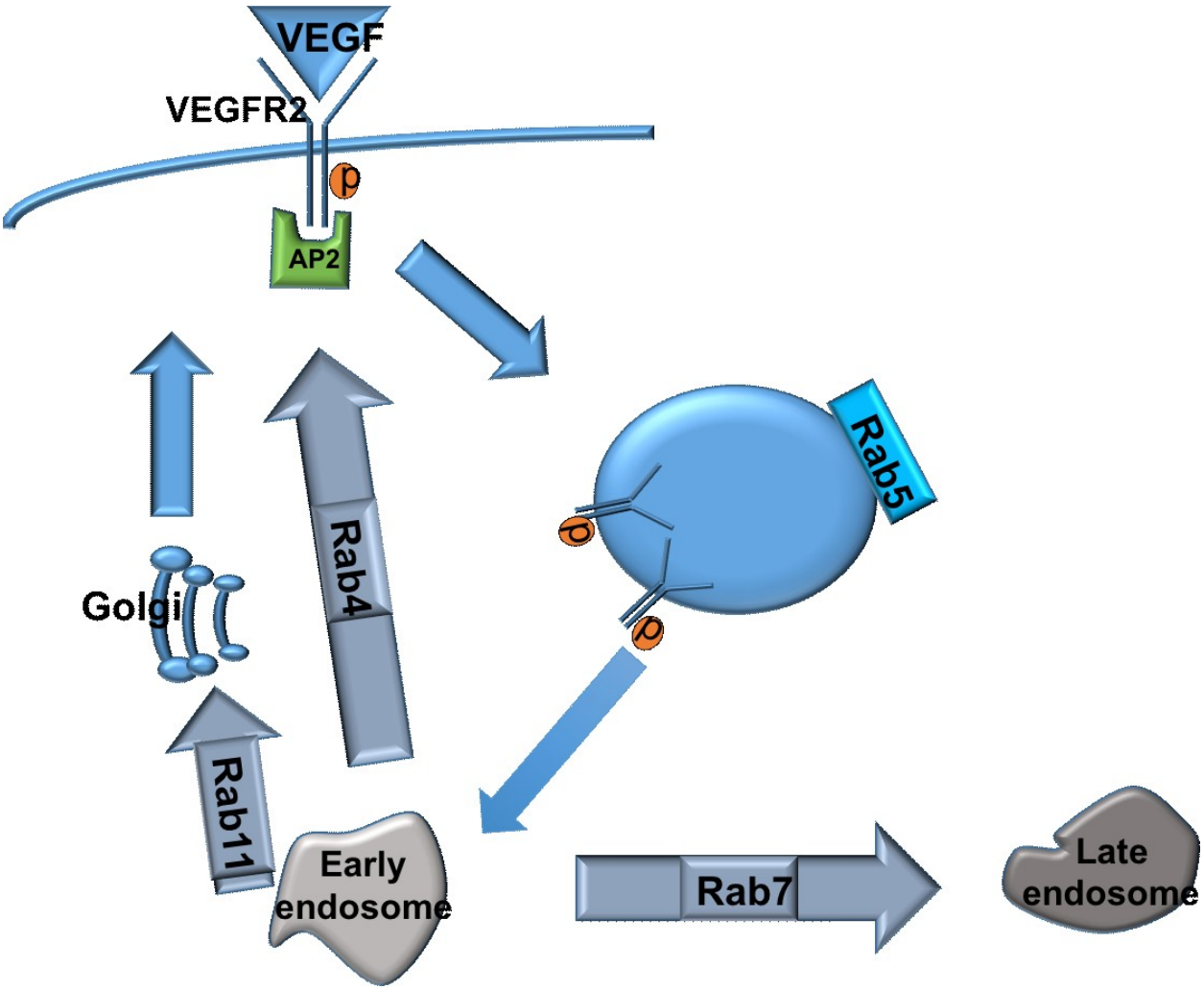

Figure 2. Trafficking of VEGFR2. VEGFR2 is endocytosed by a clarthin-mediated mechanism to Rab5 vesicles. Rab4 and 11 regulates VEGFR2 recycling pathway, whereas Rab7 regulates VEGFR2 degradation pathway.

Figure 3. The structure of FGD5. Zinc-finger domain (FYVE), Rho guanine exchange factor domain (Rho GEF) and pleckstrin homology domain (PH).

References

1. Carmeliet P, Jain RK. Angiogenesis in cancer and other diseases. *Nature*. 2000;407(6801):249-257.

2. Folkman J. Tumor angiogenesis: Therapeutic implications. *N Engl J Med*. 1971;285(21):1182-1186. doi: 10.1056/NEJM197111182852108.

3. Risau W. Mechanisms of angiogenesis. *Nature*. 1997;386(6626):671-674. doi: 10.1038/386671a0.

4. Ferguson JE,3rd, Kelley RW, Patterson C. Mechanisms of endothelial differentiation in embryonic vasculogenesis. *Arterioscler Thromb Vasc Biol*. 2005;25(11):2246-2254. doi: 01.ATV.0000183609.55154.44 [pii].

5. Risau W. Differentiation of endothelium. *FASEB J*. 1995;9(10):926-933.

6. Schmidt A, Brixius K, Bloch W. Endothelial precursor cell migration during vasculogenesis. *Circ Res*. 2007;101(2):125-136. doi: 101/2/125 [pii].

7. Douglas J, Poole TJ. Endothelial cell origin and migration in embryonic heart and cranial blood vessel development. *Anat Rec*. 1991;231(3):383-395.

8. Carmeliet P, Ferreira V, Breier G, et al. Abnormal blood vessel development and lethality in embryos lacking a single VEGF allele. *Nature*. 1996;380(6573):435-439. doi: 10.1038/380435a0.

9. Nagy JA, Dvorak AM, Dvorak HF. VEGF-A and the induction of pathological angiogenesis. *Annu.Rev.Pathol.Mech.Dis.* 2007;2:251-275.

10. Gerhardt H. VEGF and endothelial guidance in angiogenic sprouting. In: *VEGF in development.* Springer; 2008:68-78.

11. Carmeliet P, De Smet F, Loges S, Mazzone M. Branching morphogenesis and antiangiogenesis candidates: Tip cells lead the way. *Nature reviews Clinical oncology*. 2009;6(6):315-326.

12. van Hinsbergh VW, Koolwijk P. Endothelial sprouting and angiogenesis: Matrix metalloproteinases in the lead. *Cardiovasc Res*. 2008;78(2):203-212. doi: cvm102 [pii].

13. Small JV, Stradal T, Vignal E, Rottner K. The lamellipodium: Where motility begins. *Trends Cell Biol*. 2002;12(3):112-120.

14. Chien S. Mechanotransduction and endothelial cell homeostasis: The wisdom of the cell. *Am J Physiol Heart Circ Physiol*. 2007;292(3):H1209-24. doi: 01047.2006 [pii].

15. Gerhardt H, Golding M, Fruttiger M, et al. VEGF guides angiogenic sprouting utilizing endothelial tip cell filopodia. *J Cell Biol*. 2003;161(6):1163-1177. doi: 10.1083/jcb.200302047.

16. Siekmann AF, Lawson ND. Notch signalling limits angiogenic cell behaviour in developing zebrafish arteries. *Nature*. 2007;445(7129):781-784.

17. Gerhardt H, Ruhrberg C, Abramsson A, Fujisawa H, Shima D, Betsholtz C. Neuropilin-1 is required for endothelial tip cell guidance in the developing central nervous system. *Developmental Dynamics*. 2004;231(3):503-509.

18. Suchting S, Freitas C, le Noble F, et al. The notch ligand delta-like 4 negatively regulates endothelial tip cell formation and vessel branching. *Proc Natl Acad Sci U S A*. 2007;104(9):3225-3230. doi: 0611177104 [pii].

19. Hellström M, Phng L, Hofmann JJ, et al. Dll4 signalling through Notch1 regulates formation of tip cells during angiogenesis. *Nature*. 2007;445(7129):776-780.

20. Phng L, Potente M, Leslie JD, et al. Nrarp coordinates endothelial notch and wnt signaling to control vessel density in angiogenesis. *Developmental cell*. 2009;16(1):70-82.

21. Harrington LS, Sainson RC, Williams CK, et al. Regulation of multiple angiogenic pathways by Dll4 and notch in human umbilical vein endothelial cells. *Microvasc Res*. 2008;75(2):144-154.

22. Roca C, Adams RH. Regulation of vascular morphogenesis by notch signaling. *Genes Dev*. 2007;21(20):2511-2524. doi: 21/20/2511 [pii].

23. Ferrara N, Carver-Moore K, Chen H, et al. Heterozygous embryonic lethality induced by targeted inactivation of the VEGF gene. *Nature*. 1996;380(6573):439-442.

24. Jain RK. Normalization of tumor vasculature: An emerging concept in antiangiogenic therapy. *Science*. 2005;307(5706):58-62. doi: 10.1126/science.1104819.

25. Kurz H, Burri PH, Djonov VG. Angiogenesis and vascular remodeling by intussusception: From form to function. *News Physiol Sci*. 2003;18:65-70.

26. Djonov VG, Kurz H, Burri PH. Optimality in the developing vascular system: Branching remodeling by means of intussusception as an efficient adaptation mechanism. *Developmental dynamics*. 2002;224(4):391-402.

27. Djonov V, Baum O, Burri PH. Vascular remodeling by intussusceptive angiogenesis. *Cell Tissue Res*. 2003;314(1):107-117. doi: 10.1007/s00441-003-0784-3.

28. Burri PH, Tarek MR. A novel mechanism of capillary growth in the rat pulmonary microcirculation. *Anat Rec*. 1990;228(1):35-45.

29. Caduff JH, Fischer LC, Burri PH. Scanning electron microscope study of the developing microvasculature in the postnatal rat lung. *Anat Rec*. 1986;216(2):154-164. doi: 10.1002/ar.1092160207.

30. Burri PH, Hlushchuk R, Djonov V. Intussusceptive angiogenesis: Its emergence, its characteristics, and its significance. *Developmental Dynamics*. 2004;231(3):474-488.

31. PATAN S, ALVAREZ MJ, SCHITTNY JC, BURRI PH. Intussusceptive microvascular growth: A common alternative to capillary sprouting. *Arch Histol Cytol*. 1992;55(Suppl):65-75.

32. Jain RK. Normalizing tumor vasculature with anti-angiogenic therapy: A new paradigm for combination therapy. *Nat Med*. 2001;7(9):987-989.

33. Nagy JA, Chang SH, Shih SC, Dvorak AM, Dvorak HF. Heterogeneity of the tumor vasculature. *Semin Thromb Hemost*. 2010;36(3):321-331. doi: 10.1055/s-0030-1253454; 10.1055/s-0030-1253454.

34. Baluk P, Hashizume H, McDonald DM. Cellular abnormalities of blood vessels as targets in cancer. *Curr Opin Genet Dev*. 2005;15(1):102-111.

35. Mazzone M, Dettori D, Leite de Oliveira R, et al. Heterozygous deficiency of< i> PHD2 restores tumor oxygenation and inhibits metastasis via endothelial normalization. *Cell*. 2009;136(5):839-851.

36. Ozawa MG, Yao VJ, Chanthery YH, et al. Angiogenesis with pericyte abnormalities in a transgenic model of prostate carcinoma. *Cancer*. 2005;104(10):2104-2115.

37. Jain RK. Determinants of tumor blood flow: A review. *Cancer Res*. 1988;48(10):2641-2658.

38. Jain RK, Stylianopoulos T. Delivering nanomedicine to solid tumors. *Nature reviews clinical oncology*. 2010;7(11):653-664.

39. Carmeliet P, Jain RK. Principles and mechanisms of vessel normalization for cancer and other angiogenic diseases. *Nature reviews Drug discovery*. 2011;10(6):417-427.

40. Moeller BJ, Richardson RA, Dewhirst MW. Hypoxia and radiotherapy: Opportunities for improved outcomes in cancer treatment. *Cancer Metastasis Rev*. 2007;26(2):241-248.

41. Fukumura D, Duda DG, Munn LL, Jain RK. Tumor microvasculature and microenvironment: Novel insights through intravital imaging in Pre-Clinical models. *Microcirculation*. 2010;17(3):206-225.

42. Chung AS, Lee J, Ferrara N. Targeting the tumour vasculature: Insights from physiological angiogenesis. *Nature Reviews Cancer*. 2010;10(7):505-514.

43. Jain RK. Lessons from multidisciplinary translational trials on anti-angiogenic therapy of cancer. *Nature Reviews Cancer*. 2008;8(4):309-316.

44. Inoue M, Hager JH, Ferrara N, Gerber H, Hanahan D. VEGF-A has a critical, nonredundant role in angiogenic switching and pancreatic β cell carcinogenesis. *Cancer cell*. 2002;1(2):193-202.

45. Ferrara N, Kerbel RS. Angiogenesis as a therapeutic target. *Nature*. 2005;438(7070):967-974.

46. Shibuya M. Involvement of flt-1 (VEGF receptor-1) in cancer and preeclampsia. *Proc Japan Acad , Ser B*. 2011;87(4):167-178.

47. Shibuya M, Claesson-Welsh L. Signal transduction by VEGF receptors in regulation of angiogenesis and lymphangiogenesis. *Exp Cell Res*. 2006;312(5):549-560.

48. Alitalo K, Carmeliet P. Molecular mechanisms of lymphangiogenesis in health and disease. *Cancer cell*. 2002;1(3):219-227.

49. Ferrara N, Carver Moore K, Chen H, et al. Heterozygous embryonic lethality induced by targeted inactivation of the VEGF gene. . 1996.

50. Luttun A, Tjwa M, Moons L, et al. Revascularization of ischemic tissues by PlGF treatment, and inhibition of tumor angiogenesis, arthritis and atherosclerosis by anti-Flt1. *Nat Med*. 2002;8(8):831-840.

51. Aase K, von Euler G, Li X, et al. Vascular endothelial growth factor-B-deficient mice display an atrial conduction defect. *Circulation*. 2001;104(3):358-364.

52. Karkkainen MJ, Haiko P, Sainio K, et al. Vascular endothelial growth factor C is required for sprouting of the first lymphatic vessels from embryonic veins. *Nat Immunol*. 2004;5(1):74-80.

53. Heldin CH, Westermark B. Mechanism of action and in vivo role of platelet-derived growth factor. *Physiol Rev*. 1999;79(4):1283-1316.

54. Takahashi T, Yamaguchi S, Chida K, Shibuya M. A single autophosphorylation site on KDR/flk-1 is essential for VEGF-A-dependent activation of PLC-gamma and DNA synthesis in vascular endothelial cells. *EMBO J*. 2001;20(11):2768-2778. doi: 10.1093/emboj/20.11.2768 [doi].

55. Sakurai Y, Ohgimoto K, Kataoka Y, Yoshida N, Shibuya M. Essential role of flk-1 (VEGF receptor 2) tyrosine residue 1173 in vasculogenesis in mice. *Proc Natl Acad Sci U S A*. 2005;102(4):1076-1081. doi: 0404984102 [pii].

56. Holmqvist K, Cross MJ, Rolny C, et al. The adaptor protein shb binds to tyrosine 1175 in vascular endothelial growth factor (VEGF) receptor-2 and regulates VEGF-dependent cellular migration. *J Biol Chem*. 2004;279(21):22267-22275. doi: 10.1074/jbc.M312729200 [doi].

57. Warner AJ, Lopez-Dee J, Knight EL, Feramisco JR, Prigent SA. The shc-related adaptor protein, sck, forms a complex with the vascular-endothelial-growth-factor receptor KDR in transfected cells. *Biochem J*. 2000;347(Pt 2):501-509.

58. Sakai R, Henderson JT, O'Bryan JP, Elia AJ, Saxton TM, Pawson T. The mammalian ShcB and ShcC phosphotyrosine docking proteins function in the maturation of sensory and sympathetic neurons. *Neuron*. 2000;28(3):819-833.

59. Kroll J, Waltenberger J. The vascular endothelial growth factor receptor KDR activates multiple signal transduction pathways in porcine aortic endothelial cells. *J Biol Chem*. 1997;272(51):32521-32527.

60. Shu X, Wu W, Mosteller RD, Broek D. Sphingosine kinase mediates vascular endothelial growth factor-induced activation of ras and mitogen-activated protein kinases. *Mol Cell Biol*. 2002;22(22):7758-7768.

61. Matsumoto T, Bohman S, Dixelius J, et al. VEGF receptor-2 Y951 signaling and a role for the adapter molecule TSAd in tumor angiogenesis. *EMBO J*. 2005;24(13):2342-2353. doi: 7600709 [pii].

62. Zeng H, Sanyal S, Mukhopadhyay D. Tyrosine residues 951 and 1059 of vascular endothelial growth factor receptor-2 (KDR) are essential for vascular permeability factor/vascular

endothelial growth factor-induced endothelium migration and proliferation, respectively. *J Biol Chem*. 2001;276(35):32714-32719. doi: 10.1074/jbc.M103130200 [doi].

63. Weis M, Schlichting CL, Engleman EG, Cooke JP. Endothelial determinants of dendritic cell adhesion and migration: New implications for vascular diseases. *Arterioscler Thromb Vasc Biol*. 2002;22(11):1817-1823.

64. Abedi H, Zachary I. Vascular endothelial growth factor stimulates tyrosine phosphorylation and recruitment to new focal adhesions of focal adhesion kinase and paxillin in endothelial cells. *J Biol Chem*. 1997;272(24):15442-15451.

65. Le Boeuf F, Houle F, Huot J. Regulation of vascular endothelial growth factor receptor 2-mediated phosphorylation of focal adhesion kinase by heat shock protein 90 and src kinase activities. *J Biol Chem*. 2004;279(37):39175-39185. doi: 10.1074/jbc.M405493200 [doi].

66. Hart MJ, Callow MG, Souza B, Polakis P. IQGAP1, a calmodulin-binding protein with a rasGAP-related domain, is a potential effector for cdc42Hs. *EMBO J*. 1996;15(12):2997-3005.

67. Yamaoka-Tojo M, Ushio-Fukai M, Hilenski L, et al. IQGAP1, a novel vascular endothelial growth factor receptor binding protein, is involved in reactive oxygen species--dependent endothelial migration and proliferation. *Circ Res*. 2004;95(3):276-283. doi: 10.1161/01.RES.0000136522.58649.60 [doi].

68. Sawano A, Takahashi T, Yamaguchi S, Aonuma M, Shibuya M. Flt-1 but not KDR/flk-1 tyrosine kinase is a receptor for placenta growth factor, which is related to vascular endothelial growth factor. *Cell Growth Differ*. 1996;7(2):213-221.

69. Fong GH, Rossant J, Gertsenstein M, Breitman ML. Role of the flt-1 receptor tyrosine kinase in regulating the assembly of vascular endothelium. *Nature*. 1995;376(6535):66-70. doi: 10.1038/376066a0 [doi].

70. Hiratsuka S, Minowa O, Kuno J, Noda T, Shibuya M. Flt-1 lacking the tyrosine kinase domain is sufficient for normal development and angiogenesis in mice. *Proc Natl Acad Sci U S A*. 1998;95(16):9349-9354.

71. Katoh O, Tauchi H, Kawaishi K, Kimura A, Satow Y. Expression of the vascular endothelial growth factor (VEGF) receptor gene, KDR, in hematopoietic cells and inhibitory effect of VEGF on apoptotic cell death caused by ionizing radiation. *Cancer Res*. 1995;55(23):5687-5692.

72. Yang X, Cepko CL. Flk-1, a receptor for vascular endothelial growth factor (VEGF), is expressed by retinal progenitor cells. *J Neurosci*. 1996;16(19):6089-6099.

73. Olsson A, Dimberg A, Kreuger J, Claesson-Welsh L. VEGF receptor signalling? in control of vascular function. *Nature reviews Molecular cell biology*. 2006;7(5):359-371.

74. Shalaby F, Rossant J, Yamaguchi TP, et al. Failure of blood-island formation and vasculogenesis in flk-1-deficient mice. *Nature*. 1995;376(6535):62-66.

75. Holmes K, Roberts OL, Thomas AM, Cross MJ. Vascular endothelial growth factor receptor-2: Structure, function, intracellular signalling and therapeutic inhibition. *Cell Signal*. 2007;19(10):2003-2012.

76. Liu P, Cheng H, Roberts TM, Zhao JJ. Targeting the phosphoinositide 3-kinase pathway in cancer. *Nature reviews Drug discovery*. 2009;8(8):627-644.

77. Geng L, Tan J, Himmelfarb E, et al. A specific antagonist of the p110delta catalytic component of phosphatidylinositol 3'-kinase, IC486068, enhances radiation-induced tumor vascular destruction. *Cancer Res*. 2004;64(14):4893-4899. doi: 10.1158/0008-5472.CAN-03-3955.

78. Puri KD, Doggett TA, Douangpanya J, et al. Mechanisms and implications of phosphoinositide 3-kinase delta in promoting neutrophil trafficking into inflamed tissue. *Blood*. 2004;103(9):3448-3456. doi: 10.1182/blood-2003-05-1667 [doi].

79. Vanhaesebroeck B, Guillermet-Guibert J, Graupera M, Bilanges B. The emerging mechanisms of isoform-specific PI3K signalling. *Nature reviews Molecular cell biology*. 2010;11(5):329-341.

80. Okkenhaug K, Bilancio A, Farjot G, et al. Impaired B and T cell antigen receptor signaling in p110delta PI 3-kinase mutant mice. *Science*. 2002;297(5583):1031-1034. doi: 10.1126/science.1073560.

81. Rodriguez-Viciana P, Warne PH, Dhand R, et al. Phosphatidylinositol-3-OH kinase direct target of ras. . 1994.

82. Rodriguez-Viciana P, Warne PH, Vanhaesebroeck B, Waterfield MD, Downward J. Activation of phosphoinositide 3-kinase by interaction with ras and by point mutation. *EMBO J.* 1996;15(10):2442-2451.

83. Igarashi J, Michel T. Sphingosine 1-phosphate and isoform-specific activation of phosphoinositide 3-kinase beta. evidence for divergence and convergence of receptor-regulated

endothelial nitric-oxide synthase signaling pathways. *J Biol Chem*. 2001;276(39):36281-36288. doi: 10.1074/jbc.M105628200 [doi].

84. Ciraolo E, Iezzi M, Marone R, et al. Phosphoinositide 3-kinase p110beta activity: Key role in metabolism and mammary gland cancer but not development. *Sci Signal*. 2008;1(36):ra3. doi: 10.1126/scisignal.1161577; 10.1126/scisignal.1161577.

85. Guillermet-Guibert J, Bjorklof K, Salpekar A, et al. The p110beta isoform of phosphoinositide 3-kinase signals downstream of G protein-coupled receptors and is functionally redundant with p110gamma. *Proc Natl Acad Sci U S A*. 2008;105(24):8292-8297. doi: 10.1073/pnas.0707761105; 10.1073/pnas.0707761105.

86. Fritsch R, de Krijger I, Fritsch K, et al. RAS and RHO families of GTPases directly regulate distinct phosphoinositide 3-kinase isoforms. *Cell*. 2013;153(5):1050-1063.

87. Li J, Yen C, Liaw D, et al. PTEN, a putative protein tyrosine phosphatase gene mutated in human brain, breast, and prostate cancer. *Science*. 1997;275(5308):1943-1947.

88. Suzuki A, Hamada K, Sasaki T, Mak TW, Nakano T. Role of PTEN/PI3K pathway in endothelial cells. *Biochem Soc Trans*. 2007;35(Pt 2):172-176. doi: BST0350172 [pii].

89. Hollander MC, Blumenthal GM, Dennis PA. PTEN loss in the continuum of common cancers, rare syndromes and mouse models. *Nature Reviews Cancer*. 2011;11(4):289-301.

90. Yuan TL, Choi HS, Matsui A, et al. Class 1A PI3K regulates vessel integrity during development and tumorigenesis. *Proc Natl Acad Sci U S A*. 2008;105(28):9739-9744. doi: 10.1073/pnas.0804123105; 10.1073/pnas.0804123105.

91. Graupera M, Guillermet-Guibert J, Foukas LC, et al. Angiogenesis selectively requires the p110alpha isoform of PI3K to control endothelial cell migration. *Nature*. 2008;453(7195):662-666. doi: 10.1038/nature06892; 10.1038/nature06892.

92. Bi L, Okabe I, Bernard DJ, Wynshaw-Boris A, Nussbaum RL. Proliferative defect and embryonic lethality in mice homozygous for a deletion in the p110alpha subunit of phosphoinositide 3-kinase. *J Biol Chem*. 1999;274(16):10963-10968.

93. Bi L, Okabe I, Bernard DJ, Nussbaum RL. Early embryonic lethality in mice deficient in the p110ß catalytic subunit of PI 3-kinase. *Mammalian Genome*. 2002;13(3):169-172.

94. Haddad G, Zhabyeyev P, Farhan M, et al. Phosphoinositide 3-kinase beta mediates microvascular endothelial repair of thrombotic microangiopathy. *Blood*. 2014;124(13):2142-2149. doi: 10.1182/blood-2014-02-557975; 10.1182/blood-2014-02-557975.

95. Wojtalla A, Fischer B, Kotelevets N, et al. Targeting the phosphoinositide 3-kinase p110-alpha isoform impairs cell proliferation, survival, and tumor growth in small cell lung cancer. *Clin Cancer Res*. 2012. doi: 10.1158/1078-0432.CCR-12-1138.

96. Manning BD, Cantley LC. AKT/PKB signaling: Navigating downstream. *Cell*. 2007;129(7):1261-1274.

97. Chen J, Somanath PR, Razorenova O, et al. Akt1 regulates pathological angiogenesis, vascular maturation and permeability in vivo. *Nat Med*. 2005;11(11):1188-1196.

98. Peng XD, Xu PZ, Chen ML, et al. Dwarfism, impaired skin development, skeletal muscle atrophy, delayed bone development, and impeded adipogenesis in mice lacking Akt1 and Akt2. *Genes Dev*. 2003;17(11):1352-1365. doi: 10.1101/gad.1089403 [doi].

99. Kunz J, Henriquez R, Schneider U, Deuter-Reinhard M, Movva NR, Hall MN. Target of rapamycin in yeast, TOR2, is an essential phosphatidylinositol kinase homolog required for G< sub> 1 progression. *Cell*. 1993;73(3):585-596.

100. Keith CT, Schreiber SL. PIK-related kinases: DNA repair, recombination, and cell cycle checkpoints. *SCIENCE-NEW YORK THEN WASHINGTON-*. 1995:50-50.

101. Hara K, Maruki Y, Long X, et al. Raptor, a binding partner of target of rapamycin (TOR), mediates TOR action. *Cell*. 2002;110(2):177-189.

102. Sancak Y, Thoreen CC, Peterson TR, et al. PRAS40 is an insulin-regulated inhibitor of the mTORC1 protein kinase. *Mol Cell*. 2007;25(6):903-915.

103. Sarbassov DD, Ali SM, Kim D, et al. Rictor, a novel binding partner of mTOR, defines a rapamycin-insensitive and raptor-independent pathway that regulates the cytoskeleton. *Current biology*. 2004;14(14):1296-1302.

104. Frias MA, Thoreen CC, Jaffe JD, et al. mSin1 is necessary for akt/PKB phosphorylation, and its isoforms define three distinct mTORC2s. *Current Biology*. 2006;16(18):1865-1870.

105. Foster DA, Toschi A. Targeting mTOR with rapamycin: One dose does not fit all. *Cell Cycle*. 2009;8(7):1026-1029.

106. Guertin D, Stevens D, Thoreen C, Burds A, Kalaany N. J. 1 moffat, M. brown, KJ fitzgerald, and DM sabatini. 2006. ablation in mice of 2 the mTORC components raptor, rictor, or mLST8 reveals that mTORC2 is required 3 for signaling to akt-FOXO and PKCalpha, but not S6K1. *Dev.Cell*. ;11:859-871.

107. O'Reilly KE, Rojo F, She Q, et al. mTOR inhibition induces upstream receptor tyrosine kinase signaling and activates akt. *Cancer Res*. 2006;66(3):1500-1508.

108. Carver BS, Chapinski C, Wongvipat J, et al. Reciprocal feedback regulation of PI3K and androgen receptor signaling in PTEN-deficient prostate cancer. *Cancer cell*. 2011;19(5):575-586.

109. Jopling HM, Odell AF, Hooper NM, Zachary IC, Walker JH, Ponnambalam S. Rab GTPase regulation of VEGFR2 trafficking and signaling in endothelial cells. *Arterioscler Thromb Vasc Biol*. 2009;29(7):1119-1124. doi: 10.1161/ATVBAHA.109.186239; 10.1161/ATVBAHA.109.186239.

110. Miaczynska M, Pelkmans L, Zerial M. Not just a sink: Endosomes in control of signal transduction. *Curr Opin Cell Biol*. 2004;16(4):400-406. doi: 10.1016/j.ceb.2004.06.005.

111. Ballmer-Hofer K, Andersson AE, Ratcliffe LE, Berger P. Neuropilin-1 promotes VEGFR-2 trafficking through Rab11 vesicles thereby specifying signal output. *Blood*. 2011;118(3):816-826. doi: 10.1182/blood-2011-01-328773; 10.1182/blood-2011-01-328773.

112. Eichmann A, Simons M. VEGF signaling inside vascular endothelial cells and beyond. *Curr Opin Cell Biol*. 2012;24(2):188-193.

113. Lanahan AA, Hermans K, Claes F, et al. VEGF receptor 2 endocytic trafficking regulates arterial morphogenesis. *Developmental cell*. 2010;18(5):713-724.

114. Lampugnani MG, Orsenigo F, Gagliani MC, Tacchetti C, Dejana E. Vascular endothelial cadherin controls VEGFR-2 internalization and signaling from intracellular compartments. *J Cell Biol*. 2006;174(4):593-604. doi: 10.1083/jcb.200602080.

115. van Lessen M, Nakayama M, Kato K, Kim JM, Kaibuchi K, Adams RH. Regulation of vascular endothelial growth factor receptor function in angiogenesis by numb and numb-like. *Arterioscler Thromb Vasc Biol*. 2015;35(8):1815-1825. doi: 10.1161/ATVBAHA.115.305473 [doi].

116. Smith GA, Fearnley GW, Abdul-Zani I, et al. VEGFR2 trafficking, signaling and proteolysis is regulated by the ubiquitin isopeptidase USP8. *Traffic*. 2015.

117. Meyer RD, Srinivasan S, Singh AJ, Mahoney JE, Gharahassanlou KR, Rahimi N. PEST motif serine and tyrosine phosphorylation controls vascular endothelial growth factor receptor 2 stability and downregulation. *Mol Cell Biol*. 2011;31(10):2010-2025. doi: 10.1128/MCB.01006-10 [doi].

118. Srinivasan S, Meyer RD, Lugo R, Rahimi N. Identification of PDCL3 as a novel chaperone protein involved in the generation of functional VEGF receptor 2. *J Biol Chem*. 2013;288(32):23171-23181. doi: 10.1074/jbc.M113.473173 [doi].

119. Folkman J, Szabo S, Stovroff M, McNeil P, Li W, Shing Y. Duodenal ulcer. discovery of a new mechanism and development of angiogenic therapy that accelerates healing. *Ann Surg*. 1991;214(4):414-25; discussion 426-7.

120. Hull MA, Cullen DJ, Hudson N, Hawkey CJ. Basic fibroblast growth factor treatment for non-steroidal anti-inflammatory drug associated gastric ulceration. *Gut*. 1995;37(5):610-612.

121. Sellke FW, Laham RJ, Edelman ER, Pearlman JD, Simons M. Therapeutic angiogenesis with basic fibroblast growth factor: Technique and early results. *Ann Thorac Surg*. 1998;65(6):1540-1544.

122. Li WW, Talcott KE, Zhai AW, Kruger EA, Li VW. The role of therapeutic angiogenesis in tissue repair and regeneration. *Adv Skin Wound Care*. 2005;18(9):491-500.

123. Lee S, Won J, Lee H, et al. Angiopoietin-1 protects heart against ischemia/reperfusion injury through VE-cadherin dephosphorylation and myocardiac integrin-β1/ERK/caspase-9 phosphorylation cascade. *Molecular Medicine*. 2011;17(9):1095.

124. Vale PR, Losordo DW, Symes JF, Isner JM. Growth factors for therapeutic angiogenesis in cardiovascular diseases. *Rev Esp Cardiol*. 2001;54(10):1210-1224.

125. Simons M, Bonow RO, Chronos NA, et al. Clinical trials in coronary angiogenesis: Issues, problems, consensus: An expert panel summary. *Circulation*. 2000;102(11):E73-86.

126. Sleijfer S, Ray-Coquard I, Papai Z, et al. Pazopanib, a multikinase angiogenesis inhibitor, in patients with relapsed or refractory advanced soft tissue sarcoma: A phase II study from the european organisation for research and treatment of cancer-soft tissue and bone sarcoma group

(EORTC study 62043). *J Clin Oncol*. 2009;27(19):3126-3132. doi: 10.1200/JCO.2008.21.3223 [doi].

127. Sandler A, Herbst R. Combining targeted agents: Blocking the epidermal growth factor and vascular endothelial growth factor pathways. *Clin Cancer Res*. 2006;12(14 Pt 2):4421s-4425s. doi: 12/14/4421s [pii].

128. Shih T, Lindley C. Bevacizumab: An angiogenesis inhibitor for the treatment of solid malignancies. *Clin Ther*. 2006;28(11):1779-1802.

129. Gotink KJ, Verheul HM. Anti-angiogenic tyrosine kinase inhibitors: What is their mechanism of action? *Angiogenesis*. 2010;13(1):1-14.

130. Andreoli CM, Miller JW. Anti-vascular endothelial growth factor therapy for ocular neovascular disease. *Curr Opin Ophthalmol*. 2007;18(6):502-508. doi: 10.1097/ICU.0b013e3282f0ca54 [doi].

131. Jager RD, Mieler WF, Miller JW. Age-related macular degeneration. *N Engl J Med*. 2008;358(24):2606-2617.

132. Hussain RM, Harris A, Siesky B, Yung C, Ehrlich R, Prall R. The effect of pegaptanib (macugen®) injection on retinal and retrobulbar blood flow in retinal ischaemic diseases. *Acta Ophthalmol*. 2015;93(5):e399-e400.

133. Krebs I, Schmetterer L, Boltz A, et al. A randomised double-masked trial comparing the visual outcome after treatment with ranibizumab or bevacizumab in patients with neovascular

age-related macular degeneration. *Br J Ophthalmol*. 2013;97(3):266-271. doi: 10.1136/bjophthalmol-2012-302391 [doi].

134. Dado DV. Vascular birthmarks, hemangiomas and malformations. *Ann Plast Surg*. 1989;23(1):91.

135. Haggstrom AN, Drolet BA, Baselga E, et al. Prospective study of infantile hemangiomas: Clinical characteristics predicting complications and treatment. *Pediatrics*. 2006;118(3):882-887. doi: 118/3/882 [pii].

136. Pope E, Krafchik BR, Macarthur C, et al. Oral versus high-dose pulse corticosteroids for problematic infantile hemangiomas: A randomized, controlled trial. *Pediatrics*. 2007;119(6):e1239-47. doi: peds.2006-2962 [pii].

137. White CW, Sondheimer HM, Crouch EC, Wilson H, Fan LL. Treatment of pulmonary hemangiomatosis with recombinant interferon alfa-2a. *N Engl J Med*. 1989;320(18):1197-1200.

138. Ezekowitz RAB, Mulliken JB, Folkman J. Interferon alfa-2a therapy for life-threatening hemangiomas of infancy. *N Engl J Med*. 1992;326(22):1456-1463.

139. Alibaz-Oner F, Karadeniz A, Ylmaz S, et al. Behcet disease with vascular involvement: Effects of different therapeutic regimens on the incidence of new relapses. *Medicine (Baltimore)*. 2015;94(6):e494. doi: 10.1097/MD.0000000000000494 [doi].

140. Elshabrawy HA, Chen Z, Volin MV, Ravella S, Virupannavar S, Shahrara S. The pathogenic role of angiogenesis in rheumatoid arthritis. *Angiogenesis*. 2015;18(4):433-448.

141. Folkman J. Angiogenesis and angiogenesis inhibition: An overview. In: *Regulation of angiogenesis.* Springer; 1997:1-8.

142. Battegay E. Angiogenesis: Mechanistic insights, neovascular diseases, and therapeutic prospects. *Journal of Molecular Medicine*. 1995;73(7):333-346.

143. Peacock DJ, Banquerigo ML, Brahn E. Angiogenesis inhibition suppresses collagen arthritis. *J Exp Med*. 1992;175(4):1135-1138.

144. Paulus HE. Minocycline treatment of rheumatoid arthritis. *Ann Intern Med*. 1995;122(2):147-148.

145. Jain RK. Antiangiogenic therapy for cancer: Current and emerging concepts. *Oncology (Williston Park)*. 2005;19(4 Suppl 3):7-16.

146. Saltz LB, Lenz HJ, Kindler HL, et al. Randomized phase II trial of cetuximab, bevacizumab, and irinotecan compared with cetuximab and bevacizumab alone in irinotecan-refractory colorectal cancer: The BOND-2 study. *J Clin Oncol*. 2007;25(29):4557-4561. doi: 10.1200/JCO.2007.12.0949.

147. Kindler H, Niedzwiecki D, Hollis D, et al. A double-blind, placebo-controlled, randomized phase III trial of gemcitabine plus bevacizumab versus gemcitabine plus placebo in patients with advanced pancreatic cancer: A preliminary analysis of cancer and leukemia group B (CALGB) 80303. *J Clin Oncol*. 2007;25(18S):4508.

148. Miller KD, Sweeney CJ, Sledge Jr GW. Can tumor angiogenesis be inhibited without resistance? In: *Mechanisms of angiogenesis.* Springer; 2005:95-112.

149. Casanovas O, Hicklin DJ, Bergers G, Hanahan D. Drug resistance by evasion of antiangiogenic targeting of VEGF signaling in late-stage pancreatic islet tumors. *Cancer cell*. 2005;8(4):299-309.

150. Blouw B, Song H, Tihan T, et al. The hypoxic response of tumors is dependent on their microenvironment. *Cancer cell*. 2003;4(2):133-146.

151. Kerbel RS. Therapeutic implications of intrinsic or induced angiogenic growth factor redundancy in tumors revealed. *Cancer cell*. 2005;8(4):269-271.

152. Rubenstein JL, Kim J, Ozawa T, et al. Anti-VEGF antibody treatment of glioblastoma prolongs survival but results in increased vascular cooption. *Neoplasia*. 2000;2(4):306-314.

153. Relf M, LeJeune S, Scott PA, et al. Expression of the angiogenic factors vascular endothelial cell growth factor, acidic and basic fibroblast growth factor, tumor growth factor beta-1, platelet-derived endothelial cell growth factor, placenta growth factor, and pleiotrophin in human primary breast cancer and its relation to angiogenesis. *Cancer Res*. 1997;57(5):963-969.

154. Batchelor TT, Sorensen AG, di Tomaso E, et al. AZD2171, a pan-VEGF receptor tyrosine kinase inhibitor, normalizes tumor vasculature and alleviates edema in glioblastoma patients. *Cancer cell*. 2007;11(1):83-95.

155. Bertolini F, Mancuso P, Shaked Y, Kerbel RS. Molecular and cellular biomarkers for angiogenesis in clinical oncology. *Drug Discov Today*. 2007;12(19):806-812.

156. Bertolini F, Shaked Y, Mancuso P, Kerbel RS. The multifaceted circulating endothelial cell in cancer: Towards marker and target identification. *Nature Reviews Cancer*. 2006;6(11):835-845.

157. Bocci G, Man S, Green SK, et al. Increased plasma vascular endothelial growth factor (VEGF) as a surrogate marker for optimal therapeutic dosing of VEGF receptor-2 monoclonal antibodies. *Cancer Res*. 2004;64(18):6616-6625. doi: 10.1158/0008-5472.CAN-04-0401.

158. Xu L, Duda DG, di Tomaso E, et al. Direct evidence that bevacizumab, an anti-VEGF antibody, up-regulates SDF1alpha, CXCR4, CXCL6, and neuropilin 1 in tumors from patients with rectal cancer. *Cancer Res*. 2009;69(20):7905-7910. doi: 10.1158/0008-5472.CAN-09-2099; 10.1158/0008-5472.CAN-09-2099.

159. Batchelor TT, Duda DG, di Tomaso E, et al. Phase II study of cediranib, an oral pan-vascular endothelial growth factor receptor tyrosine kinase inhibitor, in patients with recurrent glioblastoma. *J Clin Oncol*. 2010;28(17):2817-2823. doi: 10.1200/JCO.2009.26.3988; 10.1200/JCO.2009.26.3988.

160. Balkwill F. Cancer and the chemokine network. *Nature Reviews Cancer*. 2004;4(7):540-550.

161. Sciumè G, Santoni A, Bernardini G. Chemokines and glioma: Invasion and more. *J Neuroimmunol*. 2010;224(1):8-12.

162. Rempel SA, Dudas S, Ge S, Gutierrez JA. Identification and localization of the cytokine SDF1 and its receptor, CXC chemokine receptor 4, to regions of necrosis and angiogenesis in human glioblastoma. *Clin Cancer Res*. 2000;6(1):102-111.

163. Duda DG, Kozin SV, Kirkpatrick ND, Xu L, Fukumura D, Jain RK. CXCL12 (SDF1alpha)-CXCR4/CXCR7 pathway inhibition: An emerging sensitizer for anticancer therapies? *Clin Cancer Res*. 2011;17(8):2074-2080. doi: 10.1158/1078-0432.CCR-10-2636; 10.1158/1078-0432.CCR-10-2636.

164. Bleul CC, Farzan M, Choe H, et al. The lymphocyte chemoattractant SDF-1 is a ligand for LESTR/fusin and blocks HIV-1 entry. . 1996.

165. Tashiro K, Tada H, Heilker R, Shirozu M, Nakano T, Honjo T. Signal sequence trap: A cloning strategy for secreted proteins and type I membrane proteins. *Science*. 1993;261(5121):600-603.

166. Nagasawa T, Kikutani H, Kishimoto T. Molecular cloning and structure of a pre-B-cell growth-stimulating factor. *Proc Natl Acad Sci U S A*. 1994;91(6):2305-2309.

167. Oberlin E, Amara A. The CXC chemokine SDF-1 is the ligand for LESTR/fusin and prevents infection by T-cell-line-adapted HIV-1. . 1996.

168. Aiuti A, Webb IJ, Bleul C, Springer T, Gutierrez-Ramos JC. The chemokine SDF-1 is a chemoattractant for human CD34+ hematopoietic progenitor cells and provides a new mechanism to explain the mobilization of CD34+ progenitors to peripheral blood. *J Exp Med*. 1997;185(1):111-120.

169. Lyden D, Hattori K, Dias S, et al. Impaired recruitment of bone-marrow–derived endothelial and hematopoietic precursor cells blocks tumor angiogenesis and growth. *Nat Med*. 2001;7(11):1194-1201.

170. Nagasawa T, Hirota S, Tachibana K, et al. Defects of B-cell lymphopoiesis and bone-marrow myelopoiesis in mice lacking the CXC chemokine PBSF/SDF-1. *Nature*. 1996;382(6592):635-638.

171. Forster R, Kremmer E, Schubel A, et al. Intracellular and surface expression of the HIV-1 coreceptor CXCR4/fusin on various leukocyte subsets: Rapid internalization and recycling upon activation. *J Immunol*. 1998;160(3):1522-1531.

172. Delézay O, Koch N, Yahi N, et al. Co-expression of CXCR4/fusin and galactosylceramide in the human intestinal epithelial cell line HT-29. *AIDS*. 1997;11(11):1311-1318.

173. Volin MV, Joseph L, Shockley MS, Davies PF. Chemokine receptor CXCR4 expression in endothelium. *Biochem Biophys Res Commun*. 1998;242(1):46-53.

174. Gupta SK, Lysko PG, Pillarisetti K, Ohlstein E, Stadel JM. Chemokine receptors in human endothelial cells. functional expression of CXCR4 and its transcriptional regulation by inflammatory cytokines. *J Biol Chem*. 1998;273(7):4282-4287.

175. Feil C, Augustin HG. Endothelial cells differentially express functional CXC-chemokine receptor-4 (CXCR-4/fusin) under the control of autocrine activity and exogenous cytokines. *Biochem Biophys Res Commun*. 1998;247(1):38-45.

176. Stratman AN, Davis MJ, Davis GE. VEGF and FGF prime vascular tube morphogenesis and sprouting directed by hematopoietic stem cell cytokines. *Blood*. 2011;117(14):3709-3719. doi: 10.1182/blood-2010-11-316752; 10.1182/blood-2010-11-316752.

177. Unoki N, Murakami T, Nishijima K, Ogino K, van Rooijen N, Yoshimura N. SDF-1/CXCR4 contributes to the activation of tip cells and microglia in retinal angiogenesis. *Invest Ophthalmol Vis Sci*. 2010;51(7):3362-3371. doi: 10.1167/iovs.09-4978; 10.1167/iovs.09-4978.

178. Ara T, Tokoyoda K, Okamoto R, Koni PA, Nagasawa T. The role of CXCL12 in the organ-specific process of artery formation. *Blood*. 2005;105(8):3155-3161. doi: 2004-07-2563 [pii].

179. Lima e Silva R, Shen J, Hackett SF, et al. The SDF-1/CXCR4 ligand/receptor pair is an important contributor to several types of ocular neovascularization. *FASEB J*. 2007;21(12):3219-3230. doi: fj.06-7359com [pii].

180. Salcedo R, Wasserman K, Young HA, et al. Vascular endothelial growth factor and basic fibroblast growth factor induce expression of CXCR4 on human endothelial cells: In vivo neovascularization induced by stromal-derived factor-1α. *The American journal of pathology*. 1999;154(4):1125-1135.

181. Kryczek I, Lange A, Mottram P, et al. CXCL12 and vascular endothelial growth factor synergistically induce neoangiogenesis in human ovarian cancers. *Cancer Res*. 2005;65(2):465-472.

182. Hiratsuka S, Duda DG, Huang Y, et al. C-X-C receptor type 4 promotes metastasis by activating p38 mitogen-activated protein kinase in myeloid differentiation antigen (gr-1)-positive

cells. *Proc Natl Acad Sci U S A*. 2011;108(1):302-307. doi: 10.1073/pnas.1016917108; 10.1073/pnas.1016917108.

183. Rubin JB, Kung AL, Klein RS, et al. A small-molecule antagonist of CXCR4 inhibits intracranial growth of primary brain tumors. *Proc Natl Acad Sci U S A*. 2003;100(23):13513-13518. doi: 10.1073/pnas.2235846100.

184. Porvasnik S, Sakamoto N, Kusmartsev S, et al. Effects of CXCR4 antagonist CTCE-9908 on prostate tumor growth. *Prostate*. 2009;69(13):1460-1469.

185. Kozin SV, Kamoun WS, Huang Y, Dawson MR, Jain RK, Duda DG. Recruitment of myeloid but not endothelial precursor cells facilitates tumor regrowth after local irradiation. *Cancer Res*. 2010;70(14):5679-5685. doi: 10.1158/0008-5472.CAN-09-4446; 10.1158/0008-5472.CAN-09-4446.

186. Kioi M, Vogel H, Schultz G, Hoffman RM, Harsh GR, Brown JM. Inhibition of vasculogenesis, but not angiogenesis, prevents the recurrence of glioblastoma after irradiation in mice. *J Clin Invest*. 2010;120(3):694-705. doi: 10.1172/JCI40283; 10.1172/JCI40283.

187. Redjal N, Chan JA, Segal RA, Kung AL. CXCR4 inhibition synergizes with cytotoxic chemotherapy in gliomas. *Clin Cancer Res*. 2006;12(22):6765-6771. doi: 10.1158/1078-0432.CCR-06-1372.

188. Devic E, Rizzoti K, Bodin S, Knibiehler B, Audigier Y. Amino acid sequence and embryonic expression of msr/apj, the mouse homolog of XenopusX-msr and human APJ. *Mech Dev*. 1999;84(1):199-203.

189. O'Dowd BF, Heiber M, Chan A, et al. A human gene that shows identity with the gene encoding the angiotensin receptor is located on chromosome 11. *Gene*. 1993;136(1-2):355-360.

190. Fredriksson R, Lagerstrom MC, Lundin LG, Schioth HB. The G-protein-coupled receptors in the human genome form five main families. phylogenetic analysis, paralogon groups, and fingerprints. *Mol Pharmacol*. 2003;63(6):1256-1272. doi: 10.1124/mol.63.6.1256 [doi].

191. Tatemoto K, Hosoya M, Habata Y, et al. Isolation and characterization of a novel endogenous peptide ligand for the human APJ receptor. *Biochem Biophys Res Commun*. 1998;251(2):471-476.

192. Scott IC, Masri B, D'Amico LA, et al. The g protein-coupled receptor agtrl1b regulates early development of myocardial progenitors. *Developmental cell*. 2007;12(3):403-413.

193. Jaffredo T, Gautier R, Brajeul V, Dieterlen-Lievre F. Tracing the progeny of the aortic hemangioblast in the avian embryo. *Dev Biol*. 2000;224(2):204-214.

194. Mandal L, Banerjee U, Hartenstein V. Evidence for a fruit fly hemangioblast and similarities between lymph-gland hematopoiesis in fruit fly and mammal aorta-gonadal-mesonephros mesoderm. *Nat Genet*. 2004;36(9):1019-1023.

195. Cox CM, D'Agostino SL, Miller MK, Heimark RL, Krieg PA. Apelin, the ligand for the endothelial G-protein-coupled receptor, APJ, is a potent angiogenic factor required for normal vascular development of the frog embryo. *Dev Biol*. 2006;296(1):177-189.

196. Sorli SC, Van den Berghe L, Masri B, Knibiehler B, Audigier Y. Therapeutic potential of interfering with apelin signalling. *Drug Discov Today*. 2006;11(23):1100-1106.

197. Sorli SC, Le Gonidec S, Knibiehler B, Audigier Y. Apelin is a potent activator of tumour neoangiogenesis. *Oncogene*. 2007;26(55):7692-7699.

198. Tatemoto K, Takayama K, Zou M, et al. The novel peptide apelin lowers blood pressure via a nitric oxide-dependent mechanism. *Regul Pept*. 2001;99(2):87-92.

199. Lee DK, Cheng R, Nguyen T, et al. Characterization of apelin, the ligand for the APJ receptor. *J Neurochem*. 2000;74(1):34-41.

200. Szokodi I, Tavi P, Foldes G, et al. Apelin, the novel endogenous ligand of the orphan receptor APJ, regulates cardiac contractility. *Circ Res*. 2002;91(5):434-440.

201. Kasai A, Shintani N, Kato H, et al. Retardation of retinal vascular development in apelin-deficient mice. *Arterioscler Thromb Vasc Biol*. 2008;28(10):1717-1722. doi: 10.1161/ATVBAHA.108.163402 [doi].

202. del Toro R, Prahst C, Mathivet T, et al. Identification and functional analysis of endothelial tip cell-enriched genes. *Blood*. 2010;116(19):4025-4033. doi: 10.1182/blood-2010-02-270819; 10.1182/blood-2010-02-270819.

203. Kunduzova O, Alet N, Delesque-Touchard N, et al. Apelin/APJ signaling system: A potential link between adipose tissue and endothelial angiogenic processes. *FASEB J*. 2008;22(12):4146-4153. doi: 10.1096/fj.07-104018 [doi].

204. Visser YPd, Walther FJ, Laghmani EH, Laarse Avd, Wagenaar GT. Apelin attenuates hyperoxic lung and heart injury in neonatal rats. *American journal of respiratory and critical care medicine*. 2010;182(10):1239-1250.

205. Kasai A. Pathological role of apelin in angiogenic eye disease. *Yakugaku Zasshi*. 2011;131(8):1201-1206. doi: JST.JSTAGE/yakushi/131.1201 [pii].

206. Masri B, van den Berghe L, Sorli C, Knibiehler B, Audigier Y. Apelin signalisation and vascular physiopathology. *J Soc Biol*. 2009;203(2):171-179. doi: 10.1051/jbio/2009021 [doi].

207. Li L, Zeng H, Chen JX. Apelin-13 increases myocardial progenitor cells and improves repair postmyocardial infarction. *Am J Physiol Heart Circ Physiol*. 2012;303(5):H605-18. doi: 10.1152/ajpheart.00366.2012 [doi].

208. Wang W, McKinnie SM, Patel VB, et al. Loss of apelin exacerbates myocardial infarction adverse remodeling and ischemia-reperfusion injury: Therapeutic potential of synthetic apelin analogues. *J Am Heart Assoc*. 2013;2(4):e000249. doi: 10.1161/JAHA.113.000249 [doi].

209. Nobes CD, Hall A. Rho, rac, and cdc42 GTPases regulate the assembly of multimolecular focal complexes associated with actin stress fibers, lamellipodia, and filopodia. *Cell*. 1995;81(1):53-62.

210. Nobes C, Hall A. Regulation and function of the rho subfamily of small GTPases. *Curr Opin Genet Dev*. 1994;4(1):77-81.

211. Bourne HR, Sanders DA, McCormick F. The GTPase superfamily: A conserved switch for diverse cell functions. *Nature*. 1990;348(6297):125-132. doi: 10.1038/348125a0 [doi].

212. Hart MJ, Eva A, Evans T, Aaronson SA, Cerione RA. Catalysis of guanine nucleotide exchange on the CDC42Hs protein by the dbl oncogene product. *Nature*. 1991;354(6351):311-314. doi: 10.1038/354311a0 [doi].

213. Manser E, Leung T, Monfries C, Teo M, Hall C, Lim L. Diversity and versatility of GTPase activating proteins for the p21rho subfamily of ras G proteins detected by a novel overlay assay. *J Biol Chem*. 1992;267(23):16025-16028.

214. Itoh RE, Kurokawa K, Ohba Y, Yoshizaki H, Mochizuki N, Matsuda M. Activation of rac and cdc42 video imaged by fluorescent resonance energy transfer-based single-molecule probes in the membrane of living cells. *Mol Cell Biol*. 2002;22(18):6582-6591.

215. Pertz O, Hodgson L, Klemke RL, Hahn KM. Spatiotemporal dynamics of RhoA activity in migrating cells. *Nature*. 2006;440(7087):1069-1072.

216. Beckers CM, van Hinsbergh VW, van Nieuw Amerongen, Geerten P. Driving rho GTPase activity in endothelial cells regulates barrier integrity. *Thrombosis & Haemostasis*. 2010;19(1):40.

217. Rameh LE, Arvidsson A, Carraway KL, et al. A comparative analysis of the phosphoinositide binding specificity of pleckstrin homology domains. *J Biol Chem*. 1997;272(35):22059-22066.

218. Das B, Shu X, Day GJ, et al. Control of intramolecular interactions between the pleckstrin homology and dbl homology domains of vav and Sos1 regulates rac binding. *J Biol Chem*. 2000;275(20):15074-15081. doi: 10.1074/jbc.M907269199 [doi].

219. Côté J, Motoyama AB, Bush JA, Vuori K. A novel and evolutionarily conserved PtdIns (3, 4, 5) P3-binding domain is necessary for DOCK180 signalling. *Nat Cell Biol*. 2005;7(8):797-807.

220. Michiels F, Stam JC, Hordijk PL, et al. Regulated membrane localization of Tiam1, mediated by the NH2-terminal pleckstrin homology domain, is required for rac-dependent membrane ruffling and C-jun NH2-terminal kinase activation. *J Cell Biol*. 1997;137(2):387-398.

221. Aghazadeh B, Lowry WE, Huang X, Rosen MK. Structural basis for relief of autoinhibition of the dbl homology domain of proto-oncogene vav by tyrosine phosphorylation. *Cell*. 2000;102(5):625-633.

222. Crespo P, Schuebel KE, Ostrom AA, Gutkind JS, Bustelo XR. Phosphotyrosine-dependent activation of rac-1 GDP/GTP exchange by the vav proto-oncogene product. . 1997.

223. Hart MJ, Jiang X, Kozasa T, et al. Direct stimulation of the guanine nucleotide exchange activity of p115 RhoGEF by Galpha13. *Science*. 1998;280(5372):2112-2114.

224. Kozasa T, Jiang X, Hart MJ, et al. p115 RhoGEF, a GTPase activating protein for Galpha12 and Galpha13. *Science*. 1998;280(5372):2109-2111.

225. Su ZJ, Hahn CN, Goodall GJ, et al. A vascular cell-restricted RhoGAP, p73RhoGAP, is a key regulator of angiogenesis. *Proc Natl Acad Sci U S A*. 2004;101(33):12212-12217. doi: 10.1073/pnas.0404631101 [doi].

226. Sprang SR. G protein mechanisms: Insights from structural analysis. *Annu Rev Biochem*. 1997;66(1):639-678.

227. Ross EM. Coordinating speed and amplitude in G-protein signaling. *Current Biology*. 2008;18(17):R777-R783.

228. Kurogane Y, Miyata M, Kubo Y, et al. FGD5 mediates proangiogenic action of vascular endothelial growth factor in human vascular endothelial cells. *Arterioscler Thromb Vasc Biol*. 2012;32(4):988-996. doi: 10.1161/ATVBAHA.111.244004; 10.1161/ATVBAHA.111.244004.

229. Nakhaei-Nejad M, Haddad G, Zhang QX, Murray AG. Facio-genital dysplasia-5 regulates matrix adhesion and survival of human endothelial cells. *Arterioscler Thromb Vasc Biol*. 2012;32(11):2694-2701. doi: 10.1161/ATVBAHA.112.300074; 10.1161/ATVBAHA.112.300074.

230. Korn C, Augustin HG. Born to die: Blood vessel regression research coming of age. *Circulation*. 2012;125(25):3063-3065. doi: 10.1161/CIRCULATIONAHA.112.112755; 10.1161/CIRCULATIONAHA.112.112755.

231. Gillooly D, SIMONSEN A, STENMARK H. Cellular functions of phosphatidylinositol 3-phosphate and FYVE domain proteins. *Biochem J*. 2001;355:249-258.

232. Burd CG, Emr SD. Phosphatidylinositol (3)-phosphate signaling mediated by specific binding to RING FYVE domains. *Mol Cell*. 1998;2(1):157-162.

233. Gaullier J, Simonsen A, D'Arrigo A, Bremnes B, Stenmark H, Aasland R. FYVE fingers bind PtdIns (3) P. *Nature*. 1998;394(6692):432-433.

234. Patki V, Lawe DC, Corvera S, Virbasius JV, Chawla A. A functional PtdIns (3) P-binding motif. *Nature*. 1998;394(6692):433-434.

235. Pasteris NG, Cadle A, Logie LJ, et al. Isolation and characterization of the faciogenital dysplasia (aarskog-scott syndrome) gene: A putative RhoRac guanine nucleotide exchange factor. *Cell*. 1994;79(4):669-678.

236. Cheng C, Haasdijk R, Tempel D, et al. Endothelial cell-specific FGD5 involvement in vascular pruning defines neovessel fate in mice. *Circulation*. 2012;125(25):3142-3158. doi: 10.1161/CIRCULATIONAHA.111.064030; 10.1161/CIRCULATIONAHA.111.064030.

237. Gazit R, Mandal PK, Ebina W, et al. Fgd5 identifies hematopoietic stem cells in the murine bone marrow. *J Exp Med*. 2014;211(7):1315-1331. doi: 10.1084/jem.20130428; 10.1084/jem.20130428.

238. Moake JL. Thrombotic microangiopathies. *N Engl J Med*. 2002;347(8):589-600.

239. Laszik Z, Silva F. Hemolytic uremic syndrome, thrombotic thrombocytopenia purpura, and other thrombotic microangiopathies and coagulopathies. *Heptinstall's Pathology of the Kidney, ed*. 2007;6:699-762.

240. Moschcowitz E. Hyaline thrombosis of the terminal arterioles and capillaries: A hitherto undescribed disease. . 1924;24:21-24.

241. Levy GG, Nichols WC, Lian EC, et al. Mutations in a member of the ADAMTS gene family cause thrombotic thrombocytopenic purpura. *Nature*. 2001;413(6855):488-494.

242. Fujimura Y, Matsumoto M, Isonishi A, et al. Natural history of Upshaw–Schulman syndrome based on ADAMTS13 gene analysis in japan. *Journal of Thrombosis and Haemostasis*. 2011;9(s1):283-301.

243. Motto DG, Chauhan AK, Zhu G, et al. Shigatoxin triggers thrombotic thrombocytopenic purpura in genetically susceptible ADAMTS13-deficient mice. *J Clin Invest*. 2005;115(10):2752-2761. doi: 10.1172/JCI26007 [doi].

244. George JN, Chen Q, Deford CC, Al-Nouri Z. Ten patient stories illustrating the extraordinarily diverse clinical features of patients with thrombotic thrombocytopenic purpura and severe ADAMTS13 deficiency. *J Clin Apheresis*. 2012;27(6):302-311.

245. George JN. How I treat patients with thrombotic thrombocytopenic purpura: 2010. *Blood*. 2010;116(20):4060-4069. doi: 10.1182/blood-2010-07-271445 [doi].

246. Furlan M, Robles R, Morselli B, Sandoz P, Lämmle B. Recovery and half-life of von willebrand factor-cleaving protease after plasma therapy in patients with thrombotic thrombocytopenic purpura. *Thromb Haemost*. 1999;81(1):8-13.

247. Naik S, Mahoney DH. Successful treatment of congenital TTP with a novel approach using plasma-derived factor VIII. *J Pediatr Hematol Oncol*. 2013;35(7):551-553. doi: 10.1097/MPH.0b013e3182755c38 [doi].

248. AMOROSI EL, ULTMANN JE. Thrombotic thrombocytopenic purpura: Report of 16 cases and review of the literature. *Medicine*. 1966;45(2):139-160.

249. Rock GA, Shumak KH, Buskard NA, et al. Comparison of plasma exchange with plasma infusion in the treatment of thrombotic thrombocytopenic purpura. *N Engl J Med*. 1991;325(6):393-397.

250. Kaplan BS, Chesney RW, Drummond KN. Hemolytic uremic syndrome in families. *N Engl J Med*. 1975;292(21):1090-1093.

251. Farr MJ, Roberts S, Morley AR, Dewar DF, Uldall PR. The haemolytic uraemic syndrome--a family study. *Q J Med*. 1975;44(174):161-188.

252. Warwicker P, Goodship TH, Donne RL, et al. Genetic studies into inherited and sporadic hemolytic uremic syndrome. *Kidney Int*. 1998;53(4):836-844.

253. Stahl AL, Vaziri-Sani F, Heinen S, et al. Factor H dysfunction in patients with atypical hemolytic uremic syndrome contributes to complement deposition on platelets and their activation. *Blood*. 2008;111(11):5307-5315. doi: 10.1182/blood-2007-08-106153 [doi].

254. Legendre CM, Licht C, Muus P, et al. Terminal complement inhibitor eculizumab in atypical hemolytic–uremic syndrome. *N Engl J Med*. 2013;368(23):2169-2181.

255. Nishimura J, Yamamoto M, Hayashi S, et al. Genetic variants in C5 and poor response to eculizumab. *N Engl J Med*. 2014;370(7):632-639.

256. JAVETT SN, SENIOR B. Syndrome of hemolysis, thrombopenia and nephropathy in infancy. *Pediatrics*. 1962;29:209-223.

257. Riley LW, Remis RS, Helgerson SD, et al. Hemorrhagic colitis associated with a rare escherichia coli serotype. *N Engl J Med*. 1983;308(12):681-685.

258. Kamali M, Petric M, Lim C, Fleming P, Steele B. Sporadic cases of hemolytic uremic syndrome associated with fecal cytotoxin and cytotoxin producing escherichia coli in stools. *Lancet i*. 1983;619:620.

259. Tarr PI, Gordon CA, Chandler WL. Shiga-toxin-producing escherichia coli and haemolytic uraemic syndrome. *The Lancet*. 2005;365(9464):1073-1086.

260. Karpac CA, Li X, Terrell DR, et al. Sporadic bloody diarrhoea-associated thrombotic thrombocytopenic purpura-haemolytic uraemic syndrome: An adult and paediatric comparison. *Br J Haematol*. 2008;141(5):696-707.

261. Pennington H. Escherichia coli O157. *The Lancet*. 2010;376(9750):1428-1435.

262. Bell BP, Goldoft M, Griffin PM, et al. A multistate outbreak of escherichia coli o157: H7—associated bloody diarrhea and hemolytic uremic syndrome from hamburgers: The washington experience. *JAMA*. 1994;272(17):1349-1353.

263. Buchholz U, Bernard H, Werber D, et al. German outbreak of escherichia coli O104: H4 associated with sprouts. *N Engl J Med*. 2011;365(19):1763-1770.

264. Huang J, Motto DG, Bundle DR, Sadler JE. Shiga toxin B subunits induce VWF secretion by human endothelial cells and thrombotic microangiopathy in ADAMTS13-deficient mice. *Blood*. 2010;116(18):3653-3659. doi: 10.1182/blood-2010-02-271957 [doi].

265. Robinson L, Hurley R, Lingwood C, Matsell D. Escherichia coli verotoxin binding to human paediatric glomerular mesangial cells. *Pediatric Nephrology*. 1995;9(6):700-704.

266. Ergonul Z, Clayton F, Fogo AB, Kohan DE. Shigatoxin-1 binding and receptor expression in human kidneys do not change with age. *Pediatric Nephrology*. 2003;18(3):246-253.

267. Hughes AK, Ergonul Z, Stricklett PK, Kohan DE. Molecular basis for high renal cell sensitivity to the cytotoxic effects of shigatoxin-1: Upregulation of globotriaosylceramide expression. *J Am Soc Nephrol*. 2002;13(9):2239-2245.

268. Chandler WL, Jelacic S, Boster DR, et al. Prothrombotic coagulation abnormalities preceding the hemolytic–uremic syndrome. *N Engl J Med*. 2002;346(1):23-32.

269. Garg AX, Suri RS, Barrowman N, et al. Long-term renal prognosis of diarrhea-associated hemolytic uremic syndrome: A systematic review, meta-analysis, and meta-regression. *JAMA*. 2003;290(10):1360-1370.

270. Rosales A, Hofer J, Zimmerhackl LB, et al. Need for long-term follow-up in enterohemorrhagic escherichia coli-associated hemolytic uremic syndrome due to late-emerging sequelae. *Clin Infect Dis*. 2012;54(10):1413-1421. doi: 10.1093/cid/cis196 [doi].

271. Edwards IR, Aronson JK. Adverse drug reactions: Definitions, diagnosis, and management. *The Lancet*. 2000;356(9237):1255-1259.

272. Webb RF, Ramirez AM, Hocken AG, Pettit JE. Acute intravascular haemolysis due to quinine. *N Z Med J*. 1980;91(651):14-16.

273. Gottschall JL, Neahring B, McFarland JG, Wu G, Weitekamp LA, Aster RH. Quinine-induced immune thrombocytopenia with hemolytic uremic syndrome: Clinical and serological findings in nine patients and review of literature. *Am J Hematol*. 1994;47(4):283-289.

274. Kojouri K, Vesely SK, George JN. Quinine-associated thrombotic thrombocytopenic purpura–hemolytic uremic syndrome: Frequency, clinical features, and long-term outcomes. *Ann Intern Med*. 2001;135(12):1047-1051.

275. Huynh M, Chee K, Lau DH. Thrombotic thrombocytopenic purpura associated with quetiapine. *Ann Pharmacother*. 2005;39(7-8):1346-1348. doi: aph.1G067 [pii].

276. Saif MW, Xyla V, Makrilia N, Bliziotis I, Syrigos K. Thrombotic microangiopathy associated with gemcitabine: Rare but real. *Expert opinion on drug safety*. 2009;8(3):257-260.

277. Bougie DW, Wilker PR, Aster RH. Patients with quinine-induced immune thrombocytopenia have both "drug-dependent" and "drug-specific" antibodies. *Blood*. 2006;108(3):922-927. doi: 108/3/922 [pii].

278. Glynne P, Salama A, Chaudhry A, Swirsky D, Lightstone L. Quinine-induced immune thrombocytopenic purpura followed by hemolytic uremic syndrome. *American journal of kidney diseases*. 1999;33(1):133-137.

279. Sartelet H, Toupance O, Lorenzato M, et al. Sirolimus-induced thrombotic microangiopathy is associated with decreased expression of vascular endothelial growth factor in kidneys. *American journal of transplantation*. 2005;5(10):2441-2447.

280. Eremina V, Jefferson JA, Kowalewska J, et al. VEGF inhibition and renal thrombotic microangiopathy. *N Engl J Med*. 2008;358(11):1129-1136.

281. Russo P, Doyon J, Sonsino E, Ogier H, Saudubray J. A congenital anomaly of vitamin B 12 metabolism: A study of three cases. *Hum Pathol*. 1992;23(5):504-512.

282. Geraghty MT, Perlman EJ, Martin LS, et al. Cobalamin C defect associated with hemolytic-uremic syndrome. *J Pediatr*. 1992;120(6):934-937.

283. Coppola A, Davi G, De Stefano V, Mancini FP, Cerbone AM, Di Minno G. Homocysteine, coagulation, platelet function, and thrombosis. *Semin Thromb Hemost*. 2000;26(3):243-254. doi: 10.1055/s-2000-8469 [doi].

284. Hosenpud JD, Bennett LE, Keck BM, Boucek MM, Novick RJ. The registry of the international society for heart and lung transplantation: Eighteenth official report-2001. *J Heart Lung Transplant*. 2001;20(8):805-815. doi: S1053-2498(01)00323-0 [pii].

285. Libby P, Pober JS. Chronic rejection. *Immunity*. 2001;14(4):387-397.

286. Hirsch GM, Kearsey J, Burt T, Karnovsky MJ, Lee T. Medial smooth muscle cell loss in arterial allografts occurs by cytolytic cell induced apoptosis. *European journal of cardio-thoracic surgery*. 1998;14(1):89-97.

287. Skaro AI, Liwski RS, Zhou J, Vessie EL, Lee TD, Hirsch GM. CD8+ T cells mediate aortic allograft vasculopathy by direct killing and an interferon-gamma-dependent indirect pathway. *Cardiovasc Res*. 2005;65(1):283-291. doi: S0008-6363(04)00426-2 [pii].

288. Costello JP, Mohanakumar T, Nath DS. Mechanisms of chronic cardiac allograft rejection. *Texas Heart Institute Journal*. 2013;40(4).

289. Billingham ME. Histopathology of graft coronary disease. *J Heart Lung Transplant*. 1992;11(3 Pt 2):S38-44.

290. Ramzy D, Rao V, Brahm J, Miriuka S. Cardiac allograft vasculopathy: A review. *Canadian journal of surgery*. 2005;48(4):319.

291. Lu W, Palatnik K, Fishbein GA, et al. Diverse morphologic manifestations of cardiac allograft vasculopathy: A pathologic study of 64 allograft hearts. *The Journal of Heart and Lung Transplantation*. 2011;30(9):1044-1050.

292. Rahmani M, Cruz RP, Granville DJ, McManus BM. Allograft vasculopathy versus atherosclerosis. *Circ Res*. 2006;99(8):801-815. doi: 99/8/801 [pii].

293. Fishbein GA, Fishbein MC. Arteriosclerosis: Rethinking the current classification. *Arch Pathol Lab Med*. 2009;133(8):1309-1316.

294. Schmauss D, Weis M. Cardiac allograft vasculopathy: Recent developments. *Circulation*. 2008;117(16):2131-2141. doi: 10.1161/CIRCULATIONAHA.107.711911 [doi].

295. Taylor DO, Yowell RL, Kfoury AG, Hammond EH, Renlund DG. Allograft coronary artery disease: Clinical correlations with circulating anti-HLA antibodies and the immunohistopathologic pattern of vascular rejection. *The Journal of heart and lung transplantation*. 2000;19(6):518-521.

296. Weis M, Von Scheidt W. Coronary artery disease in the transplanted heart. *Annu Rev Med*. 2000;51(1):81-100.

297. Pinney SP, Mancini D. Cardiac allograft vasculopathy: Advances in understanding its pathophysiology, prevention, and treatment. *Curr Opin Cardiol*. 2004;19(2):170-176.

298. Lázaro IS, Bonet LA, López JM, et al. Influence of traditional cardiovascular risk factors in the recipient on the development of cardiac allograft vasculopathy after heart transplantation. . 2008;40(9):3056-3057.

299. Behrendt D, Ganz P. Endothelial function: From vascular biology to clinical applications. *Am J Cardiol*. 2002;90(10):L40-L48.

300. Patel RP, Levonen A, Crawford JH, Darley-Usmar VM. Mechanisms of the pro- and anti-oxidant actions of nitric oxide in atherosclerosis. *Cardiovasc Res*. 2000;47(3):465-474. doi: S0008636300000869 [pii].

301. Chehal MK, Granville DJ. Cytochrome p450 2C (CYP2C) in ischemic heart injury and vascular dysfunction this paper is one of a selection of papers published in this special issue, entitled young investigator's forum. *Can J Physiol Pharmacol*. 2006;84(1):15-20.

302. Epstein FH, Ross R. Atherosclerosis—an inflammatory disease. *N Engl J Med*. 1999;340(2):115-126.

303. Weis M, Cooke JP. Cardiac allograft vasculopathy and dysregulation of the NO synthase pathway. *Arterioscler Thromb Vasc Biol*. 2003;23(4):567-575. doi: 10.1161/01.ATV.0000067060.31369.F9 [doi].

304. Lai JC, Tranfield EM, Walker DC, et al. Ultrastructural evidence of early endothelial damage in coronary arteries of rat cardiac allografts. *The Journal of heart and lung transplantation*. 2003;22(9):993-1004.

305. Fish RD, Nabel EG, Selwyn AP, et al. Responses of coronary arteries of cardiac transplant patients to acetylcholine. *J Clin Invest*. 1988;81(1):21-31. doi: 10.1172/JCI113297 [doi].

306. Weis M, Peter-Wolfa W, Mazzilli N, et al. Variations of segmental endothelium-dependent and endothelium-independent vasomotor tone after cardiac transplantation (qualitative changes in endothelial function). *Am Heart J*. 1997;134(2):306-315.

307. Drexler H, Fischell TA, Pinto FJ, et al. Effect of L-arginine on coronary endothelial function in cardiac transplant recipients. relation to vessel wall morphology. *Circulation*. 1994;89(4):1615-1623.

308. Hasdai D, Gibbons RJ, Holmes DR,Jr, Higano ST, Lerman A. Coronary endothelial dysfunction in humans is associated with myocardial perfusion defects. *Circulation*. 1997;96(10):3390-3395.

309. Davis SF, Yeung AC, Meredith IT, et al. Early endothelial dysfunction predicts the development of transplant coronary artery disease at 1 year posttransplant. *Circulation*. 1996;93(3):457-462.

310. Hollenberg SM, Klein LW, Parrillo JE, et al. Coronary endothelial dysfunction after heart transplantation predicts allograft vasculopathy and cardiac death. *Circulation*. 2001;104(25):3091-3096.

311. Shears LL, Kawaharada N, Tzeng E, et al. Inducible nitric oxide synthase suppresses the development of allograft arteriosclerosis. *J Clin Invest*. 1997;100(8):2035-2042. doi: 10.1172/JCI119736 [doi].

312. Lee PC, Wang ZL, Qian S, et al. Endothelial nitric oxide synthase protects aortic allografts from the development of transplant arteriosclerosis. *Transplantation*. 2000;69(6):1186-1192.

313. Iwata A, Sai S, Nitta Y, et al. Liposome-mediated gene transfection of endothelial nitric oxide synthase reduces endothelial activation and leukocyte infiltration in transplanted hearts. *Circulation*. 2001;103(22):2753-2759.

314. Vejlstrup NG, Andersen CB, Boesgaard S, Mortensen SA, Aldershvile J. Temporal changes in myocardial endothelial nitric oxide synthase expression following human heart transplantation. *The Journal of heart and lung transplantation*. 2002;21(2):211-216.

315. Weis M, Wildhirt SM, Schulze C, et al. Coronary vasomotor dysfunction in the cardiac allograft: Impact of different immunosuppressive regimens. *J Cardiovasc Pharmacol*. 2000;36(6):776-784.

316. Lee S, Willoughby WF, Smallwood CJ, Dawson A, Orloff MJ. Heterotopic heart and lung transplantation in the rat. *Am J Pathol*. 1970;59(2):279-298.

317. Wilhelm M, Pratschke J, Beato F, et al. Activation of proinflammatory mediators in heart transplants from brain-dead donors: Evidence from a model of chronic rat cardiac allograft rejection. . 2002;34(6):2359-2360.

318. Lemstrom K, Sihvola R, Bruggeman C, Hayry P, Koskinen P. Cytomegalovirus infection-enhanced cardiac allograft vasculopathy is abolished by DHPG prophylaxis in the rat. *Circulation*. 1997;95(12):2614-2616.

319. Choy JC, Cruz RP, Kerjner A, et al. Granzyme B induces endothelial cell apoptosis and contributes to the development of transplant vascular disease. *American journal of transplantation*. 2005;5(3):494-499.

320. Isik FF, McDonald TO, Ferguson M, Yamanaka E, Gordon D. Transplant arteriosclerosis in a rat aortic model. *Am J Pathol*. 1992;141(5):1139-1149.

321. Wagoner LE, Zhao L, Bishop DK, Chan S, Xu S, Barry WH. Lysis of adult ventricular myocytes by cells infiltrating rejecting murine cardiac allografts. *Circulation*. 1996;93(1):111-119.

322. Kawahara K, Sutherland DE, Rynasiewicz JJ, Najarian JS. Prolongation of heterotopic cardiac allografts in rats by cyclosporin A. *Surgery*. 1980;88(4):594-600. doi: 0039-6060(80)90136-1 [pii].

323. Fuchs E. The tortoise and the hair: Slow-cycling cells in the stem cell race. *Cell*. 2009;137(5):811-819.

324. Orkin SH, Zon LI. Hematopoiesis: An evolving paradigm for stem cell biology. *Cell*. 2008;132(4):631-644.

325. Barker N. Adult intestinal stem cells: Critical drivers of epithelial homeostasis and regeneration. *Nature reviews Molecular cell biology*. 2014;15(1):19-33.

326. Hoath SB, Leahy D. The organization of human epidermis: Functional epidermal units and phi proportionality. *J Invest Dermatol*. 2003;121(6):1440-1446.

327. Altschul R. Endothelium. Its development, morphology, function, and pathology. *Am J Med Sci*. 1956;232(1):116.

328. Florentin R, Nam S, Lee K, Thomas W. Increased 3H-thymidine incorporation into endothelial cells of swine fed cholesterol for 3 days. *Exp Mol Pathol*. 1969;10(3):250-255.

329. Poole J, Sanders A, Florey H. The regeneration of aortic endothelium. *J Pathol Bacteriol*. 1958;75(1):133-143.

330. ROBERTSON HR, MOORE JR, MERSEREAU WA. Observations on thrombosis and endothelial repair following application of external pressure to a vein. *Can J Surg*. 1959;3:5-16.

331. Stehbens W. Endothelial cell mitosis and permeability. *Q J Exp Physiol Cogn Med Sci*. 1965;50(1):90-92.

332. Wright HP. Endothelial mitosis around aortic branches in normal guinea-pigs. . 1968.

333. Caplan BA, Schwartz CJ. Increased endothelial cell turnover in areas of in vivo evans blue uptake in the pig aorta. *Atherosclerosis*. 1973;17(3):401-417.

334. Prescott MF, Muller KR. Endothelial regeneration in hypertensive and genetically hypercholesterolemic rats. *Arteriosclerosis*. 1983;3(3):206-214.

335. Schwartz SM, Benditt EP. Aortic endothelial cell replication. I. effects of age and hypertension in the rat. *Circ Res*. 1977;41(2):248-255.

336. Schwartz SM, Gajdusek CM, Reidy MA, Selden SC,3rd, Haudenschild CC. Maintenance of integrity in aortic endothelium. *Fed Proc*. 1980;39(9):2618-2625.

337. Schwartz SM, Benditt EP. Clustering of replicating cells in aortic endothelium. *Proc Natl Acad Sci U S A*. 1976;73(2):651-653.

338. Li F, Downing BD, Smiley LC, et al. Neurofibromin-deficient myeloid cells are critical mediators of aneurysm formation in vivo. *Circulation*. 2014;129(11):1213-1224. doi: 10.1161/CIRCULATIONAHA.113.006320 [doi].

339. Wara AK, Manica A, Marchini JF, et al. Bone marrow-derived kruppel-like factor 10 controls reendothelialization in response to arterial injury. *Arterioscler Thromb Vasc Biol*. 2013;33(7):1552-1560. doi: 10.1161/ATVBAHA.112.300655 [doi].

340. Schwartz SM, Gajdusek CM, Selden SC,3rd. Vascular wall growth control: The role of the endothelium. *Arteriosclerosis*. 1981;1(2):107-126.

341. Tannock IF, Hayashi S. The proliferation of capillary endothelial cells. *Cancer Res*. 1972;32(1):77-82.

342. Hobson B, Denekamp J. Endothelial proliferation in tumours and normal tissues: Continuous labelling studies. *Br J Cancer*. 1984;49(4):405-413.

343. Ding B, Nolan DJ, Guo P, et al. Endothelial-derived angiocrine signals induce and sustain regenerative lung alveolarization. *Cell*. 2011;147(3):539-553.

344. Haudenschild C, Studer A. Early interactions between blood cells and severely damaged rabbit aorta. *Eur J Clin Invest*. 1971;2(1):1-7.

345. Schwartz SM, Stemerman MB, Benditt EP. The aortic intima. II. repair of the aortic lining after mechanical denudation. *Am J Pathol*. 1975;81(1):15-42.

346. Asahara T, Murohara T, Sullivan A, et al. Isolation of putative progenitor endothelial cells for angiogenesis. *Science*. 1997;275(5302):964-966.

347. Purhonen S, Palm J, Rossi D, et al. Bone marrow-derived circulating endothelial precursors do not contribute to vascular endothelium and are not needed for tumor growth. *Proc Natl Acad Sci U S A*. 2008;105(18):6620-6625. doi: 10.1073/pnas.0710516105 [doi].

348. Hagensen MK, Shim J, Thim T, Falk E, Bentzon JF. Circulating endothelial progenitor cells do not contribute to plaque endothelium in murine atherosclerosis. *Circulation*. 2010;121(7):898-905. doi: 10.1161/CIRCULATIONAHA.109.885459 [doi].

349. Tsuzuki M. Bone marrow-derived cells are not involved in reendothelialized endothelium as endothelial cells after simple endothelial denudation in mice. *Basic Res Cardiol*. 2009;104(5):601-611.

350. Hagensen MK, Raarup MK, Mortensen MB, et al. Circulating endothelial progenitor cells do not contribute to regeneration of endothelium after murine arterial injury. *Cardiovasc Res*. 2012;93(2):223-231. doi: 10.1093/cvr/cvr278 [doi].

351. Itoh Y, Toriumi H, Yamada S, Hoshino H, Suzuki N. Resident endothelial cells surrounding damaged arterial endothelium reendothelialize the lesion. *Arterioscler Thromb Vasc Biol*. 2010;30(9):1725-1732. doi: 10.1161/ATVBAHA.110.207365 [doi].

352. Nishimura R, Nishiwaki T, Kawasaki T, et al. Hypoxia-induced proliferation of tissue-resident endothelial progenitor cells in the lung. *Am J Physiol Lung Cell Mol Physiol*. 2015;308(8):L746-58. doi: 10.1152/ajplung.00243.2014 [doi].

353. STUMP MM, JORDAN GL,Jr, DEBAKEY ME, HALPERT B. Endothelium grown from circulating blood on isolated intravascular dacron hub. *Am J Pathol*. 1963;43:361-367.

354. Medina RJ, O'Neill CL, Sweeney M, et al. Molecular analysis of endothelial progenitor cell (EPC) subtypes reveals two distinct cell populations with different identities. *BMC Med Genomics*. 2010;3:18-8794-3-18. doi: 10.1186/1755-8794-3-18 [doi].

355. Au P, Daheron LM, Duda DG, et al. Differential in vivo potential of endothelial progenitor cells from human umbilical cord blood and adult peripheral blood to form functional long-lasting vessels. *Blood*. 2008;111(3):1302-1305. doi: blood-2007-06-094318 [pii].

356. Yoder MC, Mead LE, Prater D, et al. Redefining endothelial progenitor cells via clonal analysis and hematopoietic stem/progenitor cell principals. *Blood*. 2007;109(5):1801-1809. doi: blood-2006-08-043471 [pii].

357. Meneveau N, Deschaseaux F, Séronde M, et al. Presence of endothelial colony-forming cells is associated with reduced microvascular obstruction limiting infarct size and left ventricular remodelling in patients with acute myocardial infarction. *Basic Res Cardiol*. 2011;106(6):1397-1410.

358. Massa M, Campanelli R, Bonetti E, Ferrario M, Marinoni B, Rosti V. Rapid and large increase of the frequency of circulating endothelial colony-forming cells (ECFCs) generating late

outgrowth endothelial cells in patients with acute myocardial infarction. *Exp Hematol*. 2009;37(1):8-9.

359. Folkman J. Angiogenesis in cancer, vascular, rheumatoid and other disease. *Nat Med*. 1995;1(1):27-30.

360. Ferrara N. Vascular endothelial growth factor and the regulation of angiogenesis. *Recent Prog Horm Res*. 2000;55:15-35; discussion 35-6.

361. Cotran R, Kumar V, Robbins S, Schoen F. Inflammation and repair. *Robbins pathologic basis of disease*. 1994;5:51-92.

362. Polverini P. Role of the macrophage in angiogenesis-dependent diseases. *Cellular and Molecular Life Sciences-Supplements Only*. 1997;79:11-28.

363. Moulton KS, Vakili K, Zurakowski D, et al. Inhibition of plaque neovascularization reduces macrophage accumulation and progression of advanced atherosclerosis. *Proc Natl Acad Sci U S A*. 2003;100(8):4736-4741. doi: 10.1073/pnas.0730843100 [doi].

364. Nykanen AI, Krebs R, Saaristo A, et al. Angiopoietin-1 protects against the development of cardiac allograft arteriosclerosis. *Circulation*. 2003;107(9):1308-1314.

365. Lemstrom KB, Krebs R, Nykanen AI, et al. Vascular endothelial growth factor enhances cardiac allograft arteriosclerosis. *Circulation*. 2002;105(21):2524-2530.

366. Denton MD, Magee C, Melter M, Dharnidharka VR, Sayegh MH, Briscoe DM. TNP-470, an angiogenesis inhibitor, attenuates the development of allograft vasculopathy. *Transplantation*. 2004;78(8):1218-1221.

367. Kang DH, Kanellis J, Hugo C, et al. Role of the microvascular endothelium in progressive renal disease. *J Am Soc Nephrol*. 2002;13(3):806-816.

368. Ichinose K, Maeshima Y, Yamamoto Y, et al. Antiangiogenic endostatin peptide ameliorates renal alterations in the early stage of a type 1 diabetic nephropathy model. *Diabetes*. 2005;54(10):2891-2903. doi: 54/10/2891 [pii].

369. Carmeliet P. Manipulating angiogenesis in medicine. *J Intern Med*. 2004;255(5):538-561.

370. Libby P, Zhao DX. Allograft arteriosclerosis and immune-driven angiogenesis. *Circulation*. 2003;107(9):1237-1239.

371. Adamis AP, Aiello LP, D'Amato RA. Angiogenesis and ophthalmic disease. *Angiogenesis*. 1999;3(1):9-14.

372. Kang D, Nakagawa T, Feng L, Johnson RJ. Nitric oxide modulates vascular disease in the remnant kidney model. *The American journal of pathology*. 2002;161(1):239-248.

373. Blann AD, Woywodt A, Bertolini F, et al. Circulating endothelial cells. *Thromb Haemost*. 2005;93:228-235.

374. Kang D, Anderson S, Kim Y, et al. Impaired angiogenesis in the aging kidney: Vascular endothelial growth factor and thrombospondin-1 in renal disease. *American journal of kidney diseases*. 2001;37(3):601-611.

375. Masuda Y, Shimizu A, Mori T, et al. Vascular endothelial growth factor enhances glomerular capillary repair and accelerates resolution of experimentally induced glomerulonephritis. *The American journal of pathology*. 2001;159(2):599-608.

376. Iruela-Arispe L, Gordon K, Hugo C, et al. Participation of glomerular endothelial cells in the capillary repair of glomerulonephritis. *Am J Pathol*. 1995;147(6):1715-1727.

377. Khachigian LM, Lindner V, Williams AJ, Collins T. Egr-1-induced endothelial gene expression: A common theme in vascular injury. *Science*. 1996;271(5254):1427-1431.

378. Baffert F, Le T, Sennino B, et al. Cellular changes in normal blood capillaries undergoing regression after inhibition of VEGF signaling. *Am J Physiol Heart Circ Physiol*. 2006;290(2):H547-59. doi: 00616.2005 [pii].

379. Mancuso MR, Davis R, Norberg SM, et al. Rapid vascular regrowth in tumors after reversal of VEGF inhibition. *J Clin Invest*. 2006;116(10):2610-2621. doi: 10.1172/JCI24612 [doi].

380. Shimizu A, Masuda Y, Mori T, et al. Vascular endothelial growth factor165 resolves glomerular inflammation and accelerates glomerular capillary repair in rat anti-glomerular basement membrane glomerulonephritis. *J Am Soc Nephrol*. 2004;15(10):2655-2665. doi: 15/10/2655 [pii].

381. Reinders ME, Briscoe DM. Angiogenesis and allograft rejection. *Graft*. 2002;5(2):96.

382. Reinders ME, Sho M, Izawa A, et al. Proinflammatory functions of vascular endothelial growth factor in alloimmunity. *J Clin Invest*. 2003;112(11):1655-1665. doi: 10.1172/JCI17712 [doi].

383. Jaffe EA, Nachman RL, Becker CG, Minick CR. Culture of human endothelial cells derived from umbilical veins. identification by morphologic and immunologic criteria. *J Clin Invest*. 1973;52(11):2745.

384. Rouwkema J, Rivron NC, van Blitterswijk CA. Vascularization in tissue engineering. *Trends Biotechnol*. 2008;26(8):434-441.

385. Koike N, Fukumura D, Gralla O, Au P, Schechner JS, Jain RK. Tissue engineering: Creation of long-lasting blood vessels. *Nature*. 2004;428(6979):138-139.

386. Booyse FM, Sedlak BJ, Rafelson ME,Jr. Culture of arterial endothelial cells: Characterization and growth of bovine aortic cells. *Thromb Diath Haemorrh*. 1975;34(3):825-839.

387. Schwartz SM. Selection and characterization of bovine aortic endothelial cells. *In Vitro Cellular & Developmental Biology-Plant*. 1978;14(12):966-980.

388. Brugger W, Heimfeld S, Berenson RJ, Mertelsmann R, Kanz L. Reconstitution of hematopoiesis after high-dose chemotherapy by autologous progenitor cells generated ex vivo. *N Engl J Med*. 1995;333(5):283-287.

389. Flamme I, Risau W. Induction of vasculogenesis and hematopoiesis in vitro. *Development*. 1992;116(2):435-439.

390. Weiss MJ, Orkin SH. In vitro differentiation of murine embryonic stem cells. new approaches to old problems. *J Clin Invest*. 1996;97(3):591-595. doi: 10.1172/JCI118454 [doi].

391. Kollet O, Shivtiel S, Chen YQ, et al. HGF, SDF-1, and MMP-9 are involved in stress-induced human CD34+ stem cell recruitment to the liver. *J Clin Invest*. 2003;112(2):160-169. doi: 10.1172/JCI17902 [doi].

392. Capillo M, Mancuso P, Gobbi A, et al. Continuous infusion of endostatin inhibits differentiation, mobilization, and clonogenic potential of endothelial cell progenitors. *Clin Cancer Res*. 2003;9(1):377-382.

393. Khakoo AY, Finkel T. Endothelial progenitor cells*. *Annu Rev Med*. 2005;56:79-101.

394. Richard L, Velasco P, Detmar M. A simple immunomagnetic protocol for the selective isolation and long-term culture of human dermal microvascular endothelial cells. *Exp Cell Res*. 1998;240(1):1-6.

395. Detmar M, Imcke E, RUSZCZAK Z, Orfanos C. Effects of tumor necrosis factor-alpha (TNF) on cultured microvascular endothelial-cells derived from human dermis. . 1989;93(4):546-547.

396. Detmar M, Tenorio S, Hettmannsperger U, Ruszczak Z, Orfanos CE. Cytokine regulation of proliferation and ICAM-1 expression of human dermal microvascular endothelial cells in vitro. *J Invest Dermatol*. 1992;98(2):147-153.

397. Ades EW, Candal FJ, Swerlick RA, et al. HMEC-1: Establishment of an immortalized human microvascular endothelial cell line. *J Invest Dermatol*. 1992;99(6):683-690.

398. Haraldsen G, Kvale D, Lien B, Farstad IN, Brandtzaeg P. Cytokine-regulated expression of E-selectin, intercellular adhesion molecule-1 (ICAM-1), and vascular cell adhesion molecule-1 (VCAM-1) in human microvascular endothelial cells. *J Immunol*. 1996;156(7):2558-2565.

399. Robinson KA, Candal FJ, Scott NA, Ades EW. Seeding of vascular grafts with an immortalized human dermal microvascular endothelial cell line. *Angiology*. 1995;46(2):107-113.

400. Bouïs D, Hospers GA, Meijer C, Molema G, Mulder NH. Endothelium in vitro: A review of human vascular endothelial cell lines for blood vessel-related research. *Angiogenesis*. 2001;4(2):91-102.

401. Lawley TJ, Kubota Y. Induction of morphologic differentiation of endothelial cells in culture. *J Invest Dermatol*. 1989;93(2 Suppl):59S-61S.

402. Auerbach R, Lewis R, Shinners B, Kubai L, Akhtar N. Angiogenesis assays: A critical overview. *Clin Chem*. 2003;49(1):32-40.

403. Staton CA, Reed MW, Brown NJ. A critical analysis of current in vitro and in vivo angiogenesis assays. *Int J Exp Pathol*. 2009;90(3):195-221. doi: 10.1111/j.1365-2613.2008.00633.x; 10.1111/j.1365-2613.2008.00633.x.

404. Zimrin AB, Villeponteau B, Maciag T. Models of in vitro angiogenesis: Endothelial cell differentiation on fibrin but not matrigel is transcriptionally dependent. *Biochem Biophys Res Commun*. 1995;213(2):630-638. doi: 10.1006/bbrc.1995.2178.

405. Liu J, Wang XB, Park DS, Lisanti MP. Caveolin-1 expression enhances endothelial capillary tubule formation. *J Biol Chem*. 2002;277(12):10661-10668. doi: 10.1074/jbc.M110354200.

406. Kanzawa S, Endo H, Shioya N. Improved in vitro angiogenesis model by collagen density reduction and the use of type III collagen. *Ann Plast Surg*. 1993;30(3):244-251.

407. Nakatsu MN, Hughes CC. An optimized three-dimensional in vitro model for the analysis of angiogenesis. *Methods Enzymol*. 2008;443:65-82.

408. Gagnon E, Cattaruzzi P, Griffith M, et al. Human vascular endothelial cells with extended life spans: In vitro cell response, protein expression, and angiogenesis. *Angiogenesis*. 2002;5(1-2):21-33.

409. Baker M, Robinson SD, Lechertier T, et al. Use of the mouse aortic ring assay to study angiogenesis. *Nature Protocols*. 2011;7(1):89-104.

410. Blacher S, Devy L, Burbridge MF, et al. Improved quantification of angiogenesis in the rat aortic ring assay. *Angiogenesis*. 2001;4(2):133-142.

411. Folkman J. Angiogenesis: initiation and control. *Ann N Y Acad Sci*. 2006;401(1):212-226.

412. Nicosia RF, Zhu WH, Fogel E, Howson KM, Aplin AC. A new ex vivo model to study venous angiogenesis and arterio-venous anastomosis formation. *J Vasc Res*. 2005;42(2):111-119.

413. Gimbrone Jr MA, Cotran RS, Leapman SB, Folkman J. Tumor growth and neovascularization: An experimental model using the rabbit cornea. *J Natl Cancer Inst*. 1974;52(2):413-427.

414. Muthukkaruppan V, Auerbach R. Angiogenesis in the mouse cornea. *Science*. 1979;205(4413):1416-1418.

415. Vogel HB, Berry RG. Chorioallantoic membrane heterotransplantation of human brain tumors. *International Journal of Cancer*. 1975;15(3):401-408.

416. Auerbach R, Arensman R, Kubai L, Folkman J. Tumor-induced angiogenesis: Lack of inhibition by irradiation. *International Journal of Cancer*. 1975;15(2):241-245.

417. Ausprunk DH, Folkman J. Vascular injury in transplanted tissues. *Virchows Archiv B*. 1976;21(1):31-44.

418. Ausprunk D, Knighton D, Folkman J. Vascularization of normal and neoplastic tissues grafted to the chick chorioallantois. role of host and preexisting graft blood vessels. *The American journal of pathology*. 1975;79(3):597.

419. Passaniti A, Taylor RM, Pili R, et al. A simple, quantitative method for assessing angiogenesis and antiangiogenic agents using reconstituted basement membrane, heparin, and fibroblast growth factor. *Lab Invest*. 1992;67(4):519-528.

420. Grant DS, Kinsella JL, Fridman R, et al. Interaction of endothelial cells with a laminin A chain peptide (SIKVAV) in vitro and induction of angiogenic behavior in vivo. *J Cell Physiol*. 1992;153(3):614-625.

421. Akhtar N, Dickerson EB, Auerbach R. The sponge/matrigel angiogenesis assay. *Angiogenesis*. 2002;5(1-2):75-80.

422. Rubinstein AL. Zebrafish: From disease modeling to drug discovery. *Current Opinion in Drug Discovery and Development*. 2003;6(2):218-223.

423. Lawson ND, Weinstein BM. Arteries and veins: Making a difference with zebrafish. *Nature Reviews Genetics*. 2002;3(9):674-682.

424. Motoike T, Loughna S, Perens E, et al. Universal GFP reporter for the study of vascular development. *Genesis*. 2000;28(2):75-81.

425. Cross LM, Cook MA, Lin S, Chen JN, Rubinstein AL. Rapid analysis of angiogenesis drugs in a live fluorescent zebrafish assay. *Arterioscler Thromb Vasc Biol*. 2003;23(5):911-912. doi: 10.1161/01.ATV.0000068685.72914.7E [doi].

426. Currie PD, Ingham PW. Induction of a specific muscle cell type by a hedgehog-like protein in zebrafish. . 1996.

427. Zheng L, Ling P, Wang Z, et al. A novel polypeptide from shark cartilage with potent anti-angiogenic activity. *Cancer biology & therapy*. 2007;6(5):775-780.

428. Touchot N, Chardin P, Tavitian A: Four additional members of the ras gene superfamily isolated by an oligonucleotide strategy: molecular cloning of YPT-related cDNAs from a rat brain library. Proc Natl Acad Sci USA. 1987, 84: 8210-8214.

429. Bock JB, Matern HT, Peden AA, Scheller RH: A genomic perspective on membrane compartment organization. Nature. 2001, 409: 839-841. 10.1038/35057024.

430. Zerial M, McBride H: Rab proteins as membrane organizers. Nat Rev Mol Cell Biol. 2001, 2: 107-117. 10.1038/35052055.

431. Stenmark H, Parton RG, Steele-Mortimer O, Lütcke A, Gruenberg J, Zerial M: Inhibition of rab5 GTPase activity stimulates membrane fusion in endocytosis. EMBO J. 1994, 13: 1287-1296.

432. HUTAGALUNG AH, NOVICK PJ. Role of Rab GTPases in Membrane Traffic and Cell Physiology. *Physiological reviews*. 2011;91(1):119-149. doi:10.1152/physrev.00059.2009.

433. Anant JS, Desnoyers L, Machius M, Demeler B, Hansen JC, Westover KD, Deisenhofer J, Seabra MC: Mechanism of Rab geranylgeranylation: formation of the catalytic ternary complex. Biochemistry. 1998, 37: 12559-12568. 10.1021/bi980881a.

434. Dirac-Svejstrup AB, Sumizawa T, Pfeffer SR: Identification of a GDI displacement factor that releases endosomal Rab GTPases from Rab-GDI. EMBO J. 1997, 16: 465-472. 10.1093/emboj/16.3.465.

Chapter II: Materials and Methods

1 Materials and methods for chapter III

1.1 Reagents

Medium 199 (M199), Hank's Balanced Salt Solution (HBSS), fetal bovine serum (FBS), and endothelial cell growth supplement were purchased from Invitrogen (Burlington, ON). VEGF-A was from Peprotech (Princeton, NJ). Rapamycin, PP242, a highly specific mTOR active-site inhibitor [1], and anti-tubulin-α was from Millipore (Temecula, CA). Ku-0063794, a second specific mTOR inhibitor [2] was from Sigma (St. Louis, MO). Anti-Akt1 was from Protein Tech (Chicago, IL). Hiperfect, non-silencing short interfering RNA (siRNA) and Akt1 silencing siRNA were from Qiagen Inc (Mississauga, ON). Human tumor necrosis factor-α (TNFα) was from Cedarlane (Mississauga, ON). Cycloheximide, phalloidin-FITC, anti-vinculin, and DAPI were from Sigma. Anti-S6K was from Abcam (Cambridge, UK). Anti-phospho-AktS473, anti-phospho-S6KT389, anti-FAK, anti-phospho-FAKY397, anti-raptor, anti-rictor, and rictor siRNA were from Cell Signaling Technology (Danvers, MA). ON-TARGETplus human raptor siRNA-SMARTpool was from Thermo Scientific (Waltham, MA).

1.2 Cell culture

Human umbilical vein ECs (HUVECs) were isolated from unidentified donors as described previously [3]. The protocol for HUVEC isolation was approved by the Research ethics Board of the University of Alberta. The human microvascular endothelial cell line (HMEC-1; ATCC, Manassas, VA). To facilitate study of VEGF as the only proangiogenic factor, cells were washed with M199 twice and incubated in M199 with 10% FBS and 20 ng/mL VEGF for 18 hours

before performing the experiments. To optimize VEGF-induced signals, HUVECs were starved in M199 + 1% FBS overnight, then stimulated with 20 ng/ml VEGF. Caki-1 human renal cell carcinoma cells (ATCC; Manassas, VA) were grown in Minimum Essential Medium (MEM; invitrogen).

1.3 RNA interference

HUVECs were seeded at 70-80% confluency and transfected serially twice over two days with either 50 nM non-silencing (siNS) or specific siRNA using Hiperfect transfection reagent according to the manufacturer's protocol. After transfection, HUVECs were left to recover in a complete media overnight. Protein expression was evaluated by Western blot. AllStars Negative Control siRNA (Qiagen) was used in all experiments to exclude off target effects.

1.4 Western blot

HUVEC monolayers were washed once with ice cold phosphate buffered solution (PBS) and then lysed immediately on ice by RIPA buffer (10 mM Tris, pH 7.4, 100 mM NaCl, 1 mM EDTA, 1 mM EGTA, 5 mM NaF, 2 mM Na3VO4, 0.1% SDS, 0.5% Na deoxycholate, 1% Triton X-100, 10% glycerol, 1 mM PMSF) followed by boiling at 95°C for 5 minutes. The lysates were resolved by SDS-PAGE, blotted on nitrocellulose membranes (Biorad), then immunostained overnight at 4°C in blocking buffer (5% BSA/TBS-Tween20). Proteins were detected using Luminata forte (EMD Millipore, Billerica, MA) and a Fluorchem FC2 CCD camera (Alpha Innotech). Protein bands were equally contrast enhanced by Adobe Photoshop CS3 then quantified by ImageJ.

1.5 Angiogenesis

A 3D angiogenesis assay in vitro was done as previously described [4]. Briefly, HUVECs were transfected with siNS or siRictor and were labeled with CellTracker Green (Life Technologies). Cytodex beads were coated with HUVECs (~400 cells/bead) and cultured for 4 hours in (M199, 10%FBS, 20 ng/ml VEGF). The beads were washed twice, suspended in fibrinogen (2 mg/mL) containing aprotinin (0.15 U/mL), and 0.625 U/mL thrombin was added. Angiogenesis growth media (M199, 10% FBS, 50 ng/ml VEGF) was then added on top. To inhibit mTORC1 versus mTORC1/2, rapamycin (5 nM) or PP242 (1-10 mM) were added, respectively, to both the fibrin gel and the growth media. To study tumor angiogenesis in vitro, HUVECs were pre-treated with PP242 (1 uM), ku-0063794 (50 nM) or rapamycin (5 nM) for 24 hours, then labeled with CellTracker Green (Life Technologies). Caki-1 human renal cell carcinoma cells (ATCC; Manassas, VA) were labeled with CellTracker Red. Cytodex beads were coated with HUVECs or Caki-1 (~400 cells/bead) then embedded in fibrin gel. Growth media (M199, 8% FBS) containing Caki-1 (20,000/well) in suspension was then added on top. At least 90 beads per treatment from each experiment were imaged after 18-20 hours incubation in 5% CO2 at 37° C, using a 20X objective lens and a CCD camera equipped inverted fluorescence microscope (Leica, Concord, ON). Scoring was done using OpenLab (PerkinElmer; Waltham, MA).

Assay of angiogenesis in vivo was performed as described previously [5]. Briefly, collagen onplants were generated by superimposing two square-gridded nylon meshes on which 30 µl of 4.73 mg/ml rat tail collagen with VEGF (100 ng/onplant) was placed. Following collagen polymerization, the onplants were placed on the chorio-allantoic membrane (CAM) of 10-day-old shell-less chick embryos. Embryos were incubated for 64 hours at 37° C, then the extent of onplant vascularization was quantified. Newly formed vessels were identified by imaging the

upper mesh of the onplant with a dissecting microscope. Images were captured at 6.3x using a StereoLumar V12 fluorescence dissection microscope (Carl Zeiss). The angiogenic index of each onplant was determined as the percentage of grids with newly formed blood vessels out of the total number of grids in the upper mesh.

1.6 Electrical cell-substrate impedance sensing (ECIS)

Cell-matrix adhesion and cell migration were tested using the ECIS device (Applied BioPhysics Inc., Troy, NY). HUVECs were treated with PP242, siAkt1, siRictor, or siRaptor as indicated. Equal numbers of cells were seeded into gelatin-coated ECIS plates (Applied BioPhysics Inc.) with VEGF (20 ng/ml). Adhesion and migration were then assessed by continuous resistance measurements in optimum growth conditions over 12 hours. Electrical impedance in each experiment was normalized to the readings from empty wells.

1.7 Apoptosis assay

Apoptosis was measured in HUVECs in optimum growth conditions and after inducing apoptosis. To induce apoptosis, EC monolayers were washed, then incubated with cycloheximide (CHX; 3 μg/mL) and tumor necrosis factor-α (TNFα; 10 ng/mL) for 4 hours. HUVECs were incubated with the FITC-conjugated active caspase-3 reporter, DEVD-FMK, for 30 minutes at 37°C as directed by the manufacturer (Promokine, Heidelberg, Germany). Cells were trypsinized and combined with the floating cells in the medium. After brief washes, cells were analyzed by flow cytometry (LSR-Fortessa).

1.8 Immunofluorescence microscopy

HUVECs were cultured on gelatin-coated glass bottom microwell dishes (MatTek Corp., Ashland, MA). Cells were fixed for 10 minutes in 3% fresh paraformaldehyde in PBS, washed with PBS, then permeabilized and blocked in 3% BSA + 0.1% Triton X-100 in PBS for 30 minutes. Cells were washed in PBS then incubated with phalloidin-FITC or anti-vinculin-FITC, and DAPI in 1% BSA for 1 hour in room temperature. The cells were washed 3 times with PBS. Filamentous actin and vinculin were visualized at 40X using an inverted fluorescence microscope (Leica, Concord, ON), and focal adhesions were enumerated as described [6].

1.9 G-actin/F-actin in vivo assay

The separation of filamentous actin (F-actin) and globular actin (G-actin) was done according to the manufacturer's instruction (Cytoskeleton, Denver, CO, USA) by ultracentrifugation. The ratios of F-actin to G-actin in ECs were estimated by Western blot [7]. Cytochalasion D was used as a negative control and Phalloidin was used as a positive control [8].

1.10 Statistical analyses

Data are shown as mean ± SEM. Statistical analysis was performed by 1-way ANOVA as appropriate followed by the Bonferroni post-hoc test. Pairwise comparisons were done by paired Student t-test using Prism 5 (Graphpad, San Diego, CA). P values <0.05 were considered significant. Each experiment was done at least three times.

2 Materials and methods for chapter IV

2.1 Reagents

M199, HBSS, FBS, and endothelial cell growth supplement were purchased from Invitrogen (Burlington, ON). VEGF-A was from Peprotech (Princeton, NJ). Anti-tubulin- α, proteasome inhibitor (MG-132) [9] and lysosome inhibitor (CA-074) [10] were from Millipore (Temecula, CA). Hiperfect, non-silencing short interfering RNA (siRNA), FGD5 silencing siRNA and Rac1 silencing siRNA were from Qiagen Inc (Mississauga, ON). Anti-phospho-CortactinY421, anti-Cortactin, anti- phospho-VEGFR2Y1175, anti- VEGFR2 and anti-Dll4 were from Cell Signaling Technology (Danvers, MA). Anti- FGD5 was from Protein Tech (Chicago, IL). Anti ESM1 and human plasmin were from Sigma-Aldrich (St. Louis, MO). The FGD5-GFP plasmid (EX-H5293-M29) was purchased from GeneCopoeia (Rockville, MD).

2.2 Cell culture

Human umbilical vein ECs (HUVECs) were isolated from unidentified donors as described previously [3]. HUVECs under passage 6 were used for all experiments. Human microvascular endothelial cell line (HMEC-1) was a kind gift from Dr. Branko Braam. To optimize VEGF-induced signals, HUVECs were starved in M199 + 1% FBS overnight, then stimulated with 30 ng/ml VEGF. Caki-1 human renal cell carcinoma cells (ATCC; Manassas, VA) were grown in Minimum Essential Medium (MEM; invitrogen).

2.3 RNA interference

HUVECs were seeded at 70-80% confluency and transfected serially twice over two days with either 50 nM non-silencing (siNS) or specific siRNA using Hiperfect transfection reagent

according to the manufacturer's protocol. Protein expression was evaluated by Western blot. The coding sequence FGD5 siRNA (TTGGATGACATGGACCATGAA; cat no.: SI386680) were from Qiagen Inc (Mississauga, ON, Canada). The second sequence, siFGD5#2, is against the 3 untranslated regions of FGD5 and was purchased from Thermo Scientific (cat no. L-028077-01-0005; Lafayette, CO).

2.4 Western blot and immunoprecipitation

HUVEC monolayers were washed once with ice cold PBS and then lysed immediately on ice by RIPA buffer (10 mM Tris, pH 7.4, 100 mM NaCl, 1 mM EDTA, 1 mM EGTA, 5 mM NaF, 2 mM Na3VO4, 0.1% SDS, 0.5% Na deoxycholate, 1% Triton X-100, 10% glycerol, 1 mM PMSF) followed by boiling at 95°C for 5 minutes. Electrophoresis was done by SDS-PAGE. Electroblotting was on nitrocellulose membranes (Biorad). The membranes were immunoblotted overnight at 4°C in blocking buffer (5% BSA/TBS- Tween20). Proteins were detected using Luminata forte (EMD Millipore, Billerica, MA) and a Fluorchem FC2 CCD camera (Alpha Innotech). Protein bands were equally contrast enhanced by Adobe Photoshop CS3 then quantified by ImageJ.

For immunoprecipitation, Dynabeads Protein G (LifeTechnologies) were incubated with anti-FGD5, anti-VEGFR2 or non-specific IgG then the beads-Ab complex was incubated with cell lysate for 1 hour at room temperature. The Ab-Ag complex was eluted by SDS sample buffer then resolved by SDS-PAGE. For control, total cell lysate (TCL) was incubated with uncoated Dynabeads, eluted, then resolved by SDS-PAGE in parallel with the experimental samples.

2.5 Flow cytometry

FGD5 deficient or control HUVECs were starved overnight, stimulated with VEGF for one hour, fixed and stained with Alexa Fluor conjugated VEGFR2 rabbit mAb (Cell Signaling). After staining, cells were analyzed in a FACScan flow cytometer (LSR-Fortessa). Alexa Fluor conjugated rabbit IgG was used as the negative control.

2.6 Quantitative PCR

Total cellular RNA was extracted by using QIAzol® (Qiagen) and RNeasy Mini Kit (Qiagen) according to the manufacturer's instructions. A total 300 ng of RNA was used to synthesize cDNA by using QuantiTect Reverse Transcription Kit (Qiagen) following the manufacturer's instructions. qRT-PCR was carried out using the Mastercycler®ep realplex real-time PCR system (Eppendorf). The reaction mixture consisted of 1 μl of cDNA, 1 μl of 10 μM primers, and 10 μl of SYBR® Select Master Mix (Applied Biosystems) in a total volume of 20 μl. Experimental samples were first normalized to internal control HPRT and then to the control samples, and the fold changes were calculated based on $2^{-\Delta\Delta CT}$ method. The PCR primers used are listed in the table below. Abul Azad did the PCR experiments in this chapter.

2.7 Migration assay

A scratch was made across a confluent HUVEC monolayer using a sterile pipette tip. VEGF-driven cellular migration to cover the scratch area was monitored at the indicated time points [11]. Images of the exact same field were taken by 5X objective lens and a CCD camera−equipped inverted microscope (Leica, Concord, ON). Data represent the distance of cellular migration (the difference in size between the time zero scratch area, and the scratch area at each time point).

2.8 Protrusion assay

HUVECs were cultured on gelatin-coated delta T4 glass bottomed culture dishes, Bioptechs (Butler, PA), until confluency and then scratched by a sterile pipette. The growth media used was only supplied with VEGF to exclude involvement of other signaling pathways. The early protrusions formed by the polarized cells at the scratch edge were monitored by life cell imaging for 10 minutes 12. The protrusions from at least 30 cells per experiment were measured by ImageJ. Videos were recorded by 40X objective lens and a CCD camera−equipped inverted microscope with a heated stage, Bioptechs (Butler, PA).

2.9 Angiogenesis

A 3D angiogenesis assay in vitro was done as previously described [4]. Briefly, HUVECs were transfected with siNS or siFDG5 and were labeled with CellTracker Green (Life Technologies). Cytodex beads were coated with HUVECs (~400 cells/bead) and cultured for 4 hours in (M199, 8%FBS, 30ng/ml VEGF). The beads were washed twice, suspended in fibrinogen (2 mg/mL) containing aprotinin (0.15 U/mL), and 0.625 U/mL thrombin was added. Then angiogenesis growth media (M199, 8% FBS, 50 ng/ml VEGF) was added on top. To study tumor angiogenesis in vitro 13, HUVECs were labeled with CellTracker Green (Life Technologies) and Caki-1 human renal cell carcinoma cells (ATCC; Manassas, VA) were labeled with CellTracker Red. Cytodex beads were coated with HUVECs or Caki-1 (~400 cells/bead) then embedded in fibrin gel. Growth media (M199, 8% FBS) containing Caki-1 (20,000/well) in suspension was then added on top.

At least 30 beads per treatment from each experiment were imaged after 18-20 hours incubation in 5% CO2 at 37°C, using a 20X objective lens and a CCD camera−equipped inverted

fluorescence microscope (Leica, Concord, ON). Scoring was done using OpenLab (PerkinElmer; Waltham, MA).

Filopodia were imaged by 40X objective lens and an EMCCD camera−equipped spinning disk confocal (Quorum Technologies). Extended focus datasets were merged to produce the final images. Data represents the cumulative of 30 tip cells from three independent experiments.

To extract protein from the HUVEC sprouts, polymerized fibrin was treated by active plasmin (0.01 units; Sigma Aldrich) then HUVECs were isolated from the digested fibrin by centrifugation. HUVECs were lysed by RIPA buffer, and proteins expression was studied by Western blot.

2.10 Immunofluorescence Microscopy

Cells were fixed with 3% formaldehyde for 10 min. Cells were blocked and permeabilized with 3%BSA and 0.1% Triton x-100 for 30 minutes and then incubated with the following antibodies, diluted in 3% BSA: anti-VEGFR2, anti-phospho VEGFR2Y1175 (Cell Signaling), anti-FGD5 (Biorbyt Ltd), anti-Rab4, 7, 11 (Bioss Inc), anti-actin (Cytoskeleton Inc), processed for immunofluorescence and visualized using spinning disc confocal microscope with a 63X objective. Quantification of colocalized pixels was performed using Volocity software (PerkinElmir) on extended focus merge of datasets. FITC-conjugated anti mouse IgG was used as negative control. Colocalization measurements were obtained from three different regions in the cytosol for each cell. Data represents the cumulative of 45 cells from three independent experiments.

2.11 Statistical analyses

Data are shown as mean ± SEM. Statistical analysis was performed by 1-way ANOVA as appropriate followed by the Bonferroni post-hoc test. Pairwise comparisons were done by paired Student t-test using Prism 5 (Graphpad, San Diego, CA). P values <0.05 were considered significant. Each experiment was done at least three separate times.

3 Materials and methods for chapter V

3.1 Reagents

M199, HBSS, FBS, and endothelial cell growth supplement were purchased from Invitrogen (Burlington, ON). VEGF-A was from Peprotech (Princeton, NJ). Recombinant human SDF1, Cdc42 inhibitor (ML141) [14] from TORCIS, RAC1 inhibitor from Calbiochem. Hiperfect, non-silencing short interfering RNA (siRNA), FGD5 silencing siRNA and CXCR4 silencing siRNA were from Qiagen Inc (Mississauga, ON). S1P agonist, CYM5442 hydrochloride, was from TOCRIS Bioscience [15]. Anti-phospho-FAKY397, anti-FAK, anti- phospho-AktS473, anti-Akt, anti-CXR4, and anti-ERK were from Cell Signaling Technology (Danvers, MA). Anti-FGD5 was from Protein Tech (Chicago, IL).

3.2 Cell culture

Human umbilical vein ECs (HUVECs) were isolated as described previously [3]. All cells used in the experiments were under passage 6. Human microvascular endothelial cell line (HMEC-1) was a kind gift from Dr. Branko Braam. Unless otherwise specified, EC were incubated in low

serum media supplemented with VEGF for 12-18 hours prior to experimemts to upregulate CXCR4 and augment SDF1 effect.

3.3 Migration assay

A scratch was made across a confluent HUVEC monolayer using a sterile pipette tip. VEGF- or SDF1-driven cellular migration to cover the scratch area was monitored at the indicated time points. Images were taken by 5X objective lens and a CCD camera−equipped inverted microscope (Leica, Concord, ON). Data represent the distance of cellular migration (the difference in size between the time zero scratch area and the scratch area at each time point).

3.4 Angiogenesis

A 3D angiogenesis assay in vitro was done as previously described [4]. Briefly, HUVECs were labeled with CellTracker Green (Life Technologies). Cytodex beads were coated with HUVECs (~400 cells/bead) and cultured for 4 hours in (M199, 8%FBS). The beads were washed and suspended in fibrin (2 mg/mL). Then angiogenesis growth media (M199, 8% FBS, 50 ng/ml VEGF or 100ng/ml SDF1) was added on top. At least 30 beads per treatment from each experiment were imaged after 18-20 hours incubation in 5% CO2 at 37oC, using a 20X objective lens and a CCD camera−equipped inverted fluorescence microscope (Leica, Concord, ON). Scoring was done using OpenLab (PerkinElmer; Waltham, MA).

3.5 Immunofluorescence Microscopy

Cells were fixed with 3% formaldehyde for 10 min. Cells were blocked and permeabilized with 3%BSA and 0.1% TritonX for 30 minutes and then incubated with the following antibodies, diluted in 3% BSA: anti-VEGFR2, anti-phospho VEGFR2Y1175 (Cell Signaling), anti-FGD5

(Biorbyt Ltd), anti-Rab4, 7, 11 (Bioss Inc), anti-actin (Cytoskeleton Inc), processed for immunofluorescence and visualized using spinning disc confocal microscope with a 63X objective. Quantification of colocalized pixels was performed using Volocity software (PerkinElmir) on extended focus merge of datasets. Data represents the cumulative of 30 cells from three independent experiments. FITC-conjugated anti mouse IgG was used as negative control

3.6 RNA interference

HUVECs were seeded at 70-80% confluency and transfected serially twice over two days with either 50 nM non-silencing (siNS) or specific siRNA using Hiperfect transfection reagent according to the manufacturer's protocol. Protein expression was evaluated by Western blot.

3.7 Western blot

HUVEC monolayers were washed once with ice cold PBS and then lysed immediately on ice by RIPA buffer (10 mM Tris, pH 7.4, 100 mM NaCl, 1 mM EDTA, 1 mM EGTA, 5 mM NaF, 2 mM Na3VO4, 0.1% SDS, 0.5% Na deoxycholate, 1% Triton X-100, 10% glycerol, 1 mM PMSF) followed by boiling at 95°C for 5 minutes. Electrophoresis was done by SDS-PAGE. Electroblotting was on nitrocellulose membranes (Biorad). The membranes were immunoblotted overnight at 4°C in blocking buffer (5% BSA/TBS-Tween20). Proteins were detected using Luminata forte (EMD Millipore, Billerica, MA) and a Fluorchem FC2 CCD camera (Alpha Innotech). Protein bands were equally contrast enhanced by Adobe Photoshop CS3 then quantified by ImageJ.

3.8 Flow cytometry

FGD5 deficient or control HUVECs were incubated with VEGF for 18 hours, then fixed and stained with Alexa Fluor conjugated CXCR4 rabbit mAb (Cell Signaling). After 1 hour of staining and triple wash, cells were analyzed in a FACScan flow cytometer. Alexa Fluor conjugated rabbit IgG was used as the negative control.

3.9 Statistical analyses

Data are shown as mean ± SEM. Statistical analysis was performed by 1-way ANOVA as appropriate followed by the Bonferroni post-hoc test. Pairwise comparisons were done by paired Student t-test using Prism 5 (Graphpad, San Diego, CA). P values <0.05 were considered significant. Each experiment was done at least three separate times.

4 Materials and methods for chapter VI

4.1 Apelin knockout mice

The APLN -deficient ($APLN^{-/y}$) mice were generated and bred in a C57BL/6 background as previously described [16]. Apelin is deleted after exon 1, and functions as a null allele. Apelin is coded on the X chromosome. Therefore, mutant male mice are denoted as $apelin^{-/y}$, and are derived from intercrosses in a colony using $apelin^{-/+}$ females bred against wild type males. The mutant mice were backcrossed onto C57BL/6 mice, so they display $H\text{-}2^{b}$ Major Histocompatibility Complex class I. The mice genotype was confirmed by PCR and southern blotting in Gavin Oudit laboratory at the University of Alberta. Since heart function is normal in

unstressed APLN$^{-/y}$ mice until 6 months, all donor hearts were obtained from 8-14 week old mice for transplantation. C57BL/6 mice were purchased from Jackson Laboratories. The C57BL/6 mice subjected to surgery were 14-16 weeks old. All animal experiments were carried out in accordance with the Canadian Council on Animal Care Guidelines, and animal protocols were reviewed and approved by the Animal Care and Use Committee at the University of Alberta.

4.2 Cardiac allograft vasculopathey (CAV) mouse model

Hearts from 8-14 weeks donors were transplanted heterotropically as previously described [17,18]. Briefly, the inferior and superior vena cavae, and the pulmonary veins of the donor heart were ligated. Then the donor aorta and pulmonary artery were anastomosed to the recipient's abdominal aorta and inferior vena cava, below the renal arteries. Transplantation of male donor HY+ minor-MHC hearts to littermate females induced the immune response in the recipients and resulted in features of early coronary arterial endothelial injury as early as 2 weeks post transplantation, and severe progressive CAV by 8 weeks post transplantation. Of note, myocardial inflammation or injury was not documented in this mouse model [18]. Heart allograft function was successfully maintained over 12 weeks post transplantation. Surgeries were done by Dr Lin-Fu Zhu.

4.3 Marilyn mice

Marilyn Rag2-/- PD-1-/- (programmed death-1 [PD-1]-/-) mice lack the PD-1 expression and have monoclonal CD4+ T cells that are specific for the HY antigen. Marilyn Rag2-/- PD-1-/- mice were generated by intercrossing the T-cell receptor (TCR) transgenic Rag2-/- Marilyn mice

with C57BL/6-Pdcd1-/- mice [19]. All procedures followed the guidelines of the Canadian Council on Animal Care. The Marilyn mice were bred in Colin Anderson lab at the University of Alberta.

4.4 In vivo proliferation assay

Splenocytes from naïve female Marilyn Rag2-/- PD-1-/- mice were labeled with 5 μM CelltraceTM Violet proliferation dye (Invitrogen) according to manufacturer's protocols. Labeled splenocytes containing a total of 2.3-3.0 x 10^6 single positive anti-HY CD4+ T cells in PBS were transferred into the recipients through I.V. via tail vein.

4.5 Flow cytometry

Peripheral blood samples from the recipient mice on 1 and 3 days post adoptive cell transfer, and recipient splenocytes were stained after incubation with an FcR block. Fluorescent antibodies to mouse: TCR-β chain (TCRβ; H57–597), CD4 (GK1.5), CD8β (53–6.7), CD45R (B220; RA3–6B2) were purchased from eBioscience. BD LSR II (BD Biosciences) was used for the data acquisition. Flow cytometric data analysis was performed using FlowJo (Treestar software, Portland, OR). Gating strategies are shown in the figure below. The in vivo proliferation assay and the flow cytometry analysis were done by Jiaxin Lin from Dr Anderson's laboratory.

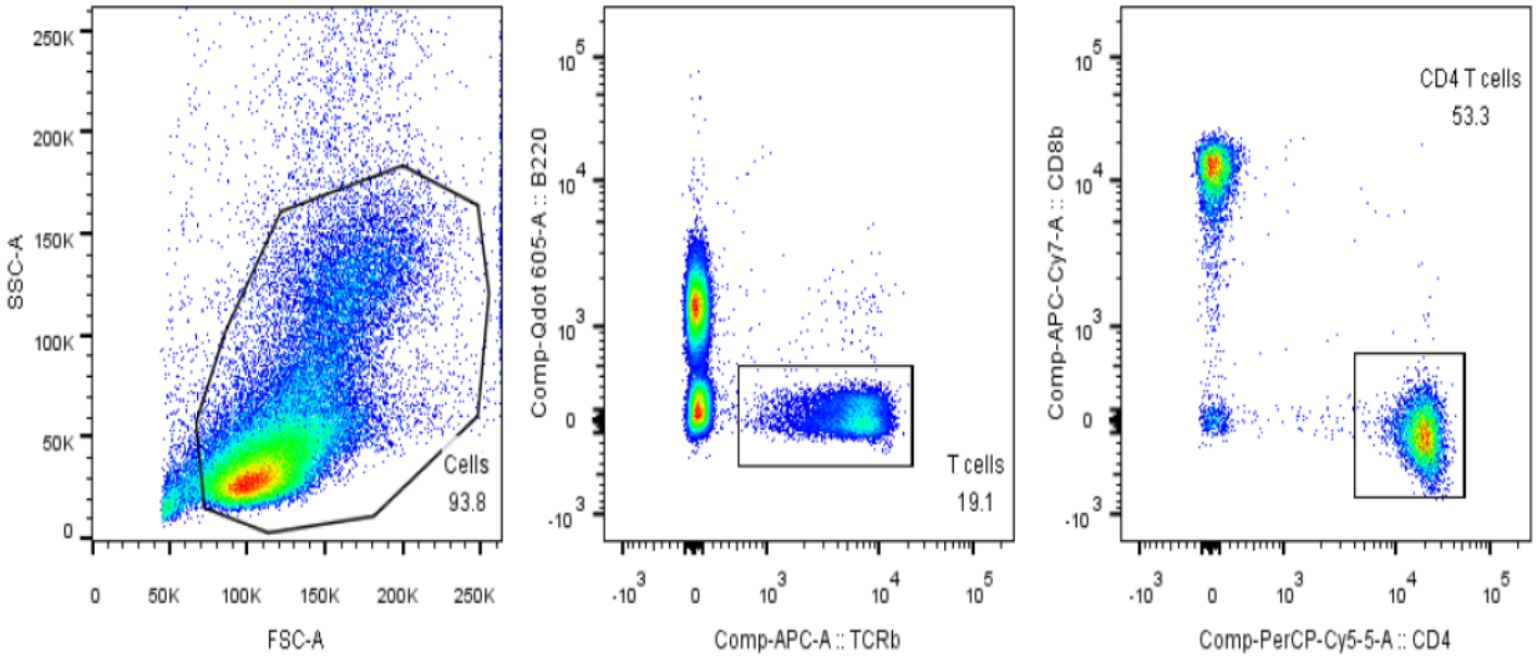

Fig 2. 1

4.6 Electrocardiographic (ECG) recordings

Mice were anesthetized using 2% isofluorane and body temperature was maintained using a heating pad. For native heart, electrodes were placed on the chest in lead I configuration. For transplanted heart, electrodes were placed on the abdomen near the base of the heart to improve P-wave detection. Native and transplanted hearts were recorded for 5 min simultaneously using two channel configuration of ACQ-7700 under control of ECG module of Ponemah Physiology platform (DSI, Data Sciences International; USA). Recordings were analyzed offline in ECG module of Ponemah Physiology platform. The following intervals were measured for native and transplanted hearts: RR, PR, QRS, and QT. Two types of QT correction were applied Bazett's and Federicia's [20,21]. Dr Pavel Zhabyeyev from Dr Oudit's laboratory provided technical support in regard to ECG recordings.

4.7 Histology and Immunohistochemical Staining

Mice were euthanized 2 weeks or 6 weeks post transplantation. Hearts were collected from euthanized mice, placed in IHC zinc fixative (BD Pharmingen™). The base of the heart that represents the origin of the coronaries was dissected and processed further. The tissues in the zinc fixative were paraffin embedded, sectioned and stained at the Hisotlogy Core Facility at the University of Alberta. Five um sections were taken every 100 um thickness of myocardium to ensure capturing the whole span of the base of the heart, then stained with Hematoxylin & Eosin (H & E) and Van Gieson specific eslastin stain. To quantitate CAV lesions, a region of interest was drawn at the internal elastic lamina and the endothelium margin of the coronary arteries in cross-section, then the relative area of proliferated intima was calculated.

4.8 Western blot

HUVECs were serum starved in M199 + 1% FBS (Invitrogen, Burlington, ON), then stimulated with 100 ng/ml human derived stromal factor 1 (SDF1) or 0.1 uM of apelin peptides as indicated. HUVECs were washed once with ice cold PBS, and lysed immediately on ice with RIPA buffer (Thermo Fischer Scientific). Cell lysates were boiled at 95°C for 5 min, resolved bySDS-PAGE, then electroblotted on nitrocellulose membranes (Bio-Rad). The membranes were immunoblotted using anti-phospho-eNOSS1177, antiphospho-AktS473 (Cell Signaling Technology, Danvers, MA), anti-actin (Cytoskeleton, Denver, CO) and anti-Akt (Protein Tech, Chicago, IL) and proteins were detected using Luminata forte (EMD Millipore, Billerica, MA) and a Fluorochem FC2 CCD camera (Alpha Innotech)

5 References

1. Feldman ME, Apsel B, Uotila A, et al. Active-site inhibitors of mTOR target rapamycin-resistant outputs of mTORC1 and mTORC2. PLoS biology. 2009;7(2):e1000038.

2. Garcia-Martinez JM, Moran J, Clarke RG, et al. Ku-0063794 is a specific inhibitor of the mammalian target of rapamycin (mTOR). Biochem J. 2009;421(1):29-42. doi: 10.1042/BJ20090489 [doi].

3. Zhang Q, Nakhaei-Nejad M, Haddad G, Wang X, Loutzenhiser R, Murray AG. Glomerular endothelial PI3 kinase-α couples to VEGFR2, but is not required for eNOS activation. American Journal of Physiology-Renal Physiology. 2011;301(6):F1242-F1250.

4. Nakatsu MN, Hughes CC. An optimized three-dimensional in vitro model for the analysis of angiogenesis. Methods Enzymol. 2008;443:65-82.

5. Zijlstra A, Lewis JD. Visualization and quantification of de novo angiogenesis in ex ovo chicken embryos. In: The textbook of angiogenesis and lymphangiogenesis: Methods and applications. Springer; 2012:217-240.

6. Angers-Loustau A, Cote JF, Charest A, et al. Protein tyrosine phosphatase-PEST regulates focal adhesion disassembly, migration, and cytokinesis in fibroblasts. J Cell Biol. 1999;144(5):1019-1031.

7. Hartwig JH. An ultrastructural approach to understanding the cytoskeleton. The Cytoskeleton: A Practical Approach.K.Carraway and C.Carraway, editors.Oxford University Press, Oxford, UK. 1992;23:45.

8. Casella JF, Flanagan MD, Lin S. Cytochalasin D inhibits actin polymerization and induces depolymerization of actin filaments formed during platelet shape change. . 1981.

9. Shibata T, Imaizumi T, Tamo W, et al. Proteasome inhibitor MG-132 enhances the expression of interleukin-6 in human umbilical vein endothelial cells: Involvement of MAP/ERK kinase. Immunol Cell Biol. 2002;80(3):226-230.

10. Montaser M, Lalmanach G, Mach L. CA-074, but not its methyl ester CA-074Me, is a selective inhibitor of cathepsin B within living cells. Biol Chem. 2002;383(7-8):1305-1308.

11. Liang C, Park AY, Guan J. In vitro scratch assay: A convenient and inexpensive method for analysis of cell migration in vitro. Nature protocols. 2007;2(2):329-333.

12. Meyer AS, Hughes-Alford SK, Kay JE, et al. 2D protrusion but not motility predicts growth factor-induced cancer cell migration in 3D collagen. J Cell Biol. 2012;197(6):721-729. doi: 10.1083/jcb.201201003; 10.1083/jcb.201201003.

13. Farhan MA, Carmine-Simmen K, Lewis JD, Moore RB, Murray AG. Endothelial cell mTOR complex-2 regulates sprouting angiogenesis. PloS one. 2015;10(8):e0135245.

14. Hong L, Kenney SR, Phillips GK, et al. Characterization of a Cdc42 protein inhibitor and its use as a molecular probe. J Biol Chem. 2013;288(12):8531-8543. doi: 10.1074/jbc.M112.435941 [doi].

15. Gonzalez-Cabrera PJ, Jo E, Sanna MG, et al. Full pharmacological efficacy of a novel S1P1 agonist that does not require S1P-like headgroup interactions. Mol Pharmacol. 2008;74(5):1308-1318. doi: 10.1124/mol.108.049783 [doi].

16. Kuba K, Zhang L, Imai Y, et al. Impaired heart contractility in apelin gene-deficient mice associated with aging and pressure overload. Circ Res. 2007;101(4):e32-42. doi: CIRCRESAHA.107.158659 [pii].

17. Corry RJ, Winn HJ, Russell PS. Primarily vascularized allografts of hearts in mice: The role of H-2D, H-2K, and non-H-2 antigens in rejection. Transplantation. 1973;16(4):343-350.

18. Russell PS, Chase CM, Madsen JC, et al. Coronary artery disease from isolated non-H2-determined incompatibilities in transplanted mouse hearts. Transplantation. 2011;91(8):847-852. doi: 10.1097/TP.0b013e3182122f82 [doi].

19. Thangavelu G, Gill RG, Boon L, Ellestad KK, Anderson CC. Control of in vivo collateral damage generated by T cell immunity. J Immunol. 2013;191(4):1686-1691. doi: 10.4049/jimmunol.1203240 [doi].

20. Fredericia L. Duration of systole in electrocardiogram. Acta med.Scandinav. 1920;53:469.

21. Bazett HC. An analysis of the time-relations of electrocardiograms. Heart. 1920;7:353-370.

Chapter III: Endothelial cell mTOR complex 2 regulates VEGF-induced angiogenesis

Abstract

Tumor neovascularization is targeted by inhibition of vascular endothelial growth factor (VEGF) or the receptor to prevent tumor growth, but drug resistance to angiogenesis inhibition limits clinical efficacy. Inhibition of the phosphoinositide 3 kinase pathway intermediate, mammalian target of rapamycin (mTOR), also inhibits tumor growth and may prevent escape from VEGF receptor inhibitors. mTOR is assembled into two separate multi-molecular complexes, mTORC1 and mTORC2. The direct effect of mTORC2 inhibition on the endothelium and tumor angiogenesis is poorly defined. We used pharmacological inhibitors and RNA interference to determine the function of mTORC2 *versus* Akt1 and mTORC1 in human endothelial cells (EC). Angiogenic sprouting, EC migration, cytoskeleton re-organization, and signaling events regulating matrix adhesion were studied. Sustained inactivation of mTORC1 activity up-regulated mTORC2-dependent Akt1 activation. In turn, ECs exposed to mTORC1-inhibition were resistant to apoptosis and hyper-responsive to renal cell carcinoma (RCC)-stimulated angiogenesis after relief of the inhibition. Conversely, mTORC1/2 dual inhibition or selective mTORC2 inactivation inhibited angiogenesis in response to RCC cells and VEGF. mTORC2-inactivation decreased EC migration more than Akt1- or mTORC1-inactivation. Mechanistically, mTORC2 inactivation robustly suppressed VEGF-stimulated EC actin polymerization, and inhibited focal adhesion formation and activation of focal adhesion kinase, independent of Akt1. Endothelial mTORC2 regulates angiogenesis, in part by regulation of EC focal adhesion kinase activity, matrix adhesion, and cytoskeletal remodeling, independent of Akt/mTORC1.

Introduction

Drug therapy to inhibit tumor neovascularization is used clinically as an adjuvant in chemotherapy–resistant cancers, including renal cell carcinoma, recurrent glioblastoma, and bowel cancer. The rapalog mammalian target of rapamycin (mTOR) inhibitors are used after failure of pro-angiogenic growth factor –receptor tyrosine kinase inhibitors, and in some cases as first line therapy [1]. Rapalog mTOR inhibition decreases Vascular Endothelial Growth Factor (VEGF) production by the tumor to reduce tumor neovascularization and inhibit tumor growth [2,3]. However, this therapeutic approach is limited by the development of resistance of the tumor and microvasculature to the effect of rapalog mTOR inhibition [4,5]. This "escape" of the vasculature from the effects of current mTOR inhibitors emphasizes the need for new agents with durable effects.

In mammalian cells, mTOR is assembled in two distinct signaling complexes: mTOR complex-1 (mTORC1), sensitive to inhibition by rapalog drugs, and mTOR complex-2 (mTORC2) [6]. In addition to the mTOR catalytic subunit, mTORC1 consists of raptor (regulatory associated protein of mTOR), mLST8 (also termed G-protein β-subunit-like protein, GβL, a yeast homolog of LST8), and PRAS40 (proline-rich Akt substrate 40 kDa). mTORC1 activity is best characterized by phosphorylation of ribosomal protein S6 kinase (S6K) and eukaryotic translation initiation factor 4E-binding protein 1 to regulate translation [7]. mTORC2 similarly includes mTOR and mLST8, but raptor is replaced by two mTORC2-specific proteins: rictor (rapamycin-insensitive companion of mTOR), and mSin1 (mammalian stress-activated protein kinase-interacting protein 1). The principal known target of mTORC2 is Akt, a key survival enzyme, and upstream regulator of mTORC1 [7]. The targets of mTORC1 are well-defined, but much less is known regarding mTORC2-mediated effects independent of Akt/ mTORC1.

Pro-angiogenic cues are recognized by activation of several growth factor receptors displayed on the vascular endothelium, and the diverse signals are integrated to recruit key signal transduction pathways in the endothelial cell (EC). For example, the principal endothelial VEGF receptor, VEGF-receptor 2, is coupled to phosphatidylinositide 3 (PI3)-kinase, signaling to the downstream mTOR kinase [8]. In pre-clinical models, mTORC1 inhibition reduces early vessel growth to VEGF stimulation [2,3,9]. Nevertheless, vessel development and tumor growth proceeds in humans treated with rapalog drugs, prompting the investigation of agents that inhibit mTOR in both complexes [10].

The effect of disrupted signaling of the mTORC2 branch point on the PI3 kinase pathway in the endothelium is poorly understood, but may contribute anti-angiogenic effects [11]. In this paper we report that genetic inactivation of mTORC1 activity or inhibition by rapamycin paradoxically upregulates mTORC2 and Akt activity in primary human ECs. Pharmacologic inhibition or genetic disruption of mTORC2 by rictor knock-down optimally blocks VEGF-stimulated angiogenic sprouting of human ECs *in vitro*. Mechanistically, we identify that mTORC2 activity in ECs is needed for cell migration, development of mature matrix adhesion structures, and specifically regulates VEGF-stimulated Src and focal adhesion kinase activity.

Results

Exposure to rapamycin activates endothelial Akt

In tumor cells, active mTORC1 participates in a negative regulatory loop that inhibits serine 473 (S473) phosphorylation full activation of Akt. Inhibition of mTORC1 relieves this inhibition, but

has a variable and cell-type specific effect on upstream growth factor receptor signaling [18,19]. We sought to determine if this mechanism is present in primary human ECs, since these events could contribute to resistance to rapalog anti-angiogenesis treatments. First, we treated ECs with rapamycin for 1 hour, then stimulated the cells with VEGF. Rapamycin inhibited VEGF-stimulated, mTORC1-dependent phosphorylation of S6K in dose-dependent manner (Fig 3.1A-C). We determined rapamycin 5 nM optimally inhibited VEGF-stimulated mTORC1 signaling. Next, we sought to model chronic *in vivo* exposure of ECs to rapamycin by treatment with 5 nM rapamycin for 24 hours. Paradoxically, sustained exposure to rapamycin increased Akt S473 phosphorylation, the mTORC2-dependent site, in a dose-dependent manner (Fig 3.1D, E). Rapamycin treatment at 5 and 10 nM increased Akt S473 phosphorylation ~2.4 ± 0.4 and ~2.7 ± 0.4 fold (mean ± SEM) compared to the control carrier treatment, respectively (Fig 3.1E). Similarly, sustained inhibition of mTORC1 with rapamycin in human microvascular ECs (HMEC-1) increased Akt S473 phosphorylation Fig 3.2).

To determine if mTORC2- had the same effect as mTORC1- inactivation, we specifically disrupted EC mTORC2 or mTORC1 using siRNA targeted against rictor or raptor, respectively [20,21]. We observed that sustained mTORC1 disruption persistently blocked S6K phosphorylation, but increased phosphorylation of Akt S473 ~2.5 fold and its down stream target, FOXO1/3 S319, compared to control (Fig 3.1F, G). Conversely, mTORC2 disruption markedly lowered Akt S473 phosphorylation compared to control (Fig 3.1G, G). Notably, specific disruption of mTORC2 also blocked FOXO and S6 kinase phosphorylation (Fig 3.1F, H). These data indicate sustained inactivation of mTORC1, but not mTORC2, relieves feedback inhibition to drive hyper-activation of the PI3 kinase/ Akt pathway in primary human ECs.

Next, we sought to study the effect of dual mTORC1 and mTORC2 inhibition on VEGF-stimulated EC Akt activation. Selective mTOR kinase inhibitors are active against mTOR in both complexes [12]. Pretreatment of EC with PP242 or Ku-0063794 inhibited VEGF-stimulated Akt activation in a dose-dependent manner, and we determined the optimal inhibitory concentration of the compounds (data not shown). Like rictor knock-down to disrupt mTORC2 formation (Fig 3.1F-H), sustained pharmacologic inhibition of mTORC1 + mTORC2 using either PP242 or Ku-0063794 did not increase Akt phosphorylation or Akt activity in EC (Figs 3.2 and 3.3).

mTORC1 sustained inhibition increases resistance to apoptosis and pre-sensitized EC to angiogenic cues

We evaluated the effect of sustained rapalog exposure on EC function. Akt activity mediates an important cellular pro-survival pathway, hence we sought to determine the effect of extended mTORC1/2 *versus* mTORC1 inactivation on EC apoptosis. We challenged the EC with pro-apoptotic factors, then quantified active cleaved caspase 3 expression among rapamycin-, PP242-, or Ku-0063794-pretreated ECs. We observed that extended mTORC1 inhibition increased EC resistance to apoptosis *versus* mock-treated, or mTORC1/2 inhibited EC (Fig 3.4A). Conversely, treatment with the PP242 or Ku-0063794 compound did not confer similar resistance. Further, we investigated the effect of extended mTORC1 inhibition on sprouting angiogenesis of human ECs to tumor cells. ECs were pre-treated with rapamycin, PP242 or Ku-0063794 for 24 hours, then embedded in a 3D fibrin matrix with human RCC cells in the absence of exogenous pro-angiogenic growth factors and compounds. Tumor cells stimulated EC sprouting, which was increased by rapamycin but not PP242 or Ku 0063794 pre-exposure (Fig 3.4B, C). Similarly, rapamycin pre-exposure increased EC migration toward tumor cells in Boyden chamber

chemotaxis assay (data not shown). These observations suggest that mTORC1/2 inactivation may be more effective than mTORC1 inhibition to block tumor neoangiogenesis.

mTORC1 + mTORC2 dual inhibition reduces VEGF-induced angiogenesis

Next we studied the effect of mTOR inhibition on sprouting angiogenesis of human primary ECs in response to VEGF. Primary human ECs were loaded on microcarrier beads and embedded in 3D fibrin gels, then treated with PP242. Consistent with the effect on tumor angiogenesis, PP242 treatment markedly reduced human EC sprout formation, and reduced the elongation of the few endothelial sprouts that developed in response to VEGF (Fig 3.5A, B, C). Similar findings were obtained using a second mTORC1/2 inhibitor in microvascular ECs (Fig 3.6).

To determine the effect of mTORC1/2 inhibition on VEGF-stimulated neovascularization *in vivo*, while avoiding confounding effects of the compound on stromal cell production of VEGF, PP242 or carrier was added to VEGF-loaded onplants deposited on the chick embryo CAM, then microvessel density was measured after 3 days. As shown in (Fig 3.5D) and (Fig 3.7), we observed that PP242 inhibited new vessel formation in a concentration-dependent manner. It is worth noting that the inhibitor concentration required to inhibit neovascularization was higher *in vivo* than *in vitro* likely due to the diffusion-associated loss of PP242 concentration during the CAM assay. Taken together, these data indicate that dual inhibition of mTORC1/2 activity has potent anti-angiogenesis effects, acting directly on the vascular EC.

Specific mTORC2 disruption inhibits VEGF-stimulated angiogenesis

In complementary experiments, we used RNA interference to specifically inactivate mTORC2 activity in ECs. We used two different siRNA against rictor (siRict[1] and siRict[2]) to disrupt mTORC2, and confirmed the effect of the knock-down in EC by Western blot of rictor expression, and mTORC2 activity by Akt S473 phosphorylation (Fig 3.8A). Rictor siRNA treatment reduced EC rictor and Akt S473 phosphorylation by ~80% (Fig 3.8B). Specific disruption of mTORC2 markedly inhibited VEGF-stimulated angiogenic sprouting of ECs. Primary human ECs were transfected with siRict, then evaluated for sprouting into 3D fibrin gels. We observed mTORC2 disruption reduced the number of sprouts by ~75% (Fig 3.8C, D). In addition, among the sprouts that developed, mTORC2 disruption markedly reduced EC sprout extension into the fibrin gel (Fig 3.8E). This indicates that mTORC2 activity is required for angiogenic sprouting, and inactivation of mTORC2 additionally reduces sprout length.

mTORC2 regulates EC migration and cell-matrix adhesion independent of Akt and mTORC1 activity

Next we sought to determine if Akt-dependent signaling mediates the contribution of mTORC2 to angiogenesis. Akt activity is regulated in parallel by PDK1-dependent T308 phosphorylation in the activation loop of Akt, and enhanced by S473 phosphorylation mediated by mTORC2 to regulate a subset of Akt-dependent responses [22]. Using RNA interference we selectively knocked-down expression of Akt1 (the dominant Akt isoform in ECs) or rictor, then we studied the effect of EC Akt1*versus* mTORC2 loss on ECs *in vitro.* The level of Akt1 after knockdown is shown in (Fig 3.9).

To examine migration of rictor-, Akt1-, and raptor-deficient ECs, we wounded confluent EC monolayers using a high-field electric current. We observed a modest decrease in the closure of the wound, indicating EC migration was impaired, among both Akt1- and raptor-deficient cells (Fig 3.10A and Fig 3.11). However, loss of rictor conferred a striking decrease in wound closure. EC migration and sprout elongation require EC adhesion and anchorage to the surrounding matrix. Hence we determined the effect of mTORC2-inactivation on cell-matrix interaction. Integrin-mediated cell adhesion was reduced by 73 ± 3% after mTORC1 + mTORC2-inactivation, and by 66 ± 10% (mean ± SEM) among mTORC2-disrupted ECs compared to control ECs, measured by electrical impedance after seeding ECs on gelatin-coated electrodes (Fig 3.10B and Fig 3.12). Notably, we observed disruption or PP242-mediated inhibition of mTORC2 was more potent than inactivation of Akt to block EC adhesion. These results suggest mTORC2 mediates regulation of EC movement and adhesion, independent of Akt1/mTORC1.

In yeast, TORC2 regulates cytoskeleton remodeling independent of Akt, but this is not observed in embryonic fibroblasts isolated from mTORC2-disrupted knockout mice [21,22,23]. Since cytoskeletal remodeling is involved in cell migration and angiogenic sprout elongation, we studied the effect of mTORC2 inactivation on actin polymerization among primary human ECs. Immunofluorescence staining for polymerized actin showed a paucity of stress fibers in VEGF-stimulated, mTORC2-inactivated, adherent ECs compared to control ECs (Fig 3.10C). Similarly, protein analysis showed that the ratio of filamentous to globular actin was markedly reduced in mTORC2-disrupted adherent ECs (Fig 3.10D, E). Further, the F-/G-actin ratio was significantly reduced in mTORC2-disrupted ECs compared to Akt1-deficient ECs, consistent with mTORC2-mediated, Akt1-independent regulation of actin remodeling.

mTORC2 regulates focal adhesion kinase

Defective adhesion, motility, and stress fiber formation in mTORC2-inactivated ECs suggested formation of focal adhesion complex structures that mediate cell interactions with extracellular matrix might be defective. Focal adhesion kinase (FAK) is a principal regulator linking growth factor signals to cell-matrix adhesion and cytoskeleton remodeling [24]. Therefore, we investigated the effect of mTORC2-disruption on FAK activity. VEGF-stimulated FAK Y397 auto-phosphorylation was reduced in mTORC2-disrupted EC monolayers compared to controls, whereas Akt1 knockdown had no effect (Fig 3.13A, B). Moreover, VEGF-stimulated FAK phosphorylation and Src Y418 phosphorylation, an upstream regulator of FAK subcellular localization and activity [25] was completely inhibited in mTORC2- *versus* Akt1-inactivated ECs (Fig 3.13C, D). Similarly, inhibition of mTORC2 for 18 hours dramatically decreased FAK phosphorylation among PP242- (Fig 3.13E, F) or Ku-0063794- (Fig 3.2) treated EC, whereas mTORC1 inhibition with rapamycin did not affect FAK activity. In contrast, phosphorylation of eNOS, a known substrate of Akt, was similarly blunted by rictor or Akt1 knockdown in response to VEGF stimulation (Fig 3.13C).

Finally, we directly examined the effect of mTORC2 inactivation on matrix adhesion structures in EC. Adherent mTORC2-disrupted ECs were immunostained for the focal adhesion complex protein, vinculin, and the number of complexes were quantitated (Fig 3.14A, B). We observed the number of focal adhesions per EC was reduced in mTORC2-inactivated ECs by 69 ± 2 % (mean ± SEM) *versus* control ECs (Fig 3.14B). Together, these results indicate that mTORC2 regulates FAK activation and EC focal adhesion formation independent of Akt1.

Discussion

At therapeutic concentrations, rapalog drugs primarily inhibit tumor neovascularization through inhibition of mTORC1-dependent VEGF production [2,3], to blunt tumor angiogenesis [9,26,27]. However, rapalog treatment is limited by escape of the tumor and vasculature from drug inhibition, and subsequent tumor progression [5,28,29]. Indeed withdrawal or interruption of angiogenesis inhibitor treatment may be associated with a flare of angiogenesis and tumor growth [30,31,32,33]. Understanding the events in the endothelial cell underlying the inhibitor drug effects on angiogenesis will guide development of better drugs that target tumor neovascularization. We examined the differential effects on angiogenesis of mTORC2 inactivation or dual mTORC1/2 inhibition *versus* selective mTORC1 inhibition in EC.

We observed that sustained inhibition of mTORC1 with rapamycin paradoxically up-regulated endothelial mTORC2 and Akt activity, promoted resistance of the EC to pro-apoptotic stress conditions, and sensitized EC to cancer cell-stimulated angiogenic sprouting. Conversely, dual inhibition of mTORC1/2 prevented hyper-stimulation of the PI3 kinase pathway, and markedly decreased tumor- and VEGF-mediated angiogenic sprouting among human primary ECs in 3D angiogenesis *in vitro*. Selective gene silencing experiments showed that mTORC2 disruption was sufficient to prevent PI3 kinase pathway hyper-activation in the endothelium, did not confer increased sensitivity to VEGF pro-angiogenic stimulation, and inhibited angiogenesis both *in vitro* and *in vivo* more effectively than mTORC1 inhibition. Moreover, disruption of mTORC2 had an additive effect to Akt1 loss to directly inhibit angiogenic sprouting. We demonstrated that

mTORC2 activity regulates EC sprout extension in 3D matrices, which correlates with defects in migration, cell-matrix adhesion, cytoskeleton remodelling, and focal adhesion formation. These effects are linked to Akt1-/mTORC1-independent, but mTORC2-dependent regulation of VEGF-stimulated FAK activation in ECs.

VEGF-receptor recruitment of the PI3 kinase/ Akt/ mTORC1 pathway in the EC plays a critical role in embryonic vascular development, and postnatal neovascularization in several important clinical contexts. Pathological tumor angiogenesis is linked to VEGF-stimulated PI3 kinase/ Akt and mTORC1 activation in the endothelium [2,9,34]. These direct effects of mTORC1 inhibitors on the endothelium likely contribute to an anti-angiogenic effect of rapalog drug adjuvant treatments for advanced cancers. However, escape of the vasculature from the effects of current rapalog mTORC1 inhibitors may by blocked by investigational agents with dual effects to inhibit mTOR activity in both complexes [10,35]. Emerging preclinical studies of mTOR active site inhibitors demonstrate variable control of tumor growth [11,36,37,38,39,40]. However, the relative effects of investigational mTOR active-site inhibitory drugs on tumor cell growth, production of vascular growth factors, *versus* direct effects on the host vasculature in *in vivo* mouse xenograft models are difficult to determine. The current data indicate that the mTOR active site inhibitory agents have direct anti-angiogenic effect on the vascular endothelium.

Recent work has identified complex feedback regulation between mTORC1 inhibition and growth factor-dependent PI3 kinase activity in cancer cells, and cancer cell responses to both receptor tyrosine kinase and androgen receptor stimulation [18,41]. The signal transduction

pathway is mediated upstream by PI3 kinase isoform activation by the receptor, then direct and indirect activation of downstream mTORC2, Akt, and mTORC1 to regulate cell metabolism and growth. Inhibition of mTORC1 with rapamycin relieves constitutive inhibition, and further hyper-activates the upstream pathway [18,41]. Our data indicate that a similar EC adaptation to sustained disruption of mTORC1 signalling can prime the endothelium to resist growth factor deprivation, and to respond robustly to tumor-derived pro-angiogenic cues upon interruption in drug administration. Among tumor cells, chronic mTORC2 inhibition may be insufficient to prevent PI3 kinase pathway hyper-stimulation, and hyper-phosphorylation of the Akt target, FOXO1/3 [42]. Our data highlights that a tumor may nevertheless be targeted indirectly through the normal EC mTOR signaling pathway which maintains sensitivity to mTORC2 inhibition.

In addition to the important regulatory effects of mTORC2 on cell metabolism and regulation of growth factor receptor activity mediated through Akt-dependent signaling, we identify a new mTORC2-dependent pathway to regulate cytoskeletal remodelling in angiogenic EC. In yeast, TORC2 regulation of actin structures is recognized, and is shown to be mediated through a PKC homolog [23]. However, mTORC2 regulation of cytoskeleton dynamics in mammalian cells has been controversial. Although disruption of mTORC2 by RNA interference in tumor cell lines affects cell shape, no effect of mTORC2 loss is seen in mouse embryonic fibroblasts derived from either rictor or mLST8-knockout mice [22]. In response to VEGF stimulation, we observe a reduction in angiogenic sprouting of primary human ECs, and a marked decrease in the length of sprout extension after inactivation of mTORC2 in VEGF-stimulated 3D angiogenesis. Defective EC adhesion, migration, and actin remodeling were strikingly more pronounced by mTORC2 inactivation compared to Akt1 knockdown, consistent with an independent contribution of

mTORC2 signalling. This correlates with defective formation of organized focal adhesion complexes that anchor actin stress fibres to enable cell contractility and movement.

We identify FAK as a novel downstream effector coupled to VEGF-stimulated mTORC2 activity, independent of Akt/mTORC1. Once EC bind to extracellular matrix, the integrin intracellular domain promotes local assembly of structural and signal transduction molecules, such as Src and FAK, to support actin polymerization and cell migration [43,44]. VEGF stimulation induces remodelling of the complexes associated with Src and FAK phosphorylation. Observations in FAK knockout mice provide direct evidence supporting the role of FAK in angiogenesis, as genetic deletion of FAK in mice is embryonic lethal due to cardiovascular defects [24,45]. Similarly, both rictor and mLST8 subunits of mTORC2 are strongly expressed in the developing vasculature, and mTORC2-disrupted mutant mice die with defective vascular development [22].

The current data suggest mTORC2 indirectly regulates FAK activity, since FAK Y397 phosphorylation is not expected to be mediated by the mTOR serine-threonine kinase activity. The integrin-linked kinase (ILK) has been previously identified both outside and as a component of the mTORC2, and shown to participate in regulation of Akt [46]. Our data indicates that FAK regulation is dependent on mTOR activity, rather than ILK, since FAK phosphorylation is abolished both with disruption of mTORC2 formation after rictor knock-down, and by specific pharmacologic inhibition of mTOR activity. Finally, our data is consistent with previous findings that VEGF-stimulated FAK activation is dependent on VEGFR2 association with integrin, and

induction of Src activity in an amplification loop [25,47,48,49]. Our data indicates VEGF-stimulated mTORC2 activity is required upstream of both Src and FAK to remodel matrix adhesion sites.

In summary, our results show that sustained mTORC1 inhibition activates maladaptive PI3 kinase signaling to Akt and responsiveness to proangiogenic growth factors in primary human ECs. In contrast, mTORC2 inactivation prevents Akt and downstream FOXO1/3, or S6 kinase hyper-stimulation. Moreover, mTORC2 regulates EC matrix adhesion, motility, and angiogenesis *in vitro* independent of downstream Akt-regulated events. These data indicate that mTORC2 in the endothelium is an attractive target to inhibit pathologic neoangiogenesis.

Acknowledgements

The authors would like to acknowledge Maria Obeidat, Qui-Xia Zhang, and Steve Kulak for their technical support.

Figures

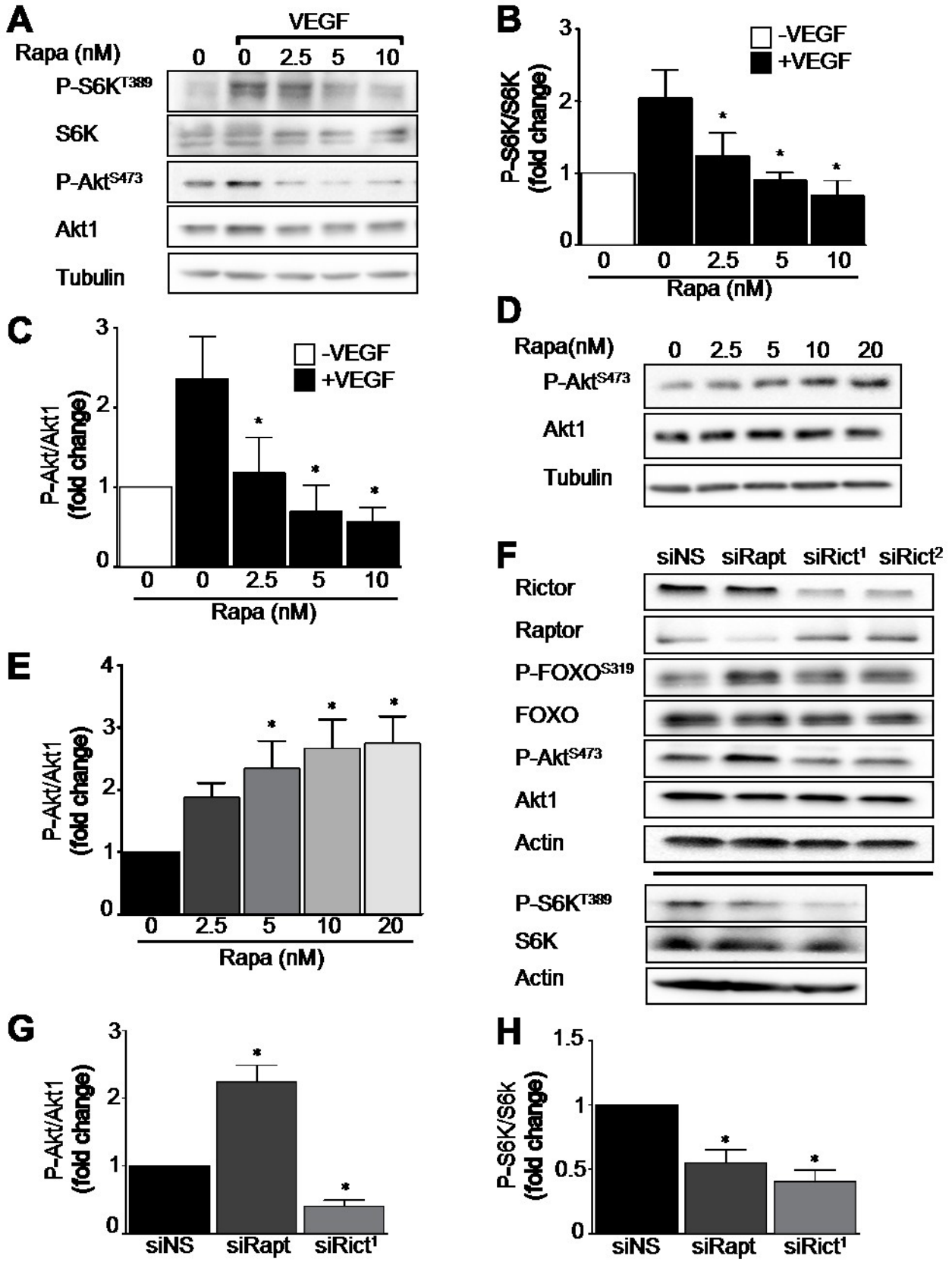
A
VEGF
Rapa (nM)
0
0
2.5
5
10
P-S6K^{T389}
S6K
P-Akt^{S473}
Akt1
Tubulin
B
-VEGF
+VEGF
P-S6K/S6K (fold change)
Rapa (nM)
C
-VEGF
+VEGF
P-Akt/Akt1 (fold change)
Rapa (nM)
D
Rapa(nM)
0
2.5
5
10
20
P-Akt^{S473}
Akt1
Tubulin
E
P-Akt/Akt1 (fold change)
Rapa (nM)
F
siNS
siRapt
siRict^{1}
siRict^{2}
Rictor
Raptor
P-FOXO^{S319}
FOXO
P-Akt^{S473}
Akt1
Actin
P-S6K^{T389}
S6K
Actin
G
P-Akt/Akt1 (fold change)
siNS
siRapt
siRict^{1}
H
P-S6K/S6k (fold change)
siNS
siRapt
siRict^{1}

Fig 3. 1

Fig 3.1. Sustained mTORC1, but not mTORC2, inhibition activates Akt. HUVECs were treated by rapamycin, two different small interfering RNAs against rictor (siRict[1] and siRict[2]) or raptor (siRapt), or non-silencing siRNA (siNS), then stimulated with 20 ng/mL VEGF as indicated. Akt phosphorylation and S6K phosphorylation were evaluated as described in Materials and Methods. **A**) A representative Western blot of the effect of Rapamycin pretreatment for 1 hour on VEGF-stimulated Akt and S6 kinase phosphorylation in HUVECs. **B)** Quantitation of phospho-S6K. **C)** Quantitation of phospho-Akt (n=5 independent experiments, $*P<0.05$ by ANOVA). The effect of rapamycin treatment of HUVEC for 24 hours. **D)** A representative Western blot of HUVEC phospho-Akt, total-Akt1 and tubulin over a range of concentration of rapamycin exposure. **E)** Quantitation of phospho-Akt (n=5 independent experiments, $*P<0.05$ by ANOVA). The effect of mTORC1 *versus* mTORC2 disruption on Akt signaling in EC. **F)** A representative Western blot of HUVEC rictor, raptor, phospho-Forkhead box protein O1/3 (P-FOXO1/3), phospho-Akt, total Akt1, phospho-S6K, total S6K, and actin after treatment with siRapt, siRict or siNS. **G)** Quantitation of phospho-Akt. **H)** Quantitation of phospho-S6K (n=3 independent experiments, $*P<0.05$ by ANOVA).

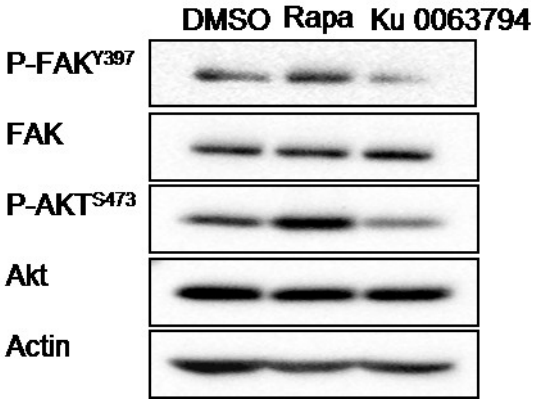

Fig 3. 2

Fig 3.2. Sustained mTORC1+2, but not mTORC1, inhibition reduces EC Akt and focal adhesion kinase activation. **A)** HMEC-1were treated with the mTORC1/2 inhibitor Ku 0063794 (50 nM), or Rapamycin, and stimulated with VEGF overnight. A representative Western blot of EC phospho-FAK, total FAK, phospho-Akt, total Akt and actin (n=3 independent experiments).

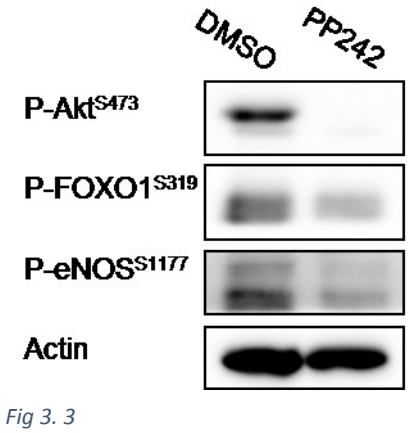

Fig 3.3. Sustained mTORC1+2 inhibition reduces Akt activity. HUVECs were treated with PP242 overnight. A representative Western blot of EC phospho-Akt, phospho-FOXO1/2, phospho-eNOS and actin (n=3 independent experiments).

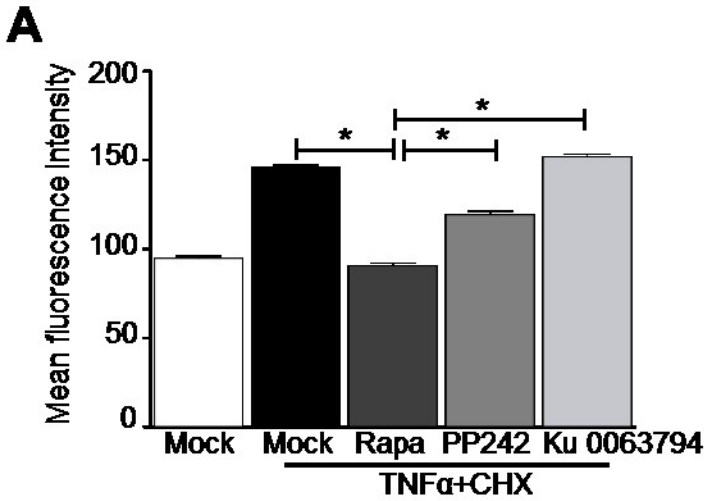
A
Mean fluorescence intensity
200
150
100
50
0
*
*
*
Mock
Mock
Rapa
PP242
Ku 0063794
TNFα+CHX

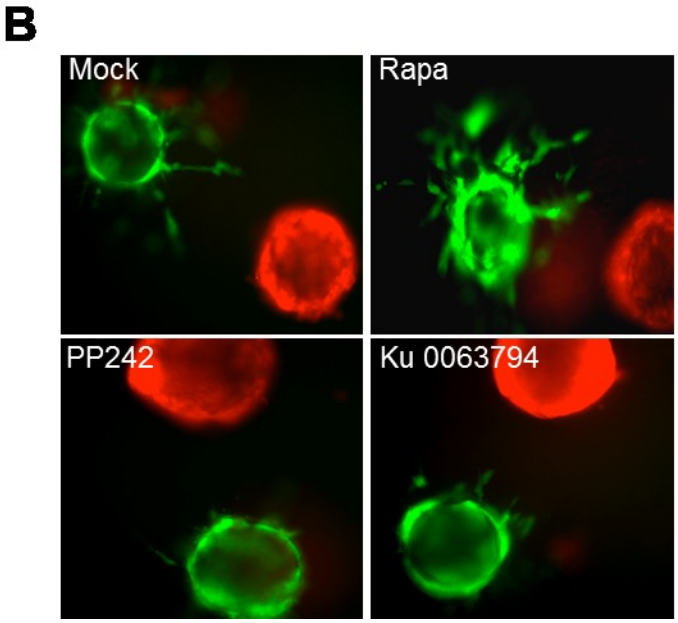
B
Mock
Rapa
PP242
Ku 0063794

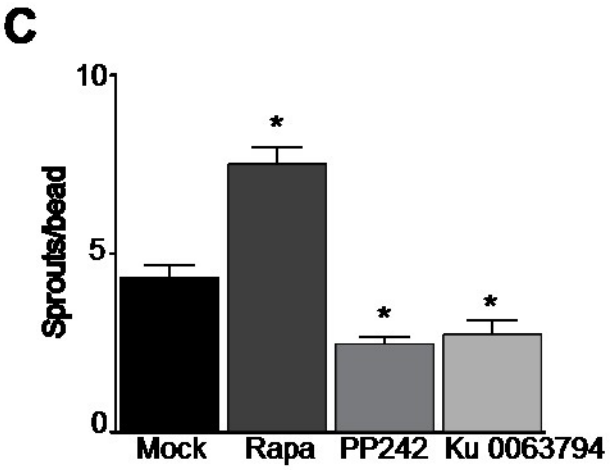
C
Sprouts/bead
10
5
0
*
*
*
Mock
Rapa
PP242
Ku 0063794

Fig 3. 4

Fig 3.4. mTORC1 inhibition primes endothelial cells to resist apoptosis and to respond to tumour-derived pro-angiogenic cues. HUVECs were treated with Rapamycin (5 nM), PP242 (1 uM), or Ku 0063794 (50 nM) for 24 hours. **A)** The EC were challenged with tumor necrosis factor-□ (TNFα) + cycloheximide (CHX) for 4 hours in normal growth conditions. Active cleaved caspase-3 was detected by DEVD-FMK-FITC and analyzed by flow cytometry as described in Methods. Quantitation of active caspase-3 in mock-, rapamycin-, PP242-, and Ku 0063794-treated ECs (n=4 independent experiments, *P<0.05 by ANOVA). **B)** Evaluation of EC angiogenic sprouting to tumor-derived growth factors *in vitro*. HUVEC were pretreated with Rapamycin (5 nM), PP242 (1 uM), or Ku 0063794 (50 nM) for 24 hours, then mounted on Cytodex beads (green) and were embedded with renal cell carcinoma cell-coated beads (red) in 3D fibrin gels as described in Methods, then co-cultured without additional growth factor supplementation or inhibitors. Representative images of EC sprouts after 18 hours incubation. **C)** Quantitation of the number of sprouts per bead (n=3 independent experiments, *P<0.05 by ANOVA).

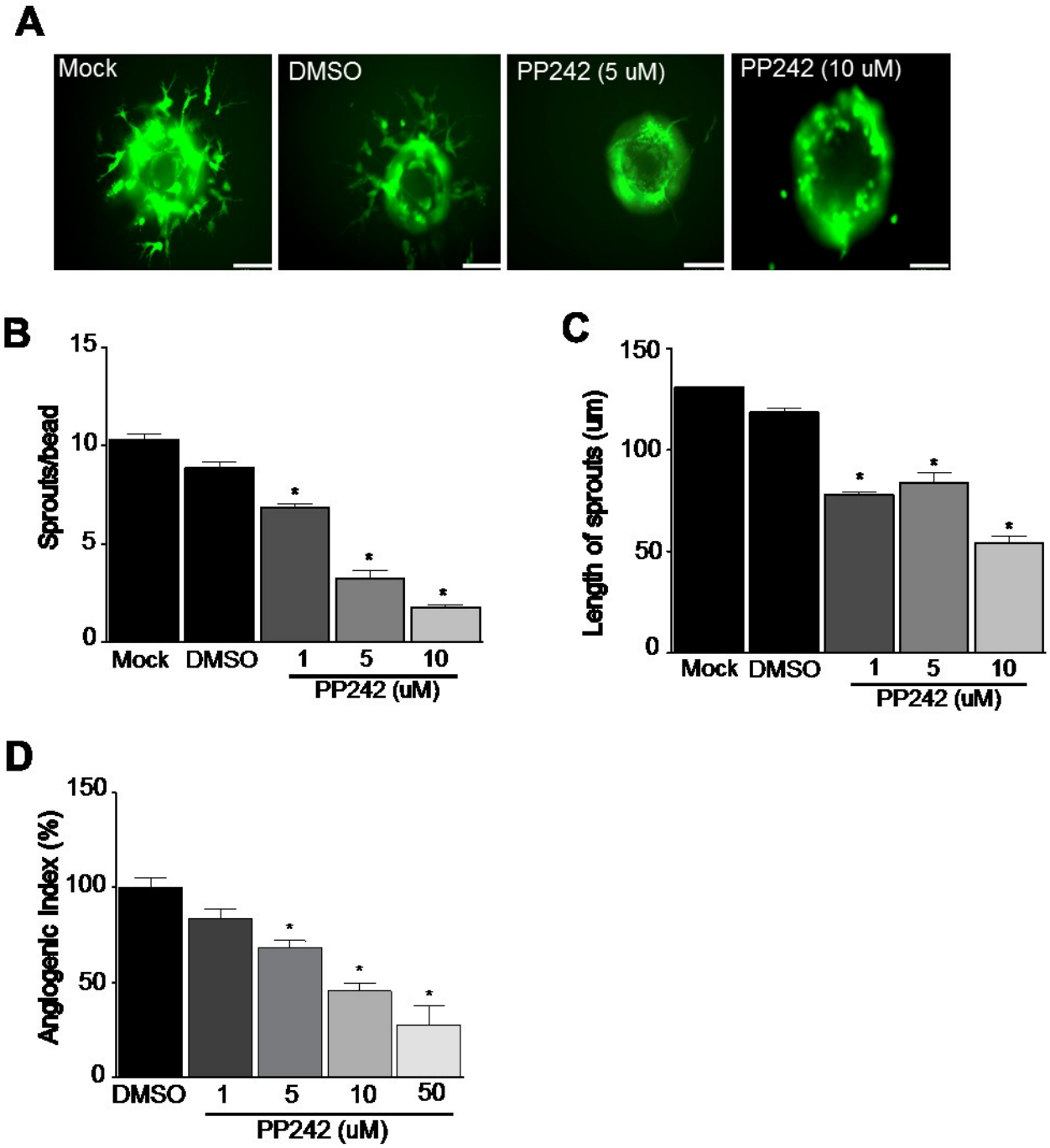
A
Mock
DMSO
PP242 (5 uM)
PP242 (10 uM)
B
Sprouts/bead
15
10
5
0
Mock
DMSO
1
5
10
PP242 (uM)
C
Length of sprouts (um)
150
100
50
0
Mock
DMSO
1
5
10
PP242 (uM)
D
Angiogenic Index (%)
150
100
50
0
DMSO
1
5
10
50
PP242 (uM)

Fig 3. 5

Fig 3.5. mTORC1/2 dual inhibition blocks VEGF-mediated angiogenesis. HUVEC-coated Cytodex beads were embedded in fibrin gels as in Fig 2, then the EC were stimulated with 50 ng/ml VEGF, and were treated with PP242 or carrier as indicated. **A)** Representative images of EC sprouts after 18 hours incubation. **B)** Quantitation of the number of sprouts per bead. **C)** Quantitation of the length of the sprouts (n=3 independent experiments, *P<0.05 by ANOVA, scale bar=95 um). **D)** Collagen gel onplants containing VEGF (100 ng/onplant) and PP242 or carrier, were placed on chicken embryo CAM as described in Methods. Quantitation of neovascularization after 64 hours of exposure to VEGF supplemented with 1, 5, 10 or 50 uM PP242 (n > 48 onplants or 16 chicken embryos per group, *P<0.05 by ANOVA).

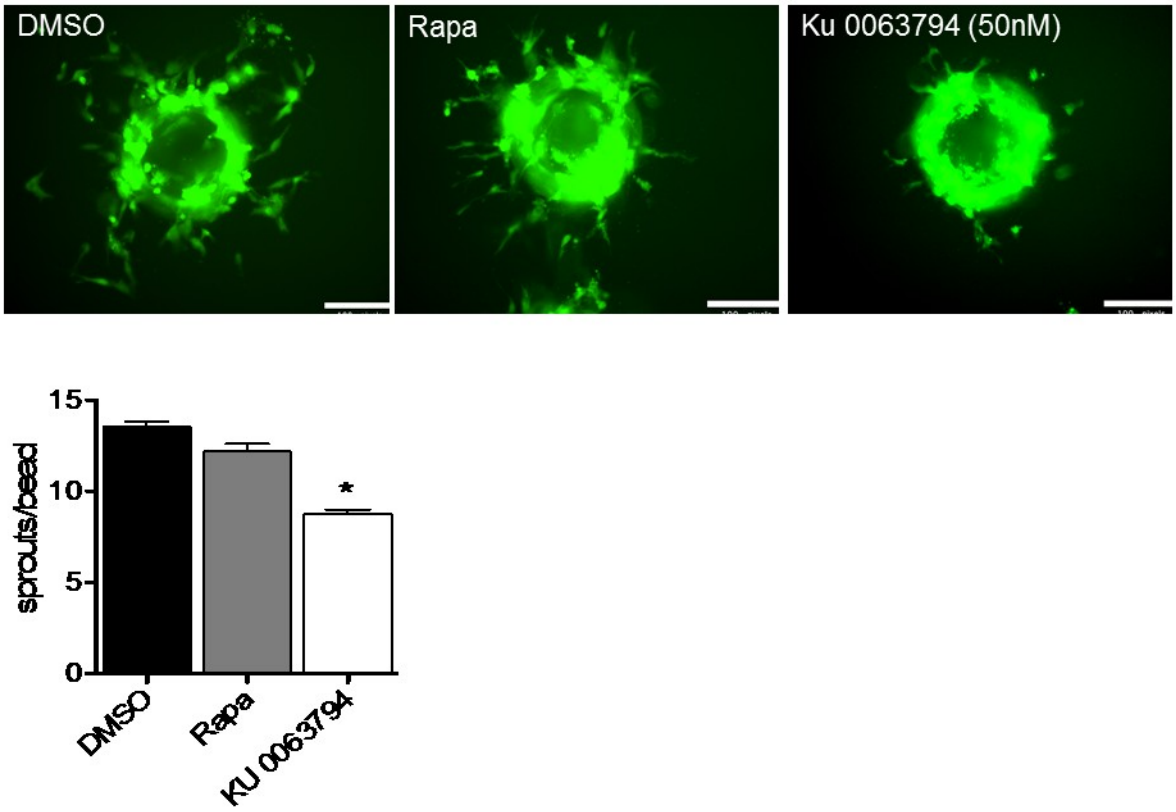

Fig 3. 6

Fig 3.6. mTORC1+2 inhibition reduces VEGF-stimulated sprouting angiogenesis in microvascular EC. HMEC-1 mounted on Cytodex beads were embedded in a fibrin gel as in Fig 3, were treated by Ku 0063794 (50 nM), Rapamycin, or carrier, and stimulated with VEGF for 18 hours. Representative images of angiogenic sprouting are shown in the upper panels. Quantitation of the number of sprouts per bead (lower panel; n=4 independent experiments, *P<0.05 by ANOVA, scale bar=95 um).

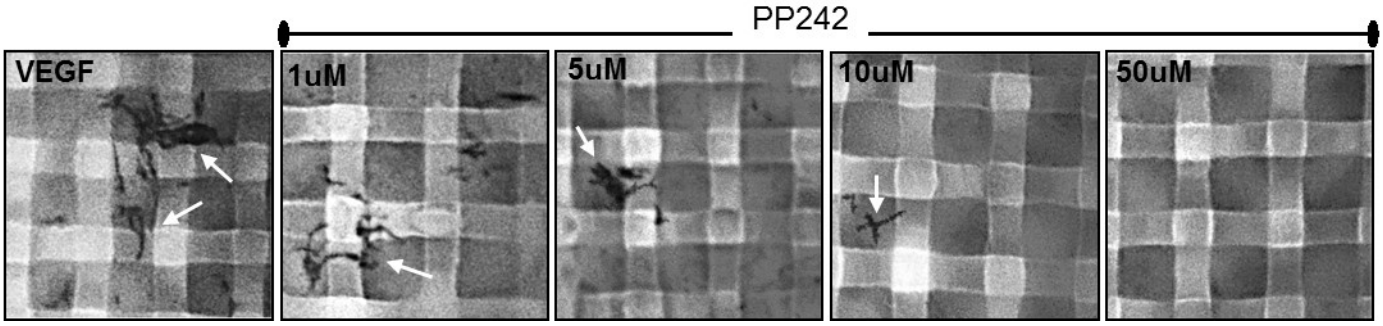

Fig 3. 7

Fig 3.7. mTORC1 + 2 inhibition inhibits angiogenesis *in vivo*. Collagen gels containing VEGF 100 ng/mL, or VEGF + PP242 at the indicated concentration, were cultured on chick CAMs as described in Methods. Newly formed vessels growing through the nylon mesh into the implant (arrows) are identified.

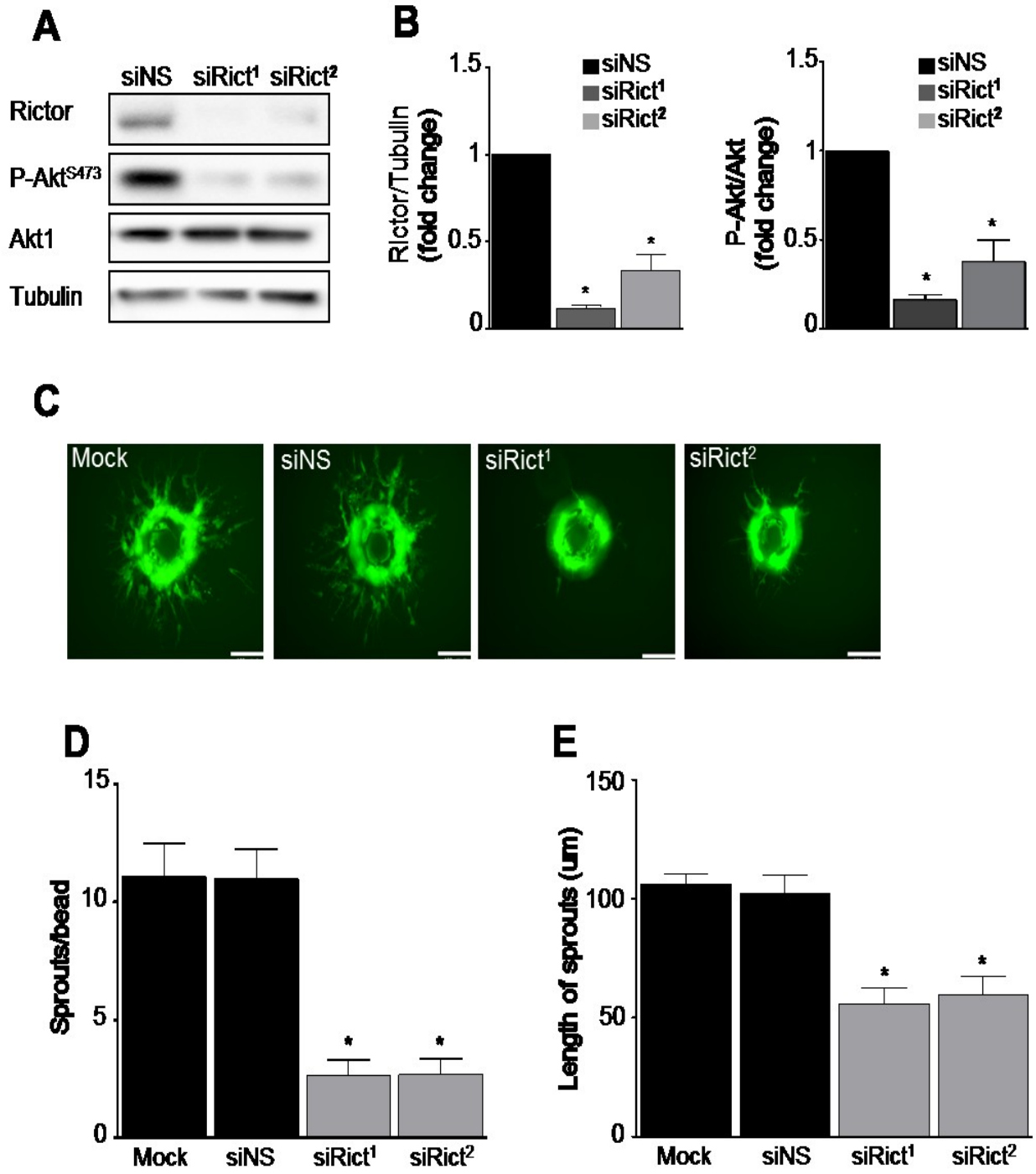
A
siNS
siRict1
siRict2
Rictor
P-AktS473
Akt1
Tubulin
B
Rictor/Tubulin (fold change)
P-Akt/Akt (fold change)
siNS
siRict1
siRict2
C
Mock
siNS
siRict1
siRict2
D
Sprouts/bead
E
Length of sprouts (um)
Mock
siNS
siRict1
siRict2

Fig 3. 8

Fig 3.8. mTORC2 inactivation inhibits VEGF-mediated angiogenesis. HUVECs were transfected with either of two small interfering RNAs (siRNAs) targeting rictor (siRict[1] and siRict[2]) or a non-silencing siRNA (siNS) control. **A)** Representative Western blot of the effect of rictor knockdown on rictor, and phospho-Akt. **B)** Quantitation of rictor and phospho-Akt (n=3 independent experiments, *P<0.05 by ANOVA). **C)** The effect of rictor knockdown on angiogenic sprouting *in vitro*. HUVEC were transfected with siRict[1], siRict[2], or siNS, then mounted on Cytodex beads, embedded in a fibrin gel, and stimulated with 50 ng/ml VEGF as in Fig 3. Representative images of EC sprouts after 18 hours incubation. **D)** Quantitation of the number of sprouts per bead. **E)** Quantitation of the length of the sprouts (n=3 independent experiments, *P<0.05 by ANOVA, scale bar=95 um).

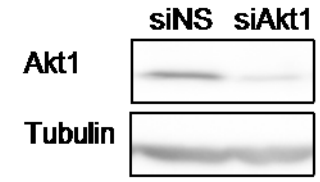

Fig 3. 9

Fig 3.9. The effect of RNAi targeted to EC Akt1. HUVECs were transfected with non-silencing (siNS) or siRNA against Akt1 (siAkt1). Representative Western blot of EC Akt1 and tubulin.

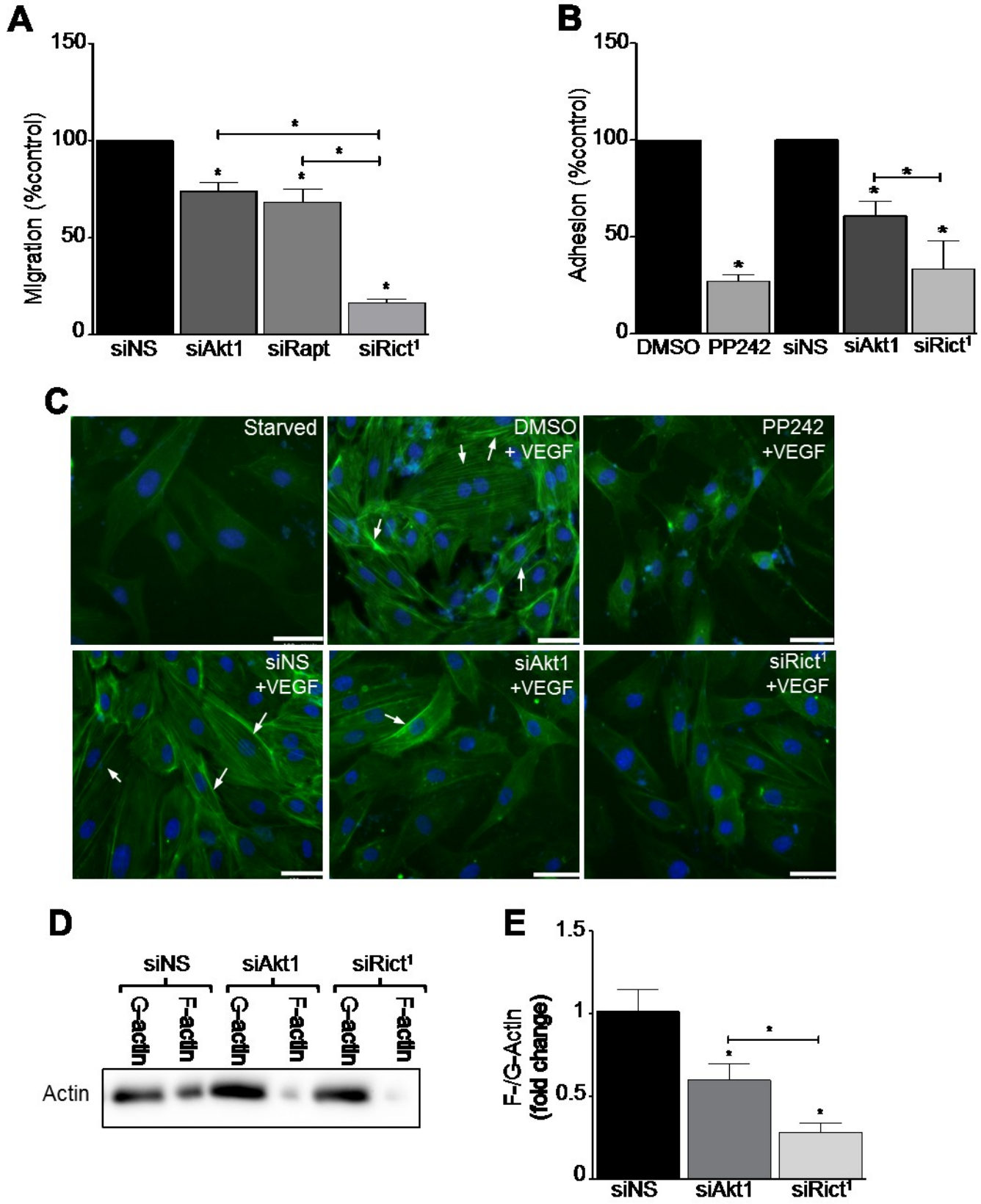
A
Migration (%control)
150
100
50
0
siNS
siAkt1
siRapt
siRict1
B
Adhesion (%control)
DMSO
PP242
siNS
siAkt1
siRict1
C
Starved
DMSO
+ VEGF
PP242
+VEGF
siNS
+VEGF
siAkt1
+VEGF
siRict1
+VEGF
D
siNS
siAkt1
siRict1
G-actin
F-actin
Actin
E
F-/G-Actin
(fold change)
1.5
1
0.5
0

Fig 3. 10

Fig 3.10. mTORC2 inactivation reduces EC migration, matrix adhesion, and actin polymerization. HUVECs were transfected with siRNA targeting Akt1 (siAkt1), rictor (siRict[1]) or raptor (siRapt). **A)** The ECs were seeded on gelatin-coated electrodes at equal density to reach confluence. The recovery of electric impedance was measured following delivery of a high electric current through an electrode to create a defect in the EC monolayer as described in Methods. Data are represented as the relative rate of migration per hour *versus* the control (n=3 independent experiments, **P*<0.05 by ANOVA). HUVECs were transfected with siRict[1], or siAkt1, or treated with PP242. **B)** The EC were seeded equally on gelatin-coated electrodes, then adhesion was evaluated using electrical impedance measurements. Data are represented as the relative rate of adhesion *versus* the controls (n=3 independent experiments, **P*<0.05 by ANOVA). **C)** The EC were serum-starved overnight, and stimulated with VEGF for 10 minutes or not (upper left). Fluorescence images of phalloidin-stained filamentous (F)-actin (green) and DNA (blue) are representative of 3 independent experiments illustrating a marked decrease in VEGF-stimulated F-actin among mTORC2-inactivated EC. **D)** HUVECs were transfected with siAkt1, or siRict[1], or control siNS. The EC were stimulated with VEGF, then globular (G)-actin and F-actin were separated as described in Methods. A representative Western blot illustrates the relative abundance of the F-actin and G-actin in ECs. **E)** Quantitation of the F-/G-actin ratio (n=5 independent experiments, **P*<0.05 by ANOVA).

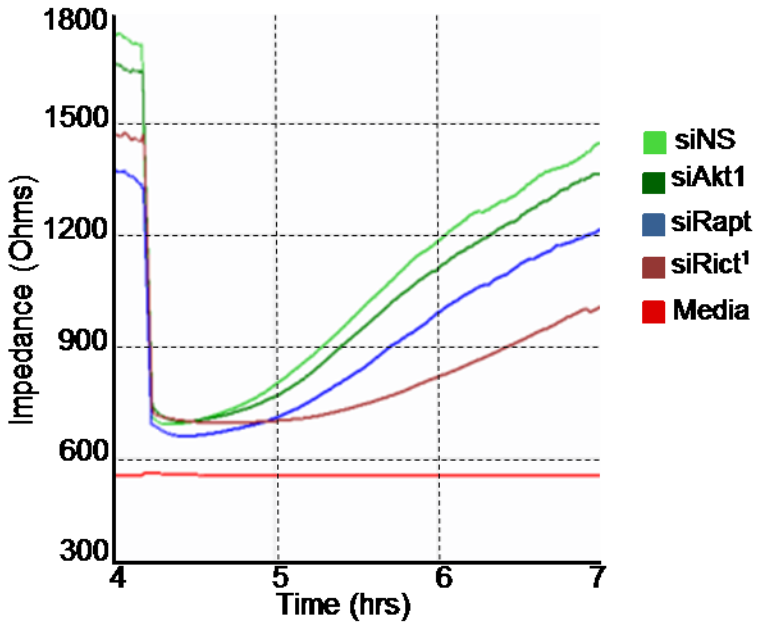

Fig 3. 11

Fig 3.11. The effect of rictor, Akt, or raptor loss on endothelial cell migration. HUVEC were transfected with siRNA against rictor, Akt, or raptor, then seeded on gelatin-coated electrodes at high density and grown to confluence as described in Methods. The monolayer was focally disrupted by an electrical pulse. Continuous electrical impedance values are shown. Representative of 3 independent experiments.

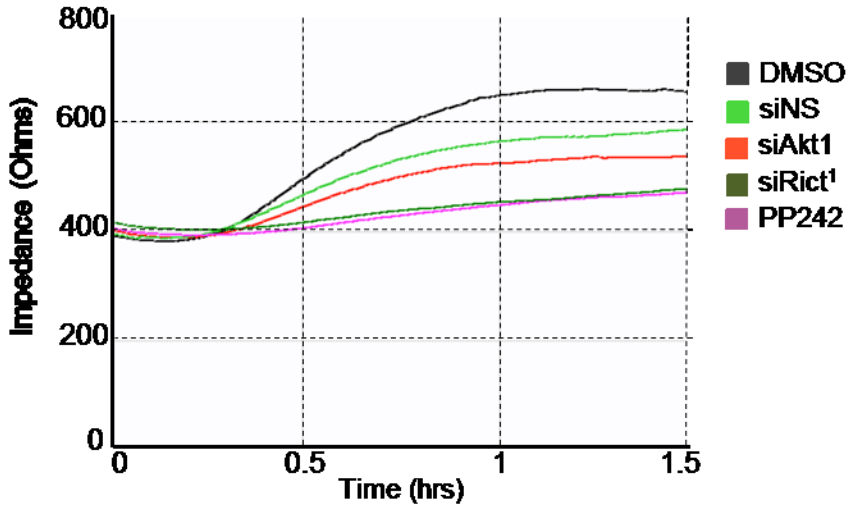

Fig 3. 12

Fig 3.12. The effect of rictor, Akt, or raptor loss on endothelial cell adhesion. HUVEC were transfected with siRNA against rictor, Akt, or raptor, or treated with PP242 as indicated. The EC were then seeded on gelatin- coated electrodes as described in Methods. Continuous electrical impedance values are shown. Representative of 3 independent experiments.

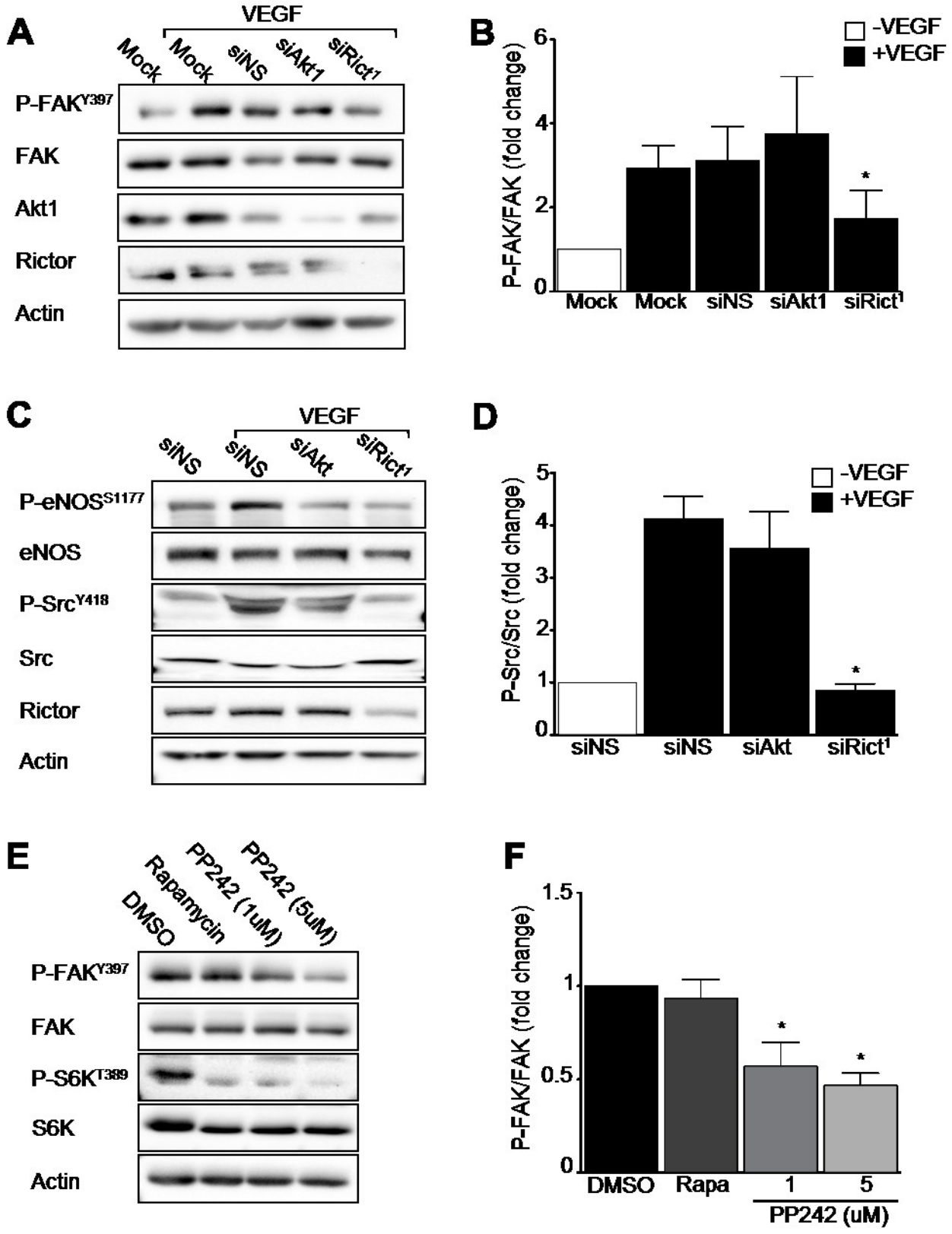
A
VEGF
Mock
Mock
siNS
siAkt1
siRict1
P-FAKY397
FAK
Akt1
Rictor
Actin
B
-VEGF
+VEGF
P-FAK/FAK (fold change)
6
4
2
0
*
Mock
Mock
siNS
siAkt1
siRict1
C
VEGF
siNS
siNS
siAkt
siRict1
P-eNOSS1177
eNOS
P-SrcY418
Src
Rictor
Actin
D
-VEGF
+VEGF
P-Src/Src (fold change)
5
4
3
2
1
0
*
siNS
siNS
siAkt
siRict1
E
DMSO
Rapamycin
PP242 (1uM)
PP242 (5uM)
P-FAKY397
FAK
P-S6KT389
S6K
Actin
F
P-FAK/FAK (fold change)
1.5
1
0.5
0
*
*
DMSO
Rapa
1
5
PP242 (uM)

Fig 3. 13

Fig 3.13. mTORC2 inactivation inhibits focal adhesion kinase activity. HUVECs were transfected with siRict[1] or siAkt1, then stimulated with 20 ng/mL VEGF for 10 minutes as indicated. **A**) A representative Western blot of EC phospho-focal adhesion kinase (P-FAK), total FAK, total Akt1, total rictor and actin. **B)** Quantitation of P-FAK (n=4 independent experiments, *P<0.05 by ANOVA). **C)** A representative Western blot of EC phospho-eNOS, and phospho-Src, illustrates that mTORC2 disruption, but not Akt1 inactivation, blocks VEGF-stimulated Src activation (n=3 independent experiments). Knockdown of either rictor or Akt1 similarly blunts eNOS phosphorylation. **D)** Quantitation of P-Src (n=3 independent experiments, *P<0.05 by ANOVA). **E)** The effect of sustained mTORC1 or mTORC1/2 inhibition on EC FAK activation. HUVECs were treated with PP242 or rapamycin and stimulated with VEGF overnight. A representative Western blot of EC P-FAK, and P-S6K (n=3 independent experiments). **F)** Quantitation of P-FAK (n=3 independent experiments, *P<0.05 by ANOVA).

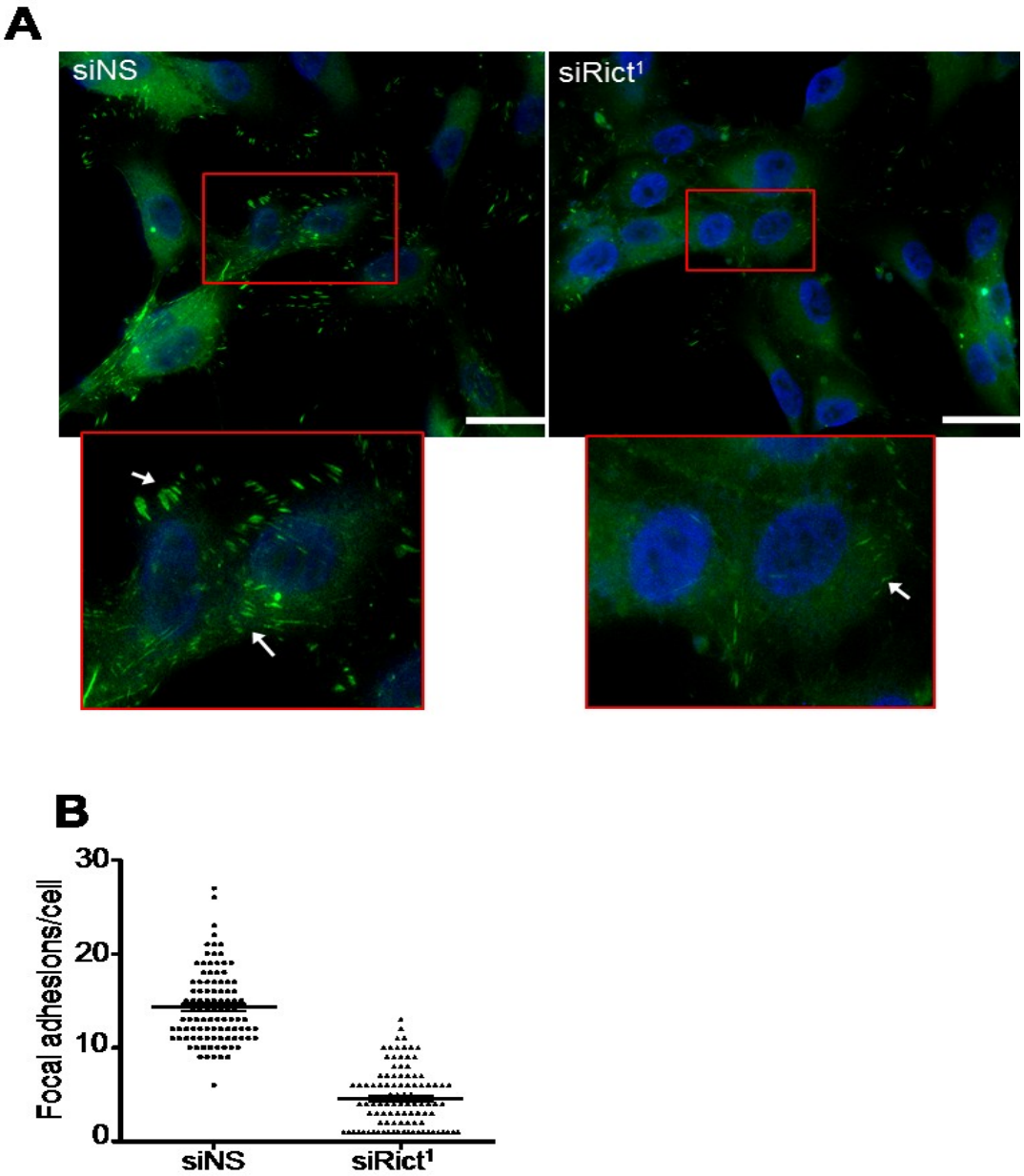

Fig 3. 14

Fig 3.14. mTORC2 inactivation inhibits focal adhesion formation. HUVECs plated on gelatin matrix were transfected with small interfering RNA against rictor (siRict[1]) or non-silencing siRNA (siNS). **A)** Representative fluorescence image of EC immuno-stained for the formation of vinculin-rich focal adhesions (green) and DNA (blue). **B)** Quantitation of the number of focal adhesions per cell, of 100 ECs pooled from three independent experiments.

References

1. Kapoor A, Figlin RA. Targeted inhibition of mammalian target of rapamycin for the treatment of advanced renal cell carcinoma. Cancer. 2009; 115: 3618-3630.

2. Del Bufalo D, Ciuffreda L, Trisciuoglio D, Desideri M, Cognetti F, Zupi G, et al. Antiangiogenic potential of the mammalian target of rapamycin inhibitor temsirolimus. Cancer Res. 2006; 66: 5549-5554.

3. Guba M, von Breitenbuch P, Steinbauer M, Koehl G, Flegel S, Hornung M, et al. Rapamycin inhibits primary and metastatic tumor growth by antiangiogenesis: involvement of vascular endothelial growth factor. Nat Med. 2002; 8: 128-135.

4. Hutson TE, Bukowski RM, Cowey CL, Figlin R, Escudier B, Sternberg CN. Sequential use of targeted agents in the treatment of renal cell carcinoma. [Review]. Crit Rev Oncol Hematol. 2011; 77: 48-62.

5. Hutson TE, Escudier B, Esteban E, Bjarnason GA, Lim HY, Pittman KB, et al. Randomized phase III trial of temsirolimus versus sorafenib as second-line therapy after sunitinib in patients with metastatic renal cell carcinoma. J Clin Oncol. 2014; 32: 760-767.

6. Takahara T, Maeda T. Evolutionarily conserved regulation of TOR signalling. . J Biochem (Tokyo). 2013; 154: 1-10.

7. Laplante M, Sabatini DM. mTOR signaling in growth control and disease. Cell. 2012; 149: 274-293.

8. Ruan GX, Kazlauskas A. Axl is essential for VEGF-A-dependent activation of PI3K/Akt. EMBO J. 2012; 31: 1692-1703.

9. Xue Q, Nagy JA, Manseau EJ, Phung TL, Dvorak HF, Benjamin LE. Rapamycin inhibition of the Akt/mTOR pathway blocks select stages of VEGF-A164-driven angiogenesis, in part by blocking S6Kinase. Arterioscler Thromb Vasc Biol. 2009; 29: 1172-1178.

10. Benjamin D, Colombi M, Moroni C, Hall MN. Rapamycin passes the torch: a new generation of mTOR inhibitors. Nat Rev Drug Discov. 2011; 10: 868-880.

11. Falcon BL, Barr S, Gokhale PC, Chou J, Fogarty J, Depeille P, et al. Reduced VEGF production, angiogenesis, and vascular regrowth contribute to the antitumor properties of dual mTORC1/mTORC2 inhibitors. Cancer Res. 2011; 71: 1573-1583.

12. Feldman ME, Apsel B, Uotila A, Loewith R, Knight ZA, Ruggero D, et al. Active-site inhibitors of mTOR target rapamycin-resistant outputs of mTORC1 and mTORC2. PLoS Biol. 2009; 7: e38.

13. Garcia-Martinez JM, Moran J, Clarke RG, Gray A, Cosulich SC, Chresta C, et al. Ku-0063794 is a specific inhibitor of the mammalian target of rapamycin (mTOR). Biochem J. 2009; 421: 29-42.

14. Zhang QX, Nakhaei-Najad M, Haddad G, Murray AG. Endothelial PI3 kinase-α couples to VEGFR2, but is not required for eNOS activation. Am J Physiol. 2011; 301: 1242-1250.

15. Nakatsu MN, Hughes CC. An optimized three-dimensional in vitro model for the analysis of angiogenesis. Methods Enzymol. 2008; 443: 65-82.

16. Zijlstra A, Lewis JD (2012) Visualization and quantification of de novo angiogenesis in ex ovo chicken embryos. In: Zudaire E, Cuttitta F, editors. The textbook of angiogenesis and lymphangiogenesis: Methods and applications. New York, NY: Springer. pp. 217-240.

17. Angers-Loustau A, C√¥t√© J-Fo, Charest A, Dowbenko D, Spencer S, Lasky LA, et al. Protein Tyrosine Phosphatase-PEST Regulates Focal Adhesion Disassembly, Migration, and Cytokinesis in Fibroblasts. The Journal of Cell Biology. 1999; 144: 1019-1031.

18. O'Reilly KE, Rojo F, She QB, Solit D, Mills GB, Smith D, et al. mTOR inhibition induces upstream receptor tyrosine kinase signaling and activates Akt. Cancer Res. 2006; 66: 1500-1508.

19. Chandarlapaty S, Sawai A, Scaltriti M, Rodrik-Outmezguine V, Grbovic-Huezo O, Serra V, et al. AKT inhibition relieves feedback suppression of receptor tyrosine kinase expression and activity. Cancer Cell. 2011; 19: 58-71.

20. Kim DH, Sarbassov DD, Ali SM, King JE, Latek RR, Erdjument-Bromage H, et al. mTOR interacts with raptor to form a nutrient-sensitive complex that signals to the cell growth machinery. Cell. 2002; 110: 163-175.

21. Sarbassov DD, Ali SM, Kim DH, Guertin DA, Latek RR, Erdjument-Bromage H, et al. Rictor, a novel binding partner of mTOR, defines a rapamycin-insensitive and raptor-independent pathway that regulates the cytoskeleton. Curr Biol. 2004; 14: 1296-1302.

22. Guertin DA, Stevens DM, Thoreen CC, Burds AA, Kalaany NY, Moffat J, et al. Ablation in mice of the mTORC components raptor, rictor, or mLST8 reveals that mTORC2 is required for signaling to Akt-FOXO and PKCalpha, but not S6K1. Dev Cell. 2006; 11: 859-871.

23. Jacinto E, Loewith R, Schmidt A, Lin S, Ruegg MA, Hall A, et al. Mammalian TOR complex 2 controls the actin cytoskeleton and is rapamycin insensitive. Nat Cell Biol. 2004; 6: 1122-1128.

24. Wary KK, Kohler EE, Chatterjee I. Focal adhesion kinase regulation of neovascularization. Microvasc Res. 2012; 83: 64-70.

25. Eliceiri BP, Puente XS, Hood JD, Stupack DG, Schlaepfer DD, Huang XZ, et al. Src-mediated coupling of focal adhesion kinase to integrin alpha(v)beta5 in vascular endothelial growth factor signaling. J Cell Biol. 2002; 157: 149-160.

26. Lane HA, Wood JM, McSheehy PM, Allegrini PR, Boulay A, Brueggen J, et al. mTOR inhibitor RAD001 (everolimus) has antiangiogenic/vascular properties distinct from a VEGFR tyrosine kinase inhibitor. Clin Cancer Res. 2009; 15: 1612-1622.

27. Saito K, Matsumoto S, Yasui H, Devasahayam N, Subramanian S, Munasinghe JP, et al. Longitudinal imaging studies of tumor microenvironment in mice treated with the mTOR inhibitor rapamycin. PLoS ONE. 2012; 7: e49456.

28. Hudes G, Carducci M, Tomczak P, Dutcher J, Figlin R, Kapoor A, et al. Temsirolimus, interferon alfa, or both for advanced renal-cell carcinoma. N Engl J Med. 2007; 356: 2271-2281.

29. Motzer RJ, Escudier B, Oudard S, Hutson TE, Porta C, Bracarda S, et al. Phase 3 trial of everolimus for metastatic renal cell carcinoma : final results and analysis of prognostic factors. Cancer. 2010; 116: 4256-4265.

30. Cacheux W, Boisserie T, Staudacher L, Vignaux O, Dousset B, Soubrane O, et al. Reversible tumor growth acceleration following bevacizumab interruption in metastatic colorectal cancer patients scheduled for surgery. Ann Oncol. 2008; 19: 1659-1661.

31. Ebos JM, Lee CR, Cruz-Munoz W, Bjarnason GA, Christensen JG, Kerbel RS. Accelerated metastasis after short-term treatment with a potent inhibitor of tumor angiogenesis. Cancer Cell. 2009; 15: 232-239.

32. Griffioen AW, Mans LA, de Graaf AM, Nowak-Sliwinska P, de Hoog CL, de Jong TA, et al. Rapid angiogenesis onset after discontinuation of sunitinib treatment of renal cell carcinoma patients. Clin Cancer Res. 2012; 18: 3961-3971.

33. Powles T, Kayani I, Sharpe K, Lim L, Peters J, Stewart G, et al. A prospective evaluation of VEGF-targeted treatment cessation in metastatic clear cell renal cancer. Ann Oncol. 2013; 24: 2098-2103.

34. Phung TL, Ziv K, Dabydeen D, Eyiah-Mensah G, Riveros M, Perruzzi C, et al. Pathological angiogenesis is induced by sustained Akt signaling and inhibited by rapamycin. Cancer Cell. 2006; 10: 159-170.

35. Kerbel RS. Tumor angiogenesis. [Review] [100 refs]. N Engl J Med. 2008; 358: 2039-2049.

36. Chresta CM, Davies BR, Hickson I, Harding T, Cosulich S, Critchlow SE, et al. AZD8055 is a potent, selective, and orally bioavailable ATP-competitive mammalian target of rapamycin kinase inhibitor with in vitro and in vivo antitumor activity. Cancer Res. 2010; 70: 288-298.

37. Gokmen-Polar Y, Liu Y, Toroni RA, Sanders KL, Mehta R, Badve S, et al. Investigational drug MLN0128, a novel TORC1/2 inhibitor, demonstrates potent oral antitumor activity in human breast cancer xenograft models. Breast Cancer Res Treat. 2012; 136: 673-682.

38. Giubellino A, Bullova P, Nolting S, Turkova H, Powers JF, Liu Q, et al. Combined inhibition of mTORC1 and mTORC2 signaling pathways is a promising therapeutic option in inhibiting

pheochromocytoma tumor growth: in vitro and in vivo studies in female athymic nude mice. Endocrinology. 2013; 154: 646-655.

39. Zhang H, Berel D, Wang Y, Li P, Bhowmick NA, Figlin RA, et al. A comparison of Ku0063794, a dual mTORC1 and mTORC2 inhibitor, and temsirolimus in preclinical renal cell carcinoma models. PLoS ONE. 2013; 8: e54918.

40. Luchman HA, Stechishin OD, Nguyen SA, Lun XQ, Cairncross JG, Weiss S. Dual mTORC1/2 blockade inhibits glioblastoma brain tumor initiating cells in vitro and in vivo and synergizes with temozolomide to increase orthotopic xenograft survival. Clin Cancer Res. 2014; 20: 5756-5767.

41. Carver BS, Chapinski C, Wongvipat J, Hieronymus H, Chen Y, Chandarlapaty S, et al. Reciprocal feedback regulation of PI3K and androgen receptor signaling in PTEN-deficient prostate cancer. Cancer Cell. 2011; 19: 575-586.

42. Rodrik-Outmezguine-VS, Chandarlapaty S, Pagano NC, Poulikakos PI, Scaltriti M, Moskatel E, et al. mTOR kinase inhibition causes feedback-dependent biphasic regulation of AKT signaling. Cancer Discov. 2011; 1: 248-259.

43. Schaller MD, Hildebrand JD, Shannon JD, Fox JW, Vines RR, Parsons JT. Autophosphorylation of the focal adhesion kinase, pp125FAK, directs SH2-dependent binding of pp60src. Mol Cell Biol. 1994; 14: 1680-1688.

44. Schaller MD, Hildebrand JD, Parsons JT. Complex formation with focal adhesion kinase: A mechanism to regulate activity and subcellular localization of Src kinases. Mol Biol Cell. 1999; 10: 3489-3505.

45. Ilic D, Furuta Y, Kanazawa S, Takeda N, Sobue K, Nakatsuji N, et al. Reduced cell motility and enhanced focal adhesion contact formation in cells from FAK-deficient mice. Nature. 1995; 377: 539-544.

46. McDonald PC, Oloumi A, Mills J, Dobreva I, Maidan M, Gray V, et al. Rictor and integrin-linked kinase interact and regulate Akt phosphorylation and cancer cell survival. Cancer Res. 2008; 68: 1618-1624.

47. Masson-Gadais B, Houle F, Laferriere J, Huot J. Integrin alphavbeta3, requirement for VEGFR2-mediated activation of SAPK2/p38 and for Hsp90-dependent phosphorylation of focal adhesion kinase in endothelial cells activated by VEGF. Cell Stress Chaperones. 2003; 8: 37-52.

48. Le Boeuf F, Houle F, Huot J. Regulation of vascular endothelial growth factor receptor 2-mediated phosphorylation of focal adhesion kinase by heat shock protein 90 and Src kinase activities. J Biol Chem. 2004; 279: 39175-39185.

49. Duval M, Le Boeuf F, Huot J, Gratton JP. Src-mediated phosphorylation of Hsp90 in response to vascular endothelial growth factor (VEGF) is required for VEGF receptor-2 signaling to endothelial NO synthase. Mol Biol Cell. 2007; 18: 4659-4668.

Chapter IV: Facio-genital dysplasia-5 (FGD5) regulates VEGFR2 coupling to PI3K and trafficking

Abstract

Vascular endothelial growth factor (VEGF)-A signaling to the endothelial cell (EC) through VEGF-receptor-2 (VEGFR2) is the principal cue driving new blood vessels formation. VEGFA is secreted by many cancer cells to promote angiogenesis and maintain blood supply to tumor tissue. Facio-genital dysplasia-5 (FGD5), a Rho-family guanine nucleotide exchange factor, is selectively expressed in EC. Deficiency of FGD5 is embryonically lethal in mice, and perturbs angiogenesis and VEGF signal transduction. However, the mechanism of FGD5 regulation of VEGFA signaling is poorly understood.

Angiogenic sprouting, tumor angiogenesis, and EC cytoskeletal remodeling were evaluated in a three dimensional in vitro model. We examined the subcellular localization of FGD5 in EC by immunofluorescent staining, and studied the association of FGD5 with VEGFR2 by immunoprecipitation.

FGD5 deficiency reduced the number of angiogenic sprouts and tip cell filopodia by ~80% and ~70%, respectively. These defects were accompanied by down regulation of the expression of tip cell-specific markers. FGD5 inactivation led to a decrease in EC migration and early protrusion (lamellipodia) formation. In resting and VEGF-stimulated EC, FGD5 forms a complex with VEGFR2 and was enriched at the leading edge of the cells and among endosomes. FGD5 loss reduced mammalian target of rapamycin complex2 (mTORC2)/Akt-dependent cortactin activation downstream of VEGFR2, but did not alter VEGFR2 plasma membrane expression, Y1175 phosphorylation, or endocytosis. However, FGD5 loss decreased endosomal VEGFR2 coupling to PI3K and diverted VEGFR2 to lysosomal degradation. This indicates FGD5

regulates VEGFR2 retention in recycling endosomes, and coupling to PI3K/mTORC2-dependent cytoskeletal remodeling.

Key points:

•FGD5 regulates VEGF-mediated angiogenesis

•FGD5 is localized to the early and recycling endosomes

•FGD5 protects VEGFR2 from degradation and regulates VEGFR2/PI3K coupling

Introduction

Angiogenesis occurs during embryonic development to support tissue growth. In adults, angiogenesis is pivotal in physiological processes such as wound healing, and contributes to many pathologies, such as tumor growth and diabetic retinopathy [1]. Angiogenesis requires endothelial cell (EC) polarization in the direction of neovessel sprout extension, to form finger-like filopodia [2]. These filopodia characteristically mark the tip cell that will lead the migration, and are thought to sense the proangiogenic cues and direct the EC migration path [3]. Tip cell filopodia mediate capillary extension and anastomoses between adjacent vessels in the formation of blood vessel networks [4]. Tip cells have a unique gene expression profile: they express relatively high levels of Delta-like 4 (DLL4), vascular endothelial growth factor receptor 2 (VEGFR2) [3], endothelial specific molecule-1 (ESM1) [5], and CXC chemokine receptor 4 (CXCR4) [6]. Hence both cytoskeletal remodeling and a gene transcription program characterize the angiogenic tip cell.

EC-specific growth factors and receptors drive EC differentiation into the tip cell. Of these, the best studied is vascular endothelial growth factor-A (VEGFA) and its receptor VEGFR2. Phosphorylation of the VEGFR2 tyrosine residue Y1175/1173 recruits the phosphoinositide 3-kinase (PI3 kinase) signaling pathway [7], an event critical to the development of new vessels [8-10]. The class IA PI3Ks stimulated by VEGFR2, consist of a catalytic subunit, and a regulatory subunit [11], p85, that mediates the interaction of PI3 kinase to VEGFR2 [12,13]. The phosphorylated lipid product of receptor-stimulated PI3 kinase activity, phosphatidylinositide-3,4,5 trisphosphate

(PIP3), creates binding sites for the pleckstrin homology (PH) domains of Phosphoinositide-dependent kinase 1 (PDK1) and Akt, and is found on the plasma membrane and early endosomes [14,15]. Activated VEGFR2 is internalized by clathrin-dependent endocytosis, then either degraded or recycled back to the plasma membrane [16]. VEGFR2 endocytosis is controlled by several Rab-family GTPases. Rab5 regulates VEGFR2 internalization and transfer to early endosomes [17,18]. Later, Rab4 and Rab11 will drive VEGFR2 recycling, whereas Rab7 will direct VEGFR2 to late endosomes and subsequently to degradation [17]. VEGFR2 continues to signal from within the endosomes, and the receptor trafficking among these endosome compartments can affect signal output from the receptor [19-21].

In polarized EC, receptor signaling from the plasma membrane or the endosome may initiate cytoskeletal remodeling involved in angiogenic sprouting. In the tip cell, filopodia arise from a cortical actin base [22,23]. The cortical actin polymerization is initiated by the actin related protein (Arp) 2/3 complex, under the regulation of actin nucleation promoting factors (NPFs) [24]. One of these is cortactin, which activates Rac1 [25] and in turn the Arp2/3 complex. Tyrosine phosphorylation of cortactin is involved in the migration of EC [26,27], and promotes VEGFR2-mediated angiogenesis [28]. Similarly, remodeling of the EC basement matrix contacts is required for EC movement and vessel formation [29]. Focal adhesion kinase, a non-receptor tyrosine kinase enriched at matrix contact sites, critically regulates remodeling of these adhesion structures.

Facio-genital dysplasia-5 (FGD5) is selectively expressed in EC, and is a member of the FYVE, Rho GTP/ GDP exchange factor, and PH domain containing family [30,31]. Deletion of FGD5 expression results in early fetal loss, attributed to defective vascular development [32,33]. The FYVE domain is predicted to mediate interactions with phosphatidylinositol- 3´-phosphate [34] and

suggests a role in endosomal trafficking [35-37]. In a previous report we showed that FGD5-loss impairs angiogenesis and the activation of Akt 30. However, a mechanistic understanding of the role FGD5 plays in VEGF-mediated angiogenesis, and how it regulates the VEGF/ PI3 kinase/ Akt pathway are still to be determined.

In the current paper we sought to study the function of FGD5 in the early events in angiogenesis, and the role of FGD5 in the regulation of VEGFR2 signaling. We report a marked inhibition of VEGFA-dependent angiogenic sprouting and filopodia formation after FGD5 loss among primary human EC spheroids. The resultant phenotype is accompanied by decreased expression of the tip cell markers DLL4, VEGFR2, and CXCR4. These defects in EC cytoskeletal remodeling are reflected in monolayer cultures as reduced EC migration and lamellipodia formation. We show that FGD5 is localized to the EC membrane ruffles, recycling endosomes, and complexes with VEGFR2 in EC. Further, FGD5 facilitates VEGFR2/PI3K coupling in the endosome, regulates VEGFR2 PI3 kinase-dependent signaling to cortactin, and protects VEGFR2 from lysosomal degradation.

Results

FGD5 deficiency inhibits VEGF-dependent sprouting angiogenesis and tip cell specialization.

To recapitulate tumor angiogenesis in vitro, we co-cultured human umbilical vein EC-coated micro-carrier beads with human renal cell carcinoma-coated beads in a three dimensional (3D) fibrin gel. We reduced the expression of FGD5 in the EC using RNA interference (Figure. 4.1 A). We observed EC sprouting stimulated by tumor cell-secreted angiogenic cues, however, the sprouting was markedly impaired among FGD5-deficient EC-coated beads (Figure. 4.1 B, C). Since vascular endothelial growth factor-A (VEGFA) potently induces angiogenesis, and angiogenic tip cells via the receptor VEGFR2 [3], we confirmed the effect of EC FGD5 loss on VEGFA-dependent sprouting angiogenesis. Compared to non-specific siRNA-treated controls, FGD5 loss lead to ~ 80% decrease in the number of sprouts, and shortened the formed sprouts by ~ 20% (Figure. 4.1 D, E). These results were replicated in Human microvascular endothelial cells (HMEC1) using a different sequence of siRNA targeting FGD5 (siFGD5#2) (Figure 4.2.). Similarly, we examined the effect of FGD5 deficiency on filopodia formation in 3D culture. We found VEGF-stimulated filopodia formation was reduced by 70% among tip cells in the FGD5-deficient EC cultures (Figure. 4.1 F, G). Moreover, the length of the filopodia was reduced by ~ 40% (Figure. 4.1 G). These data indicate that FGD5 is required in VEGFA-guided angiogenesis, and FGD5 loss is specifically associated with defective cytoskeletal remodeling during endothelial tip cell formation.

We investigated whether the defect in endothelial cytoskeletal remodeling due to FGD5 loss was accompanied by altered expression of endothelial tip cell-specific markers: VEGFR2, Delta-like ligand-4 (DLL4), CXC chemokine receptor 4 (CXCR4) and Endothelial specific molecule-1 (ESM1). First, to establish a model where the tip cell markers were highly induced, we compared two dimensional (2D) to 3D cell cultures. VEGFR2, CXCR4 and DLL4 were detected by Western blot among 2D cultures, but VEGFA stimulation did not change their expression. In contrast, VEGF stimulation induced expression of these markers in 3D spheroid cultures (Figure. 4.3 A, B). To confirm these data, we isolated the RNA from the 3D EC cultures. RT-PCR analysis showed 4-fold increase in the abundance of DLL4, ESM1 and CXCR4, and 2-fold increase in VEGFR2 after VEGF stimulation (Figure. 4.3 C). Next, we investigated the effect of FGD5 deficiency on the EC tip cell markers in 3D EC cultures. Compared to the controls, FGD5 loss reduced the expression of DLL4 by ~ 40 %, and slightly lowered VEGFR2 and CXCR4 expression (Supplemental Figure. 4.3 D, E). RT-PCR analysis showed a similar pattern of decreased DLL4, VEGFR2 and CXCR4 expression (Supplemental Figure. 4.3 F). These data show that FGD5 regulates the VEGF-stimulated increase in the expression of tip cell genes during 3D angiogenesis. Taken together with the observation of defective VEGF-stimulated cytoskeletal remodeling, the data suggest FGD5 loss impairs VEGF receptor coupling to signal transduction pathway(s) required to mediate these events.

FGD5 regulates EC migration and VEGFR2 signaling to the cytoskeleton.

Endothelial migration is initiated by lamellipodia formation, a process dependent on actin polymerization. Of note, the activity of regulatory pathways for lamellipodia formation in monolayer cultures is highly correlated to migration in 3 dimensional (3D) cultures [43]. Thus, we sought to determine if FGD5 loss is accompanied by migration defects in wounded EC monolayers. The polarized edge of the migrating ECs following VEGFA stimulation revealed a striking defect in lamellipodia formation after FGD5 loss (Figure. 4.4 A). The defect in lamellipodia formation in FGD5-deficient cells was comparable to Rac1- (an essential molecule for lamellipodia formation) deficient cells (Figure. 4.5 A, B) [44,45]. Consistent with this observation, VEGFA-stimulated closure of a scratch-wound in a confluent EC monolayer was delayed among FGD5-deficient cells (Figure. 4.5 C and Figure. 4.4 B). Taken together, FGD5 is indispensable to EC cytoskeletal remodeling and in turn migration. This may contribute to the defects in sprout extension after FGD5 loss.

Next, we investigated the effect of FGD5 loss on VEGFR2-dependent downstream signals involved in cytoskeletal remodeling. We observed that FGD5 loss markedly decreased p-FAKY397 (Figure. 4.5 D, E). Further, we observed the VEGFA-stimulated phosphorylation of cortical actin binding protein, cortactin on Y421, which promotes lamellipodia formation, was reduced among FGD5-deficient EC (Figure 4.5 D, E) [46]. Thus the defect in lamellipodia formation evident as early as 10 minutes after polarizing the cells by the scratch-wound, were temporally correlated with the decrease in FAK and cortactin phosphorylation 10 minutes after VEGFA stimulation (Figure. 4.5 D, E). Further, in agreement with our previous report [30] we found a modest reduction in Akt S473 phosphorylation (data not shown). Focal adhesion kinase Y397 phosphorylation after VEGF stimulation is dependent on PI3 kinase and mTORC2 activity

[42]. To determine if the cortactin Y421 phosphorylation defect is linked to PI3K/Akt signaling, we genetically targeted Akt1 with short interfering RNA, and replicated the defect in cortactin Y421 phosphorylation after VEGFA stimulation (Figure. 4.5 F, G). These results suggest FGD5 regulates VEGFR2 coupling to PI3 kinase-dependent downstream signals in EC.

FGD5 is associated with the leading edge and early endosomes.

Next, we studied FGD5 subcellular localization in ECs. EC were stimulated with VEGF then immunostained for FGD5 and actin. FGD5 co-localized to the actin-rich lamellipodia as well as cytoplasmic structures (Figure. 4.6 A). To confirm this polarized compartmentalization of FGD5, EC were transfected to express GFP-tagged FGD5, then we examined FGD5 localization by live-cell imaging of subconfluent EC monolayers. FGD5 localized to the migratory leading edge (Figure. 4.6 B). Since polarized VEGFR2 activation defines the leading edge of a migrating EC, we evaluated if FGD5 complexed with VEGFR2. When immunoprecipitated, FGD5 formed complexes with VEGFR2 under VEGF stimulation (Figure. 4.7 A). Similarly, reciprocal immunoprecipitation of VEGFR2 demonstrated association between VEGFR2, FGD5 and p85 (Figure. 4.7 B). Taken together, these data suggest the FGD5/VEGFR2 complex might assemble at the cellular leading edge, or directly after VEGFR2 is activated and undergoes endocytosis.

Since activated VEGFR2 is targeted to early endosomes [16], we sought to investigate FGD5 colocalization with early endosomes, marked by Rab5. ECs were stimulated with VEGF then fixed and immunostained for VEGFR2, FGD5 and Rab5 simultaneously. We observed that FGD5 was colocalized with both VEGFR2 and Rab5 (Figure. 4.7 C). These results indicate that

FGD5 and VEGFR2 are complexed shortly after VEGFR2 activation and become internalized in a Rab5 positive early endosomal compartment.

Next, we sought to characterize the distribution of FGD5 among endosome compartments, i.e. Rab4-, 11- or 7-associated vesicles. VEGF-stimulated ECs showed marked co-localization of FGD5 with the recycling vesicles labeled with Rab4, or Rab11 after 30 minutes of stimulation (Figure. 4.8 A, B). FGD5 also co-localized to Rab7 vesicles but to a lower extent (Figure. 4.8 A, B). Thus, FGD5 is preferentially distributed among recycling endosomes. To confirm this observation, we examined FGD5 co-localization with the transferrin receptor, another marker for early and recycling endosomes [47]. As predicted, we found FGD5 co-localized with the transferrin receptor in VEGF-stimulated ECs (Figure. 4.9).

It is known the VEGFR2 pool residing in the early endosomes is sorted either to Rab7 vesicles for degradation, or Rab4/11 vesicles for recycling [17,48]. Since we have shown that FGD5 is associated with VEGFR2 shortly after activation and is present among recycling endosomes, these data suggest that FGD5 could play a role in activated VEGFR2 endocytosis, trafficking, and/or coupling to PI3 kinase.

FGD5 does not regulate VEGFR2 activation or endocytosis.

To evaluate the effect of FGD5 loss on VEGFR2 activation we studied VEGFR2 Y1175 phosphorylation [7]. After 10 minutes of VEGF stimulation, VEGFR2 Y1175 phosphorylation among FGD5-deficient EC was unchanged compared to control EC (Figure. 4.10 A, B). Further,

at later time points after stimulation with VEGF the pattern of VEGFR2 Y1175 phosphorylation was similar among the control and FGD5-deficient EC (Figure. 4.10 C, D). This indicates intact VEGFR2 activity after FGD5 loss. However, we observed a decrease in the total VEGFR2 protein after 10 minutes of VEGF stimulation among the FGD5-deficient ECs (Figure. 4.10 C). Hence, we hypothesized that FGD5 loss alters VEGFR2 endocytosis and/or trafficking.

We studied the endocytosis of both the phosphorylated VEGFR2 Y1175 and the total VEGFR2. Flow cytometry analysis of surface membrane VEGFR2 expression showed a decrease in VEGFR2 after one hour of VEGF stimulation, indicating receptor endocytosis. However, ECs did not show any change in surface membrane VEGFR2 expression after FGD5 loss (Figure. 4.10 E). Next, we investigated phospho-VEGFR2 Y1175 co-localization with Rab5 or EEA1, markers of early endosomes [47], at 10 minutes after VEGF stimulation. The fraction of phospho-Y1175 VEGFR2 co-localized with early endosomes did not change among FGD5-deficient versus control EC (Figure. 4.11 A-D). Taken together, FGD5 deficiency did not alter VEGFR2 availability or activation by VEGF, and activated VEGFR2 underwent prompt endocytosis despite FGD5 loss.

FGD5 loss targets VEGFR2 to lysosomal degradation.

FGD5 loss decreased the level of VEGFR2 by 25% and 50% at 30 and 60 minutes of VEGF stimulation, respectively (Figure. 4.12 A, B). This suggests that VEGFR2 is degraded more quickly in the absence of FGD5. Since protein degradation occurs mainly through the lysosomal or proteasome pathway, we aimed to identify which system was involved in the increased

degradation rate of VEGFR2 in the absence of FGD5. Treatment of HUVECs with the lysosome inhibitor CA-074 (20 uM) [39], but not the proteasome inhibitor MG-132 (20 uM) [38], protected VEGRF2 from degradation after VEGF stimulation (Figure. 4.12 C. D and Figure 4.13). Similarly, CA-074, but not MG-132, rescued the accelerated degradation of VEGFR2 associated with FGD5 deficiency (Figure. 4.12 C, D). Consistent with this observation, we find that the fraction of VEGFR2 co-localized with Rab7 vesicles among FGD5-deficient ECs was more than double of that in the control ECs (Figure. 4.13 A, B, C). Together, these two lines of evidence indicate that VEGFR2 retention in early endosome compartments is mediated by FGD5.

FGD5 is required for efficient VEGFR2 and PI3K coupling.

The early endosome compartment is a VEGFR2/PI3K coupling site, and we detected both FGD5 and VEGFR2 complexed with p85 (Figure. 4.7 B), the regulatory subunit of PI3K. Therefore, we hypothesized that FGD5 is required for VEGFR2/PI3K coupling. After VEGF stimulation we noticed a robust decrease in VEGFR2/p85 coupling by anti-VEGFR2 immunoprecipitation in FGD5-deficient EC (Figure. 4.15 A, B). Further, immunostaining showed markedly reduced p85 colocalization with phospho-Y1175 VEGFR2 in early endosomes among FGD5-deficient EC (Figure. 4.15 C, D). However, p85 coupling to phospho-Y1175 VEGFR2 on the membrane was intact (Figure. 4.15 C). These results indicate that FGD5 is critical for VEGFR2/PI3K coupling in the early endosome compartments.

Discussion

Pro-angiogenic signaling to the endothelial cell through the VEGF receptor-2 is critical for developmental angiogenesis and has been targeted in the adult to block neoangiogenesis required for tumor growth. VEGFR2 coupling to the PI3 kinase pathway in the EC is essential to support new vessel development. In earlier work, we identified the endothelial-restricted Rho GTP-GDP exchange factor, FGD5, as a regulator of the PI3 kinase pathway recruitment after VEGF stimulation [30]. In vivo, loss of VEGFR2, PI3 kinase-alpha, and FGD5 are each associated with failed embryonic vascular development and embryonic demise.

In the current work, we identify that loss of FGD5 induced by RNA interference in human ECs markedly impairs angiogenic sprouting to tumor cell-secreted growth factors or VEGF. FGD5 loss reduces filopodia and sprout extension from tip cells in 3D endothelial spheroid cultures, and lamellapodia extension in monolayer culture. We link these events to VEGF-stimulated, PI3 kinase-dependent phosphorylation of focal adhesion kinase [49,50] and cortactin [26,28], proteins known to regulate cytoskeletal remodeling, and show the pathway requires FGD5 expression. We demonstrate that VEGFR2, PI3 kinase, and FGD5 associate in a complex, and localize the complex formation to the endosome compartment. Strikingly, FGD5 is required for recruitment of PI3 kinase to activated VEGFR2, and for VEGFR2 trafficking through recycling endosomes. In this way, FGD5 functions to shape VEGFR2 downstream signaling in the endothelial cell by modifying the signal output, and the function of the receptor for sustained signal propagation to enable cytoskeleton remodeling.

VEGFR2 undergoes clathrin-mediated endocytosis after stimulation with VEGFA, and rapidly enters Rab5-, and EEA1-positive endosomes [17,51,52]. A large fraction of the receptor is then recycled to the cell surface sequentially via Rab4- and Rab11 endosomes. Alternatively, the remaining VEGFR2 can be degraded by the proteasome or sorted from Rab5- or Rab4- through Rab7-endosomes for lysosomal degradation [19,53-55]. Dysregulated trafficking of the activated receptor through these compartments impairs vascular development [21,56].

After FGD5 loss, we observe no reduction in the cell-surface level of VEGFR2 assessed by flow cytometry. However, the overall abundance of VEGFR2 in the EC after receptor activation is decreased in the setting of FGD5 knockdown. Inhibition of lysosomal proteases rescues this effect of FGD5 loss on VEGFR2, suggesting FGD5 loss preferentially shunts VEGFR2 to the lysosomal degradation pathway. Consistent with this observation, FGD5 loss increases the fraction of VEGFR2 co-localized to Rab7-positive vesicles, indicating FGD5 functions to retain VEGFR2 in the recycling endosome compartments. Few regulators of this VEGF receptor sorting are known. NRP1, a co-receptor for VEGFA, interacts with VEGFR2 and favours VEGFR2 transfer to recycling Rab11 endosomes [19]. Further, VEGFR2 de-ubiquitinylation by USP8, promotes VEGFR2 recycling and signaling [55]. Conversely, serine phosphorylation of the PEST domain of VEGFR2, and recruitment of PDCL3 are implicated to guide receptor trafficking toward the degradation pathway [54,57]. This dephosphorylation and recycling of the activated VEGFR2 from the early endosome to the plasma membrane is a feature of VEGFR2 distinct from the degradation typical of other activated receptor tyrosine kinases in EC [19]. The molecular events relating FGD5 function to direct receptor sorting away from Rab7-vesicles requires further investigation. However, FGD5 represents an endothelial-restricted molecule

specialized to guide the cell-type-specific adaptation of VEGFR2 endosomal storage and trafficking.

Internalization of VEGFR2 by endocytosis is known to promote stable, sustained signaling events. Activation of VEGFR2, reflected by Y1175 phosphorylation, is required to recruit PI3 kinase pathway signaling [58,59]. The VEGFR2/PI3K coupling is found in Rab5-endosomes, and is extinguished by the time VEGFR2 traffics to the Rab11-endosome [19]. Perturbation of endocytic trafficking of VEGFR2 is associated with altered signaling. For example, retention of VEGFR2 to the plasma membrane, by association with VE-cadherin, promotes receptor de-phosphorylation [52]. Moreover, delayed endocytosis induced by loss of Numb activity is also associated with decreased Akt phosphorylation despite VEGF receptor activation [60]. Indeed, essential VEGFR2 signaling occurs from EEA1+ subcellular compartments, upstream of Rab 11- or Rab 7-labelled endosomes, since knockdown of either Rab GTPase rescues the effect of disordered VEGFR2 traffic [21]. Signaling may even persist in the Rab7 endosome, since lysosome pharmacological inhibition prolongs Akt phosphorylation [53]. Our data indicate the Rab5/ EEA1-positive endosome as the principal subcellular location of the assembly of a VEGF-stimulated PI3 kinase signaling complex involved in VEGF-stimulated polarized remodeling of the cell cytoskeleton.

Spatial receptor signaling contributes to cell polarization and directed migration. We observe that FGD5 is enriched at the lead edge of the EC in subconfluent culture, and regulates polarized lamellae extension and EC migration. Consistent with this impaired EC cytoskeletal remodeling, activation of both cortactin and FAK are impaired by FGD5 loss. We determine that both VEGF-

stimulated cortactin and FAK activation requires PI3 kinase activity in the EC [42]. VEGF-stimulated recruitment of these molecules is dependent on engagement of the co-receptor NRP1 [61,62], and requires VEGFR2 phospho-Y1175-dependent PI3 kinase activity [59]. Loss of FGD5 does not affect phospho-Y1175 VEGFR2 endocytosis, but decreases PI3 kinase association with the activated VEGFR2 in co-immunoprecipitation of whole cell lysates. Further, we provide direct evidence that FGD5 loss is associated with decreased recruitment of PI3 kinase, p85, to phospho-VEGFR2 in the EEA1+ endosome. Taken together, these observations indicate polarized cytoskeletal remodeling in the EC are dependent on early endosome assembly of PI3 kinase with VEGFR2, and recruitment of mTORC2-dependent pathways [42].

In summary, we identify the function of FGD5 in regulation of tip cell-cytoskeletal remodelling in VEGF-guided sprouting angiogenesis. Moreover, we identify a novel role for FGD5 to regulate the coupling of PI3K to activated VEGFR2 in the early endosome compartment, and to retain VEGFR2 in recycling endosome compartment. These data indicate that FGD5 is a potential target to regulate pathological angiogenesis.

Figures

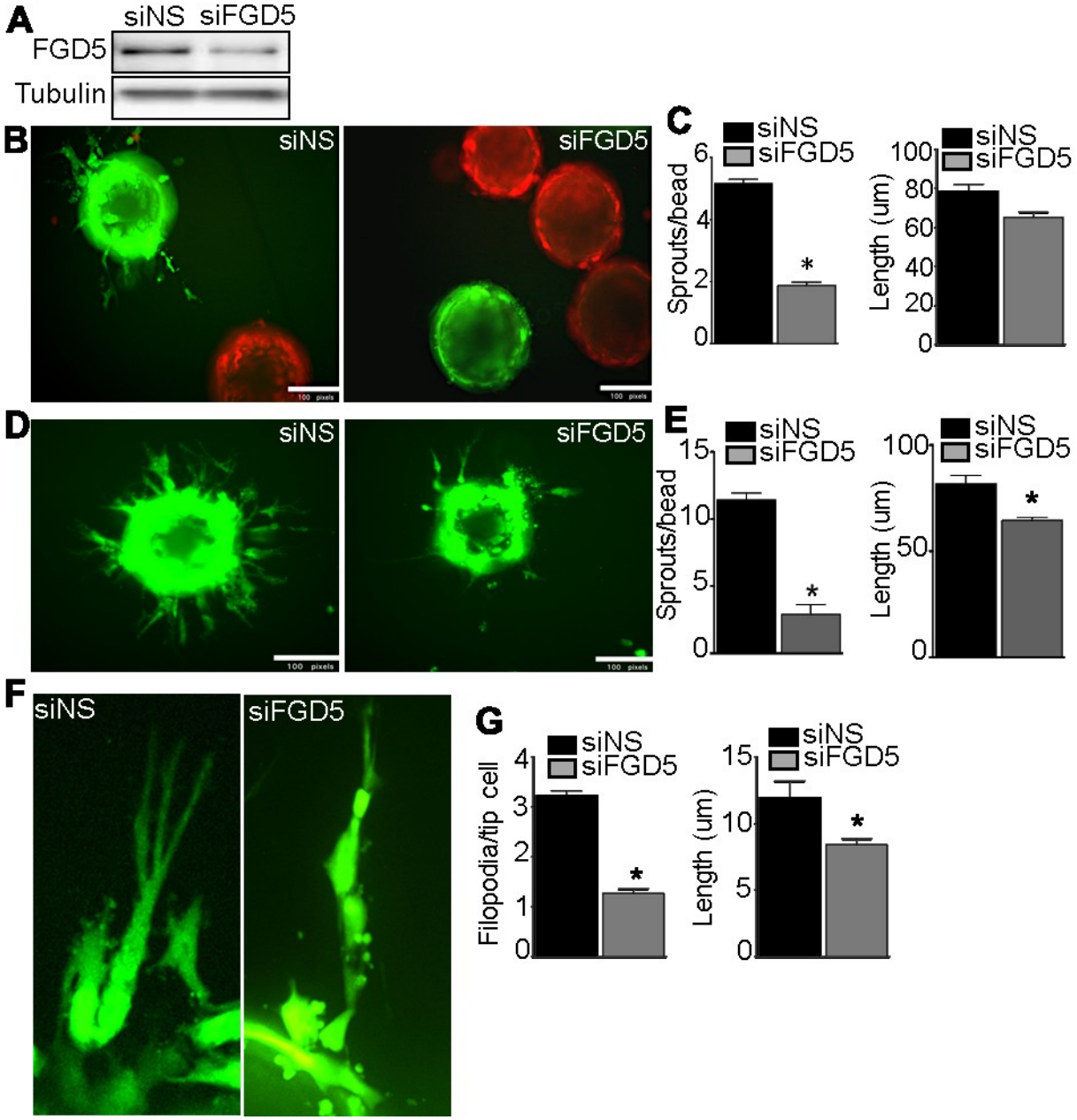

Fig 4. 1

Figure 4.1. FGD5 loss inhibits sprouting angiogenesis, filopodia formation and endothelial migration. Human umbilical vein endothelial cells HUVECs were transfected with non-silencing siRNA (siNS) or siRNA against FGD5 (siFGD5). A) A representative image of FGD5 and Tubulin Western blot. To Evaluate EC angiogenic sprouting to tumor-derived growth factors in vitro, FGD5 deficient HUVECs or control HUVECs were mounted on Cytodex beads (green) and were embedded with renal cell carcinoma cell-coated beads (red) in 3D fibrin gels as described in Methods, and co-cultured without additional growth factor supplementation. B) Representative images of EC sprouts after 18 hours incubation. C) Quantitation of the length and number of sprouts per bead (n=3 independent experiments, *P<0.05 by student t-test). Cytodex beads coated with FGD5 deficient HUVECs or control HUVECs were embedded in fibrin gel supplemented with M199+ 8% FBS+ 50ng/m VEGF. D) Representative images of HUVECs sprouting after 18 hours incubation. E) Quantitation of number of sprouts per bead and length of sprouts (n=3 independent experiments, *P<0.05 by student t-test). F) Representative images of filopodia formed from FGD5 deficient tip cells and control tip cells. G) Quantitation of number of filopodia/ tip cell and length of filopodia (n=3 independent experiments, *P<0.05 by student t-test).

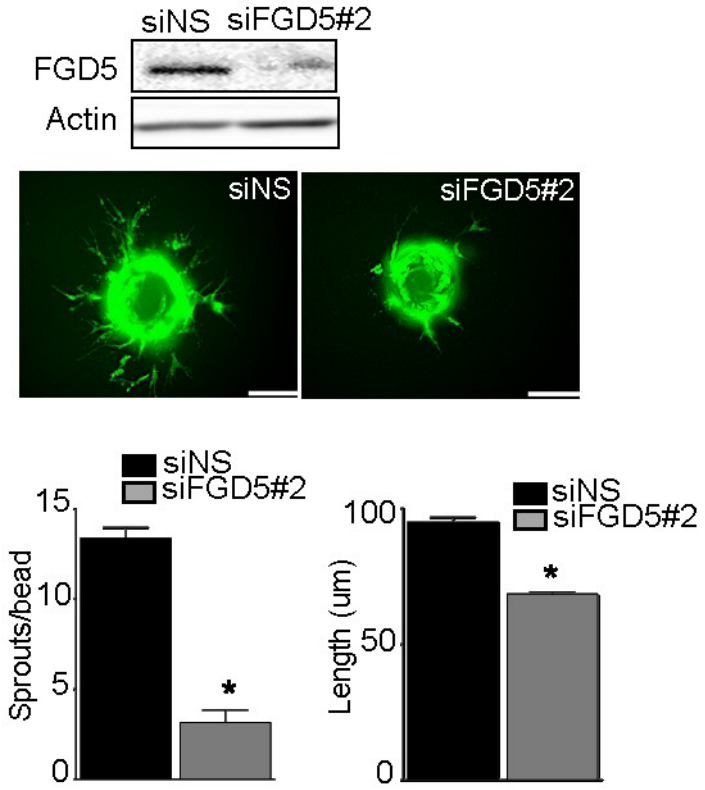

Fig 4. 2

Figure 4.2. FGD5 loss inhibits sprouting angiogenesis in HMEC1. Human Microvascular endothelial cells HMEC1 were transfected with non-silencing siRNA (siNS) or siRNA against FGD5 (siFGD5#2). **A)** A representative image of FGD5 and Actin Western blot. Cytodex beads coated with FGD5 deficient HMEC1 or control HMEC1 were embedded in fibrin gel supplemented with M199+ 8% FBS+ 50ng/m VEGF. **B)** Representative images of HMEC1 sprouting after 18 hours incubation. **C)** Quantitation of number of sprouts per bead and length of sprouts (n=3 independent experiments, *P<0.05 by student t-test).

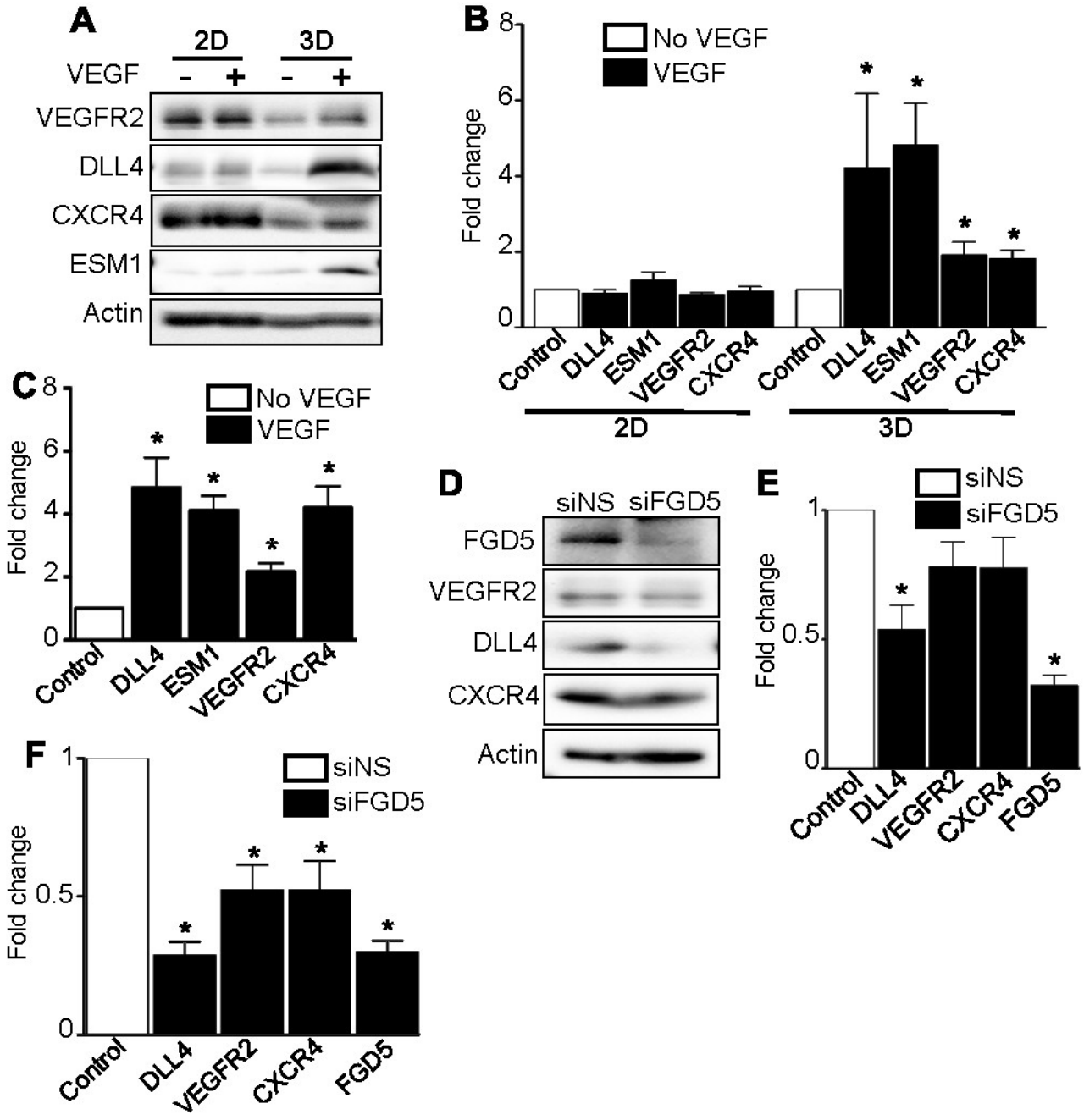
A
2D
3D
VEGF
- + - +
VEGFR2
DLL4
CXCR4
ESM1
Actin
B
No VEGF
VEGF
Fold change
Control
DLL4
ESM1
VEGFR2
CXCR4
2D
3D
C
No VEGF
VEGF
Fold change
Control
DLL4
ESM1
VEGFR2
CXCR4
D
siNS siFGD5
FGD5
VEGFR2
DLL4
CXCR4
Actin
E
siNS
siFGD5
Fold change
Control
DLL4
VEGFR2
CXCR4
FGD5
F
siNS
siFGD5
Fold change
Control
DLL4
VEGFR2
CXCR4
FGD5

Fig 4. 3

Figure 4.3. FGD5-deficient tip cells express less tip cell markers. HUVECs were grown in a two dimensional culture (2D) or a three dimensional (3D) culture, then incubated with VEGF (50ng/ml) as indicated. Protein and RNA were extracted from the 2D culture and from the sprouting HUVECs in 3D culture, then analyzed by Western blot or RT-PCR for the expression of DLL4, ESM1, VEGFR2 and CXR4. **A)** Representative image of VEGFR2, DLL4, CXCR4, ESM1 and actin Western blot. **B)** Quantitation of DLL4, ESM1, VEGFR2 and CXCR4 (n=3 independent experiments, *P<0.05 by ANOVA). **C)** Quantitation of the fold change in DLL4, ESM1, VEGFR2 and CXCR4 expression by RT-PCR (n=3 independent experiments, *P<0.05 by ANOVA). HUVECs were transfected with non-silencing siRNA (siNS) or siRNA against FGD5 (siFGD5). Protein and RNA were extracted from sprouting FGD5-deficient HUVECs and sprouting control-HUVECs, then analyzed by Western blot or RT-PCR for the expression of DLL4, VEGFR2, CXR4 and FGD5. **D)** Representative image of FGD5, VEGFR2, DLL4, CXCR4 and actin Western blot. **E)** Quantitation of DLL4, VEGFR2, CXCR4 and FGD5 (n=3 independent experiments, *P<0.05 by ANOVA). **F)** Quantitation of the fold change in DLL4, VEGFR2, CXCR4 and FGD5 expression by RT-PCR (n=3 independent experiments, *P<0.05 by ANOVA).

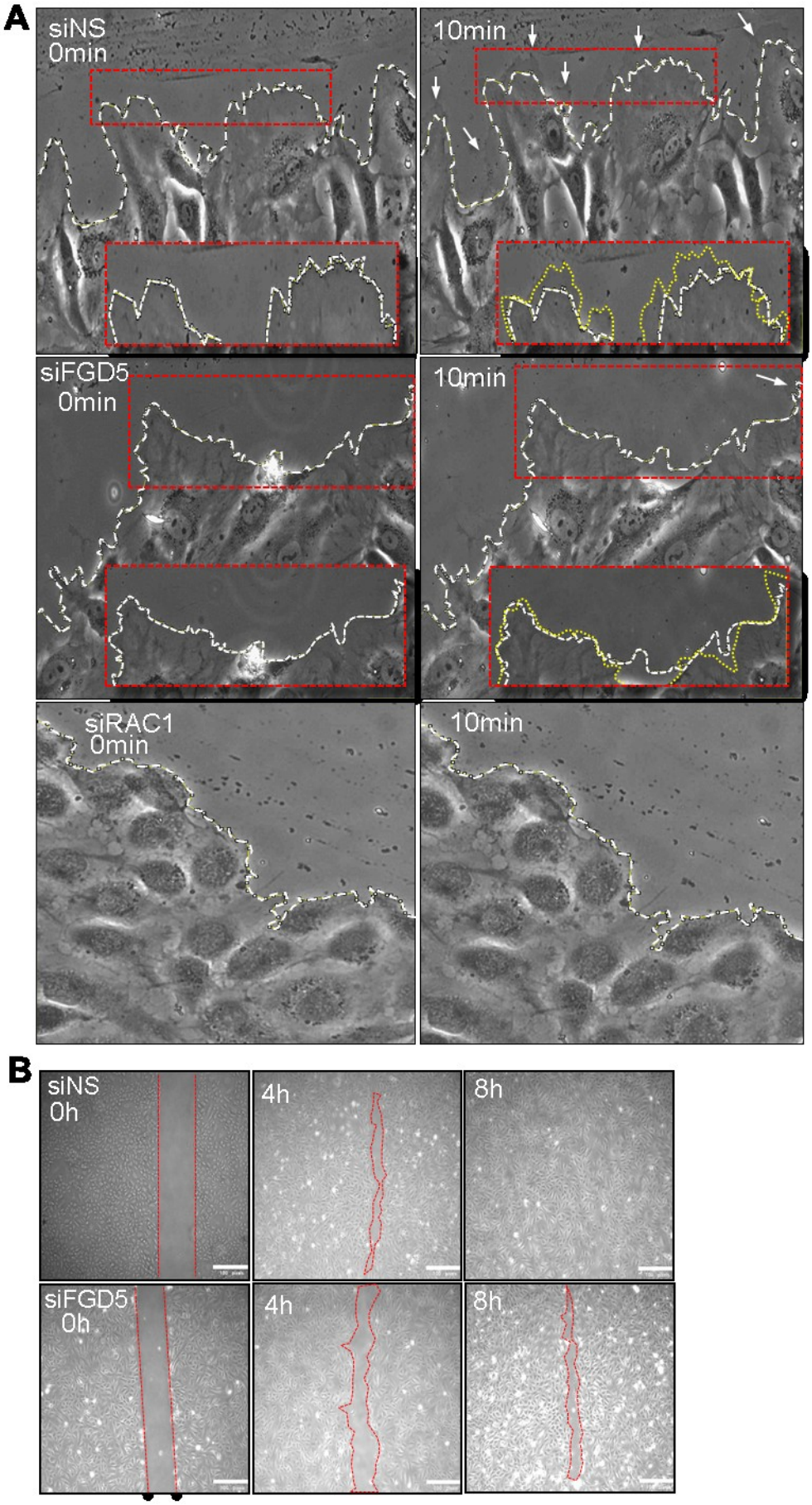
A
siNS
0min
10min
siFGD5
0min
10min
siRAC1
0min
10min
B
siNS
0h
4h
8h
siFGD5
0h
4h
8h

Figure 4.4. FGD5 inhibition negatively regulates HUVECs migration and lamellipodia formation. HUVECs were transfected with non-silencing siRNA (siNS), siRNA against FGD5 (siFGD5) or siRNA against Rac1 (siRac1). FGD5-deficient and Rac1-deficient HUVECs were subjected to protrusion assay as described in materials and methods, and compared to VEGF-stimulated or unstimulated control HUVECs. **A)** Representative images of cellular protrusions (lamellipodia) at 0 min (white line) and 10 min (yellow line) showing reduction in lamellipodia formation in the Rac-deficient and FGD5-deficient HUVECs.

FGD5-deficient and control HUVECs were subjected to migration assay as described in materials and methods. **B)** Representative images of migration assay at 0, 4 and 8 hours.

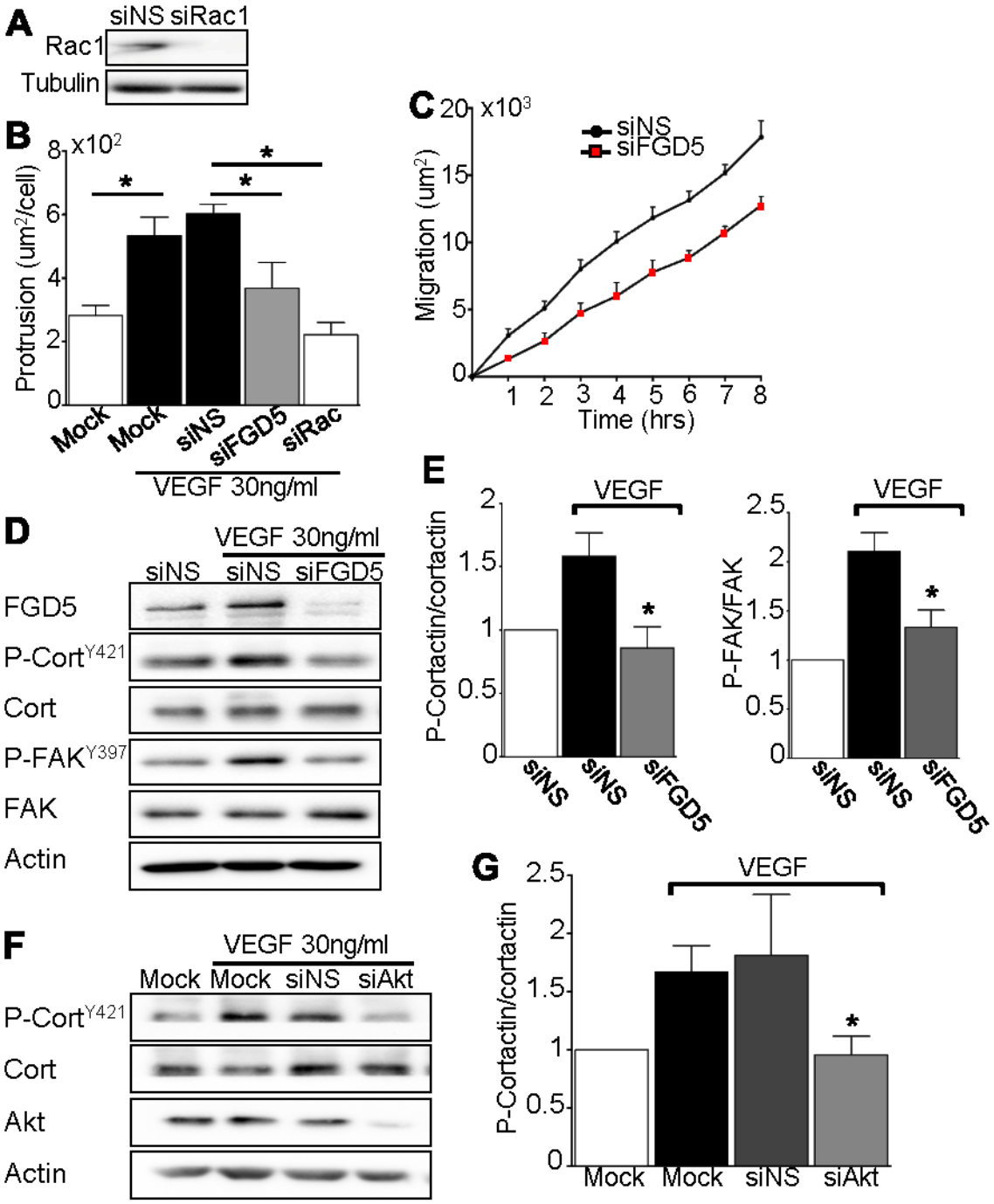
A
siNS siRac1
Rac1
Tubulin
B
x10²
Protrusion (um²/cell)
Mock
Mock
siNS
siFGD5
siRac
VEGF 30ng/ml
C
x10³
siNS
siFGD5
Migration (um²)
Time (hrs)
D
VEGF 30ng/ml
siNS
siNS
siFGD5
FGD5
P-Cort Y421
Cort
P-FAK Y397
FAK
Actin
E
VEGF
P-Cortactin/cortactin
P-FAK/FAK
siNS
siNS
siFGD5
F
VEGF 30ng/ml
Mock
Mock
siNS
siAkt
P-Cort Y421
Cort
Akt
Actin
G
VEGF
P-Cortactin/cortactin
Mock
Mock
siNS
siAkt

Fig 4. 5

Figure 4.5. FGD5 inhibition perturbs cortactin phosphorylation. HUVECs were transfected with non-silencing siRNA (siNS), siRNA targeting Rac1 (siRac1), or siRNA targeting FGD5 (siFGD5). **A)** Representative image of Rac1 and tubulin western blot. FGD5-deficient and Rac1-deficient HUVECs were subjected to protrusion assay as described in materials and methods, and compared to VEGF-stimulated or unstimulated control HUVECs. **B)** Quantitation of protrusion surface area (n=3 independent experiments, *P<0.05 by ANOVA). FGD5-deficient and control HUVECs were subjected to migration assay as described in materials and methods. **C)** Quantitation of cellular migration for 8 hours after the scratch (n=4 independent experiments). HUVECs were transfected with non-silencing siRNA (siNS), siRNA targeting FGD5 (siFGD5) or Akt (siAkt) then stimulated with 30ng/ml VEGF for 10 minutes. **D)** Representative image of FGD5, phospho-cortactinY421 (p-cortY421), total cortactin (cort), phospho-FAKY397 (p-FAKY397), total FAK and Actin Western blot. **E)** Quantitation of p-cortY421 and p-FAKY397 (n=3 independent experiments, *P<0.05 by ANOVA). **F)** Representative image of phospho-cortactinY421 (p-cortY421), total cortactin (cort), total Akt and Actin Western blot. **G)** Quantitation of p-cortY421 (n=3 independent experiments, *P<0.05 by ANOVA).

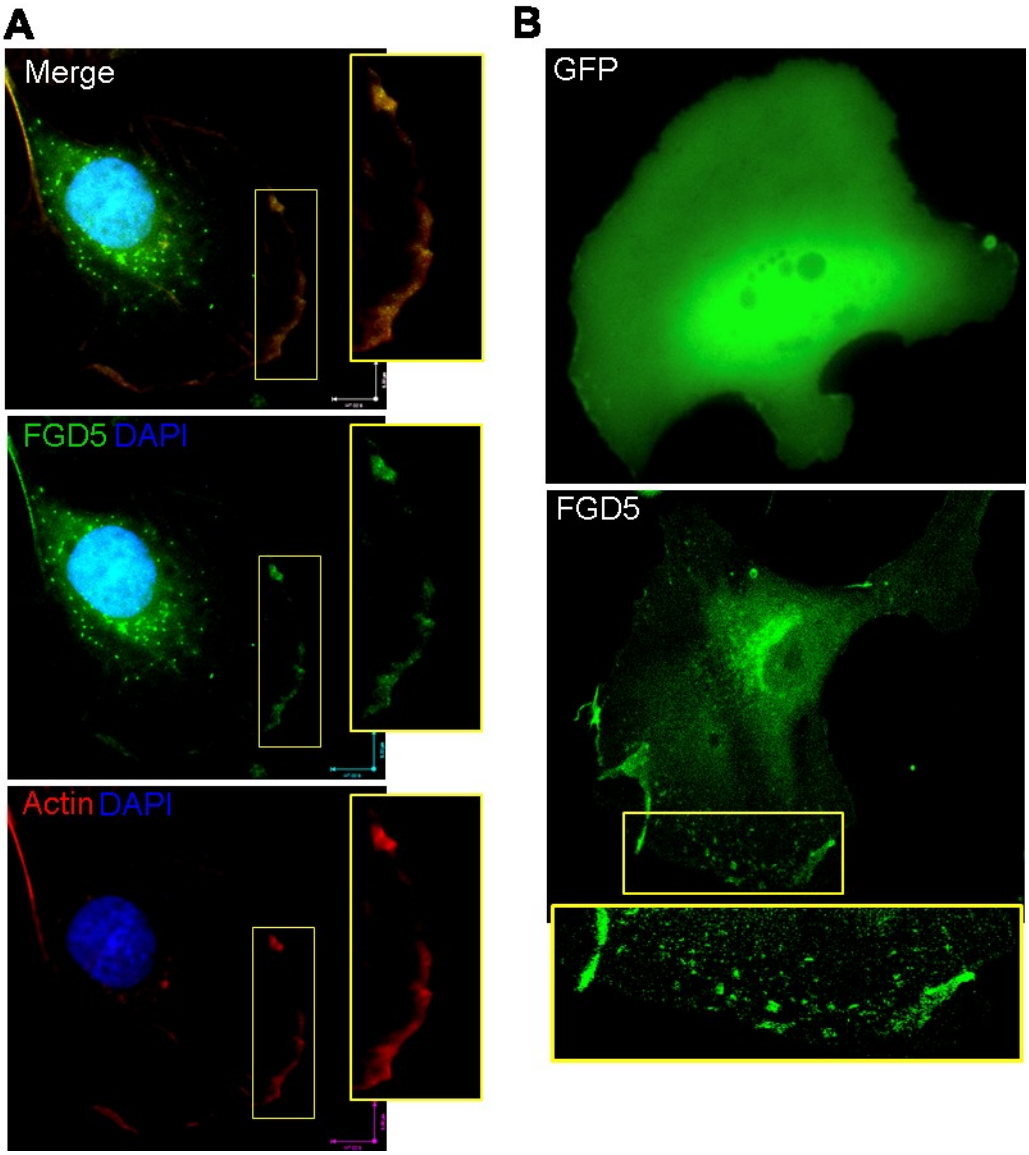

Fig 4. 6

Figure 4.6. FGD5 is localized to EC leading edge. HUVECs were stimulated with VEGF for 30 minutes then fixed and immunostained for actin (red), FGD5 (green) and DAPI (blue). **A)** Representative images of FGD5 colocalized with actin at the leading edge with 63X objective lens. Scale bar: 8um. Human microvascular endothelial cells (HMEC-1) were transfected by EX-FGD5-GFP-M29 plasmid (FGD5) to over express FGD5-GFP, or by the control EX-GFP-M29 plasmid (GFP). **B)** Representative images of FGD5-GFP or GFP over expression in HMEC1 (n= 30 cells from 3 independent experiments).

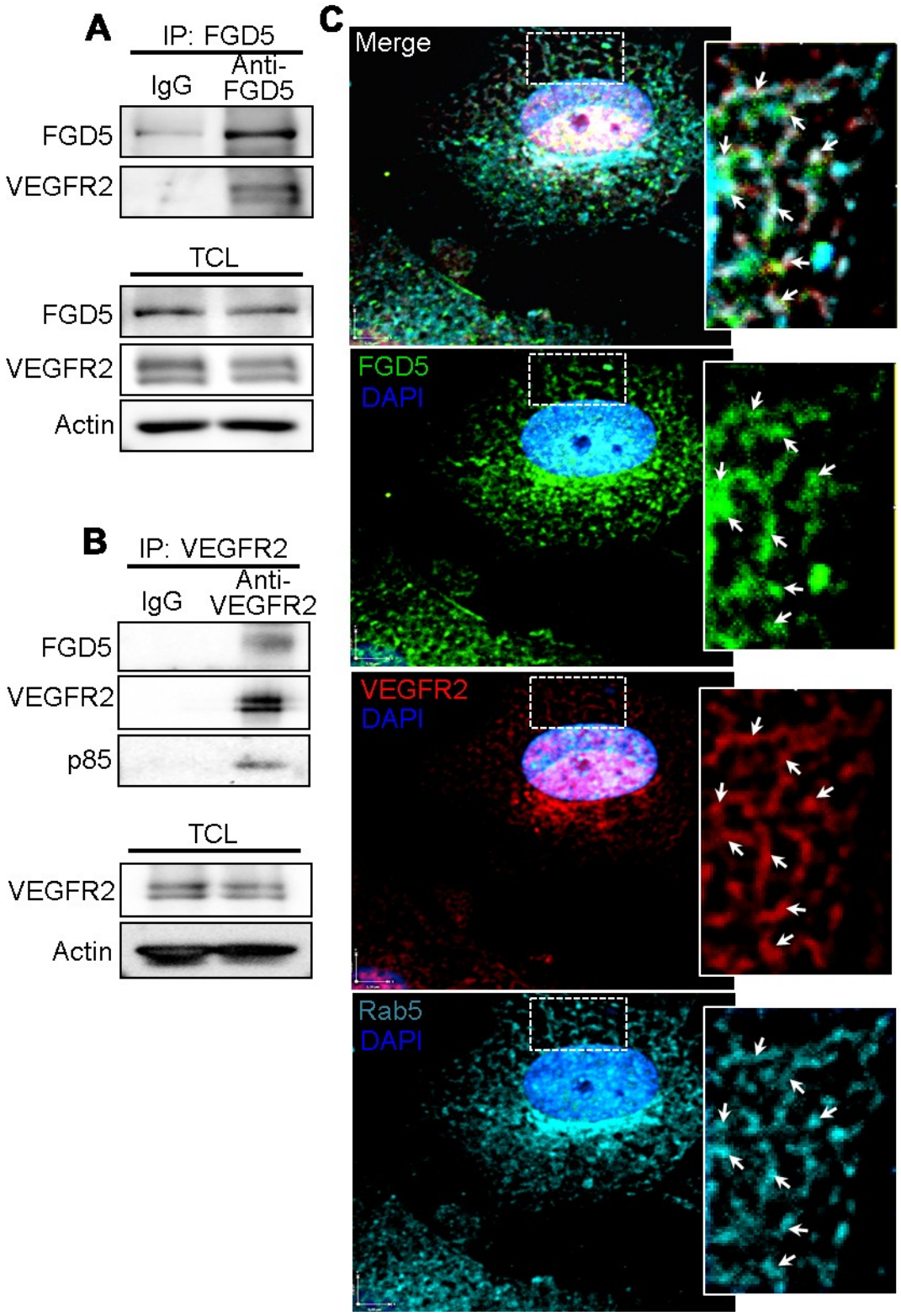
A
IP: FGD5
IgG
Anti-FGD5
FGD5
VEGFR2
TCL
FGD5
VEGFR2
Actin
B
IP: VEGFR2
IgG
Anti-VEGFR2
FGD5
VEGFR2
p85
TCL
VEGFR2
Actin
C
Merge
FGD5
DAPI
VEGFR2
DAPI
Rab5
DAPI

Fig 4. 7

Figure 4.7. FGD5 is associated with VEGFR2. HUVECs were stimulated with VEGF for 30 minutes then cells were lysed and FGD5 or VEGFR2 were immunoprecipitated. **A)** Representative image of FGD5, VEGFR2 and p85 Western blot after immunoprecipitating VEGFR2. Total cell lysate (TCL) shows the basal level of VEGFR2 and actin. **B)** Representative image of FGD5 and VEGFR2 Western blot after immunoprecipitating FGD5. Total cell lysate (TCL) shows the basal level of FGD5, VEGFR2 and actin. **C)** HUVECs were starved overnight, stimulated with 30ng/ml VEGF for 30 min then fixed and stained for FGD5 (green), VEGFR2 (red) and Rab5 (cyan). FGD5 and VEGFR2 colocalized with Rab5 (arrows). Scale bar: 5.5um.

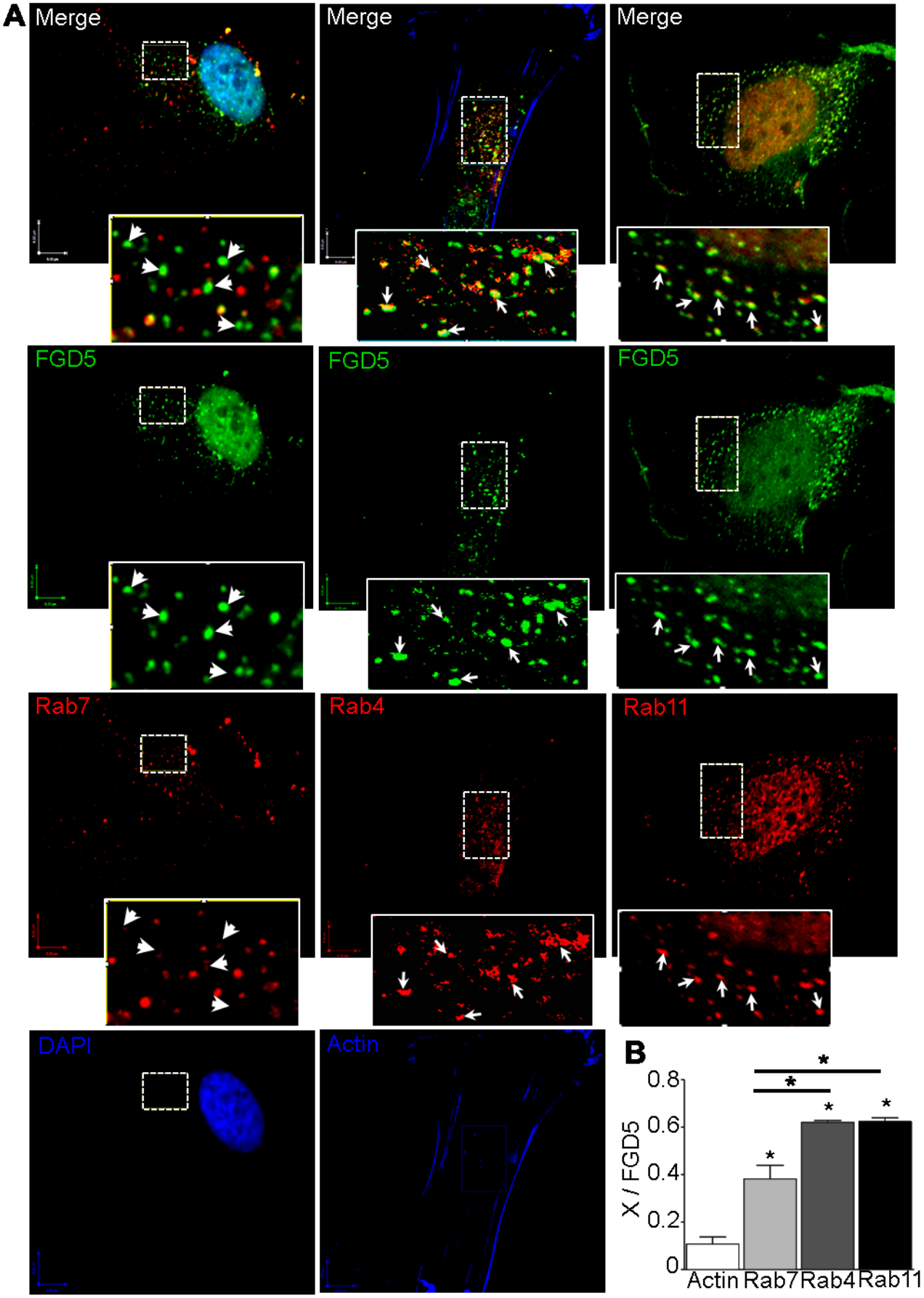
A
Merge
Merge
Merge
FGD5
FGD5
FGD5
Rab7
Rab4
Rab11
DAPI
Actin
B
X / FGD5
0.8
0.6
0.4
0.2
0
Actin
Rab7
Rab4
Rab11
*
*
*
*
*

Figure 4.8. FGD5 is colocalized with the recycling Rab vesicles (Rab4, 11) more than the degradation Rab vesicles (Rab7). A) HUVECs were starved overnight, stimulated with 30ng/ml VEGF for 30 min then fixed and stained for FGD5 (green), Rab7/4/11 (red), and Actin/DAPI (blue). FGD5 colocalizes with Rab4 and Rab11 (arrows) more than Rab7 (arrow heads). Scale bar: 8um. **B)** Quantitaion of the colocalization of FGD5 with the indicated Rab vesicles by pearson's correlation. The bars represent the mean of three random regions of interest per cell. At least 45 cells per group were pooled from three different experiments (n=3 independent experiments, *P<0.05 by ANOVA). Random colocalization was excluded by quantitation of FGD5 colocalization with actin.

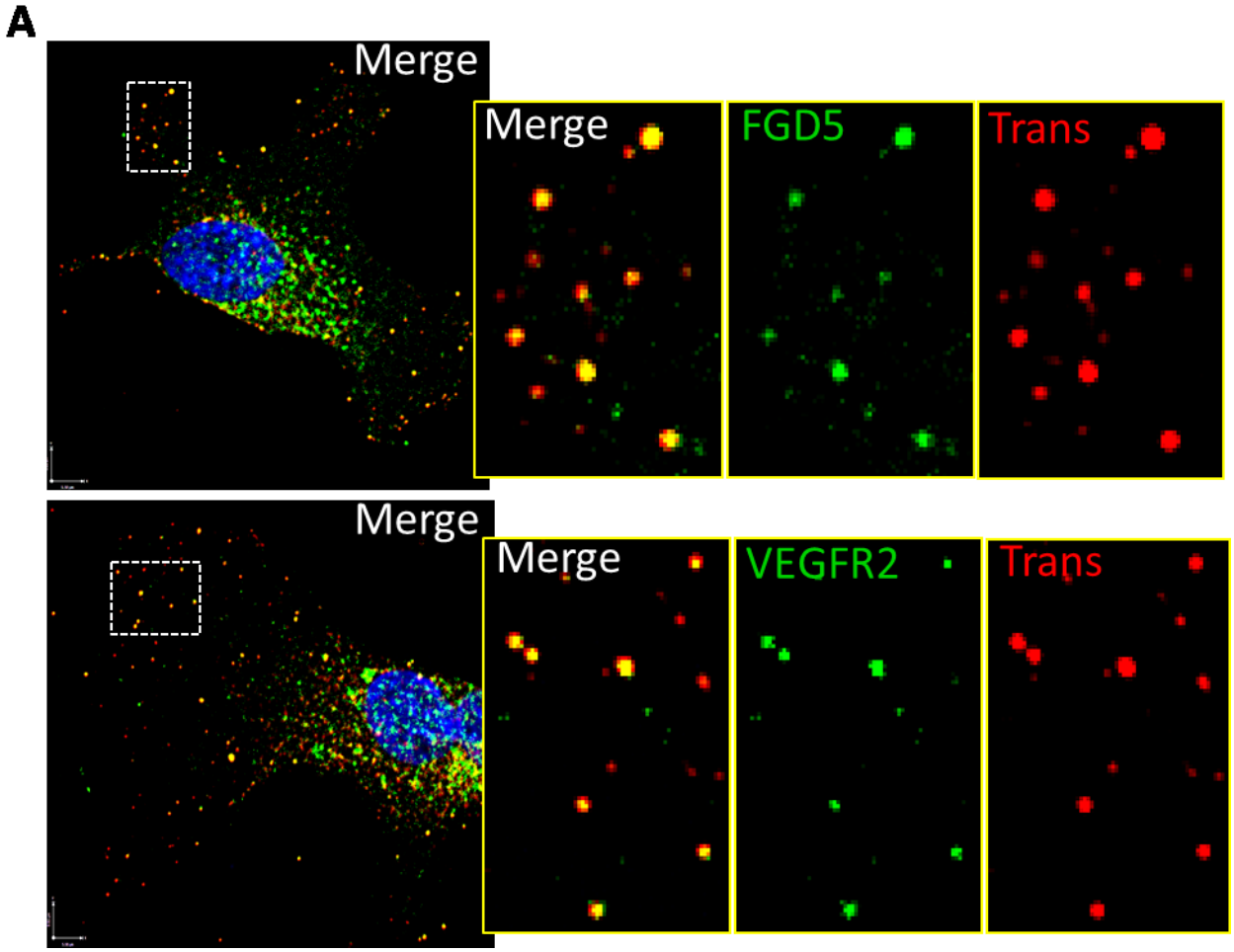

Fig 4. 9

Figure 4.9. FGD5 and VEGFR2 are colocalized with transferrin receptor (early and recycling endosomes marker). A) HUVECs were starved overnight, stimulated with 30ng/ml VEGF for 30 min then fixed and stained for FGD5 (green), VEGFR2 (green), transferrin receptor (Trans) (red), DAPI (blue). Both FGD5 and VEGFR2 colocalize with Trans. Scale bar: 8um.

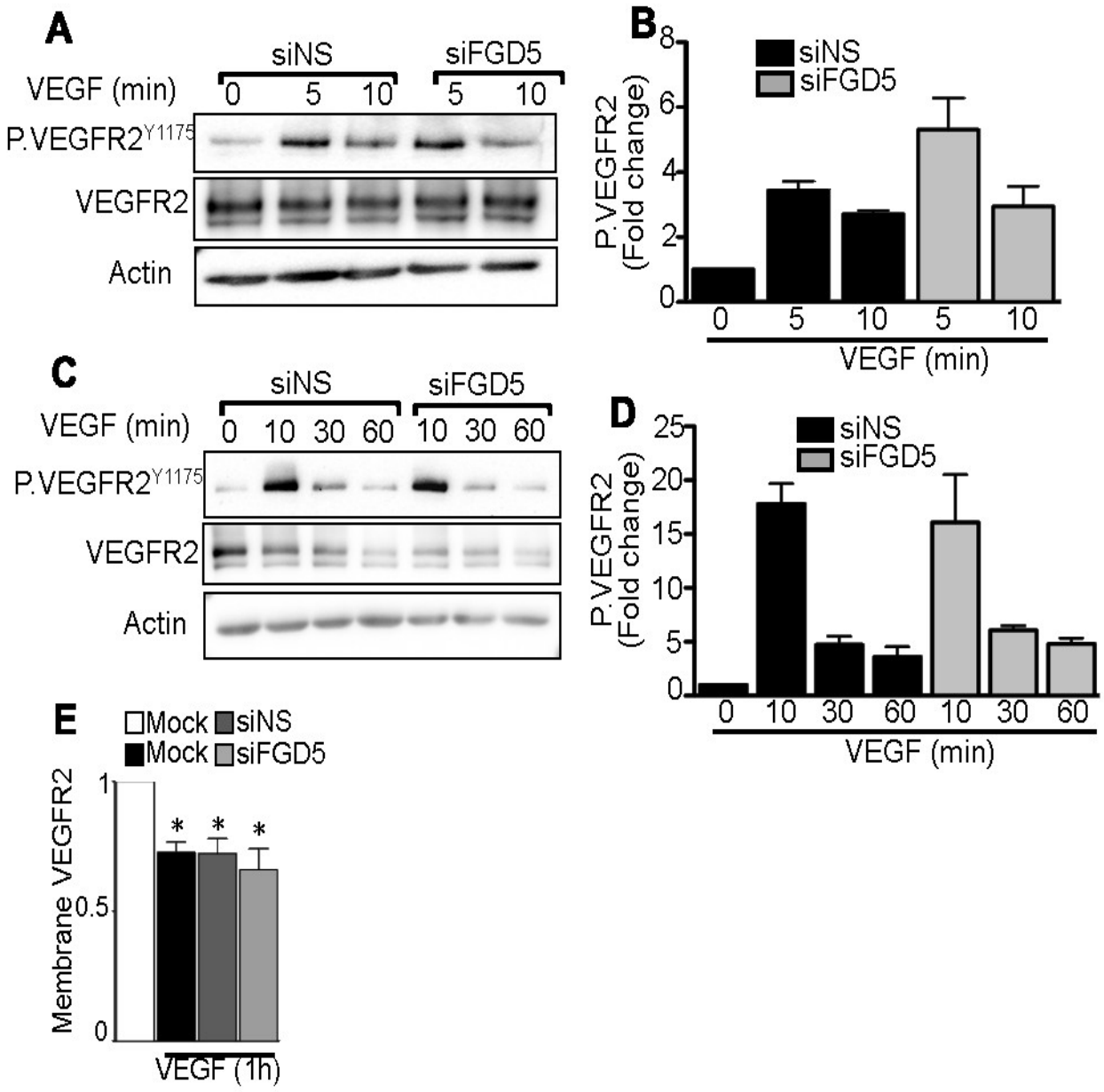
A
siNS
siFGD5
VEGF (min)
0 5 10 5 10
P.VEGFR2Y1175
VEGFR2
Actin
B
siNS
siFGD5
P.VEGFR2 (Fold change)
0 2 4 6 8
0 5 10 5 10
VEGF (min)
C
siNS
siFGD5
VEGF (min)
0 10 30 60 10 30 60
P.VEGFR2Y1175
VEGFR2
Actin
D
siNS
siFGD5
P.VEGFR2 (Fold change)
0 5 10 15 20 25
0 10 30 60 10 30 60
VEGF (min)
E
Mock
siNS
Mock
siFGD5
Membrane VEGFR2
0 0.5 1
*
*
*
VEGF (1h)

Fig 4. 10

Figure 4.10. FGD5 loss does not affect VEGFR2 phosphorylation or membrane expression in HUVECs. HUVECs were transfected with non-silencing siRNA (siNS) or siRNA against FGD5 (siFGD5). After 18 hours of starvation, HUVECs were stimulated by 30 ng/ml VEGF at the indicated time points. **A)** Representative P-VEGFR2, VEGFR2 and actin Western blot. **B)** Quantitation of P-VEGFR2 (n=3 independent experiments, *P<0.05 by ANOVA). To study the effect of FGD5 loss on the longer time points of VEGF stimulation, cells were stimulated for 60 min. **C)** Representative P-VEGFR2, VEGFR2 and actin Western blot. **D)** Quantitation of P-VEGFR2 (n=3 independent experiments, *P<0.05 by ANOVA). siNS or siFGD5 HUVECs were starved overnight then stimulated with VEGF (30 ng/ml) for one hour. **E)** Quantitation of membrane VEGFR2 expression by flowcytometry (n=3 independent experiments, *P<0.05 by ANOVA).

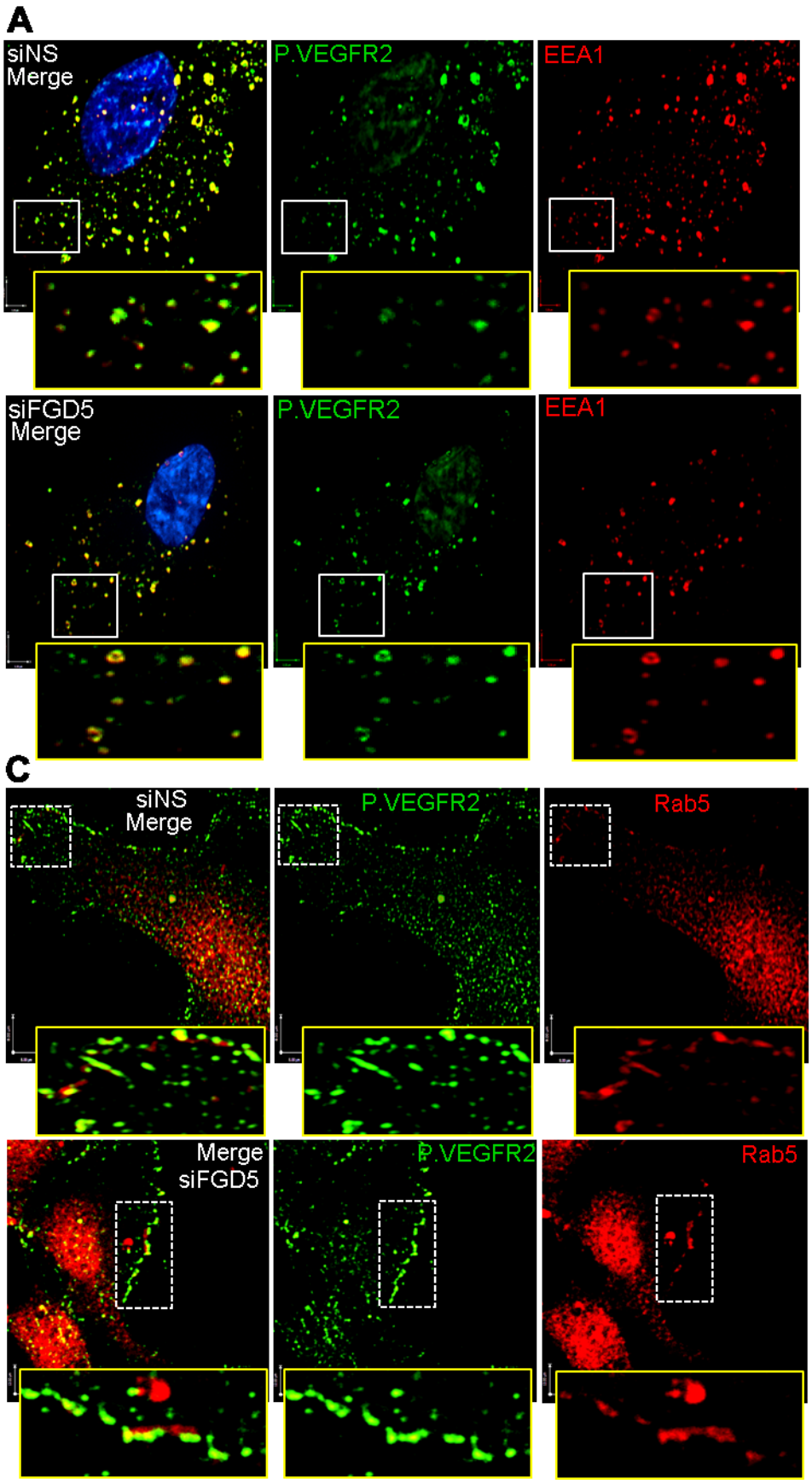
A
siNS
Merge
P.VEGFR2
EEA1
siFGD5
Merge
P.VEGFR2
EEA1
C
siNS
Merge
P.VEGFR2
Rab5
Merge
siFGD5
P.VEGFR2
Rab5

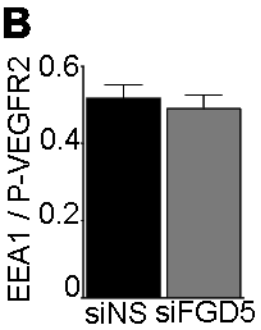
B
EEA1 / P-VEGFR2
0.6
0.4
0.2
0
siNS
siFGD5

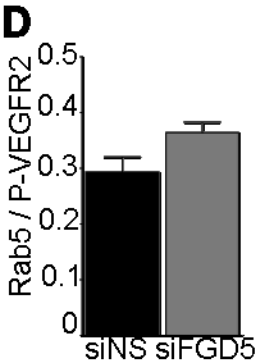
D
Rab5 / P-VEGFR2
0.5
0.4
0.3
0.2
0.1
0
siNS
siFGD5

Figure 4.11. FGD5 loss does not affect VEGFR2 endocytosis. Control (siNS) or FGD5-deficient HUVECs (siFGD5) were starved overnight, stimulated with VEGF (30 ng/ml) for 10 min then fixed and stained for phospho-VEGFR2^{Y1175} (green), early endosome antigen 1 (EEA1) (red) and DAPI (blue). **A)** Representative images of no change in p.VEGFR2 colocalization with EEA1 after FGD5 loss. **B)** Quantitation of p.VEGFR2 colocalization with EEA1 by pearson's correlation. Data represents the mean colocalization from 45 cells pooled from three different experiments. siNS or siFGD5 HUVECs were starved overnight, stimulated with VEGF (30 ng/ml) for 10 min then fixed and stained for phospho-VEGFR2^{Y1175} (green) and Rab5 (red). **C)** Representative images of no change in p.VEGFR2 expression on the cell membrane nor in p.VEGFR2 colocalization with Rab5 after FGD5 loss. **D)** Quantitation of p.VEGFR2 colocalization with Rab5 by pearson's correlation. Data represents the mean colocalization from 45 cells pooled from three different experiments.

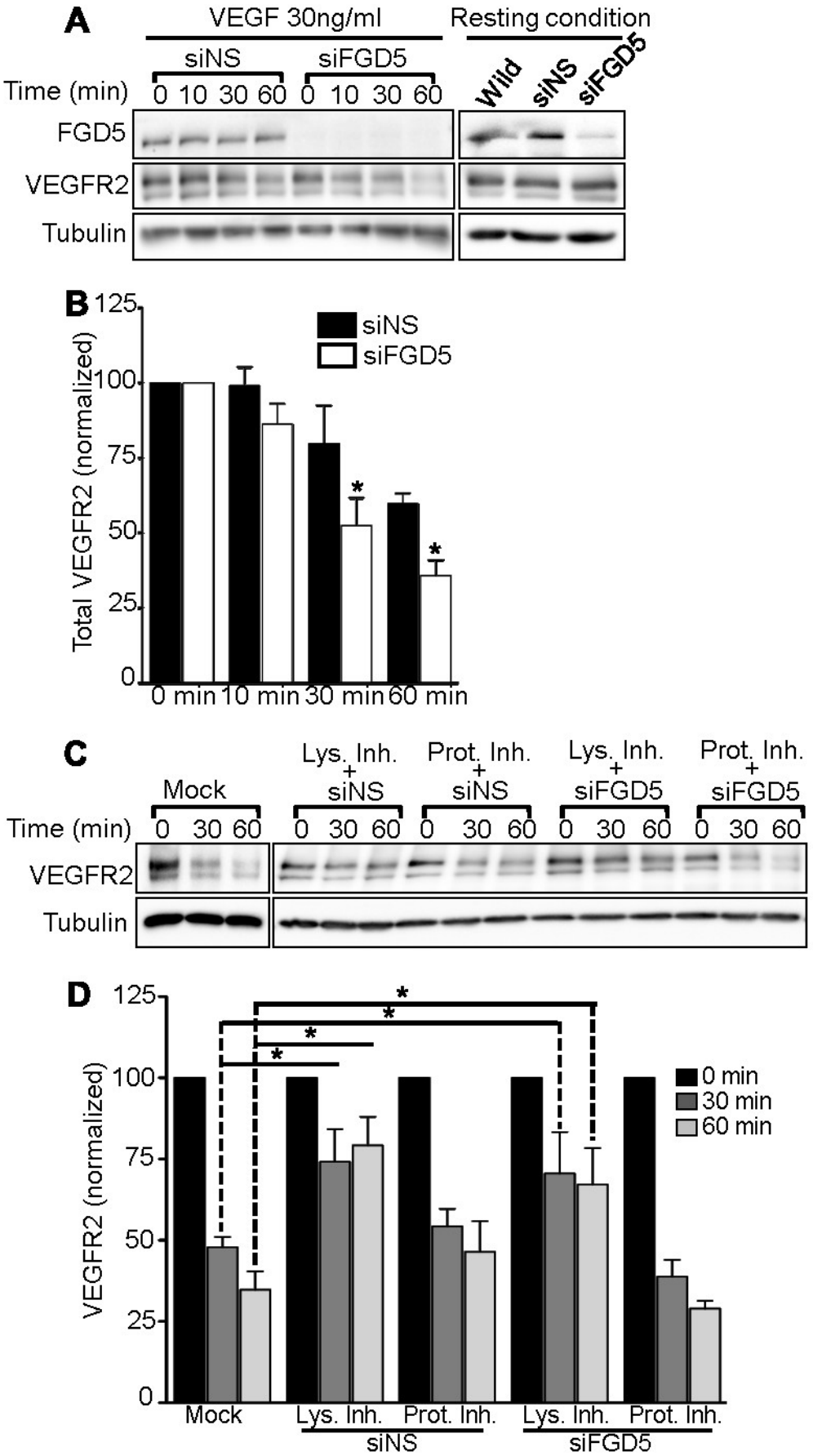
A
VEGF 30ng/ml
Resting condition
siNS
siFGD5
Time (min)
0 10 30 60 0 10 30 60
Wild
siNS
siFGD5
FGD5
VEGFR2
Tubulin
B
Total VEGFR2 (normalized)
125
100
75
50
25
0
siNS
siFGD5
0 min 10 min 30 min 60 min
C
Mock
Lys. Inh. + siNS
Prot. Inh. + siNS
Lys. Inh. + siFGD5
Prot. Inh. + siFGD5
Time (min)
0 30 60 0 30 60 0 30 60 0 30 60 0 30 60
VEGFR2
Tubulin
D
VEGFR2 (normalized)
125
100
75
50
25
0
0 min
30 min
60 min
Mock
Lys. Inh.
Prot. Inh.
siNS
Lys. Inh.
Prot. Inh.
siFGD5

Fig 4. 12

Figure 4.12. FGD5 loss reduces total VEGFR2 levels in HUVECs. HUVECs were transfected with non-silencing siRNA (siNS) or siRNA against FGD5 (siFGD5). After 18 hours of starvation HUVECs were stimulated by 30 ng/ml VEGF at the indicated time points. Under resting condition, VEGFR2 level did not chang excluding any change in protein synthesis after FGD5 loss. **A)** Representative FGD5, VEGFR2 and Tubulin Western blot. **B)** Quantitation of VEGFR2 (n=5 independent experiments, *P<0.05 by two-way ANOVA).

FGD5-deficient HUVECs or control HUVECs were incubated with CA-074 (20 uM) or MG-132 (20 uM) for one hour then stimulated with VEGF at the indicated time points. **C)** Representative VEGFR2 and Tubulin Western blot. **D)** Quantitation of VEGFR2 (n=5 independent experiments, *P<0.05 by two-way ANOVA).

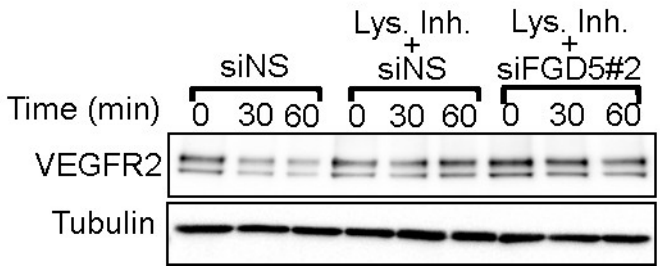

Fig 4. 13

Figure 4.13. Lysosomal inhibition rescues total VEGFR2 level in HMEC1. HMEC1 were transfected with non-silencing siRNA (siNS) or siRNA against FGD5 (siFGD5#2). FGD5-deficient HMEC1 or control HMEC1 were incubated with the lysosome inhibitor CA-074 (20 um; Lys. Inh) for one hour then stimulated with VEGF at the indicated time points. Representative VEGFR2 and Tubulin Western blot showing a decrease in VEGFR2 level after stimulation with VEGF. In addition, the lysosome inhibitor could rescue VEGFR2 even after FGD5 loss.

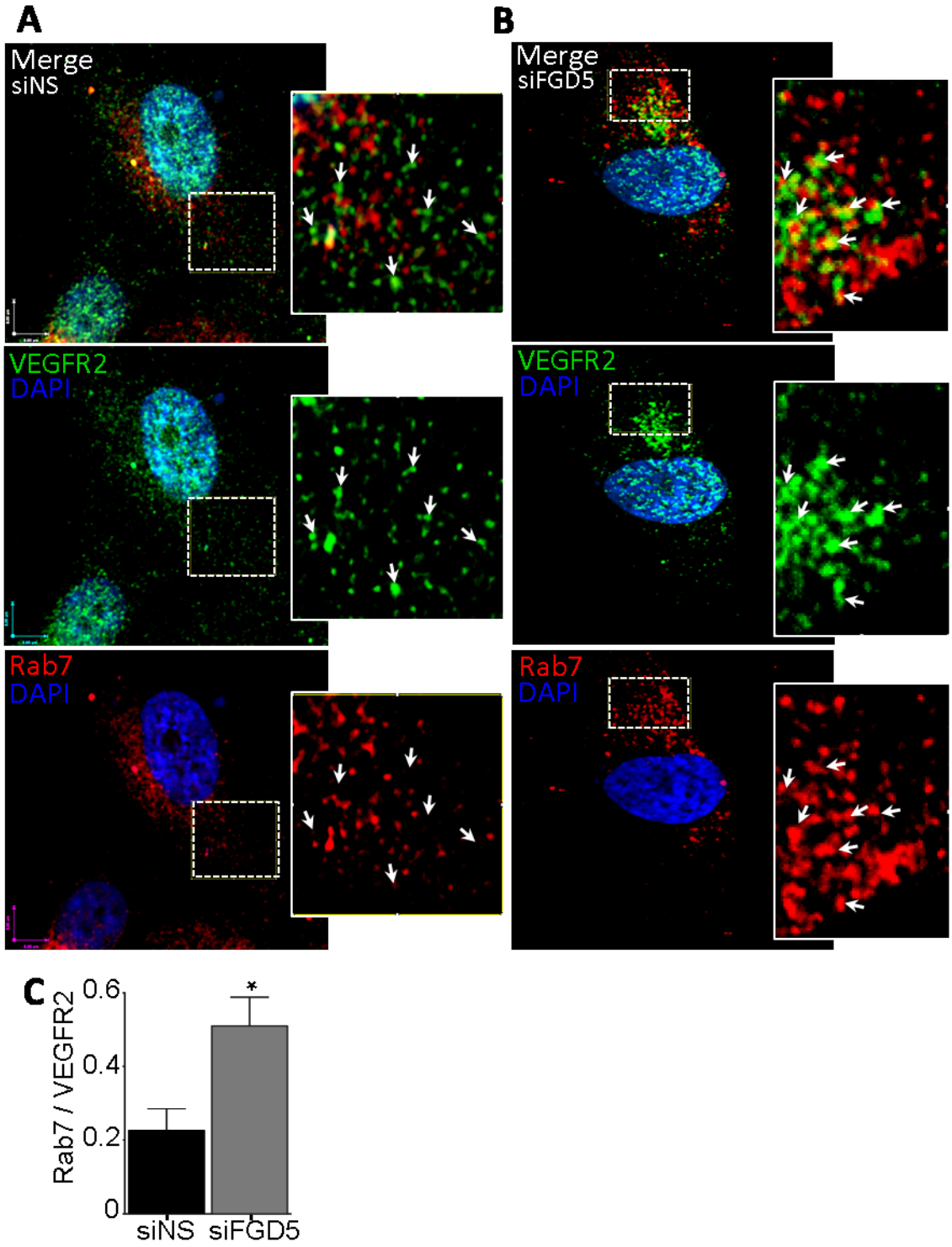
A
B
Merge
siNS
Merge
siFGD5
VEGFR2
DAPI
VEGFR2
DAPI
Rab7
DAPI
Rab7
DAPI
C
Rab7 / VEGFR2
0.6
0.4
0.2
0
*
siNS
siFGD5

Fig 4. 14

Figure 4.14. FDG5 loss targets VEGFR2 to the degradation Rab vesicles (Rab7). Control (siNS) or FGD5-deficient HUVECs (siFGD5) were starved overnight, stimulated with VEGF (30 ng/ml) for 30 min then fixed and stained for VEGFR2 (green), Rab7 (red) and DAPI (blue). **A)** Representative images of minimal colocalization of VEGFR2 with Rab7 in siNS HUVECs. **B)** Representative images of extensive colocalization of VEGFR2 with Rab7 in siFGD5 HUVECs. Scale bar: 8um. **C)** Quantitation of the colocalization of FGD5 with Rab7 vesicles by pearson's correlation. The bars represent the mean of three random regions of interest per cell. At least 45 cells per group were pooled from three different experiments (n=3 independent experiments, *P<0.05 by student t-test).

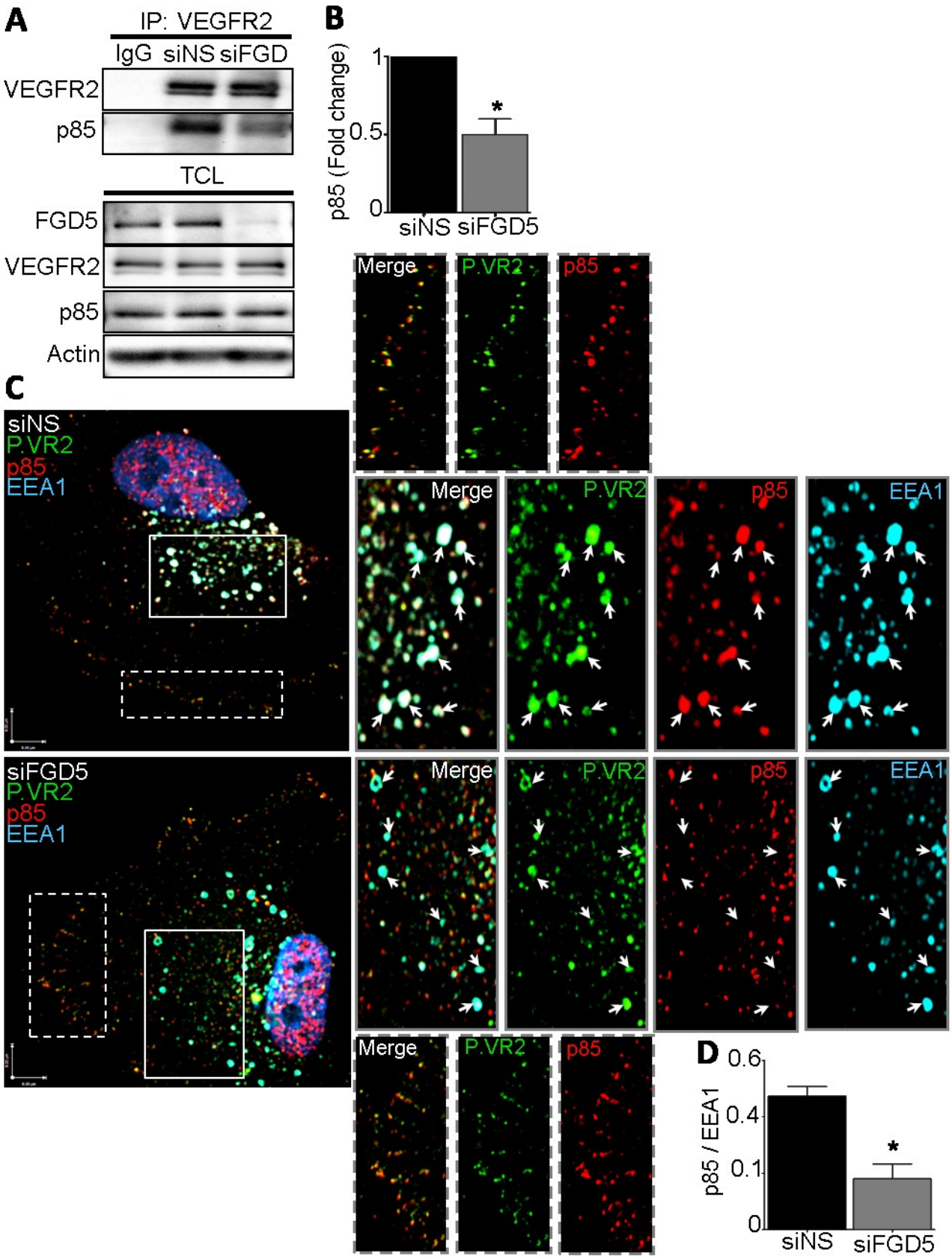
A
IP: VEGFR2
IgG siNS siFGD
VEGFR2
p85
TCL
FGD5
VEGFR2
p85
Actin
B
p85 (Fold change)
1
0.5
0
siNS siFGD5
C
siNS
P.VR2
p85
EEA1
siFGD5
P.VR2
p85
EEA1
Merge
P.VR2
p85
EEA1
D
p85 / EEA1
0.6
0.4
0.1
0
siNS siFGD5

Figure 4.15. FDG5 loss decreases VEGFR2/p85 coupling. Control (siNS) or FGD5-deficient HUVECs (siFGD5) were incubated with VEGF (30 ng/ml) overnight. HUVECs were lysed and VEGFR2 was immunoprecipitated. **A)** Representative image of VEGFR2 and p85 Western blot after immunoprecipitating VEGFR2. Total cell lysate (TCL) shows the basal level of FGD5, VEGFR2, p85 and actin. **B)** Quantitation of p85 immunoprecipitated with VEGFR2 (n=3 independent experiments, *P<0.05 by student t-test).

Control (siNS) or FGD5-deficient HUVECs (siFGD5) were starved overnight, stimulated with VEGF (30 ng/ml) for 10 min then fixed and stained for phospho Y1175 VEGFR2 (P.VR2) (green), p85 (red), EEA1 (cyan) and DAPI (blue). **C)** Representative images of P.VR2/EEA1/p85 colocalization in the cytosol (dashed-frame boxes) and P.VR2/p85 colocalization on the plasma membrane (solid-frame boxes). Arrows are showing P.VR2 positive EEA1 vesicles. Scale bar: 8um. **D)** Quantitaion of the colocalization of p85 with the EEA1 vesicles by pearson's correlation. At least 45 cells per group were pooled from three different experiments (n=3 independent experiments, *P<0.05 by student t-test).

References

1. Carmeliet P. Angiogenesis in health and disease. Nat Med. 2003;9(6):653-660.

2. De Smet F, Segura I, De Bock K, Hohensinner PJ, Carmeliet P. Mechanisms of vessel branching: Filopodia on endothelial tip cells lead the way. Arterioscler Thromb Vasc Biol. 2009;29(5):639-649.

3. Gerhardt H, Golding M, Fruttiger M, et al. VEGF guides angiogenic sprouting utilizing endothelial tip cell filopodia. J Cell Biol. 2003;161(6):1163-1177.

4. Isogai S, Lawson ND, Torrealday S, Horiguchi M, Weinstein BM. Angiogenic network formation in the developing vertebrate trunk. Development. 2003;130(21):5281-5290.

5. del Toro R, Prahst C, Mathivet T, et al. Identification and functional analysis of endothelial tip cell-enriched genes. Blood. 2010;116(19):4025-4033.

6. Strasser GA, Kaminker JS, Tessier-Lavigne M. Microarray analysis of retinal endothelial tip cells identifies CXCR4 as a mediator of tip cell morphology and branching. Blood. 2010;115(24):5102-5110.

7. Holmes K, Roberts OL, Thomas AM, Cross MJ. Vascular endothelial growth factor receptor-2: Structure, function, intracellular signalling and therapeutic inhibition. Cell Signal. 2007;19(10):2003-2012.

8. Bi L, Okabe I, Bernard DJ, Wynshaw-Boris A, Nussbaum RL. Proliferative defect and embryonic lethality in mice homozygous for a deletion in the p110alpha subunit of phosphoinositide 3-kinase. J Biol Chem. 1999;274(16):10963-10968.

9. Jiang BH, Zheng JZ, Aoki M, Vogt PK. Phosphatidylinositol 3-kinase signaling mediates angiogenesis and expression of vascular endothelial growth factor in endothelial cells. Proc Natl Acad Sci U S A. 2000;97(4):1749-1753.

10. Puri KD, Doggett TA, Douangpanya J, et al. Mechanisms and implications of phosphoinositide 3-kinase delta in promoting neutrophil trafficking into inflamed tissue. Blood. 2004;103(9):3448-3456.

11. Vanhaesebroeck B, Leevers SJ, Panayotou G, Waterfield MD. Phosphoinositide 3-kinases: A conserved family of signal transducers. Trends Biochem Sci. 1997;22(7):267-272.

12. Vanhaesebroeck B, Guillermet-Guibert J, Graupera M, Bilanges B. The emerging mechanisms of isoform-specific PI3K signalling. Nature reviews Molecular cell biology. 2010;11(5):329-341.

13. Hawkins PT, Anderson KE, Davidson K, Stephens LR. Signalling through class I PI3Ks in mammalian cells. Biochem Soc Trans. 2006;34(Pt 5):647-662.

14. Czech MP. PIP2 and PIP3: Complex roles at the cell surface. Cell. 2000;100(6):603-606.

15. Lawe DC, Patki V, Heller-Harrison R, Lambright D, Corvera S. The FYVE domain of early endosome antigen 1 is required for both phosphatidylinositol 3-phosphate and Rab5 binding. critical role of this dual interaction for endosomal localization. J Biol Chem. 2000;275(5):3699-3705.

16. Ewan LC, Jopling HM, Jia H, et al. Intrinsic tyrosine kinase activity is required for vascular endothelial growth factor receptor 2 ubiquitination, sorting and degradation in endothelial cells. Traffic. 2006;7(9):1270-1282.

17. Jopling HM, Odell AF, Hooper NM, Zachary IC, Walker JH, Ponnambalam S. Rab GTPase regulation of VEGFR2 trafficking and signaling in endothelial cells. Arterioscler Thromb Vasc Biol. 2009;29(7):1119-1124.

18. Lanzetti L, Palamidessi A, Areces L, Scita G, Di Fiore PP. Rab5 is a signalling GTPase involved in actin remodelling by receptor tyrosine kinases. Nature. 2004;429(6989):309-314.

19. Ballmer-Hofer K, Andersson AE, Ratcliffe LE, Berger P. Neuropilin-1 promotes VEGFR-2 trafficking through Rab11 vesicles thereby specifying signal output. Blood. 2011;118(3):816-826. doi: 10.1182/blood-2011-01-328773; 10.1182/blood-2011-01-328773.

20. Eichmann A, Simons M. VEGF signaling inside vascular endothelial cells and beyond. Curr Opin Cell Biol. 2012;24(2):188-193.

21. Lanahan AA, Hermans K, Claes F, et al. VEGF receptor 2 endocytic trafficking regulates arterial morphogenesis. Developmental cell. 2010;18(5):713-724.

22. Small JV, Stradal T, Vignal E, Rottner K. The lamellipodium: Where motility begins. Trends Cell Biol. 2002;12(3):112-120.

23. Ridley AJ. Rho GTPases and cell migration. J Cell Sci. 2001;114(Pt 15):2713-2722.

24. DALY R. Cortactin signalling and dynamic actin networks. Biochem J. 2004;382:13-25.

25. Lai FP, Szczodrak M, Oelkers JM, et al. Cortactin promotes migration and platelet-derived growth factor-induced actin reorganization by signaling to rho-GTPases. Mol Biol Cell. 2009;20(14):3209-3223.

26. Lua BL, Low BC. Cortactin phosphorylation as a switch for actin cytoskeletal network and cell dynamics control. FEBS Lett. 2005;579(3):577-585.

27. Huang C, Liu J, Haudenschild CC, Zhan X. The role of tyrosine phosphorylation of cortactin in the locomotion of endothelial cells. J Biol Chem. 1998;273(40):25770-25776.

28. Hashimoto A, Hashimoto S, Ando R, et al. GEP100-Arf6-AMAP1-cortactin pathway frequently used in cancer invasion is activated by VEGFR2 to promote angiogenesis. PLoS one. 2011;6(8):e23359.

29. Shen TL, Park AY, Alcaraz A, et al. Conditional knockout of focal adhesion kinase in endothelial cells reveals its role in angiogenesis and vascular development in late embryogenesis. J Cell Biol. 2005;169(6):941-952.

30. Nakhaei-Nejad M, Haddad G, Zhang QX, Murray AG. Facio-genital dysplasia-5 regulates matrix adhesion and survival of human endothelial cells. Arterioscler Thromb Vasc Biol. 2012;32(11):2694-2701.

31. Kurogane Y, Miyata M, Kubo Y, et al. FGD5 mediates proangiogenic action of vascular endothelial growth factor in human vascular endothelial cells. Arterioscler Thromb Vasc Biol. 2012;32(4):988-996.

32. Cheng C, Haasdijk R, Tempel D, et al. Endothelial cell-specific FGD5 involvement in vascular pruning defines neovessel fate in mice. Circulation. 2012;125(25):3142-3158.

33. Gazit R, Mandal PK, Ebina W, et al. Fgd5 identifies hematopoietic stem cells in the murine bone marrow. J Exp Med. 2014;211(7):1315-1331.

34. Gillooly D, SIMONSEN A, STENMARK H. Cellular functions of phosphatidylinositol 3-phosphate and FYVE domain proteins. Biochem J. 2001;355:249-258.

35. Burd CG, Emr SD. Phosphatidylinositol (3)-phosphate signaling mediated by specific binding to RING FYVE domains. Mol Cell. 1998;2(1):157-162.

36. Gaullier J, Simonsen A, D'Arrigo A, Bremnes B, Stenmark H, Aasland R. FYVE fingers bind PtdIns (3) P. Nature. 1998;394(6692):432-433.

37. Patki V, Lawe DC, Corvera S, Virbasius JV, Chawla A. A functional PtdIns (3) P-binding motif. Nature. 1998;394(6692):433-434.

38. Shibata T, Imaizumi T, Tamo W, et al. Proteasome inhibitor MG-132 enhances the expression of interleukin-6 in human umbilical vein endothelial cells: Involvement of MAP/ERK kinase. Immunol Cell Biol. 2002;80(3):226-230.

39. Montaser M, Lalmanach G, Mach L. CA-074, but not its methyl ester CA-074Me, is a selective inhibitor of cathepsin B within living cells. Biol Chem. 2002;383(7-8):1305-1308.

40. Zhang Q, Nakhaei-Nejad M, Haddad G, Wang X, Loutzenhiser R, Murray AG. Glomerular endothelial PI3 kinase-α couples to VEGFR2, but is not required for eNOS activation. American Journal of Physiology-Renal Physiology. 2011;301(6):F1242-F1250.

41. Nakatsu MN, Hughes CC. An optimized three-dimensional in vitro model for the analysis of angiogenesis. Methods Enzymol. 2008;443:65-82.

42. Farhan MA, Carmine-Simmen K, Lewis JD, Moore RB, Murray AG. Endothelial cell mTOR complex-2 regulates sprouting angiogenesis. PloS one. 2015;10(8):e0135245.

43. Meyer AS, Hughes-Alford SK, Kay JE, et al. 2D protrusion but not motility predicts growth factor-induced cancer cell migration in 3D collagen. J Cell Biol. 2012;197(6):721-729.

44. Huber AB, Kolodkin AL, Ginty DD, Cloutier J. Signaling at the growth cone: Ligand-receptor complexes and the control of axon growth and guidance. Annu Rev Neurosci. 2003;26(1):509-563.

45. Pollard TD, Borisy GG. Cellular motility driven by assembly and disassembly of actin filaments. Cell. 2003;112(4):453-465.

46. Krause M, Gautreau A. Steering cell migration: Lamellipodium dynamics and the regulation of directional persistence. Nature Reviews Molecular Cell Biology. 2014;15(9):577-590.

47. Grant BD, Donaldson JG. Pathways and mechanisms of endocytic recycling. Nature reviews Molecular cell biology. 2009;10(9):597-608.

48. Miaczynska M, Pelkmans L, Zerial M. Not just a sink: Endosomes in control of signal transduction. Curr Opin Cell Biol. 2004;16(4):400-406.

49. Tavora B, Batista S, Reynolds LE, et al. Endothelial FAK is required for tumour angiogenesis. EMBO Mol Med. 2010;2(12):516-528.

50. Braren R, Hu H, Kim YH, Beggs HE, Reichardt LF, Wang R. Endothelial FAK is essential for vascular network stability, cell survival, and lamellipodial formation. J Cell Biol. 2006;172(1):151-162.

51. Gampel A, Moss L, Jones MC, Brunton V, Norman JC, Mellor H. VEGF regulates the mobilization of VEGFR2/KDR from an intracellular endothelial storage compartment. Blood. 2006;108(8):2624-2631.

52. Lampugnani MG, Orsenigo F, Gagliani MC, Tacchetti C, Dejana E. Vascular endothelial cadherin controls VEGFR-2 internalization and signaling from intracellular compartments. J Cell Biol. 2006;174(4):593-604.

53. Bruns AF, Herbert SP, Odell AF, et al. Ligand-stimulated VEGFR2 signaling is regulated by co-ordinated trafficking and proteolysis. Traffic. 2010;11(1):161-174.

54. Meyer RD, Srinivasan S, Singh AJ, Mahoney JE, Gharahassanlou KR, Rahimi N. PEST motif serine and tyrosine phosphorylation controls vascular endothelial growth factor receptor 2 stability and downregulation. Mol Cell Biol. 2011;31(10):2010-2025.

55. Smith GA, Fearnley GW, Abdul-Zani I, et al. VEGFR2 trafficking, signaling and proteolysis is regulated by the ubiquitin isopeptidase USP8. Traffic. 2015.

56. Nakayama M, Nakayama A, van Lessen M, et al. Spatial regulation of VEGF receptor endocytosis in angiogenesis. Nat Cell Biol. 2013;15(3):249-260.

57. Srinivasan S, Meyer RD, Lugo R, Rahimi N. Identification of PDCL3 as a novel chaperone protein involved in the generation of functional VEGF receptor 2. J Biol Chem. 2013;288(32):23171-23181.

58. Dayanir V, Meyer RD, Lashkari K, Rahimi N. Identification of tyrosine residues in vascular endothelial growth factor receptor-2/FLK-1 involved in activation of phosphatidylinositol 3-kinase and cell proliferation. J Biol Chem. 2001;276(21):17686-17692.

59. Holmqvist K, Cross MJ, Rolny C, et al. The adaptor protein shb binds to tyrosine 1175 in vascular endothelial growth factor (VEGF) receptor-2 and regulates VEGF-dependent cellular migration. J Biol Chem. 2004;279(21):22267-22275.

60. van Lessen M, Nakayama M, Kato K, Kim JM, Kaibuchi K, Adams RH. Regulation of vascular endothelial growth factor receptor function in angiogenesis by numb and numb-like. Arterioscler Thromb Vasc Biol. 2015;35(8):1815-1825.

61. Herzog B, Pellet-Many C, Britton G, Hartzoulakis B, Zachary IC. VEGF binding to NRP1 is essential for VEGF stimulation of endothelial cell migration, complex formation between NRP1 and VEGFR2, and signaling via FAK Tyr407 phosphorylation. Mol Biol Cell. 2011;22(15):2766-2776.

62. Lanahan A, Zhang X, Fantin A, et al. The neuropilin 1 cytoplasmic domain is required for VEGF-A-dependent arteriogenesis. Developmental cell. 2013;25(2):156-168.

Chapter V: FGD5 regulates GPCRs signaling to PI3K

Abstract

Facio-genital dysplasia 5 (FGD5) regulates vascular endothelial growth factor- (VEGF) mediated angiogenesis. However, the role of FGD5 to regulate other pro-angiogenic signaling pathways that co-operate with VEGF has not been explored. Here, we identify a novel role of FGD5 to control G protein-coupled receptor (GPCR) signaling.

Angiogenic sprouting was evaluated in a three dimensional in vitro model. We examined the role of FGD5 to regulate GPCRs in two different EC cell lines by Western blot and immunofluorescent staining.

Stromal cell-derived factor 1 (SDF1; CXCL12) has a similar angiogenic potency to VEGF. Dual stimulation of endothelial cells (EC) with SDF1 and VEGF had synergic effect on angiogenesis more than VEGF alone. FGD5 loss in EC abolished the SDF1 angiogenic effect and SDF1 signaling to phosphatidylinositol (PI) 3 Kinase-β and Akt Cdc42 inhibition, a Rho guanine nucleotide exchange factor required for PI3 Kinase- β activity, recapitulated the signaling defects of FGD5 deficiency, indicating that FGD5 may control PI3 Kinase- β activity through Cdc42. Similarly, FGD5 deficiency blocks Apelin- but not sphingosine 1 phosphate (S1P)-stimulated phosphorylation of Akt, indicating FGD5 selectively regulates GPCR signaling. FGD5 loss did not affect CXCR4, the SDF1 receptor, expression. Further, FGD5 loss did not affect SDF1-stimulated MAP Kinase signaling. Subcellular localization of PI3 Kinase- β to the early endosomes occurred normally after SDF1 stimulation of FGD5-deficient EC. However, endosome display of S473-phosphorylated Akt, was absent in FGD5-deficient EC. Failure of Akt

activation at the PI3 Kinase- β positive endosomes suggests a defect in PI3 Kinase- β activity after FGD5 loss. This study identifies a novel role of FGD5 in regulating GPCR signaling to PI3 Kinase- β, and suggests FGD5 as a convergence node regulating multiple angiogenic pathways that may serve as a potential target for anti-angiogenic therapy.

Introduction

Understanding the signaling molecules that regulate angiogenesis can help to develop therapies for diseases characterized by hyper- or hypo-vascularity[1].

Tumors not only stimulate angiogenesis, but the formed blood vessels are abnormal in structure and function [2,3]. Tumor vessels are tortuous, connect to one another randomly, branch irregularly and are not fully differentiated into arterioles and venules [3-5]. Similarly, endothelial cells (EC) in the tumor vasculature lose their polarity, migrate away from the basement membrane with leading tip cells penetrating deep into the tissue[4-6]. Vascular endothelial growth factor (VEGF) is the key angiogeneic factor that stimulates EC growth, migration, permeability, lumen formation, and survival [7-9]. High levels of VEGF correlate with vessel abnormalities in tumors [10-12]. These observations have led to the notion that targeting tumor angiogenesis by VEGF pathway inhibition may prevent tumor growth.

VEGF receptor-2 (VEGFR2) is a receptor tyrosine kinase (RTK). Binding of VEGFR2 by its ligand (VEGF) activates phosphatidylinositide 3-kinase (PI3K) activity [13]. PI3Ks are divided into three classes according to their structural and substrate specificity [14]. Of these, the most commonly studied is class I PI3K that is further divided into: class IA isoforms, which are variably activated by RTKs, G protein-coupled receptors (GPCRs) and the small GTPase Ras;

and the single class IB isoform, which is only activated by GPCRs . The latter plays a minor role in EC compared to Class IA [15,16]. Class IA PI3K consists of a p110 catalytic subunit and a p85 regulatory subunit. EC express all three isoforms of the class IA PI3K, named according to their catalytic subunits: α , β, δ [17,18]. The lipid kinase activity of PI3K-α is regulated by RTKs and Ras, which binds directly to the Ras-binding domain (RBD) on the catalytic subunit [19,20]. In contrast, PI3K-β is less sensitive to activation by RTKs, but is an important downstream effector of GPCR signals [21,22]. Instead of Ras, Rac 1 and Cdc42 from the Rho family of small GTPases binds and activates PI3K-β via a Rho Binding Domain [23]. Of note, PI3K-α and -β are highly expressed in immortalized mouse cardiac EC and human umbilical vein EC (HUVECs), and studies have shown an essential function of class I PI3Ks in vascular development and angiogenesis [24,25]. Thus, PI3K could be a potential target to regulate VEGF-mediated angiogenesis.

Stromal cell-derived factor-1 (SDF1; CXCL12) was identified as a chemokine that induces the chemotaxis of lymphocytes, monocytes [26-29], and hematopoietic progenitor cells [30,31]. SDF1 deletion in mice is lethal shortly after birth with vascular defects noted in the gut and kidney microvasculature [32]. SDF1 binds specifically to the GPCR CXCR4, which is expressed on lymphocytes, monocytes, neutrophils, and epithelial cells [33,34]. CXCR4 was recently found to be expressed on various human EC [35-37]. Furthermore, SDF1 induces angiogenesis in vitro and in vivo [38,39]. VEGF or FGF induce the surface expression of CXCR4 only on EC, and increase EC migration and angiogenesis in response to SDF1 [38,40]. Moreover, the SDF1/CXCR4 pathway also affects tumor angiogenesis independently of the VEGF pathway [41-44]. On the basis of these findings, multiple agents are currently being developed to target the SDF1 pathway in cancer. However, blockade of the SDF1 pathway has minor tumor suppression effects on established

tumors. Moreover, CXCR4 antagonists inhibited tumor growth in some cases [45,46], but were ineffective in others [47-49]. Thus, these preclinical studies suggest that blocking the SDF1 pathway solely may not be sufficient or universally effective, but may be useful against certain solid tumors.

Facio-genital dysplasia-5 (FGD5) is a member of FYVE, RhoGEF, and PH domain-containing family, which is robustly expressed in highly vascularized organs and especially in EC [50,51]. The Rho guanine nucleotide exchange factor (GEF) domain induces Rho GTPase activity by exchanging GTP for GDP and may be specific for Cdc42 [50]. Among RhoGEFs, a PH domain typically accompanies the Rho GEF domain that mediates exchange factor activity. The PH domain is thought to play a crucial role in recruiting the protein to the cell membrane [52]. The FYVE domain may increase the binding specificity or alter sub-cellular localization of FGD5 as it likely mediates interactions with phosphatidylinositol- 3´-phosphate [53]. Recently, FGD5 has been heavily investigated to elucidate its physiological significance in EC. In a previous report we showed that FGD5-loss negatively regulates VEGF/PI3K pathway, and angiogenesis in 3 dimensional (3D) angiogenesis assay, and in vivo [51]. Further, the observation that FGD5 null mice do not survive beyond embryonic day 12 (E12) [54] and the robust expression of FGD5 in aorta-gonad mesonephros of mice embryos, which is the origin of the aorta [54], and vascular endothelial cells suggest that FGD5 may have a pivotal role in vascular development and angiogenesis. Taken together, we hypothesize that FGD5 may represent a convergence node to signals from VEGFR2 and CXCR4, and is required for tumor angiogenesis. In the current study, we investigated the role of FGD5 in regulating GPCR signalling, with emphasis on CXCR4.

Results

SDF1 is an pro-angiogenic stimulant as potent as VEGF

To investigate the role of SDF1 as an angiogenic stimulant we compared the number and length of the formed tip cells in a three dimensional (3D) fibrin matrix after stimulating endothelial cells (EC) with vascular endothelial cell growth factor (VEGF) (50ng/ml) or SDF1 (100ng/ml). In human umbilical vein EC (HUVEC), both VEGF and SDF1 exert a similar effect on tip cell sprout formation (Fig. 5.1A, B). However, after priming HUVEC or human microvascular EC (HMEC-1) with VEGF to increase endothelial CXCR4 expression [40], SDF1 stimulation increased sprouting more than VEGF alone (Fig. 5.1C; Fig. 5.2A, B). VEGF priming led to more than 30% increase in the number of tip cell sprouts in the SDF1 stimulated HUVEC (Fig. 5.1D). Similarly, adding SDF1 to VEGF increased HUVEC and HMEC-1 migration more than VEGF alone in the scratch wound-healing assay (Fig. 5.1E, F). Taken together, SDF1 is a potent angiogenic stimulant that potentiates VEGF-mediated angiogenesic sprouting.

FGD5 and CXCR4 are required for SDF1 angiogenic effect

Although CXCR4 is the specific receptor for SDF1, there is evidence that SDF1 can also bind to CXCR7 [57]. Thus, to determine if the SDF1-mediated angiogenesis is CXCR4 dependent, HUVECs and HMEC-1 were transfected with non-silencing short interfering (si)RNA, or siRNA against CXCR4. Targeting CXCR4 with siRNA led to a dramatic reduction in CXCR4

expression (Fig. 5.3B). Both CXCR4-deficient HUVEC and HMEC-1 showed ~70% reduction in tip cell sprout formation (Fig. 5.3 C-F).

Next, to investigate if Facio-genital dysplasia 5 (FGD5) regulates SDF1/CXCR4 mediated angiogenesis, we performed FGD5 loss of function experiments. Targeting FGD5 with siRNA markedly reduced FGD5 expression in EC (Fig. 5.3 A), and led to a pronounced reduction in tip cell sprout formation and sprout length in both HUVEC and HMEC-1 (Fig. 5.3 C-F). Therefore, EC CXCR4 critically mediates the pro-angiogenic effect of SDF1. Moreover, FGD5 is required for the SDF1/CXCR4 pro-angiogenic effect.

FGD5 acts upstream of mTORC2 and Akt

Focal adhesion kinase (FAK) is essential for vasculogenesis in mice [58 59], and is a key regulator of cell-matrix adhesion and cytoskeleton remodelling in response to growth factor signals[59]. In a previous report, we showed that PI3K-dependent mTORC2 activity regulates FAK Y397 phosphorylation, independent of Akt [60]. Therefore, we investigated the effect of FGD5 loss on FAK Y397-, and Akt S473- phosphorylation as read-outs of mTORC2 and upstream PI3K activity. SDF1-induced FAK Y397 auto-phosphorylation and Akt S473 phosphorylation were both reduced in FGD5-deficient HUVEC, and HMEC-1 monolayers compared to controls (Fig. 5.4A-F). This indicates that FGD5 regulates the SDF1/PI3K pathway upstream of Akt and mTORC2. Of note, PI3Kβ-inhibited EC had reduced Akt activity after SDF1 stimulation (Fig. 5.4G) but not after VEGF stimulation indicating a crucial role of PI3Kβ in mediating CXCR4 signaling to Akt.

To investigate if FGD5 loss has a broader impact on other GPCR signalling, we tested the effect of endothelial FGD5 loss on the response of the Apelin receptor and the sphingosine-1-

phosphate (S1P) receptor to their ligands. Apelin and S1P are known to play pivotal role in angiogenesis [61,62]. In EC, S1P has previously been demonstrated to couple to PI3Kβ activity [63]. Interestingly, we found FGD5 loss regulated Apelin-, but not S1PR1- mediated signalling to Akt (Fig. 5.5A-C). Further, PI3Kβ pharmacological inhibition with the isoform-selective inhibitor TGX-221 [64] blocked Apelin signalling to Akt S473, confirming Apelin receptor coupling to PI3K-β in EC (Supplemental Fig. 5.5D, E). These findings indicate that the role of FGD5 in regulating GPCRs is not restricted to CXCR4.

Cdc42 inhibition, but not Rac1, results in the same signaling defects of FGD5 loss

FGD5 is reported to mediate VEGF-stimulated Cdc42 activity in EC [50]. Cdc42 is a Rho GTPase that binds and specifically regulates the PI3Kβ isoform via the p110β Ras binding domain (RBD) [23]. Therefore, we sought to determine if Cdc42 activity links FGD5 to the SDF1/PI3Kβ pathway. Consistent with the effect of FGD5 loss, Cdc42 pharmacological inhibition reduced FAK Y397 auto-phosphorylation and Akt S473 phosphorylation in HUVEC and HMEC-1 after SDF1 stimulation (Fig. 5.6A-F).

Rac1 is another member of the RHO subfamily of small GTPases and has shown to regulate PI3Kβ [23,65]. However, Rac1 pharmacological inhibition did not affect SDF1-mediated PI3Kβ activation (Supplemental Fig. 5.7A-F). These data indicate that Cdc42, but not Rac, RHO GTPases regulate CXCR4-stimulated PI3K and Akt activity, to replicate the signalling defect associated with FGD5 loss.

Cdc42 inhibition does not regulate the MAP Kinase activity or VEGF signaling

FGD5 has shown to regulate both the MAP Kinase and the PI3K pathways in response to VEGF stimulation [50,51]. Therefore, we sought to investigate if Cdc42 inhibition also demonstrates the same effect on MAP kinase activation to determine if FGD5 regulates different pathways in tandem. In HUVEC and HMEC-1, Cdc42 pharmacological inhibition did not affect ERK1/2 T202/Y204 phosphorylation, a MAP Kinase downstream effector, after SDF1 stimulation (Fig. 5.8A-D). Next, we studied if Cdc42 inhibition replicates the effect of FGD5 deficiency to reduce the phosphorylation of Akt after VEGF stimulation. In contrast to FGD5 loss, Cdc42 inhibition did not alter Akt S473 phosphorylation in response to VEGF in HUVEC and HMEC-1 (Fig. 5.8E-H). These results suggest that FGD5 regulates different pathways with distinct mechanisms.

FGD5 loss does not affect CXCR4 expression

VEGF induces surface expression of CXCR4 in EC, and in turn increases EC migration and angiogenesis in response to SDF1 [38,40]. Hence, to confirm that FGD5 regulates CXCR4 downstream signaling to PI3K-β, we sought to exclude a change in CXCR4 expression or surface display of CXCR4 among resting, or VEGF-stimulated EC after FGD5 loss. Under resting conditions, FGD5 loss did not affect the total CXCR4 expression at the protein level in HUVEC or HMEC-1 (Fig.5.9A, D). Similarly, the surface expression of CXCR4 was similar among the controls and the FGD5-deficient HUVEC (Fig. 5.10A). Priming the EC with VEGF for 18 hours led to ~1.5 and 3 fold increase in CXCR4 total expression at the protein level in HUVEC and HMEC-1, respectively (Fig. 5.9E-H). However, FGD5 loss had no effect on this

upregulation nor CXCR4 surface expression (Fig. 5.9E-H; Fig. 5.10B). We conclude FGD5 does not regulate CXCR4 expression or the induction of CXCR4 expression after VEGF priming. These data support our observation that CXCR4 is functionally competent in FGD5-deficient EC to elicit MAP Kinase signaling after SDF1 stimulation. Taken together with our finding that FGD5 is an upstream regulator of mTORC2, these data suggest that FGD5 regulates the SDF1/CXR4 pathway as CXCR4 couples to PI3K-β.

FGD5 loss regulates PI3KB activity

Upon binding to SDF1, CXCR4 is endocytosed to the early endosomes [33,66,67]. Recent evidence supports the notion that CXCR4 endocytosis and trafficking to the different endosomal compartments can shape the downstream signaling [68,69]. In line with these findings, previous reports localized PI3K and Akt to the early endosomes [70-72]. Therefore, we hypothesized that FGD5 may regulate PI3K-β localization to the early endosomes. Surprisingly, PI3K-β in the FGD5-deficient HUVEC was successfully targeted to the early endosomes after SDF1 stimulation (Fig. 5.11A, B) indicating no change in CXCR4 endocytosis and coupling to PI3K-β. To test if the PI3K-β in the early endosomes is active or not, we compared the localization of the phosphorylated Akt S473 to the early endosomes in the control and the FGD5-deficient HUVEC. The level of phosphorylated, active, Akt S473, was significantly lower in the FGD5-deficient HUVEC indicating a defect in PI3K-β activation (Fig. 5.11C, D). Taken together, although PI3K-β was present in the early endosomes, it failed to efficiently activate Akt in absence of FGD5, suggesting a pivotal role of FGD5 in regulating PI3K-β activity.

Discussion

Stromal cell-derived factor (SDF1) signaling to the endothelial cell (EC) through the G protein-coupled receptor CXCR4 is critical for developmental angiogenesis [73,74]. Hence, some of CXCR4 inhibitors are being evaluated in clinical trials as antiangiogenic therapy [75]. Among the different CXCR4-regulated signalling pathways, the PI3K pathway in the EC is essential to support new vessel development. Previously, we identified Facio-genital dysplasia 5 (FGD5), an endothelial-restricted Rho GEF, as a regulator of the PI3K pathway in response to vascular endothelial growth factor (VEGF) stimulation [51]. However, the role of FGD5 in regulating CXCR4 and other GPCR signaling is still to be determined. In vivo, loss of VEGF receptor 2 (VEGFR2), PI3K-β, and FGD5 are each associated with failed embryonic vascular development, and embryonic demise. On the other hand, PI3K-β deficiency is well tolerated in mice [25,76], but plays a critical role in repair of the adult mouse microvasculature [77]. PI3K-β stands out from the other PI3K isoforms by its ability to be activated by both RTKs and GPCRs [22,78]. In this study we investigated the role of FGD5 in regulating the GPCRs signaling to PI3K-β

In the current work, we identify that SDF1/CXCR4 increases the pro-angiogenic efficacy of VEGF on EC spheroid sprouting in vitro. Loss of FGD5 induced by RNA interference abolishes the SDF1/CXCR4 pro-angiogenic effect. FGD5 loss inhibits SDF1-stimulated PI3Kβ-dependent mTORC2 activity, and exerts a similar effect on the Apelin receptor signaling, a second GPCR implicated in angiogenesis [61]. Further, we show that CXCR4 expression is intact in FGD5 deficient EC, but the recruitment of active Akt to the PI3K-β positive endosomes is defective. This suggests a deficiency in PI3K-β activity. We hypothesize a model by which FGD5 regulates

PI3K-β via Cdc42, since Cdc42 inhibition demonstrates the same signaling defects as FGD5 loss.

PI3K-β, uniquely among PI3K class I isoforms, is regulated by members of the Rho GTPase family members Cdc42 and Rac1, whereas the other PI3K isoforms are regulated by Ras [23]. The association of PI3K-β with Rac1 and Cdc42 was reported in several studies [79-81]. Further, the basal, low-level PI3K activity induced by PI3K-β [82], can also be driven by Rac1 and Cdc42 [23,83]. Despite evidence that Rac and Cdc42 can mediate PI3K-β activity downstream of GPCRs, we show that CXCR4 signaling in EC is only Cdc42 dependent. Of note, Cdc42 triggers filopodia formation and angiogenesis [84,85]; and Cdc42-knockout mice are early embryonic-lethal due to a defect in cytoskeleton reorganization [86]. Similarly, the EC-specific Cdc42 knockout mice are reported to die early due to defects in vasculogenesis [87]. Although Cdc42 was heavily investigated, the exchange factor(s) that activate Cdc42 in the EC is elusive. In this study we show that FGD5, a Cdc42-GTP/GDP exchange factor with EC-restricted expression in the adult [50,51] represents a good candidate.

We detected differential use of FGD5 downstream of S1P versus SDF1 and Apelin stimulation. All three agonists are reported to use Gai to elicit Akt phosphorylation [88-90], and we confirm each recruits PI3K-β activity. In addition, in mouse embryonic fibroblasts, Fritsch reports that S1P stimulation of Akt phosphorylation is inhibited by expression of a p110β mutant lacking a competent Rho GTPase binding domain [23]. In fibroblasts Rac1 appears to be sufficient to activate PI3K-β. This discordant result may be accounted for by differential use of the S1P receptors between fibroblasts and EC [91]. Nevertheless the explanation for the differential

requirement among different GPCRs for FGD5 in endothelial PI3K-β activation requires further study.

The fact that VEGF, bFGF, and SDF-1 genes are widely expressed in normal organs of mice and humans and that their receptors are expressed on vascular EC [35,92,93] suggest that these angiogenic cues work in parallel to maintain the vasculature. Angiogenesis can be triggered by up-regulation of receptor levels by inflammatory mediators such as TNF-α [94] or by enhanced levels of angiogenic factors such as VEGF and bFGF, which pave the way for mediators such as SDF1 to contribute to angiogenesis. It is now clear that VEGF primes EC responses to SDF1 via up-regulation of the CXC chemokine receptor-4 [38,40]. In turn, SDF1/CXCR4 amplifies angiogenesis by inducing VEGF production from EC. In line with these findings, we have shown that SDF/VEGF combination has an additive effect to stimulate angiogenesis and EC migration compared to VEGF alone.

In earlier work we found FGD5 loss inhibited coupling of VEGF receptor-2 to PI3K- α activity. However, we could not detect any change in the VEGF-induced CXCR4 expression in the FGD5 deficient EC. Therefore, our data indicate FGD5 regulates the PI3K-β pathway independent of VEGF signaling and VEGF-stimulated CXCR4 upregulation. Consistent with this interpretation, we find that SDF1-, but not VEGF-, stimulation of endothelial PI3K activity is dependent on Cdc42. Thus FGD5 appears to regulate the recruitment of PI3K activity by VEGFR2 and CXCR4 through different mechanisms.

Angiogenesis inhibitors (AI) have been approved for targeting tumor neovascularization in several cancer types [95,96]. These drugs prevent the recruitment of the surrounding vasculature by tumor tissue through stabilizing the quiescent EC and abolishing the response of the vasculature to cancer cell-secreted proangiogenic cues. Although VEGF is the dominant pro-angiogenic cue in development and tumor neoangiogenesis, limitations to AI targeting of VEGF or its receptor have been reported in tumor therapy [97-99]. Of these, a reduction in efficacy as the tumors escape the effect of VEGF/ VEGF receptor inhibitors is most problematic. Persistent tumour ischemia appears to elicit alternate angiogenic cues, such as the SDF1/CXCR4 pathway, to recruit new vessels. Therefore, our current findings, taken with our earlier report on the effect of FGD5 on VEGF receptor function [51], indicate that FGD5 serves as a convergence node on different angiogenic pathways, and represents a potential candidate to prevent tumor escape from AI therapies.

Figures

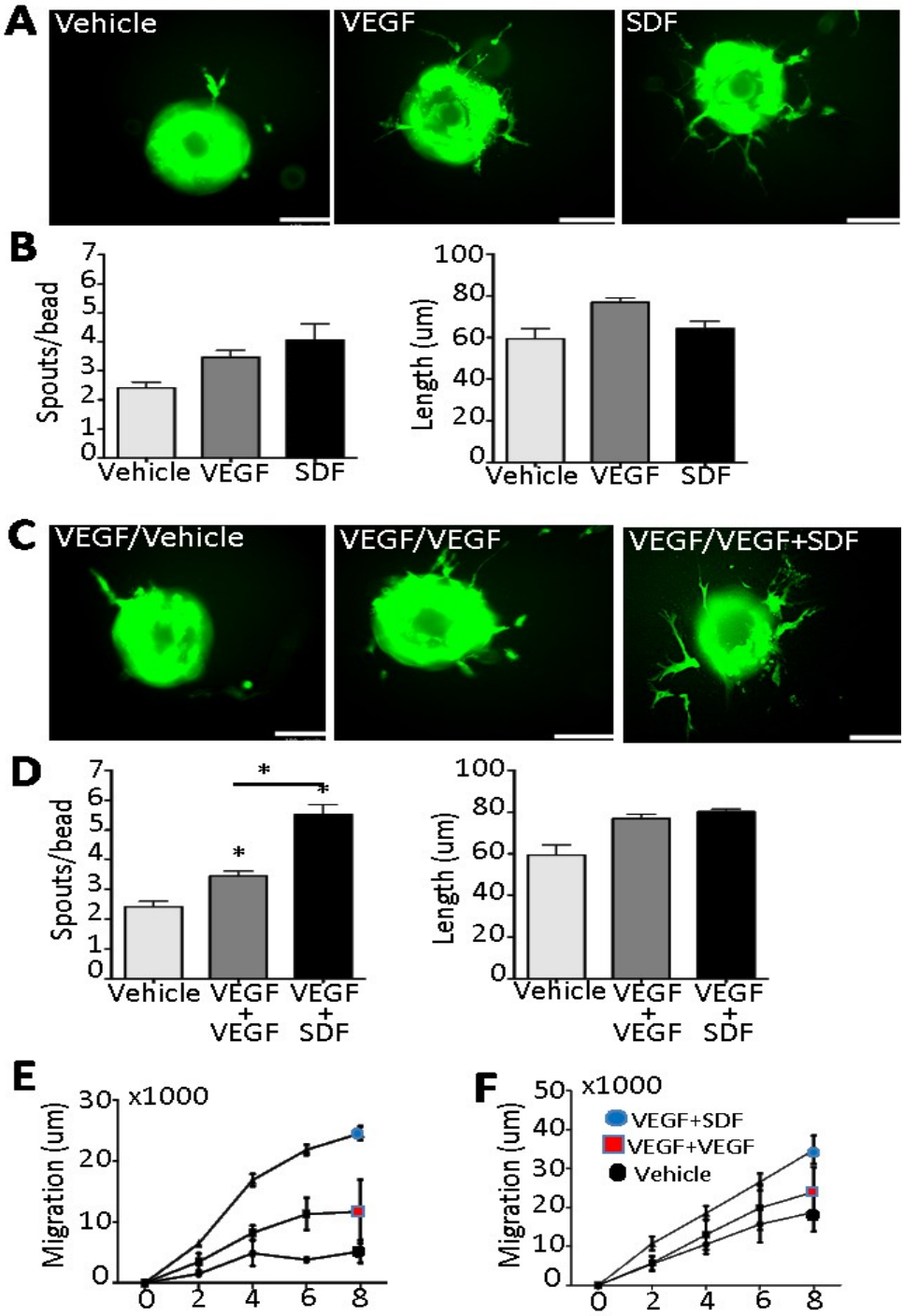
A
Vehicle
VEGF
SDF
B
Spouts/bead
Vehicle VEGF SDF
Length (um)
Vehicle VEGF SDF
C
VEGF/Vehicle
VEGF/VEGF
VEGF/VEGF+SDF
D
Spouts/bead
Vehicle VEGF + VEGF VEGF + SDF
Length (um)
Vehicle VEGF + VEGF VEGF + SDF
E
x1000
Migration (um)
F
x1000
VEGF+SDF
VEGF+VEGF
Vehicle
Migration (um)

Fig 5. 1

Figure 5.1. SDF increases the angiogenic effect of VEGF. Human umbilical vein endothelial cells (HUVECs) were mounted on Cytodex beads, embedded in 3D fibrin gels as described in Methods, and cultured with growth media supplemented with vehicle, 50ng/ml VEGF, or 100ng/ml SDF. **A)** Representative images of EC sprouts after 18 hours incubation. **B)** Quantitation of the number and length of sprouts per bead (n=3 independent experiments, *P<0.05 by ANOVA). Cytodex beads coated with VEGF-preincubated HUVECs were embedded in fibrin gel and supplied with vehicle, 50ng/m VEGF, or 50ng/ml VEGF+100ng/ml SDF. **C)** Representative images of HUVECs sprouting after 18 hours incubation. **D)** Quantitation of number of sprouts per bead and length of sprouts (n=3 independent experiments, *P<0.05 by ANOVA). HUVECs or human microvascular endothelial cells (HMEC-1) were preincubated with VEGF overnight, then stimulated with vehicle, 50ng/ml VEGF, or 50ng/ml VEGF+100ng/ml SDF; and subjected to scratch wound migration assay. **E)** Quantitation of distance migrated by HUVECs to cover the scratch wound area. **F)** Quantitation of distance migrated by HMEC-1 to cover the scratch wound area (n=3 independent experiments, *P<0.05 by two way ANOVA).

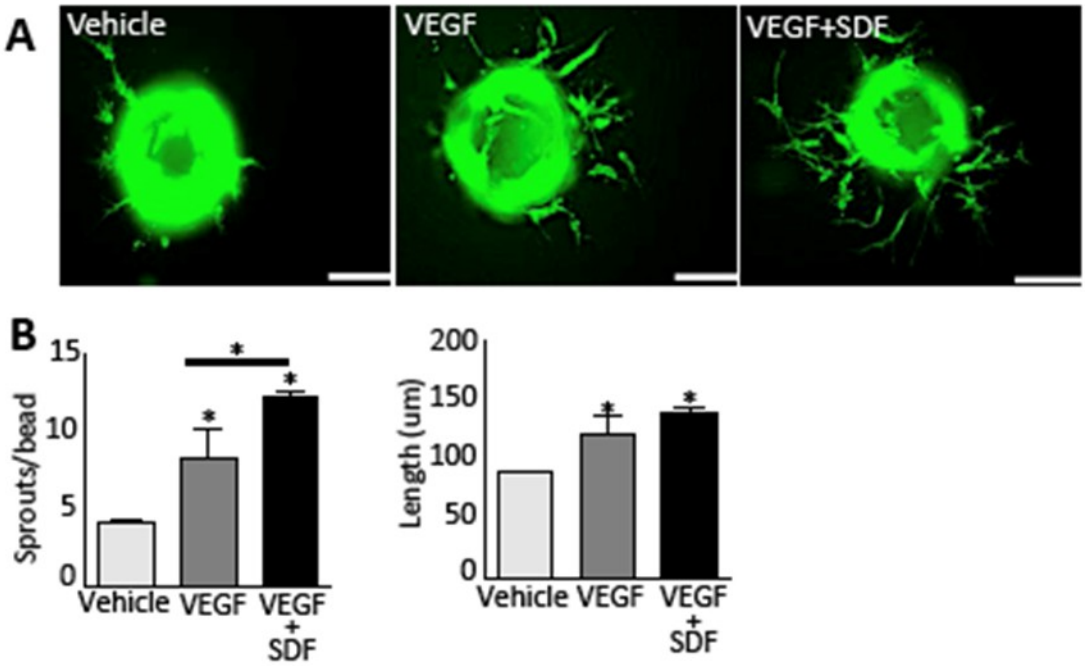

Fig 5. 2

Figure 5.2. SDF1 increases the angiogenic effect of VEGF in HMEC1. Cytodex beads coated with VEGF-preincubated HMEC1 were embedded in fibrin gel and supplemented with vehicle, 50ng/ml VEGF, or 50 ng/ml VEGF+100ng/ml SDF1. **A)** Representative images of HMEC1 sprouting after 18 hours incubation. **B)** Quantitation of number of sprouts per bead and length of sprouts (n=3 independent experiments. *P<0.05 by ANOVA).

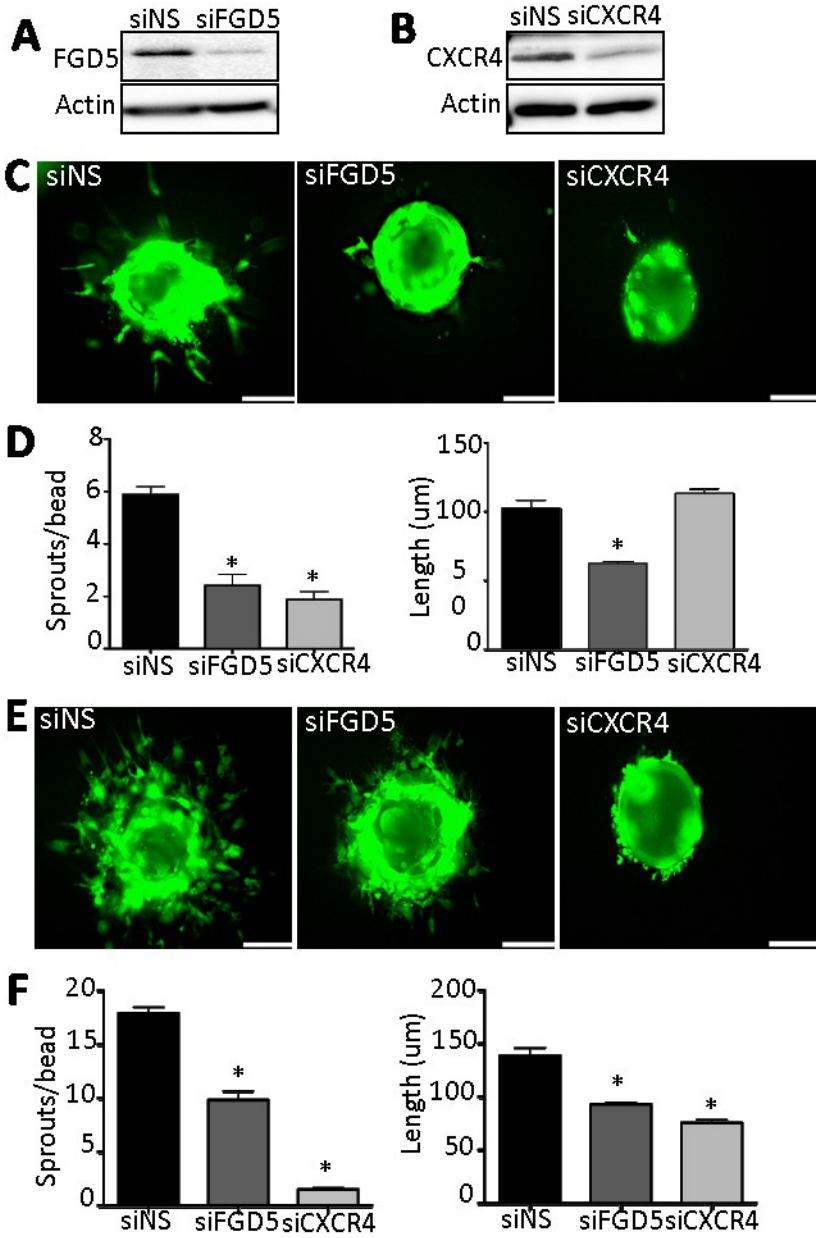
A
siNS siFGD5
FGD5
Actin
B
siNS siCXCR4
CXCR4
Actin
C
siNS
siFGD5
siCXCR4
D
Sprouts/bead
Length (um)
siNS siFGD5 siCXCR4
E
siNS
siFGD5
siCXCR4
F
Sprouts/bead
Length (um)
siNS siFGD5 siCXCR4

Fig 5. 3

Figure 5.3. FGD5 and CXCR4 are required for SDF angiogenic effect. Human umbilical vein endothelial cells HUVECs or human microvascular endothelial cells (HMEC-1) were transfected with non-silencing siRNA (siNS), siRNA against FGD5 (siFGD5), or siRNA against CXCR4. **A)** A representative image of FGD5 and Actin Western blot. **B)** A representative image of CXCR4 and Actin Western blot. FGD5 deficient-, CXCR4 deficient-, or control-HUVECs were preincubated with VEGF overnight. Then, mounted on Cytodex beads, embedded in 3D fibrin gels as described in Methods, and supplied with 100ng/ml SDF. **C)** Representative images of HUVECs sprouting after 18 hours incubation. **D)** Quantitation of the length and number of sprouts per bead (n=3 independent experiments, *$P<0.05$ by ANOVA). **E)** Representative images of HMEC-1 sprouting after 18 hours incubation. **F)** Quantitation of number of sprouts per bead and length of sprouts (n=3 independent experiments, *$P<0.05$ by ANOVA).

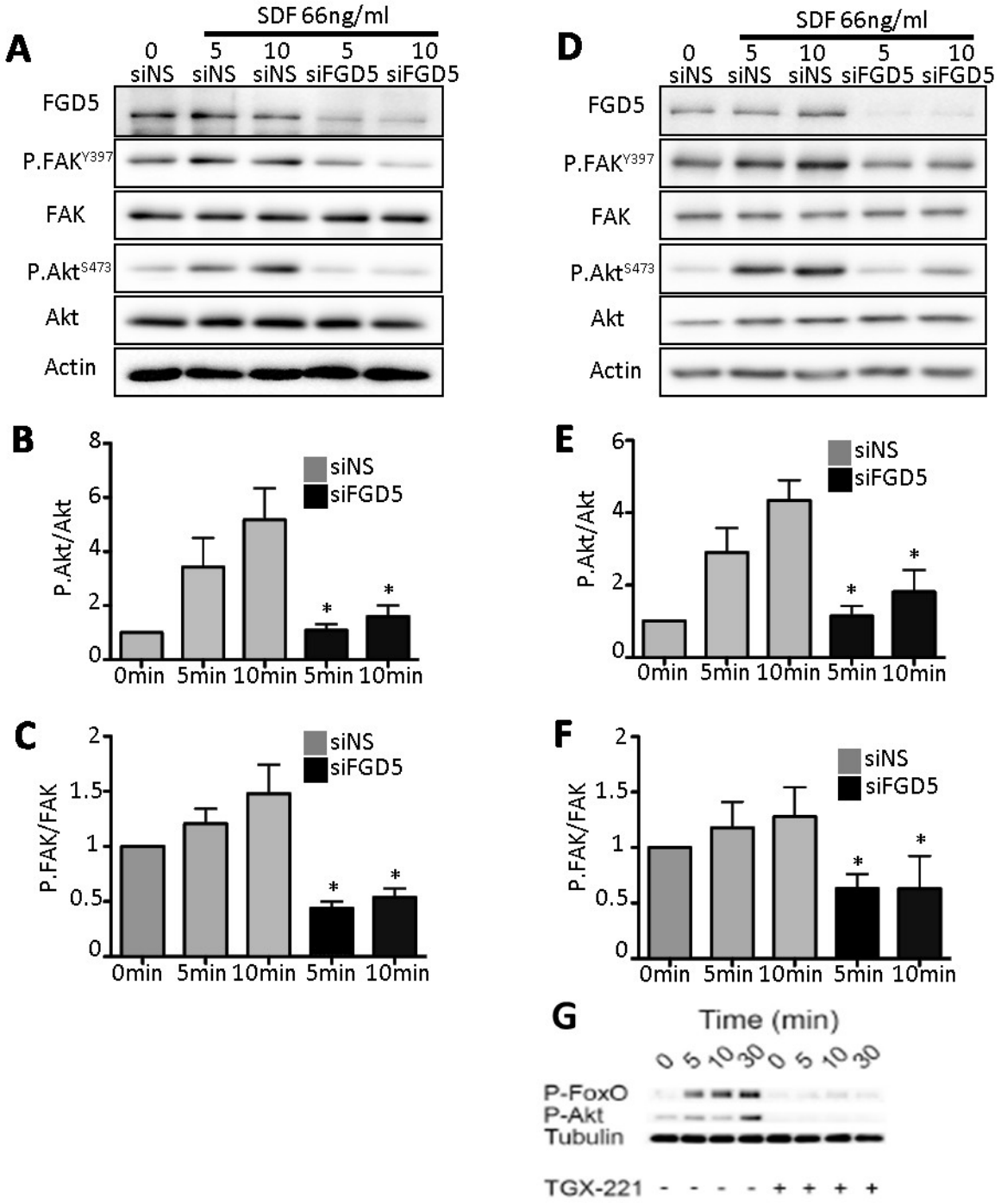
A
SDF 66ng/ml
0 siNS
5 siNS
10 siNS
5 siFGD5
10 siFGD5
FGD5
P.FAKY397
FAK
P.AktS473
Akt
Actin
D
B
P.Akt/Akt
siNS
siFGD5
0min 5min 10min 5min 10min
E
C
P.FAK/FAK
F
G
Time (min)
0 5 10 30 0 5 10 30
P-FoxO
P-Akt
Tubulin
TGX-221 - - - - + + + +

Fig 5. 4

Figure 5.4. FGD5 loss decreases Akt and FAK activation. Human umbilical vein endothelial cells (HUVECs) or human microvascular endothelial cells (HMEC-1) were transfected with non-silencing siRNA (siNS) or siRNA targeting FGD5 (siFGD5) then stimulated with 66ng/ml SDF. **A)** Representative image of FGD5, phospho-FAK^{Y397} (P.FAK^{Y397}), total FAK, phospho-Akt^{S473} (P.Akt^{S473}), total Akt, and Actin Western blot in HUVECs. **B)** Quantitation of P.Akt^{S473}. **C)** Quantitation of P.FAK^{Y397} (n=3 independent experiments, *P<0.05 by ANOVA). **D)** Representative image of FGD5, phospho-FAK^{Y397} (P.FAK^{Y397}), total FAK, phospho-Akt^{S473} (P.Akt^{S473}), total Akt, and Actin Western blot in HMEC-1. **E)** Quantitation of P.Akt^{S473}. **F)** Quantitation of P.FAK^{Y397} (n=3 independent experiments, *P<0.05 by ANOVA). **G)** Representative image of P-FOXO, P-Akt and Tubulin after inhibiting PI3KB with TGX-221. Image taken from (Blood. 2014;124(13):2142-2149)

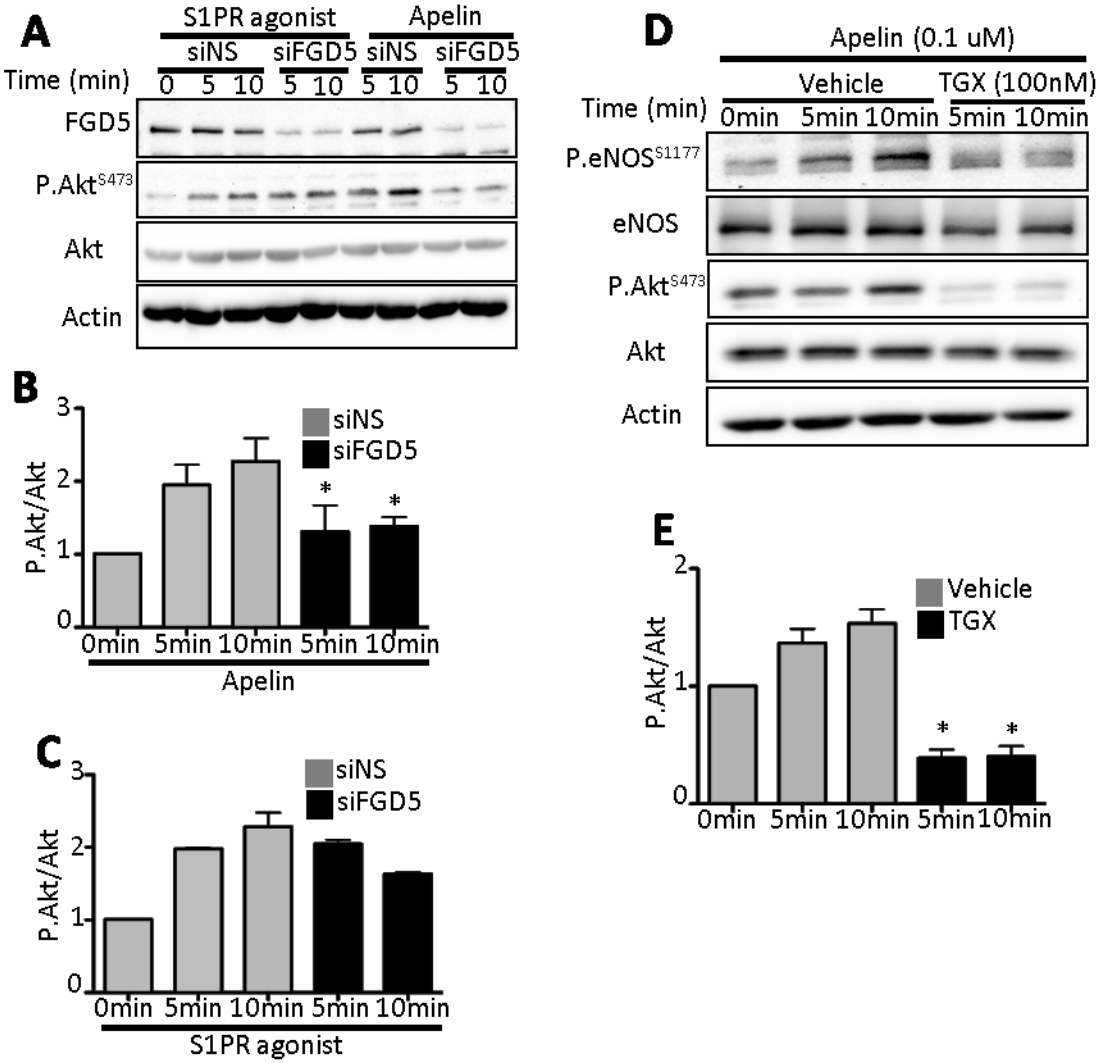
A
S1PR agonist
Apelin
siNS
siFGD5
siNS
siFGD5
Time (min)
0 5 10 5 10 5 10 5 10
FGD5
P.Akt S473
Akt
Actin
B
siNS
siFGD5
P.Akt/Akt
0min 5min 10min 5min 10min
Apelin
C
siNS
siFGD5
P.Akt/Akt
0min 5min 10min 5min 10min
S1PR agonist
D
Apelin (0.1 uM)
Vehicle
TGX (100nM)
Time (min)
0min 5min 10min 5min 10min
P.eNOS S1177
eNOS
P.Akt S473
Akt
Actin
E
Vehicle
TGX
P.Akt/Akt
0min 5min 10min 5min 10min

Fig 5. 5

Figure 5.5. FGD5 and PI3K regulate apelin receptor signaling but not S1P receptor. Human umbilical vein endothelial cells (HUVECs) were transfected with non-silencing siRNA (siNS) or siRNA targeting FGD5 (siFGD5) then stimulated with 3 nM of sphingosine 1 phosphate receptor (S1PR) agonist (CYM5442 hydrochloride) or 0.1 uM apelin. **A)** Representative image of FGD5, phospho-Akt^{S473} (P.Akt^{S473}), total Akt, and actin Western blot in HUVECs. **B)** Quantitation of P.Akt^{S473} in response to apelin stimulation (n=3 independent experiments, *P<0.05 by ANOVA). **C)** Quantitation of P.Akt^{S473} in response to S1PR agonist stimulation (n=3 independent experiments, *P<0.05 by ANOVA). **D)** HUVECs were treated with 100 nM of PI3KB inhibitor (TGX) or vehicle then stimulated with 0.1 uM apelin. Representative image of phospho-eNOS^{S1177} (P.eNOS^{s1177}), total eNOS, phospho-Akt^{S473} (P.Akt^{S473}), total Akt, and actin Western blot in HUVECs. **E)** Quantitation of P.Akt^{S473} (n=3 independent experiments, *P<0.05 by ANOVA).

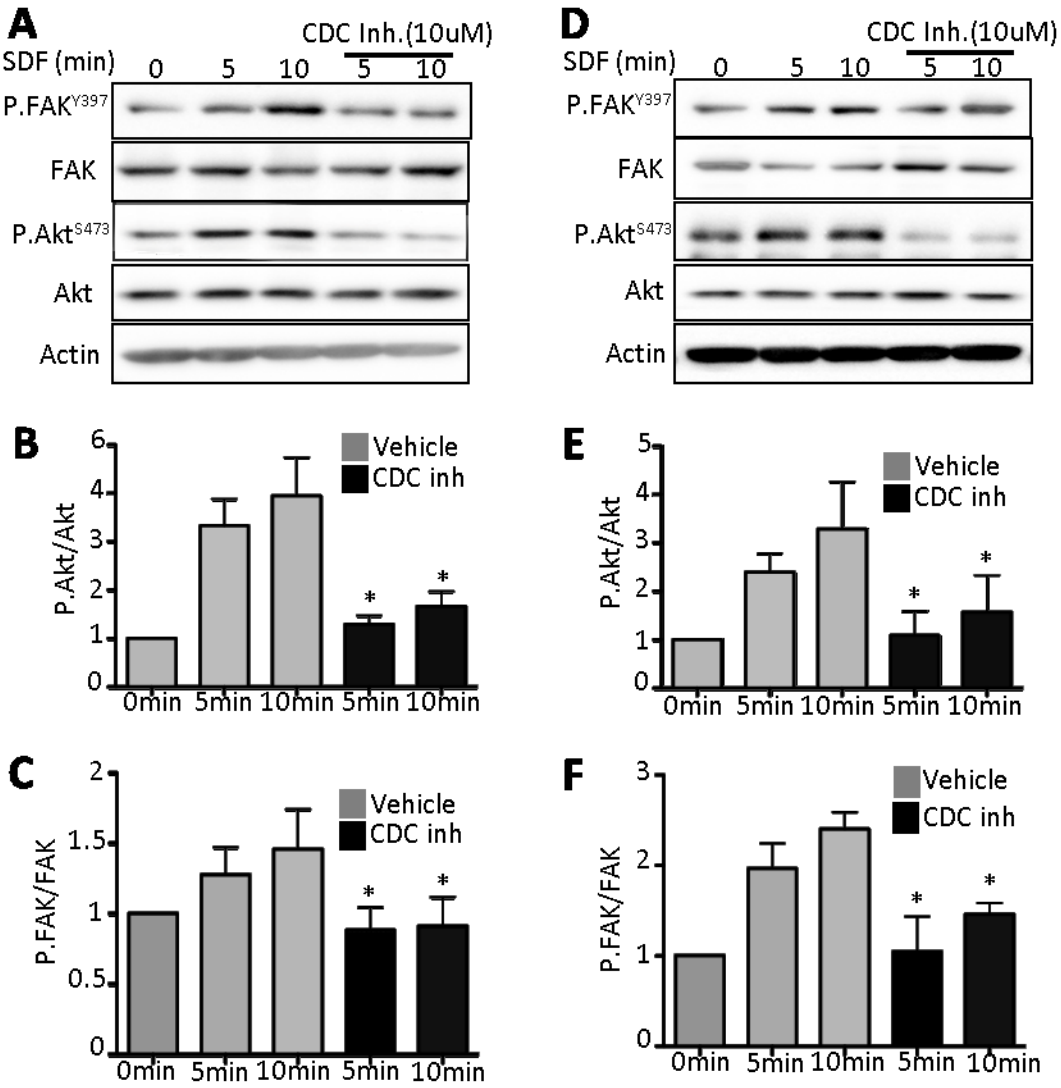
A
CDC Inh.(10uM)
SDF (min)
0
5
10
5
10
P.FAKY397
FAK
P.AktS473
Akt
Actin
D
CDC Inh.(10uM)
SDF (min)
0
5
10
5
10
P.FAKY397
FAK
P.AktS473
Akt
Actin
B
P.Akt/Akt
Vehicle
CDC inh
0min
5min
10min
5min
10min
E
P.Akt/Akt
Vehicle
CDC inh
0min
5min
10min
5min
10min
C
P.FAK/FAK
Vehicle
CDC inh
0min
5min
10min
5min
10min
F
P.FAK/FAK
Vehicle
CDC inh
0min
5min
10min
5min
10min

Fig 5. 6

Figure 5.6. CDC42 inhibition reduces AKT and FAK activation. Human umbilical vein endothelial cells (HUVECs) or human microvascular endothelial cells (HMEC-1) were treated with 10uM of CDC42 inhibitor (CDC inh) or vehicle then stimulated with 66ng/ml SDF. **A)** Representative image of phospho-FAK^{Y397} (P.FAK^{Y397}), total FAK, phospho-Akt^{S473} (P.Akt^{S473}), total Akt, and Actin Western blot in HUVECs. **B)** Quantitation of P.Akt^{S473}. **C)** Quantitation of P.FAK^{Y397} (n=3 independent experiments, *P<0.05 by ANOVA). **D)** Representative image of phospho-FAK^{Y397} (P.FAK^{Y397}), total FAK, phospho-Akt^{S473} (P.Akt^{S473}), total Akt, and Actin Western blot in HMEC-1. **E)** Quantitation of P.Akt^{S473}. **F)** Quantitation of P.FAK^{Y397} (n=3 independent experiments, *P<0.05 by ANOVA).

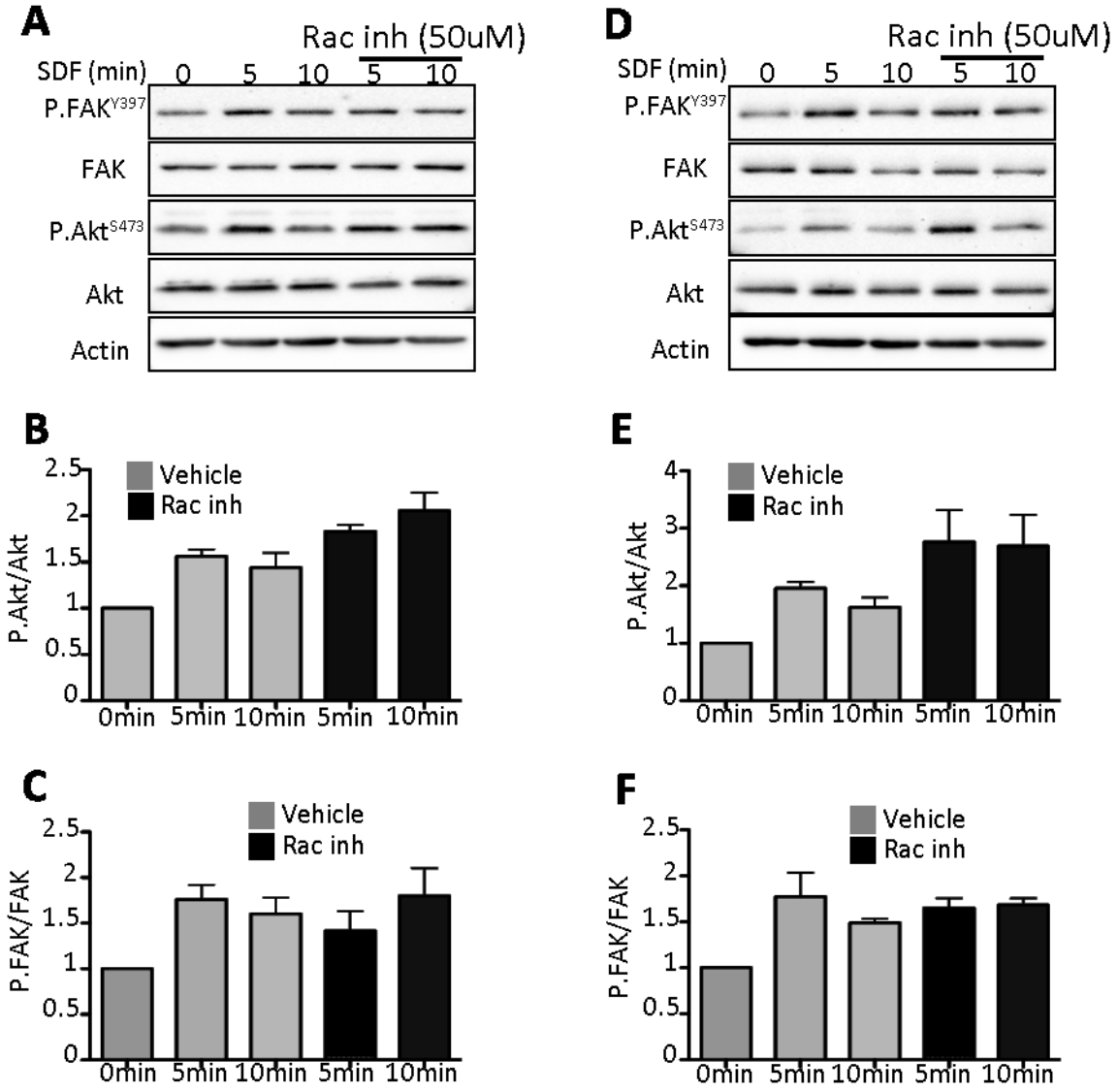
A
Rac inh (50uM)
SDF (min) 0 5 10 5 10
P.FAKY397
FAK
P.AktS473
Akt
Actin
D
Rac inh (50uM)
SDF (min) 0 5 10 5 10
P.FAKY397
FAK
P.AktS473
Akt
Actin
B
Vehicle
Rac inh
P.Akt/Akt
0min 5min 10min 5min 10min
E
Vehicle
Rac inh
P.Akt/Akt
0min 5min 10min 5min 10min
C
Vehicle
Rac inh
P.FAK/FAK
0min 5min 10min 5min 10min
F
Vehicle
Rac inh
P.FAK/FAK
0min 5min 10min 5min 10min

Fig 5. 7

Figure 5.7. Rac1 inhibition doesnot affect AKT and FAK activity. Human umbilical vein endothelial cells (HUVECs) or human microvascular endothelial cells (HMEC-1) were treated with 50uM of Rac1 inhibitor (Rac inh) or vehicle then stimulated with 66ng/ml SDF. **A)** Representative image of phospho-FAK^{Y397} (P.FAK^{Y397}), total FAK, phospho-Akt^{S473} (P.Akt^{S473}), total Akt, and Actin Western blot in HUVECs. **B)** Quantitation of P.Akt^{S473}. **C)** Quantitation of P.FAK^{Y397} (n=3 independent experiments, *P<0.05 by ANOVA). **D)** Representative image of phospho-FAK^{Y397} (P.FAK^{Y397}), total FAK, phospho-Akt^{S473} (P.Akt^{S473}), total Akt, and Actin Western blot in HMEC-1. **E)** Quantitation of P.Akt^{S473}. **F)** Quantitation of P.FAK^{Y397} (n=3 independent experiments, *P<0.05 by ANOVA).

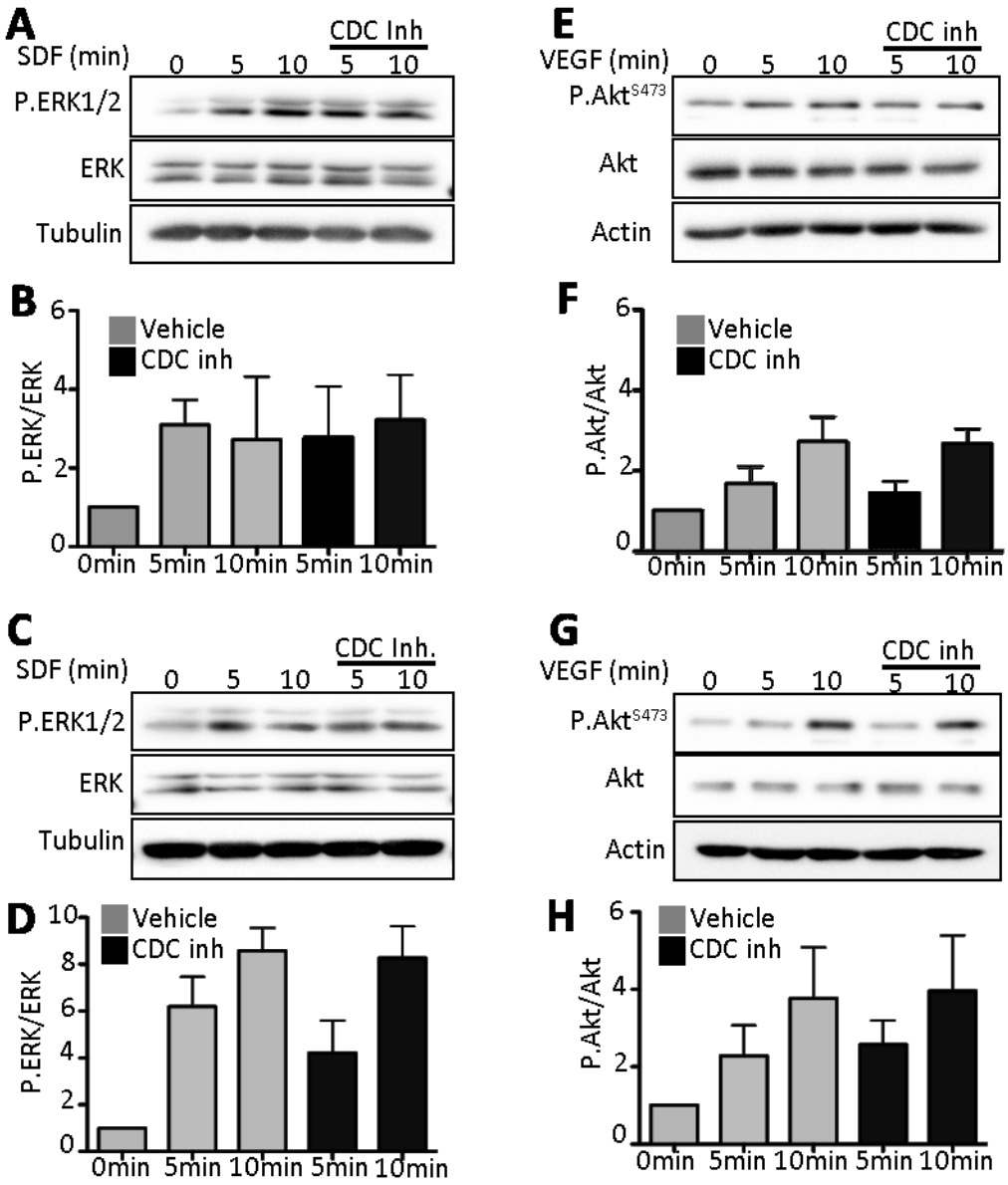
A
SDF (min)
0
5
10
CDC Inh
5
10
P.ERK1/2
ERK
Tubulin
B
Vehicle
CDC inh
P.ERK/ERK
0
2
4
6
0min
5min
10min
5min
10min
C
SDF (min)
0
5
10
CDC Inh.
5
10
P.ERK1/2
ERK
Tubulin
D
Vehicle
CDC inh
P.ERK/ERK
0
2
4
6
8
10
0min
5min
10min
5min
10min
E
VEGF (min)
0
5
10
CDC inh
5
10
P.Akt S473
Akt
Actin
F
Vehicle
CDC inh
P.Akt/Akt
0
2
4
6
0min
5min
10min
5min
10min
G
VEGF (min)
0
5
10
CDC inh
5
10
P.Akt S473
Akt
Actin
H
Vehicle
CDC inh
P.Akt/Akt
0
2
4
6
0min
5min
10min
5min
10min

Fig 5. 8

Figure 5.8. CDC42 inhibition does not regulate ERK1/2 activity or VEGF signaling. Human umbilical vein endothelial cells (HUVECs) or human microvascular endothelial cells (HMEC-1) were treated with 10uM of CDC42 inhibitor (CDC inh) or vehicle then stimulated with 66ng/ml SDF. **A)** Representative image of phospho-ERK1/2^{Y397} (P.ERK1/2^{Y397}), total ERK, and tubulin Western blot in HUVECs. **B)** Quantitation of P.ERK1/2^{S473}(n=3 independent experiments, **P*<0.05 by ANOVA). **C)** Representative image of phospho-ERK1/2^{Y397} (P.ERK1/2^{Y397}), total ERK, and tubulin Western blot in HMEC-1. **D)** Quantitation of P.ERK1/2^{Y397} (n=3 independent experiments, **P*<0.05 by ANOVA). Human umbilical vein endothelial cells (HUVECs) or human microvascular endothelial cells (HMEC-1) were treated with 10uM of CDC42 inhibitor (CDC inh) or vehicle then stimulated with 50ng/ml VEGF. **E)** Representative image of phospho-Akt^{S473} (P.Akt^{S473}), total Akt, and Actin Western blot in HUVECs. **F)** Quantitation of P.Akt^{S473} (n=3 independent experiments, **P*<0.05 by ANOVA). **G)** Representative image of phospho-Akt^{S473} (P.Akt^{S473}), total Akt, and Actin Western blot in HMEC-1. **H)** Quantitation of P.Akt^{S473} (n=3 independent experiments, **P*<0.05 by ANOVA).

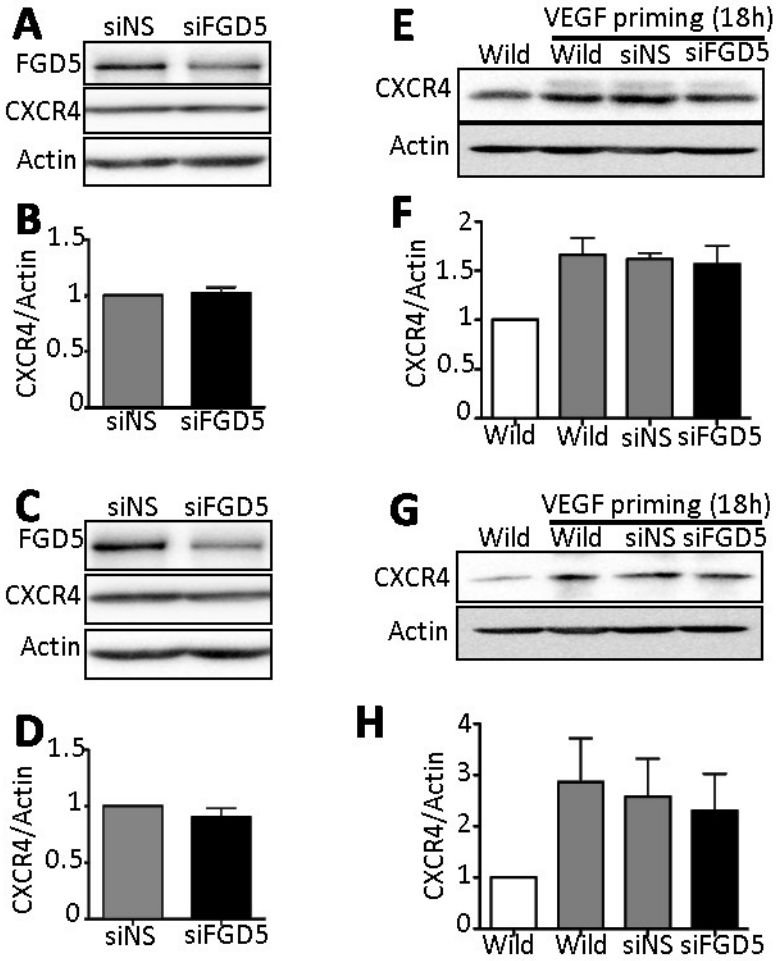
A
siNS
siFGD5
FGD5
CXCR4
Actin
B
CXCR4/Actin
1.5
1
0.5
0
siNS
siFGD5
C
siNS
siFGD5
FGD5
CXCR4
Actin
D
CXCR4/Actin
1.5
1
0.5
0
siNS
siFGD5
E
VEGF priming (18h)
Wild
Wild
siNS
siFGD5
CXCR4
Actin
F
CXCR4/Actin
2
1.5
1
0.5
0
Wild
Wild
siNS
siFGD5
G
VEGF priming (18h)
Wild
Wild
siNS
siFGD5
CXCR4
Actin
H
CXCR4/Actin
4
3
2
1
0
Wild
Wild
siNS
siFGD5

Fig 5. 9

Figure 5.9. FGD5 loss does not affect CXCR4 expression. Human umbilical vein endothelial cells (HUVECs) or human microvascular endothelial cells (HMEC-1) were transfected with non silencing RNA (siRNA) or siRNA targeting FGD5 (siFGD5) then incubated overnight without growth supplement to indicate the basal level of CXCR4 under resting conditions. **A)** Representative image of FGD5, CXCR4, and Actin Western blot in HUVECs. **B)** Quantitation of CXCR4. (n=3 independent experiments). **C)** Representative image of FGD5, CXCR4, and Actin Western blot in HMEC-1. **D)** Quantitation of CXCR4. (n=3 independent experiments). HUVECs or HMEC-1 were transfected with siRNA or siFGD5 then incubated overnight with VEGF to indicate the level of CXCR4 after VEGF priming. **E)** Representative image of CXCR4, and Actin Western blot in HUVECs. **F)** Quantitation of CXCR4. (n=3 independent experiments). **G)** Representative image of CXCR4, and Actin Western blot in HMEC-1. **H)** Quantitation of CXCR4. (n=3 independent experiments).

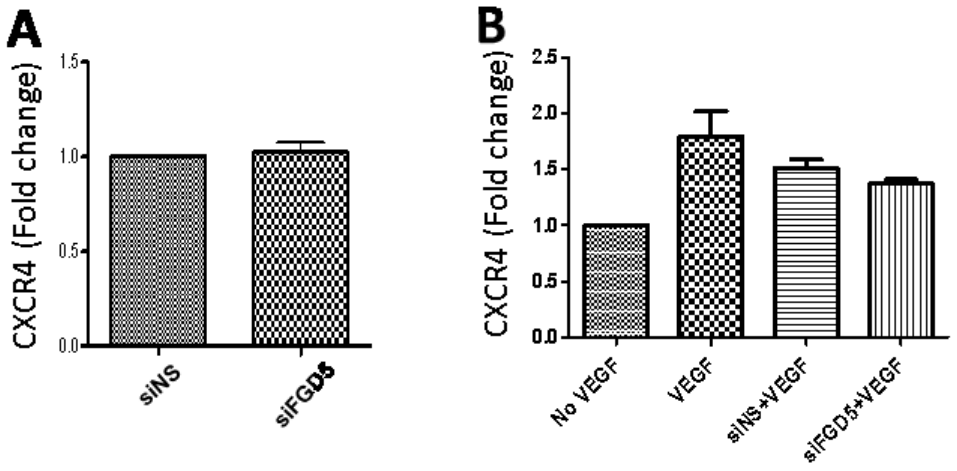

Fig 5. 10

Figure 5.10. FGD5 loss does not affect CXCR4 membrane expression. Quantitation of CXCR4 expression on the membrane by flowcytometry in resting conditions **(A),** or after VEGF priming for 18 hours **(B)** in FGD5-deficient HUVECs and control HUVECs (n=3 independent experiments).

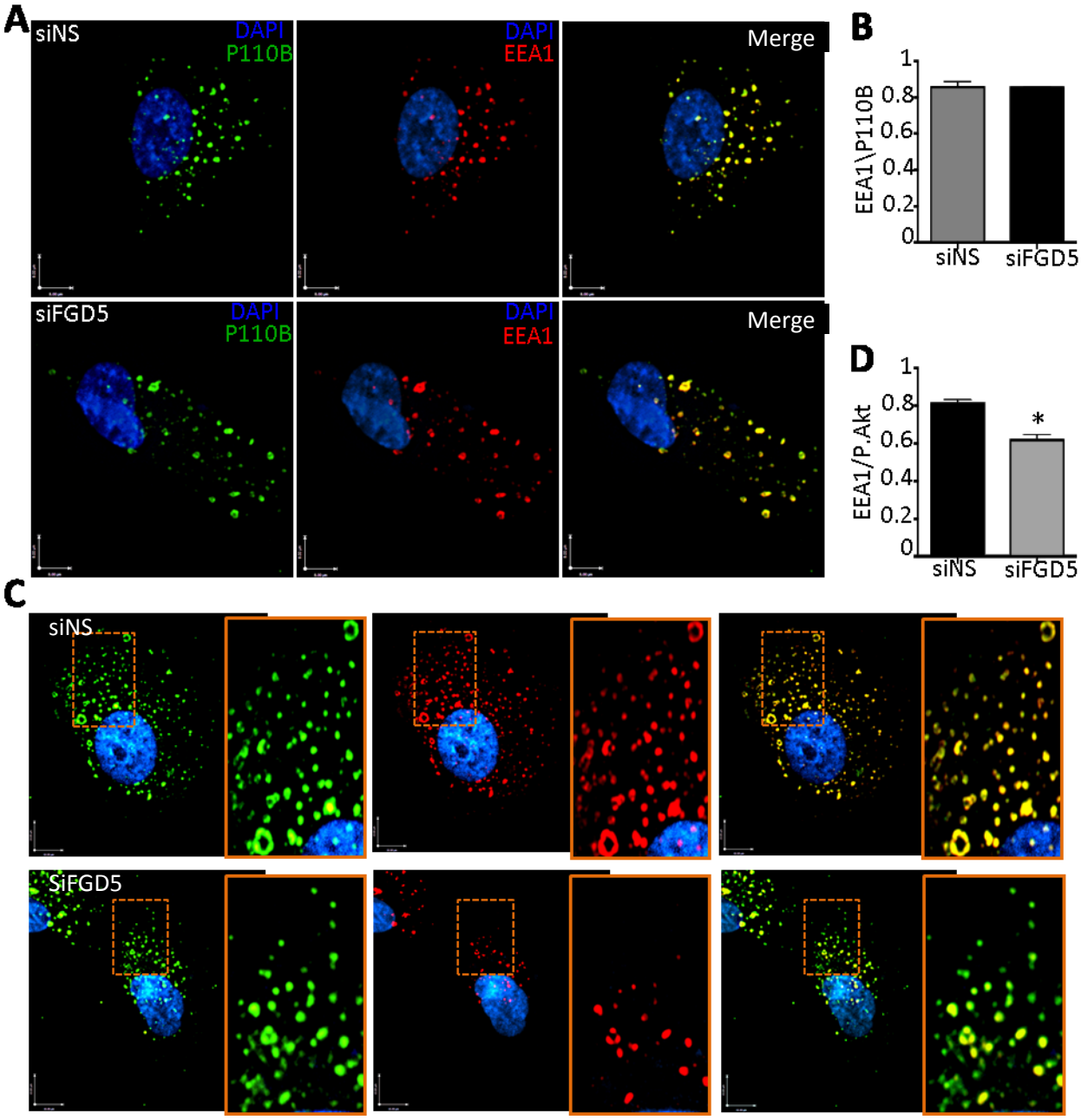
A
siNS
DAPI
P110B
DAPI
EEA1
Merge
siFGD5
DAPI
P110B
DAPI
EEA1
Merge
B
EEA1\P110B
1
0.8
0.6
0.4
0.2
0
siNS
siFGD5
D
EEA1/P.Akt
1
0.8
0.6
0.4
0.2
0
*
siNS
siFGD5
C
siNS
SiFGD5

Fig 5. 11

Figure 5.11. FGD5 loss affects P.Akt^{S473} localization to early endosomes but not P110B. Control (siNS) or FGD5-deficient HUVECs (siFGD5) were starved overnight, stimulated with SDF (66 ng/ml) for 10 min then fixed and stained for P110B (green), EEA1 (red) and DAPI (blue). **A)** Representative images of P110B colocalization with EEA1. Scale bar: 8um. **B)** Quantitation of the colocalization of P110B with EEA1 vesicles by pearson's correlation. (n=3 independent experiments, at least 35 cells per group). **C)** Representative images of P.Akt^{S473} (green) colocalization with EEA1 (red). Scale bar: 8um. **D)** Quantitation of the colocalization of P.Akt^{S473} with EEA1 vesicles by pearson's correlation. (n=3 independent experiments, at least 35 cells per group, *P<0.05 by student t-test).

References

1. Carmeliet P, Jain RK. Angiogenesis in cancer and other diseases. *Nature*. 2000;407(6801):249-257.

2. Jain RK. Normalizing tumor vasculature with anti-angiogenic therapy: A new paradigm for combination therapy. *Nat Med*. 2001;7(9):987-989.

3. Nagy JA, Chang SH, Shih SC, Dvorak AM, Dvorak HF. Heterogeneity of the tumor vasculature. *Semin Thromb Hemost*. 2010;36(3):321-331. doi: 10.1055/s-0030-1253454; 10.1055/s-0030-1253454.

4. Baluk P, Hashizume H, McDonald DM. Cellular abnormalities of blood vessels as targets in cancer. *Curr Opin Genet Dev*. 2005;15(1):102-111.

5. Mazzone M, Dettori D, Leite de Oliveira R, et al. Heterozygous deficiency of< i> PHD2 restores tumor oxygenation and inhibits metastasis via endothelial normalization. *Cell*. 2009;136(5):839-851.

6. Ozawa MG, Yao VJ, Chanthery YH, et al. Angiogenesis with pericyte abnormalities in a transgenic model of prostate carcinoma. *Cancer*. 2005;104(10):2104-2115.

7. Chung AS, Lee J, Ferrara N. Targeting the tumour vasculature: Insights from physiological angiogenesis. *Nature Reviews Cancer*. 2010;10(7):505-514.

8. Nagy JA, Dvorak AM, Dvorak HF. VEGF-A and the induction of pathological angiogenesis. *Annu.Rev.Pathol.Mech.Dis.* 2007;2:251-275.

9. Carmeliet P, Ferreira V, Breier G, et al. Abnormal blood vessel development and lethality in embryos lacking a single VEGF allele. *Nature*. 1996;380(6573):435-439. doi: 10.1038/380435a0.

10. Jain RK. Lessons from multidisciplinary translational trials on anti-angiogenic therapy of cancer. *Nature Reviews Cancer*. 2008;8(4):309-316.

11. Jain RK. Normalization of tumor vasculature: An emerging concept in antiangiogenic therapy. *Science*. 2005;307(5706):58-62. doi: 10.1126/science.1104819.

12. Inoue M, Hager JH, Ferrara N, Gerber H, Hanahan D. VEGF-A has a critical, nonredundant role in angiogenic switching and pancreatic β cell carcinogenesis. *Cancer cell*. 2002;1(2):193-202.

13. Holmes K, Roberts OL, Thomas AM, Cross MJ. Vascular endothelial growth factor receptor-2: Structure, function, intracellular signalling and therapeutic inhibition. *Cell Signal*. 2007;19(10):2003-2012.

14. Liu P, Cheng H, Roberts TM, Zhao JJ. Targeting the phosphoinositide 3-kinase pathway in cancer. *Nature reviews Drug discovery*. 2009;8(8):627-644.

15. Geng L, Tan J, Himmelfarb E, et al. A specific antagonist of the p110delta catalytic component of phosphatidylinositol 3'-kinase, IC486068, enhances radiation-induced tumor

vascular destruction. *Cancer Res*. 2004;64(14):4893-4899. doi: 10.1158/0008-5472.CAN-03-3955.

16. Puri KD, Doggett TA, Douangpanya J, et al. Mechanisms and implications of phosphoinositide 3-kinase delta in promoting neutrophil trafficking into inflamed tissue. *Blood*. 2004;103(9):3448-3456. doi: 10.1182/blood-2003-05-1667 [doi].

17. Vanhaesebroeck B, Guillermet-Guibert J, Graupera M, Bilanges B. The emerging mechanisms of isoform-specific PI3K signalling. *Nature reviews Molecular cell biology*. 2010;11(5):329-341.

18. Okkenhaug K, Bilancio A, Farjot G, et al. Impaired B and T cell antigen receptor signaling in p110delta PI 3-kinase mutant mice. *Science*. 2002;297(5583):1031-1034. doi: 10.1126/science.1073560.

19. Rodriguez-Viciana P, Warne PH, Dhand R, et al. Phosphatidylinositol-3-OH kinase direct target of ras. . 1994.

20. Rodriguez-Viciana P, Warne PH, Vanhaesebroeck B, Waterfield MD, Downward J. Activation of phosphoinositide 3-kinase by interaction with ras and by point mutation. *EMBO J*. 1996;15(10):2442-2451.

21. Ciraolo E, Iezzi M, Marone R, et al. Phosphoinositide 3-kinase p110beta activity: Key role in metabolism and mammary gland cancer but not development. *Sci Signal*. 2008;1(36):ra3. doi: 10.1126/scisignal.1161577; 10.1126/scisignal.1161577.

22. Guillermet-Guibert J, Bjorklof K, Salpekar A, et al. The p110beta isoform of phosphoinositide 3-kinase signals downstream of G protein-coupled receptors and is functionally redundant with p110gamma. *Proc Natl Acad Sci U S A*. 2008;105(24):8292-8297. doi: 10.1073/pnas.0707761105; 10.1073/pnas.0707761105.

23. Fritsch R, de Krijger I, Fritsch K, et al. RAS and RHO families of GTPases directly regulate distinct phosphoinositide 3-kinase isoforms. *Cell*. 2013;153(5):1050-1063.

24. Yuan TL, Choi HS, Matsui A, et al. Class 1A PI3K regulates vessel integrity during development and tumorigenesis. *Proc Natl Acad Sci U S A*. 2008;105(28):9739-9744. doi: 10.1073/pnas.0804123105; 10.1073/pnas.0804123105.

25. Graupera M, Guillermet-Guibert J, Foukas LC, et al. Angiogenesis selectively requires the p110alpha isoform of PI3K to control endothelial cell migration. *Nature*. 2008;453(7195):662-666. doi: 10.1038/nature06892; 10.1038/nature06892.

26. Bleul CC, Farzan M, Choe H, et al. The lymphocyte chemoattractant SDF-1 is a ligand for LESTR/fusin and blocks HIV-1 entry. . 1996.

27. Tashiro K, Tada H, Heilker R, Shirozu M, Nakano T, Honjo T. Signal sequence trap: A cloning strategy for secreted proteins and type I membrane proteins. *Science*. 1993;261(5121):600-603.

28. Nagasawa T, Kikutani H, Kishimoto T. Molecular cloning and structure of a pre-B-cell growth-stimulating factor. *Proc Natl Acad Sci U S A*. 1994;91(6):2305-2309.

29. Oberlin E, Amara A. The CXC chemokine SDF-1 is the ligand for LESTR/fusin and prevents infection by T-cell-line-adapted HIV-1. . 1996.

30. Aiuti A, Webb IJ, Bleul C, Springer T, Gutierrez-Ramos JC. The chemokine SDF-1 is a chemoattractant for human CD34+ hematopoietic progenitor cells and provides a new mechanism to explain the mobilization of CD34+ progenitors to peripheral blood. *J Exp Med*. 1997;185(1):111-120.

31. Lyden D, Hattori K, Dias S, et al. Impaired recruitment of bone-marrow–derived endothelial and hematopoietic precursor cells blocks tumor angiogenesis and growth. *Nat Med*. 2001;7(11):1194-1201.

32. Nagasawa T, Hirota S, Tachibana K, et al. Defects of B-cell lymphopoiesis and bone-marrow myelopoiesis in mice lacking the CXC chemokine PBSF/SDF-1. *Nature*. 1996;382(6592):635-638.

33. Forster R, Kremmer E, Schubel A, et al. Intracellular and surface expression of the HIV-1 coreceptor CXCR4/fusin on various leukocyte subsets: Rapid internalization and recycling upon activation. *J Immunol*. 1998;160(3):1522-1531.

34. Delézay O, Koch N, Yahi N, et al. Co-expression of CXCR4/fusin and galactosylceramide in the human intestinal epithelial cell line HT-29. *AIDS*. 1997;11(11):1311-1318.

35. Volin MV, Joseph L, Shockley MS, Davies PF. Chemokine receptor CXCR4 expression in endothelium. *Biochem Biophys Res Commun*. 1998;242(1):46-53.

36. Gupta SK, Lysko PG, Pillarisetti K, Ohlstein E, Stadel JM. Chemokine receptors in human endothelial cells. functional expression of CXCR4 and its transcriptional regulation by inflammatory cytokines. *J Biol Chem*. 1998;273(7):4282-4287.

37. Feil C, Augustin HG. Endothelial cells differentially express functional CXC-chemokine receptor-4 (CXCR-4/fusin) under the control of autocrine activity and exogenous cytokines. *Biochem Biophys Res Commun*. 1998;247(1):38-45.

38. Stratman AN, Davis MJ, Davis GE. VEGF and FGF prime vascular tube morphogenesis and sprouting directed by hematopoietic stem cell cytokines. *Blood*. 2011;117(14):3709-3719. doi: 10.1182/blood-2010-11-316752; 10.1182/blood-2010-11-316752.

39. Unoki N, Murakami T, Nishijima K, Ogino K, van Rooijen N, Yoshimura N. SDF-1/CXCR4 contributes to the activation of tip cells and microglia in retinal angiogenesis. *Invest Ophthalmol Vis Sci*. 2010;51(7):3362-3371. doi: 10.1167/iovs.09-4978; 10.1167/iovs.09-4978.

40. Salcedo R, Wasserman K, Young HA, et al. Vascular endothelial growth factor and basic fibroblast growth factor induce expression of CXCR4 on human endothelial cells: In vivo neovascularization induced by stromal-derived factor-1α. *The American journal of pathology*. 1999;154(4):1125-1135.

41. Kryczek I, Lange A, Mottram P, et al. CXCL12 and vascular endothelial growth factor synergistically induce neoangiogenesis in human ovarian cancers. *Cancer Res*. 2005;65(2):465-472.

42. Hiratsuka S, Duda DG, Huang Y, et al. C-X-C receptor type 4 promotes metastasis by activating p38 mitogen-activated protein kinase in myeloid differentiation antigen (gr-1)-positive cells. *Proc Natl Acad Sci U S A*. 2011;108(1):302-307. doi: 10.1073/pnas.1016917108; 10.1073/pnas.1016917108.

43. Yoon Y, Liang Z, Zhang X, et al. CXC chemokine receptor-4 antagonist blocks both growth of primary tumor and metastasis of head and neck cancer in xenograft mouse models. *Cancer Res*. 2007;67(15):7518-7524. doi: 67/15/7518 [pii].

44. de Nigris F, Rossiello R, Schiano C, et al. Deletion of yin yang 1 protein in osteosarcoma cells on cell invasion and CXCR4/angiogenesis and metastasis. *Cancer Res*. 2008;68(6):1797-1808. doi: 10.1158/0008-5472.CAN-07-5582 [doi].

45. Rubin JB, Kung AL, Klein RS, et al. A small-molecule antagonist of CXCR4 inhibits intracranial growth of primary brain tumors. *Proc Natl Acad Sci U S A*. 2003;100(23):13513-13518. doi: 10.1073/pnas.2235846100.

46. Porvasnik S, Sakamoto N, Kusmartsev S, et al. Effects of CXCR4 antagonist CTCE-9908 on prostate tumor growth. *Prostate*. 2009;69(13):1460-1469.

47. Kozin SV, Kamoun WS, Huang Y, Dawson MR, Jain RK, Duda DG. Recruitment of myeloid but not endothelial precursor cells facilitates tumor regrowth after local irradiation. *Cancer Res*. 2010;70(14):5679-5685. doi: 10.1158/0008-5472.CAN-09-4446; 10.1158/0008-5472.CAN-09-4446.

48. Kioi M, Vogel H, Schultz G, Hoffman RM, Harsh GR, Brown JM. Inhibition of vasculogenesis, but not angiogenesis, prevents the recurrence of glioblastoma after irradiation in mice. *J Clin Invest*. 2010;120(3):694-705. doi: 10.1172/JCI40283; 10.1172/JCI40283.

49. Redjal N, Chan JA, Segal RA, Kung AL. CXCR4 inhibition synergizes with cytotoxic chemotherapy in gliomas. *Clin Cancer Res*. 2006;12(22):6765-6771. doi: 10.1158/1078-0432.CCR-06-1372.

50. Kurogane Y, Miyata M, Kubo Y, et al. FGD5 mediates proangiogenic action of vascular endothelial growth factor in human vascular endothelial cells. *Arterioscler Thromb Vasc Biol*. 2012;32(4):988-996. doi: 10.1161/ATVBAHA.111.244004; 10.1161/ATVBAHA.111.244004.

51. Nakhaei-Nejad M, Haddad G, Zhang QX, Murray AG. Facio-genital dysplasia-5 regulates matrix adhesion and survival of human endothelial cells. *Arterioscler Thromb Vasc Biol*. 2012;32(11):2694-2701. doi: 10.1161/ATVBAHA.112.300074; 10.1161/ATVBAHA.112.300074.

52. Korn C, Augustin HG. Born to die: Blood vessel regression research coming of age. *Circulation*. 2012;125(25):3063-3065. doi: 10.1161/CIRCULATIONAHA.112.112755; 10.1161/CIRCULATIONAHA.112.112755.

53. Gillooly D, SIMONSEN A, STENMARK H. Cellular functions of phosphatidylinositol 3-phosphate and FYVE domain proteins. *Biochem J*. 2001;355:249-258.

54. Gazit R, Mandal PK, Ebina W, et al. Fgd5 identifies hematopoietic stem cells in the murine bone marrow. *J Exp Med*. 2014;211(7):1315-1331. doi: 10.1084/jem.20130428; 10.1084/jem.20130428.

55. Zhang Q, Nakhaei-Nejad M, Haddad G, Wang X, Loutzenhiser R, Murray AG. Glomerular endothelial PI3 kinase-α couples to VEGFR2, but is not required for eNOS activation. *American Journal of Physiology-Renal Physiology*. 2011;301(6):F1242-F1250.

56. Nakatsu MN, Hughes CC. An optimized three-dimensional in vitro model for the analysis of angiogenesis. *Methods Enzymol*. 2008;443:65-82.

57. Balabanian K, Lagane B, Infantino S, et al. The chemokine SDF-1/CXCL12 binds to and signals through the orphan receptor RDC1 in T lymphocytes. *J Biol Chem*. 2005;280(42):35760-35766. doi: M508234200 [pii].

58. Eliceiri BP, Puente XS, Hood JD, et al. Src-mediated coupling of focal adhesion kinase to integrin alpha(v)beta5 in vascular endothelial growth factor signaling. *J Cell Biol*. 2002;157(1):149-160. doi: 10.1083/jcb.200109079 [doi].

59. Wary KK, Kohler EE, Chatterjee I. Focal adhesion kinase regulation of neovascularization. *Microvasc Res*. 2012;83(1):64-70.

60. Farhan MA, Carmine-Simmen K, Lewis JD, Moore RB, Murray AG. Endothelial cell mTOR complex-2 regulates sprouting angiogenesis. *PloS one*. 2015;10(8):e0135245.

61. Kasai A, Shintani N, Kato H, et al. Retardation of retinal vascular development in apelin-deficient mice. *Arterioscler Thromb Vasc Biol*. 2008;28(10):1717-1722. doi: 10.1161/ATVBAHA.108.163402 [doi].

62. Lee O, Kim Y, Lee YM, et al. Sphingosine 1-phosphate induces angiogenesis: Its angiogenic action and signaling mechanism in human umbilical vein endothelial cells. *Biochem Biophys Res Commun*. 1999;264(3):743-750.

63. Igarashi J, Michel T. Sphingosine 1-phosphate and isoform-specific activation of phosphoinositide 3-kinase beta. evidence for divergence and convergence of receptor-regulated endothelial nitric-oxide synthase signaling pathways. *J Biol Chem*. 2001;276(39):36281-36288. doi: 10.1074/jbc.M105628200 [doi].

64. Bird JE, Smith PL, Bostwick JS, Shipkova P, Schumacher WA. Bleeding response induced by anti-thrombotic doses of a phosphoinositide 3-kinase (PI3K)-β inhibitor in mice. *Thromb Res*. 2011;127(6):560-564.

65. Sanematsu F, Hirashima M, Laurin M, et al. DOCK180 is a rac activator that regulates cardiovascular development by acting downstream of CXCR4. *Circ Res*. 2010;107(9):1102-1105. doi: 10.1161/CIRCRESAHA.110.223388 [doi].

66. Signoret N, Rosenkilde MM, Klasse PJ, et al. Differential regulation of CXCR4 and CCR5 endocytosis. *J Cell Sci*. 1998;111 (Pt 18)(Pt 18):2819-2830.

67. Amara A, Gall SL, Schwartz O, et al. HIV coreceptor downregulation as antiviral principle: SDF-1alpha-dependent internalization of the chemokine receptor CXCR4 contributes to inhibition of HIV replication. *J Exp Med*. 1997;186(1):139-146.

68. Yang W, Wang D, Richmond A. Role of clathrin-mediated endocytosis in CXCR2 sequestration, resensitization, and signal transduction. *J Biol Chem*. 1999;274(16):11328-11333.

69. Daaka Y, Luttrell LM, Ahn S, et al. Essential role for G protein-coupled receptor endocytosis in the activation of mitogen-activated protein kinase. *J Biol Chem*. 1998;273(2):685-688.

70. Ballmer-Hofer K, Andersson AE, Ratcliffe LE, Berger P. Neuropilin-1 promotes VEGFR-2 trafficking through Rab11 vesicles thereby specifying signal output. *Blood*. 2011;118(3):816-826. doi: 10.1182/blood-2011-01-328773; 10.1182/blood-2011-01-328773.

71. Nazarewicz RR, Salazar G, Patrushev N, et al. Early endosomal antigen 1 (EEA1) is an obligate scaffold for angiotensin II-induced, PKC-alpha-dependent akt activation in endosomes. *J Biol Chem*. 2011;286(4):2886-2895. doi: 10.1074/jbc.M110.141499 [doi].

72. Pálfy M, Reményi A, Korcsmáros T. Endosomal crosstalk: Meeting points for signaling pathways. *Trends Cell Biol*. 2012;22(9):447-456.

73. Ma Q, Jones D, Borghesani PR, et al. Impaired B-lymphopoiesis, myelopoiesis, and derailed cerebellar neuron migration in CXCR4- and SDF-1-deficient mice. *Proc Natl Acad Sci U S A*. 1998;95(16):9448-9453.

74. Tachibana K, Hirota S, Iizasa H, et al. The chemokine receptor CXCR4 is essential for vascularization of the gastrointestinal tract. *Nature*. 1998;393(6685):591-594.

75. Hotte SJ, Hirte HW, Chen EX, et al. A phase 1 study of mapatumumab (fully human monoclonal antibody to TRAIL-R1) in patients with advanced solid malignancies. *Clin Cancer Res*. 2008;14(11):3450-3455. doi: 10.1158/1078-0432.CCR-07-1416 [doi].

76. Kulkarni S, Sitaru C, Jakus Z, et al. PI3Kb plays a critical role in neutrophil activation by immune complexes. *Sci Signal*. 2011;4:168.

77. Haddad G, Zhabyeyev P, Farhan M, et al. Phosphoinositide 3-kinase beta mediates microvascular endothelial repair of thrombotic microangiopathy. *Blood*. 2014;124(13):2142-2149. doi: 10.1182/blood-2014-02-557975; 10.1182/blood-2014-02-557975.

78. Kurosu H, Maehama T, Okada T, et al. Heterodimeric phosphoinositide 3-kinase consisting of p85 and p110β is synergistically activated by the βγ subunits of G proteins and phosphotyrosyl peptide. *J Biol Chem*. 1997;272(39):24252-24256.

79. Tolias KF, Cantley LC, Carpenter CL. Rho family GTPases bind to phosphoinositide kinases. *J Biol Chem*. 1995;270(30):17656-17659.

80. Bokoch GM, Vlahos CJ, Wang Y, Knaus UG, Traynor-Kaplan AE. Rac GTPase interacts specifically with phosphatidylinositol 3-kinase. *Biochem J*. 1996;315 (Pt 3)(Pt 3):775-779.

81. Zheng Y, Bagrodia S, Cerione RA. Activation of phosphoinositide 3-kinase activity by Cdc42Hs binding to p85. *J Biol Chem*. 1994;269(29):18727-18730.

82. Knight ZA, Gonzalez B, Feldman ME, et al. A pharmacological map of the PI3-K family defines a role for p110α in insulin signaling. *Cell*. 2006;125(4):733-747.

83. Kang S, Denley A, Vanhaesebroeck B, Vogt PK. Oncogenic transformation induced by the p110beta, -gamma, and -delta isoforms of class I phosphoinositide 3-kinase. *Proc Natl Acad Sci U S A*. 2006;103(5):1289-1294. doi: 0510772103 [pii].

84. Hoang MV, Nagy JA, Senger DR. Cdc42-mediated inhibition of GSK-3β improves angio-architecture and lumen formation during VEGF-driven pathological angiogenesis. *Microvasc Res*. 2011;81(1):34-43.

85. Gupton SL, Gertler FB. Filopodia: The fingers that do the walking. *Sci STKE*. 2007;2007(400):re5. doi: 10.1126/stke.4002007re5.

86. Chen F, Ma L, Parrini M, et al. Cdc42 is required for PIP 2-induced actin polymerization and early development but not for cell viability. *Current Biology*. 2000;10(13):758-765.

87. Hu GD, Chen YH, Zhang L, et al. The generation of the endothelial specific cdc42-deficient mice and the effect of cdc42 deletion on the angiogenesis and embryonic development. *Chin Med J (Engl)*. 2011;124(24):4155-4159.

88. Kanda S, Mochizuki Y, Kanetake H. Stromal cell-derived factor-1alpha induces tube-like structure formation of endothelial cells through phosphoinositide 3-kinase. *J Biol Chem*. 2003;278(1):257-262. doi: 10.1074/jbc.M204771200 [doi].

89. Masri B, Morin N, Cornu M, Knibiehler B, Audigier Y. Apelin (65-77) activates p70 S6 kinase and is mitogenic for umbilical endothelial cells. *FASEB J*. 2004;18(15):1909-1911. doi: 10.1096/fj.04-1930fje [doi].

90. Igarashi J, Bernier SG, Michel T. Sphingosine 1-phosphate and activation of endothelial nitric-oxide synthase. differential regulation of akt and MAP kinase pathways by EDG and bradykinin receptors in vascular endothelial cells. *J Biol Chem*. 2001;276(15):12420-12426. doi: 10.1074/jbc.M008375200 [doi].

91. Gaengel K, Niaudet C, Hagikura K, et al. The sphingosine-1-phosphate receptor S1PR1 restricts sprouting angiogenesis by regulating the interplay between VE-cadherin and VEGFR2. *Developmental cell*. 2012;23(3):587-599.

92. Hanahan D, Folkman J. Patterns and emerging mechanisms of the angiogenic switch during tumorigenesis. *Cell*. 1996;86(3):353-364.

93. Shirozu M, Nakano T, Inazawa J, et al. Structure and chromosomal localization of the human stromal cell-derived factor 1 (SDF1) gene. *Genomics*. 1995;28(3):495-500.

94. Yoshida S, Ono M, Shono T, et al. Involvement of interleukin-8, vascular endothelial growth factor, and basic fibroblast growth factor in tumor necrosis factor alpha-dependent angiogenesis. *Mol Cell Biol*. 1997;17(7):4015-4023.

95. Strickler JH, Hurwitz HI. Bevacizumab-based therapies in the first-line treatment of metastatic colorectal cancer. *Oncologist*. 2012;17(4):513-524. doi: 10.1634/theoncologist.2012-0003 [doi].

96. Patel M, Vogelbaum MA, Barnett GH, Jalali R, Ahluwalia MS. Molecular targeted therapy in recurrent glioblastoma: Current challenges and future directions. *Expert Opin Investig Drugs*. 2012;21(9):1247-1266.

97. Bagri A, Berry L, Gunter B, et al. Effects of anti-VEGF treatment duration on tumor growth, tumor regrowth, and treatment efficacy. *Clin Cancer Res*. 2010;16(15):3887-3900. doi: 10.1158/1078-0432.CCR-09-3100 [doi].

98. Ebos JM, Kerbel RS. Antiangiogenic therapy: Impact on invasion, disease progression, and metastasis. *Nature reviews Clinical oncology*. 2011;8(4):210-221.

99. De Bock K, Mazzone M, Carmeliet P. Antiangiogenic therapy, hypoxia, and metastasis: Risky liaisons, or not? *Nature reviews Clinical oncology*. 2011;8(7):393-404.

Chapter VI: Characterization of vascular repair of Apelin-deficient hearts in a model of CAV in mice

Abstract

Heart transplantation improves survival and the quality of life in end stage cardiac patients. However, the development of chronic vascular injury has limited the efficacy of transplantation. The injury starts in the coronary arteries, designated chronic allograft vasculopathy (CAV), reduces the blood supply to the graft tissue, and eventually leads to organ failure. CAV is associated with damage to the endothelial cells (EC) lining the blood vessels due to indolent cell- or antibody-mediated rejection. Although the pathology of CAV is well known, the mechanism of endothelial repair in response to injury is poorly understood.

Apelin, an EC specific protein, is a prominent mediator of angiogenesis in vivo and its embryonic loss causes defects in vasculature development. Currently, accumulating evidence supports the role of Apelin in vascular repair but studies about the significance of Apelin in CAV are scant. We have recently reported that loss of Apelin impairs vascular repair in myocardial infarction, and in the injured kidney glomerular microvasculature. We hypothesize that Apelin dependent pro-angiogenic signals are exploited for arterial endothelial repair in CAV.

CAV was generated using a validated model, by transplantation of male wild type hearts into female recipients to elicit a minor MHC-directed allo-immune response against the male donor hearts, and compared to control male wild type hearts into male recipients. To test our hypothesis, male Apelin$^{-/y}$ (Apelin-deficient) or Apelin$^{+/y}$ littermate control mouse hearts were transplanted into female wild-type recipient mice. Mice were sacrificed at 2 and 6 weeks post transplantation for analysis of early and late CAV lesions. At these time points, the graft function

was tested by electrocardiogram (ECG) tracing; then the base of the hearts were recovered for histomorphometric evaluation, and immunohistology to assess the degree of CAV.

We observed about 25% difference in arterial lumen compromise between Apelin$^{-/y}$ hearts and the controls at 6 weeks post transplantation. Histological examination of the myocardium indicated a severe inflammatory response in the apelin-deficient grafts. ECG tracing showed decrease in heart rate and prolongation of PR interval in the apelin-deficient grafts. Interestingly, evaluating the immune response by T cell in vivo proliferation assay in the hosts at 6 weeks post transplantation showed that apelin deficiency triggered an exagerated host immune response against the grafts.

In conclusion, our results show that apelin loss accelerates CAV development, and suggest a significant role of apelin in vascular repair of CAV.

Introduction

Heart failure confers a high morbidity and mortality on North Americans 1. Despite many advances in heart failure management, heart transplantation (HTX) remains the best therapy for individuals with end stage disease 2. However, donor hearts are in short supply, transplant rates have remained stagnant, and many potential recipients die on the wait list. A critical goal of care, then, is to maximize the survival of heart allografts.

Currently, chronic vascular injury of the transplant heart is a leading cause of death, even in the first year after transplantation, and remains limiting for long term graft survival 3-5. The classicaly recognized injury, chronic allograft vasculopathy (CAV), progressively occludes epicardial and branch arteries 6. Higher grades of CAV assosciate with progressive imparment of left ventricular (LV) function 7. Mechanistic insights may be derived from the correlation of

circulating apoptotic endothelial cells or endothelial microparticles 8, and serum level of vascular endothelial growth factors 9 in recepients with CAV, suggesting chronic vascular endothelial cell (EC) injury and repair occur in tandem as CAV progresses.

An important clinical risk factor for CAV is donor specific antibody (DSA) 10-12. Moreover, diagnostic markers for antibody mediated rejection (AMR) of the microvasculature reveal AMR may account for more early and late morbidity and death than previously recognized 13. For example, the finding of compromise of the coronary microcirculation in human HTx by imaging techniques is a powerful predictor of outcome 12, 14. Thus, vascular injury occurs in both coronary arterial and cardiac microvascular vessels, and each contributes to adverse graft outcome.

In HTx, coronary endothelial cells (EC) serve as potent stimulators, as well as targets, of allogeneic lymphocyte reactivity 15-18. Further, evidence mounts that allo-antibody dependent mechanisms recruit macrophages and NK cells to the graft to mediate EC injury 19-20. The extent of endothelial damage assosciated with CAV is found in a continuum. Without immunosuppression, allografts display progressive vascular endothelial destruction throughout the vasculature, with missing EC an areas of bare basement membrane 16,21,22.

In mouse HTx models, EC apoptosis mediated by canonical CTL effector pathways against arterial EC contributes to CAV development 23-25. Current models of CAV in HTx under immunosuppression or medited via T helper responses, display more indolent EC injury 26-28.

Microvascular injury, mediated by DSA, also contibutes to poor allograft function and survival. This data is now clear in human kidney allografts 29-31. In HTx recepients, DSA assosciated compromise of the coronary microvascular bed corrilates with the subsequent reduction in left

ventricular function 10, 14, 32. Small animal models of acute, but not chronic microvascular injury, have been reported, however these are a mix of antibody and cell mediated injury 33.

Apelin is a key mediator induced in angiogenic tip cells in vivo, and EC loss of apelin in mutant mice is linked to impaired neovascularization in the embryo 33. In the endothelial sprout, apelin signals in a paracrine fashion to trailing stalk EC and to myocytes 34,35. We have recently reported that deficient EC apelin production in myocardial infarction, and the injured kidney glomerular microvasculature, is assosciated with failed vascular repair after acute insult, and exacerbates organ dysfunction 36, 37.

Apelin signals to adjacent cells that express the receptor, APJ. Loss of APJ in knockout mice results in embryonic and early postnatal lethality assosciated with an abnormal vasculature 38. In the microvasculature, pericytes express APJ 39. In the heart, apelin has been identified as one of the most potent positive inotropic agents signaling through its receptor, APJ, to the cardio myocyte 40. This work identified apelin as an EC product, constitutively produced in coronary artery EC, and established apelin as an EC product acting as a paracrine mediator for crosstalk between the EC and myocytes. Interestingly, expression of the gene in the coronary microvasculature was upregulated after biventricular unloading of failing hearts, consistent with induction of a vascular repair program.

Results

Apelin deficiency in transplanted hearts compromises the function of the grafts

We used ECG recording as an indicator for the function of the grafts. After 2 and 6 weeks of surgery, we performed ECGs for the recepient mice. A dual ECG tracing for the native and transplanted hearts was performed simultaneously in two separate channels. This helped to distinguish the waves of the native hearts from the transplanted grafts, and to exclude any interference. Data showed no change in the ECG waves of the native hearts. However, the PR-intervals were prolonged in the apelin-deficient heart grafts compared to the wild type grafts (Fig. 6.1 B, D). Moreover, the apelin-deficient grafts showed a decrease in the heart rate six weeks post transplant (Fig. 6.1 A, C). These measures of the function of the conduction system of the heart grafts indicate more damage among apelin-deficient vs. control hearts.

Apelin loss exacerbates the vascular injury in CAV

To study the role of apelin in the development of vascular injury in CAV, we collected the heart grafts after 2 and 6 weeks of transplantation and stained the myocardium with van Gieson stain, a specific stain for the internal elastic lamina. Of note, the internal elastic lamina is normally lined with a thin layer of endothelium that provides a cushion for the circulating red blood cells (RBCs) and regulates hemostasis. In the apelin deficient grafts, we observed a marked expansion of the intima at six weeks post transplantation that obliterated ~80% of the coronary arteries' lumens (Fig. 6.2 A, B). This indicates that apelin has a protective role in the endothelium.

Marked tissue infiltration in apelin deficient hearts

Hematoxlin and eosin staining of the myocardium of the apelin deficient heart grafts showed loss of the muscle fibers contour and heavy cellular infiltration (Fig. 6.3). This finding indicates more

severe inflamatory response in the apelin deficient grafts. However, confirmation and identification of the cell population involved in the infiltirate are still to be determined.

Apelin deficient heart grafts trigger the immune respone in the recepients

The accelerted vascular lesion in the apelin deficient hearts could result from hyper reactive immune response in the host against the apelin deficient grafts. Therefore, we compared the proliferation of Marilyn T-cells in the peripheral blood of recipients with apelin deficient hearts to recipients with wild type hearts. Marilyn T lymphocytes were isolated from T cell receptor transgenic mice, that recognize only the male HY antigen. Interestingly, after six weeks of transplantation, the apelin deficient grafts triggered a prominent T lymphocyte proliferation in the host (Fig. 6.4). Whereas, the T lymphocytes proliferation was muted in recipients of wild type heart grafts.

Apelin induces eNOS activity in human umbilical vein endothelial cells

Apelin precursor is formed of 77 amino acid pre-peptide, which is subsequently processed into a family of apelin peptides. Pyr-apelin 13 and apelin 17 are the dominant apelin peptides in vivo. To begin to evaluate the mechanism of vascular protection provided by Apelin, we asked if apelin stimulates the PI3K pathway and eNOS phosphorylation in primary human endothelial cells. We used SDF1, a GPCR ligand, as a control. Interestingly, apelin 13 and 17 stimulated both Akt and eNOS activity (Fig. 6.5 A-D).

Conclusion

We have shown that apelin deficiency exacerbates the vascular lesions in an animal model of cardiac allograft vasculopathy. The vascular lesion was characterized by coronary arterial intimal expansion, an obliterated vascular lumen, and was associated with tissue infiltration. The exaggerated injury among apelin-deficient vs. wild type heart allografts is correlated with conduction system defects among the apelin-deficient hearts. We document a more aggressive immune response against the apelen deficient vs. wild type control grafts. Mechanistically this may relate to reduced eNOS activity in the endothelium of the apelin-deficient hearts.

The coronary endothelium constitutively expresses apelin. Apelin is thought to signal in an autocrine fashion to the vascular endothelium, and in a paracrine fashion to vascular and cardiac myocytes. During new vessel development, loss of apelin results in reduced EC movement and sprout extension. Repair of the injured coronary artery endothelium of the allograft has not been well studied, but likely also involves EC effacement, cell division, and movement to fill defects in the endothelial monolayer. Our data suggests repair of the allograft coronary endothelium relies on apelin-stimulated cues to mediate these events.

In earlier work we have determined that remodeling of endothelial cell-matrix contacts, and the cortical actin cytoskeleton are regulated by PI3Kinase activity. Here we show that apelin stimulation of cultured EC couples to the PI3kinase pathway, and potently stimulates mTORC2 and Akt activities. Accordingly, loss of apelin signaling is expected to reduce remnant EC effacement and motility responses to allo-immune mediated arterial endothelial monolayer disruption.

In the arterial endothelium, loss of the apelin stimulus is expected to compromise EC defense against allo-immune cell-mediated injury. For example, blunted Akt activity directly sensitizes EC to pro-apoptotic stimuli in part through release of inhibition of FOXO1/3-dependent expression of the bcl-2 family member, Bad 41, 42. Further, decreased eNOS production of nitric oxide is anticipated to release nitric oxide-dependent repulsion of leukocytes from the endothelium 43-45. Moreover, attenuation of NO production by eNOS may reduce vasodilation and contribute to tissue injury by compromise of blood flow.

Disruption of the apelin cue to the vascular and myocardial smooth muscle may contribute to maladaptive arterial remodeling and myocardial death. On the one hand apelin functions to maintain vascular smooth muscle quiescence, therefore loss of apelin may promote VSMC migration to the neointima and myofibroblast transformation to account for the increase in cellularity and matrix deposited in the formation of the CAV lesion 46. In addition, loss of apelin signals to the myocardium may directly sensitize cardiomyocyte to allo-immune cytotoxic injury. Similar increases in myocardial injury are evident following ischemia reperfusion injury in apelin knockout mice 36.

Enhanced dendritic cell trafficking into the allograft, and exaggerated tissue injury may explain our finding of markedly enhanced Marilyn T cell responses in the recipients of apelin knockout hearts. This intriguing result indicates that endothelial apelin modulates the immune response to graft HY antigen, generated in secondary lymphoid organs such as the spleen 47. This may

reflect increased release of graft antigen from the rejecting myocardium and/or higher numbers of dendritic cells that have sampled graft antigens 48. In this way apelin may function as a novel reporter to the immune system of vascular and tissue health.

In summary, we suggest a novel function of endothelial apelin production to protect the allograft from allo-immune injury. The effect is likely complex, involving both effects on immune cell surveillance of the graft, and tissue responses to allo-immune-mediated graft injury. Taken together, however, the findings suggest potential benefits to the allograft by supplementation of native apelin production, or replacement of apelin in the setting of endothelial injury or loss.

Figures

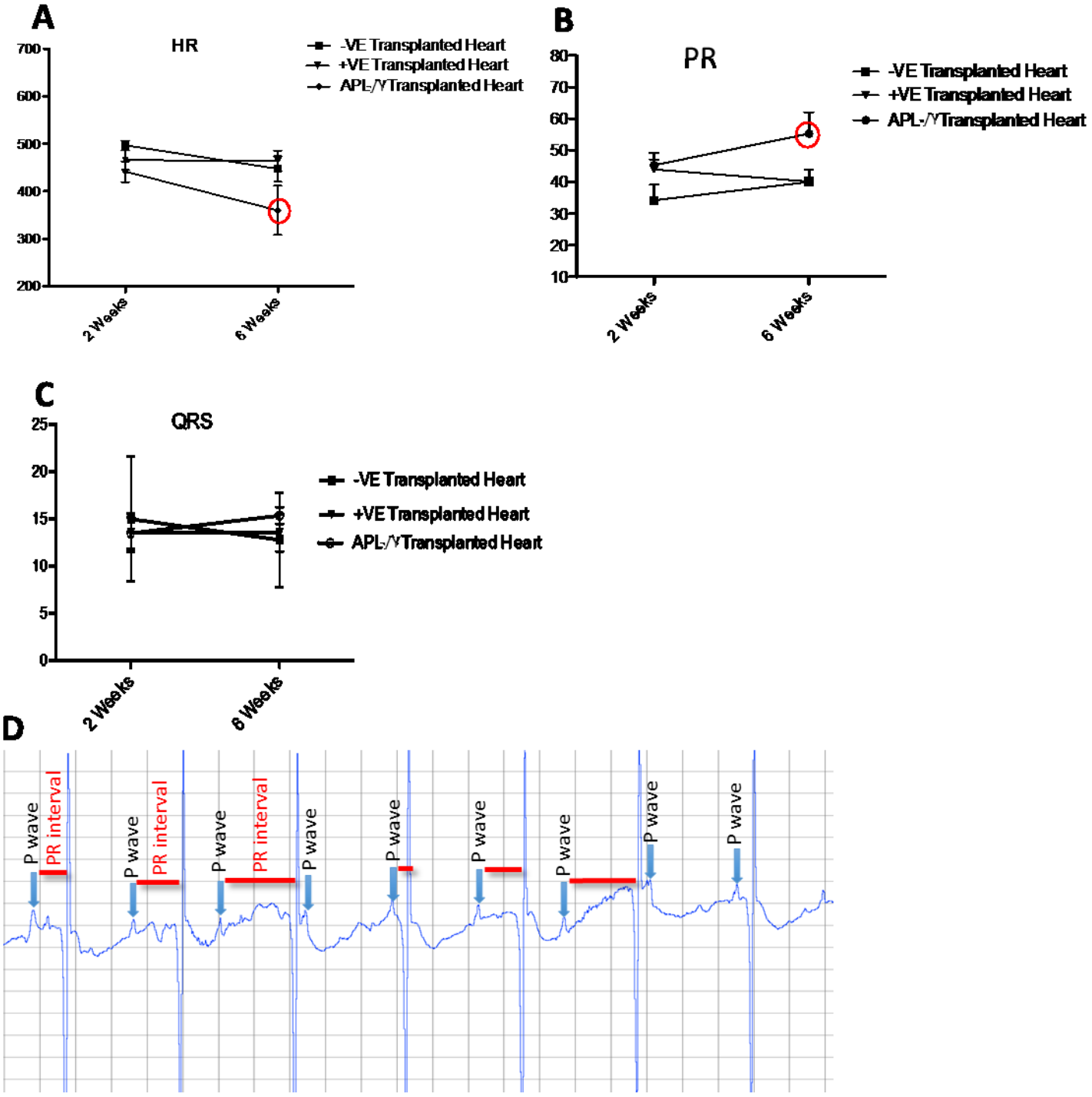

Fig 6. 1

Figure 6.1. Apelin deficiency prolongs PR interval and decreases heart rate in transplanted hearts. Hearts from male C57BL/6 mice were transplanted into male (-VE control), or female recipients (+VE control) as described in materials and methods. Alternatively, male apelin deficient hearts (APL-/Y) were transplanted into wild type females. Two and six weeks after surgery eclectrocardiogram (ECG) tracing was performed by placing the electrodes on the abdomen near the base of the heart in lead I configuration. **A)** Representative graph of heart rates form the different experimental groups (n=4 per group) indicating a significant decrease in heart rate in the APL-/Y Transplanted Heart group at 6 weeks (red circle; two way ANOVA). **B)** Representative graph of PR interval form the different experimental groups (n=4 per group) indicating a prolonged PR interval in the APL-/Y Transplanted Heart group at 6 weeks (red circle; two way ANOVA). **C)** Representative graph of QRS intervals from the different experimental groups showing no change (n=4 per group). D) Representative image of ECG tracing for the APL-/Y transplanted heart showing progressive prolongation of the PR interval in 2' heart block (red line).

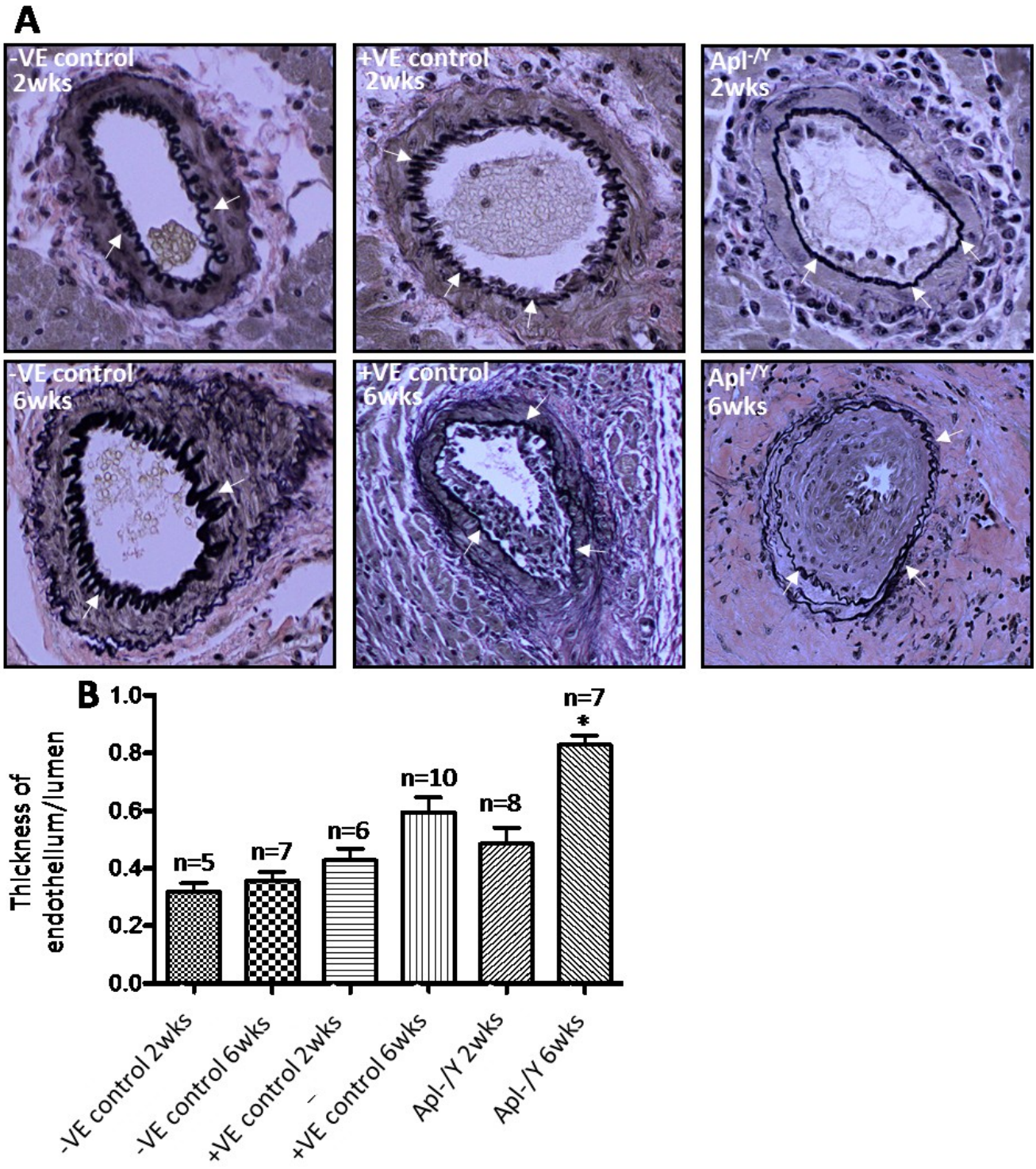
A
-VE control
2wks
+VE control
2wks
Apl-/Y
2wks
-VE control
6wks
+VE control
6wks
Apl-/Y
6wks
B
Thickness of endothellum/lumen
1.0
0.8
0.6
0.4
0.2
0.0
n=5
n=7
n=6
n=10
n=8
n=7
*
-VE control 2wks
-VE control 6wks
+VE control 2wks
+VE control 6wks
Apl-/Y 2wks
Apl-/Y 6wks

Fig 6. 2

Figure 6.2. Apelin-deficient heart grafts show increased intimal thickness. Hearts from male C57BL/6 mice were transplanted into male (negative control), or female recipients (positive control) as described in materials and methods. Alternatively, male apelin deficient hearts (APL-/Y) were transplanted into wild type females. After two (2wks) or six weeks (6wks), the transplanted hearts were recovered, fixed, sectioned and stained with van Gieson elastin stain. **A)** Representative images of coronary arteries showing the internal elastic lamina stained stained in black (arrows). **B)** Quantitation of the area of the intima as a fraction of the lumen area delimited by the internal elastic lamina as described in materials and methods. APL-/Y group shows a significant increase in intimal thickness at 6 weeks compared to controls (*$P<0.05$ by one way ANOVA).

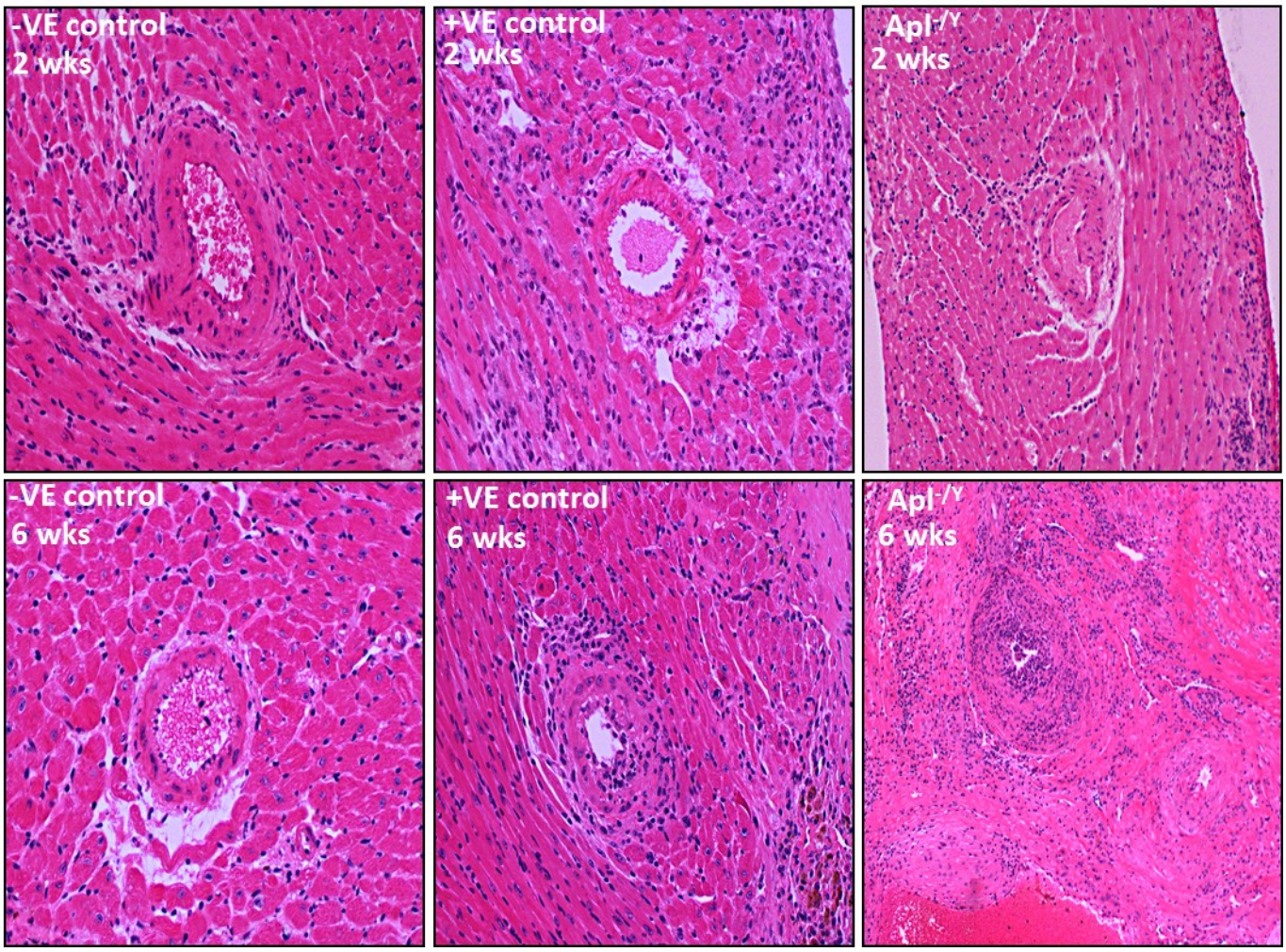

Fig 6. 3

Figure 6.3. Apelin-deficient heart grafts show marked cellular infiltration. Hearts from male C57BL/6 mice were transplanted into male (negative control), or female recipients (positive control) as described in materials and methods. Alternatively, male apelin deficient hearts (APL-/Y) were transplanted into wild type females. After two (2wks) or six weeks (6wks), hearts were recovered, fixed, sectioned and stained with H and E stain. Representative images of coronary arteries showing noticeable infiltration of the myocardium in the APL-/Y group at 6 weeks post surgery.

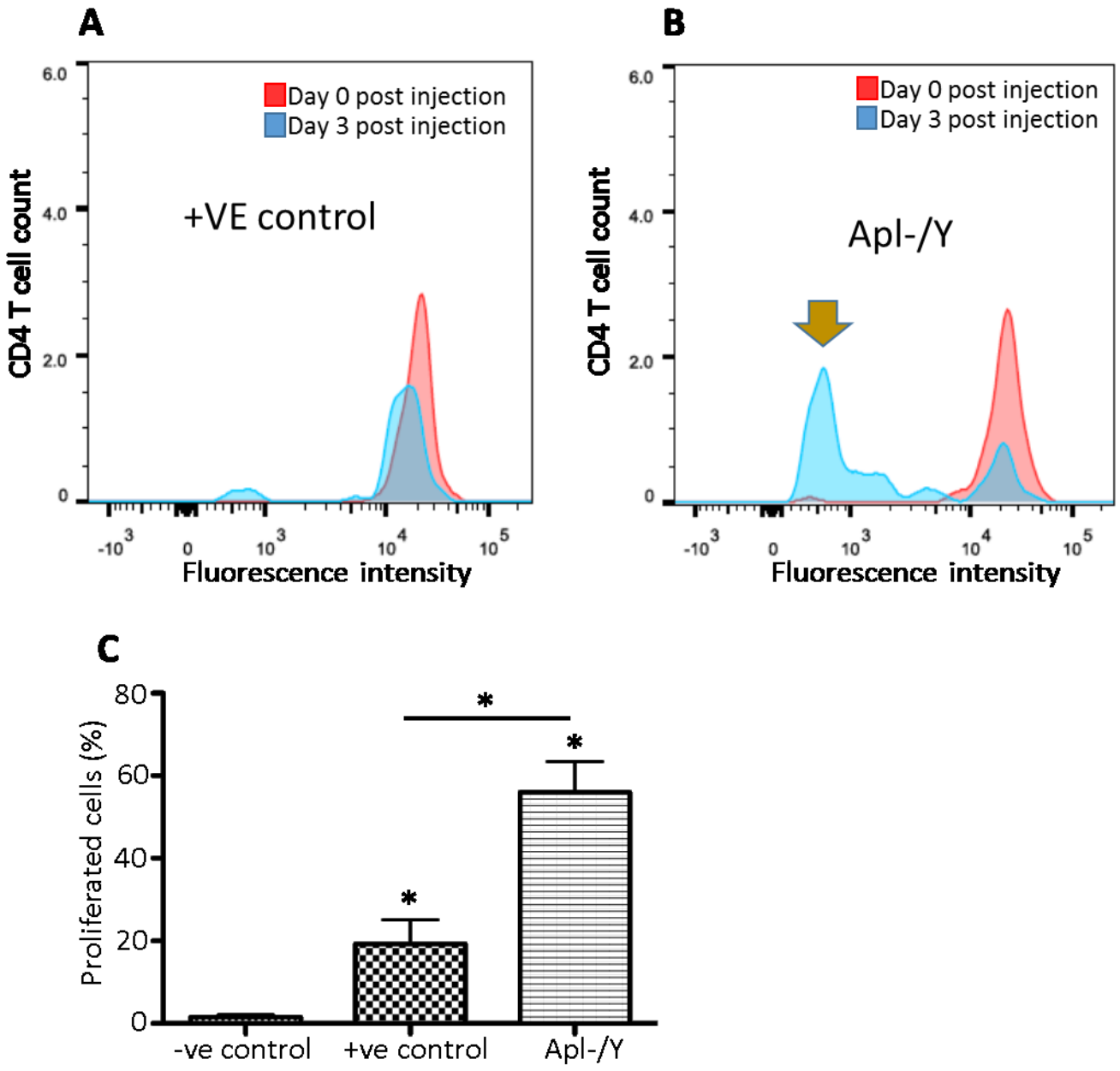
A
Day 0 post injection
Day 3 post injection
+VE control
CD4 T cell count
6.0
4.0
2.0
0
-10^3
0
10^3
10^4
10^5
Fluorescence intensity
B
Day 0 post injection
Day 3 post injection
Apl-/Y
CD4 T cell count
6.0
4.0
2.0
0
-10^3
0
10^3
10^4
10^5
Fluorescence intensity
C
Proliferated cells (%)
80
60
40
20
0
*
*
*
-ve control
+ve control
Apl-/Y

Fig 6. 4

Figure 6.4. Apelin deficient heart grafts stimulate the proliferation of CD4 T cells in the host. Hearts from male C57BL/6 mice (positive control), or apelin knock out mice (Apl-/Y) were transplanted into female C57BL/6 recipients as described in materials and methods. Equal number of fluorescent-tagged HY-specific CD4 T cells from Marilyn mice were intravenously injected in each group (red curve). Three days post injection, peripheral blood was collected and the number of fluorescent labelled T cells was evaluated by flow cytometry. **A)** Representative image of Marilyn T cell proliferation in positive control mice. **B)** Representative image of Marilyn T cell proliferation in Apl-/y group showing a large population of proliferated T cells at day 3 (yellow arrow). **B)** Quantitation of the proliferated cells by flow cytometry (negative control, n=4; positive control, n=5; APL-/Y, n=6; *$P<0.05$ by one way ANOVA).

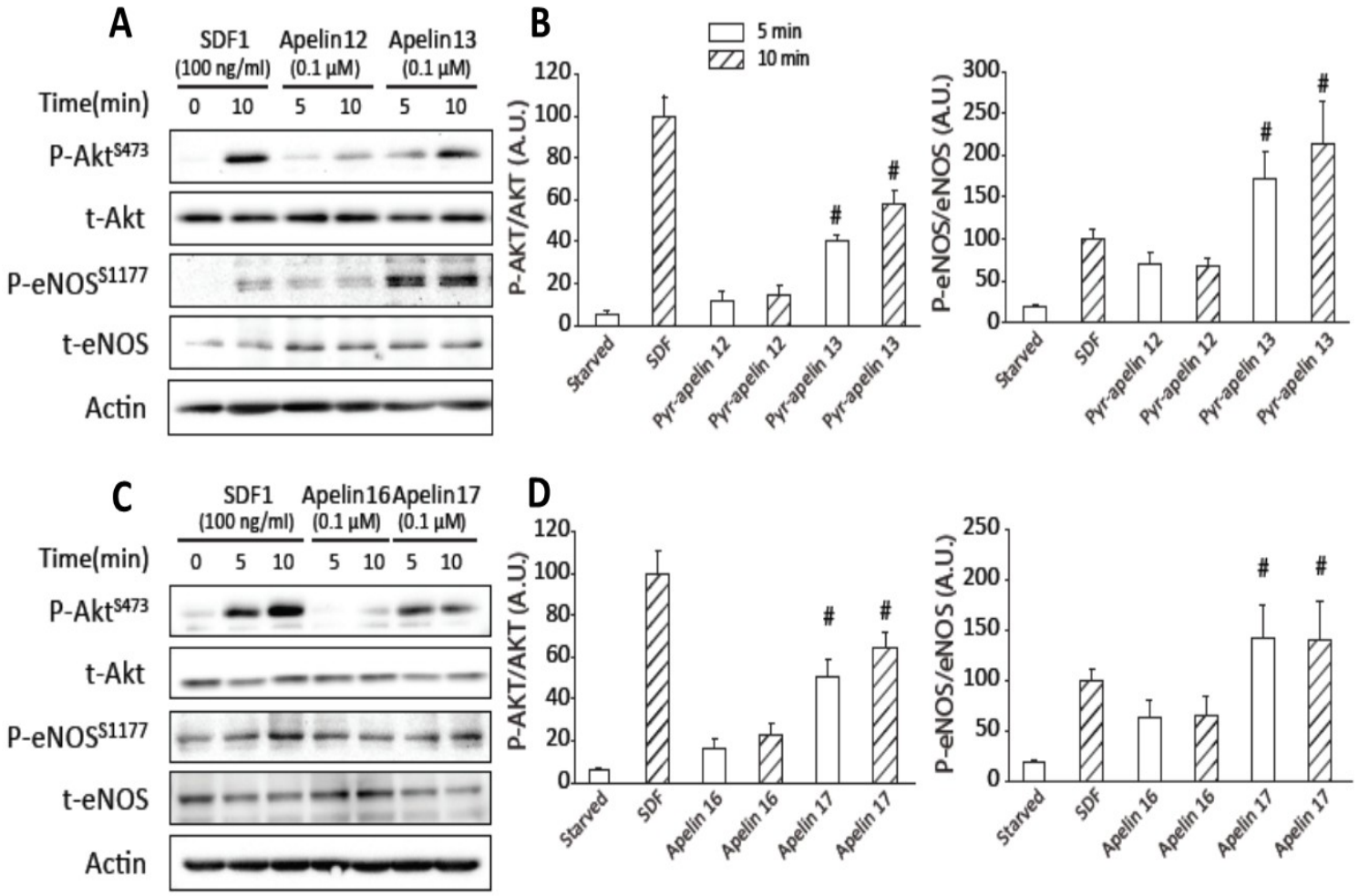
A
SDF1 (100 ng/ml)
Apelin12 (0.1 μM)
Apelin13 (0.1 μM)
Time(min)
0 10 5 10 5 10
P-Akt S473
t-Akt
P-eNOS S1177
t-eNOS
Actin
B
5 min
10 min
P-AKT/AKT (A.U.)
P-eNOS/eNOS (A.U.)
Starved
SDF
Pyr-apelin 12
Pyr-apelin 13
C
SDF1 (100 ng/ml)
Apelin16 (0.1 μM)
Apelin17 (0.1 μM)
Time(min)
0 5 10 5 10 5 10
P-Akt S473
t-Akt
P-eNOS S1177
t-eNOS
Actin
D
P-AKT/AKT (A.U.)
P-eNOS/eNOS (A.U.)
Starved
SDF
Apelin 16
Apelin 17

Fig 6. 5

Figure 6.5. Apelin increases eNOS activity in HUVECs. Human umbilical vein endothelial cells (HUVECs) were starved overnight, then stimulated with 100ng/ml stromal cell derived factor 1 (SDF1) or 0.1 uM apelin as indicated. **A)** Representative Western blot of phospho-Akt (P-Akt S473), total Akt (t-Akt), phospho-eNOS (P-eNOS S1177), total eNos (T-ENOS), and actin. **B)** Quantitation of P-Akt and P-eNOS showing increased Akt and eNOS activity after Apelin 13 treatment. **C)** Representative Western blot of P-Akt S473, t-Akt, P-eNOS S1177, t-eNos, and actin. **D)** Quantitation of P-Akt and P-eNOS showing increased Akt and eNOS activity after Apelin 17 treatment (n=3, #P<0.05 by ANOVA). Image published in Wang et al. "Angiotensin Converting Enzyme 2 Metabolizes and Partially Inactivates Pyrapelin-13 and Apelin-17: Physiological Effects in the Cardiovascular System" In Press. *Hypertension*.

References

1. Go AS. Heart disease and stroke statistics-2013 update: A report from the american heart association (vol 127, pg e6, 2013). *Circulation*. 2013;127(23):E841-E841.

2. Toyoda Y, Guy TS, Kashem A. Present status and future perspectives of heart transplantation. *Circulation Journal*. 2013;77(5):1097-1110.

3. Hiemann NE, Wellnhofer E, Knosalla C, et al. Prognostic impact of microvasculopathy on survival after heart transplantation: Evidence from 9713 endomyocardial biopsies. *Circulation*. 2007;116(11):1274-1282. doi: CIRCULATIONAHA.106.647149 [pii].

4. Lund LH, Edwards LB, Kucheryavaya AY, et al. The registry of the international society for heart and lung transplantation: Thirtieth official adult heart transplant report--2013; focus theme: Age. *J Heart Lung Transplant*. 2013;32(10):951-964.

5. Lu W, Palatnik K, Fishbein GA, et al. Diverse morphologic manifestations of cardiac allograft vasculopathy: A pathologic study of 64 allograft hearts. *The Journal of Heart and Lung Transplantation*. 2011;30(9):1044-1050.

6. Wenning C, Stypmann J, Papavassilis P, et al. Left ventricular dilation and functional impairment assessed by gated SPECT are indicators of cardiac allograft vasculopathy in heart transplant recipients. *The Journal of Heart and Lung Transplantation*. 2012;31(7):719-728.

7. Singh N, Van Craeyveld E, Tjwa M, et al. Circulating apoptotic endothelial cells and apoptotic endothelial microparticles independently predict the presence of cardiac allograft vasculopathy. *J Am Coll Cardiol*. 2012;60(4):324-331.

8. Daly KP, Seifert ME, Chandraker A, et al. VEGF-C, VEGF-A and related angiogenesis factors as biomarkers of allograft vasculopathy in cardiac transplant recipients. *The Journal of Heart and Lung Transplantation*. 2013;32(1):120-128.

9. Loupy A, Cazes A, Guillemain R, et al. Very late heart transplant rejection is associated with microvascular injury, complement deposition and progression to cardiac allograft vasculopathy. *American Journal of Transplantation*. 2011;11(7):1478-1487.

10. Chih S, Chruscinski A, Ross HJ, Tinckam K, Butany J, Rao V. Antibody-mediated rejection: An evolving entity in heart transplantation. *Journal of transplantation*. 2012;2012.

11. Topilsky Y, Gandhi MJ, Hasin T, et al. Donor-specific antibodies to class II antigens are associated with accelerated cardiac allograft vasculopathy: A three-dimensional volumetric intravascular ultrasound study. *Transplantation*. 2013;95(2):389-396. doi: 10.1097/TP.0b013e318273878c [doi].

12. Haddad F, Khazanie P, Deuse T, et al. Clinical and functional correlates of early microvascular dysfunction after heart transplantation. *Circ Heart Fail*. 2012;5(6):759-768. doi: 10.1161/CIRCHEARTFAILURE.111.962787 [doi].

13. Hofmann N, Voss A, Dickhaus H, et al. Long-Term outcome after heart transplantation predicted by quantitative myocardial blush grade in coronary angiography. *American Journal of Transplantation*. 2013;13(6):1491-1502.

14. Epperson DE, Pober JS. Antigen-presenting function of human endothelial cells. direct activation of resting CD8 T cells. *J Immunol*. 1994;153(12):5402-5412.

15. Murray AG, Petzelbauer P, Hughes CC, Costa J, Askenase P, Pober JS. Human T-cell-mediated destruction of allogeneic dermal microvessels in a severe combined immunodeficient mouse. *Proc Natl Acad Sci U S A*. 1994;91(19):9146-9150.

16. SAVAGE CO, HUGHES CC, McINTYRE BW, PICARD JK, POBER JS. HUMAN CD4 T CELLS PROLIFERATE TO HLA-DR ALLOGENEIC VASCULAR ENDOTHELIUM: IDENTIFICATION OF ACCESSORY INTERACTIONS. *Transplantation*. 1993;56(1):128-134.

17. Rahmani M, Cruz RP, Granville DJ, McManus BM. Allograft vasculopathy versus atherosclerosis. *Circ Res*. 2006;99(8):801-815. doi: 99/8/801 [pii].

18. Hirohashi T, Chase C, Della Pelle P, et al. A novel pathway of chronic allograft rejection mediated by NK cells and alloantibody. *American Journal of Transplantation*. 2012;12(2):313-321.

19. Abe T, Su C, Iida S, et al. Graft-Derived CCL2 increases graft injury during Antibody-Mediated rejection of cardiac allografts. *American Journal of Transplantation*. 2014;14(8):1753-1764.

20. Forbes RD, Guttmann RD, Gomersall M, Hibberd J. A controlled serial ultrastructural tracer study of first-set cardiac allograft rejection in the rat. evidence that the microvascular endothelium is the primary target of graft destruction. *Am J Pathol*. 1983;111(2):184-196.

21. Lai JC, Tranfield EM, Walker DC, et al. Ultrastructural evidence of early endothelial damage in coronary arteries of rat cardiac allografts. *The Journal of heart and lung transplantation*. 2003;22(9):993-1004.

22. Dong C, Wilson JE, Winters GL, McManus BM. Human transplant coronary artery disease: Pathological evidence for fas-mediated apoptotic cytotoxicity in allograft arteriopathy. *Lab Invest*. 1996;74(5):921-931.

23. Choy JC, Kerjner A, Wong BW, McManus BM, Granville DJ. Perforin mediates endothelial cell death and resultant transplant vascular disease in cardiac allografts. *The American journal of pathology*. 2004;165(1):127-133.

24. Choy JC, Cruz RP, Kerjner A, et al. Granzyme B induces endothelial cell apoptosis and contributes to the development of transplant vascular disease. *American journal of transplantation*. 2005;5(3):494-499.

25. Currie M, Zaki AM, Nejat S, Hirsch GM, Lee TD. Immunologic targets in the etiology of allograft vasculopathy: Endothelium versus media. *Transpl Immunol*. 2008;19(2):120-126.

26. Lee RS, Yamada K, Houser SL, et al. Indirect recognition of allopeptides promotes the development of cardiac allograft vasculopathy. *Proc Natl Acad Sci U S A*. 2001;98(6):3276-3281. doi: 10.1073/pnas.051584498 [doi].

27. Russell PS, Chase CM, Madsen JC, et al. Coronary artery disease from isolated non-H2-determined incompatibilities in transplanted mouse hearts. *Transplantation*. 2011;91(8):847-852. doi: 10.1097/TP.0b013e3182122f82 [doi].

28. Colvin RB, Smith RN. Antibody-mediated organ-allograft rejection. *Nature Reviews Immunology*. 2005;5(10):807-817.

29. Sis B, Jhangri GS, Bunnag S, Allanach K, Kaplan B, Halloran PF. Endothelial gene expression in kidney transplants with alloantibody indicates Antibody-Mediated damage despite lack of C4d staining. *American Journal of Transplantation*. 2009;9(10):2312-2323.

30. Sis B, Jhangri G, Riopel J, et al. A new diagnostic algorithm for Antibody-Mediated microcirculation inflammation in kidney transplants. *American journal of transplantation*. 2012;12(5):1168-1179.

31. Weis M, Hartmann A, Olbrich HG, Hör G, Zeiher AM. Prognostic significance of coronary flow reserve on left ventricular ejection fraction in cardiac transplant recipients. *Transplantation*. 1998;65(1):103-108.

32. Amano H, Bickerstaff A, Orosz CG, Novick AC, Toma H, Fairchild RL. Absence of recipient CCR5 promotes early and increased allospecific antibody responses to cardiac allografts. *J Immunol*. 2005;174(10):6499-6508. doi: 174/10/6499 [pii].

33. Kasai A, Shintani N, Kato H, et al. Retardation of retinal vascular development in apelin-deficient mice. *Arterioscler Thromb Vasc Biol*. 2008;28(10):1717-1722. doi: 10.1161/ATVBAHA.108.163402 [doi].

34. Eyries M, Siegfried G, Ciumas M, et al. Hypoxia-induced apelin expression regulates endothelial cell proliferation and regenerative angiogenesis. *Circ Res*. 2008;103(4):432-440. doi: 10.1161/CIRCRESAHA.108.179333 [doi].

35. Hashimoto T, Kihara M, Ishida J, et al. Apelin stimulates myosin light chain phosphorylation in vascular smooth muscle cells. *Arterioscler Thromb Vasc Biol*. 2006;26(6):1267-1272. doi: 01.ATV.0000218841.39828.91 [pii].

36. Wang W, McKinnie SM, Patel VB, et al. Loss of apelin exacerbates myocardial infarction adverse remodeling and ischemia-reperfusion injury: Therapeutic potential of synthetic apelin analogues. *J Am Heart Assoc*. 2013;2(4):e000249. doi: 10.1161/JAHA.113.000249 [doi].

37. Haddad G, Zhabyeyev P, Farhan M, et al. Phosphoinositide 3-kinase beta mediates microvascular endothelial repair of thrombotic microangiopathy. *Blood*. 2014;124(13):2142-2149. doi: 10.1182/blood-2014-02-557975; 10.1182/blood-2014-02-557975.

38. Kang Y, Kim J, Anderson JP, et al. Apelin-APJ signaling is a critical regulator of endothelial MEF2 activation in cardiovascular development. *Circ Res*. 2013;113(1):22-31. doi: 10.1161/CIRCRESAHA.113.301324 [doi].

39. Kleinz MJ, Skepper JN, Davenport AP. Immunocytochemical localisation of the apelin receptor, APJ, to human cardiomyocytes, vascular smooth muscle and endothelial cells. *Regul Pept*. 2005;126(3):233-240.

40. Chen MM, Ashley EA, Deng DX, et al. Novel role for the potent endogenous inotrope apelin in human cardiac dysfunction. *Circulation*. 2003;108(12):1432-1439. doi: 10.1161/01.CIR.0000091235.94914.75 [doi].

41. Sedding DG. FoxO transcription factors in oxidative stress response and ageing–a new fork on the way to longevity? *Biol Chem*. 2008;389(3):279-283.

42. Zhang X, Tang N, Hadden TJ, Rishi AK. Akt, FoxO and regulation of apoptosis. *Biochimica et Biophysica Acta (BBA)-Molecular Cell Research*. 2011;1813(11):1978-1986.

43. Bouzin C, Brouet A, De Vriese J, Dewever J, Feron O. Effects of vascular endothelial growth factor on the lymphocyte-endothelium interactions: Identification of caveolin-1 and nitric oxide as control points of endothelial cell anergy. *J Immunol*. 2007;178(3):1505-1511. doi: 178/3/1505 [pii].

44. Ibiza S, Víctor VM, Boscá I, et al. Endothelial nitric oxide synthase regulates T cell receptor signaling at the immunological synapse. *Immunity*. 2006;24(6):753-765.

45. Staykova MA, Berven LA, Cowden WB, Willenborg DO, Crouch MF. Nitric oxide induces polarization of actin in encephalitogenic T cells and inhibits their in vitro trans-endothelial migration in a p70S6 kinase-independent manner. *FASEB J*. 2003;17(10):1337-1339. doi: 10.1096/fj.02-0577fje [doi].

46. Zhang H, Gong Y, Wang Z, et al. Apelin inhibits the proliferation and migration of rat PASMCs via the activation of PI3K/akt/mTOR signal and the inhibition of autophagy under hypoxia. *J Cell Mol Med*. 2014;18(3):542-553.

47. Lakkis FG, Arakelov A, Konieczny BT, Inoue Y. Immunologic 'ignorance'of vascularized organ transplants in the absence of secondary lymphoid tissue. *Nat Med*. 2000;6(6):686-688.

48. Weis M, Schlichting CL, Engleman EG, Cooke JP. Endothelial determinants of dendritic cell adhesion and migration: New implications for vascular diseases. *Arterioscler Thromb Vasc Biol*. 2002;22(11):1817-1823.

Chapter VII: General discussion and future directions

Discussion

The notion that cancer cells are highly proliferative and antiapoptotic has founded the base of the current chemotherapy regime. However, tumors respond differently to the antiproliferative and the apoptosis-inducing chemotherapy. Further, some cancer cell clones in the same patient are more resistant than others, and the host reaction to chemotherapy and to tumors is variable. These had limited the efficacy of chemotherapy [1,2]. In part, these observations result from the variable and unstable genomes of cancer cells associated with recurrent disease and metastasis.

Recently, targeting angiogenic tumor neovascularization has been proposed as an adjuvant approach to chemotherapy [3,4]. As a result, some angiogenesis inhibitors (AI) were approved for a variety of cancer types, such as renal cell carcinoma (RCC), recurrent glioblastoma, metastatic colorectal carcinoma, and pancreatic cancers [5,6]. AI targets the quiescent vascular endothelial cells (EC) that receive constant proangiogenic signals from the growing tumor. Since the vascular endothelial growth factor (VEGF) was identified as the dominant proangiogenic cue in development, and was found to be highly expressed in rapidly-growing cancers, drugs to block VEGF/VEGF-receptor (VEGF-R) binding (e.g. bevacizumab), or VEGFR activation (e.g.

sunitinib and others) have been the focus of development of clinical agents. However, several limitations to AI therapy to block tumor neovascularization have arisen [7,8]. The noticed initial response to AI therapy could not be sustained in many cases, i.e. tumors "escape" AI inhibition. The tumors' responses to VEGF/ VEGF-R blockade were variable, and predictive biomarkers were not reliable. Moreover, VEGF/VEGF-R blockade may drive the hypoxic tumor cells to migrate to the source of nourishment (blood vessels), resulting in accelerated micrometastasis. Hence, understanding the events in the endothelial cell underlying the inhibitor drug effects on angiogenesis will guide development of better drugs that target tumor neovascularization

In this study we investigated the main pathway involved in angiogenesis and highlighted novel targets to regulate pathological angiogenesis. We first focused on the rapalog mTOR inhibitors, whose efficacy was limited by escape of the tumor microvasculature from growth factor inhibition. We compared the efficacy of mTORC2 inactivation or dual mTORC1/2 inhibition, to selective mTORC1 inhibition in EC. Our findings demonstrated that chronic inhibition of mTORC1 with rapalogs paradoxically up-regulated endothelial mTORC2 and Akt activity. Conversely, dual inhibition of mTORC1/2 prevented hyper-stimulation of the PI3 kinase pathway, and decreased VEGF-mediated angiogenic sprouting. Interestingly, mTORC2 knock-down was sufficient to prevent PI3 kinase pathway hyper-activation in the endothelium, and inhibited angiogenesis both in vitro and in vivo more dramatically than mTORC1 inhibition. Moreover, disruption of mTORC2 had an additive effect to Akt loss in inhibiting angiogenesis due to an additive inhibitory effect on focal adhesion formation.

Temsirolimus, a rapamycin analogue, is widely used for the treatment of advanced renal cell carcinoma [9]. Rapamycin binds to an intracellular receptor (FKBP12), and inhibits the assembly

of mTOR/raptor complex. Previous work has shown that mTORC1 activity is sensitive to rapamycin, while mTORC2 is nearly resistant to the drug [10-13]. Although, rapalogs blunt VEGF production, studies showed that rapalogs are largely ineffective to directly control renal cell proliferation in vitro because of robust drug transporter protein expression [14,15]. Hence clinical efficacy of rapalogs chemotherapy in tumors relies mainly on regulating the tumor microvasculature. Our results showed that although short-term treatment of EC with rapamycin inhibited both mTORC1 and mTORC2 activity, chronic exposure to rapamycin, paradoxically resulted in induction of mTORC2-mediated Akt phosphorylation. In contrast, some earlier studies showed that longer exposure to rapamycin affected mTORC2 as well as mTORC1, but these studies relied on supra-therapeutic concentrations of rapamycin [16-18]. In fact, the observation that either high doses of rapamycin or starved cells rendered rapamycin-sensitive mTORC2 confirms that mTORC 2 under normal physiological conditions and with the clinically approved dose of rapamycin is resistant to rapamycin. Vascular escape from drug inhibition is thought to be conditioned by repeated exposure to low anti-angiogenic drug concentrations that occur at prolonged dosing intervals or due to altered metabolism of the drug. Hence, we used clinically-relevant concentrations of rapamycin [19,20] under optimum growth conditions to closely model the in vivo conditions during tumor neoangiogenesis. Under the same conditions, rapalog exposure induced enhanced signalling among proximal components of the PI3 kinase pathway in ECs.

Rapalog-induced mTORC1 inhibition is known to upregulate growth factor receptor activity, and to confer resistance to chemotherapy in many tumors [21-23]. This is attributed to mTORC1- and Akt-dependent negative feedback inhibition loop that regulates both receptor phosphorylation and expression in cancer cells. Consistently, our data indicate that hyper-stimulation of the PI3

kinase pathway after mTORC1 inactivation also operates in the human vascular endothelium. In the endothelium, PI3Kinase drives numerous events, including resistance to apoptotic stress and nitric oxide-mediated vasodilation, which are maladaptive in the context of tumor neovascularization [24], and may contribute to vascular escape from the anti-mTORC1 drugs. Moreover, our data indicate that suppression of the feedback inhibition requires intact signalling through mTORC2, since loss of rictor in ECs, or dual inhibition of mTORC1/2 are not associated with hyper-stimulation of the distal PI3 kinase pathway.

Apart from the well-established regulatory effect of mTORC2 on cell metabolism, we identified a novel mTORC2-dependent pathway to regulate ECs cytoskeletal remodelling in angiogenesis. In yeast, TORC2 regulates actin reorganization through a PKC homolog [25]. However, mTORC2 involvement in cytoskeleton dynamics in mammalian cells has been controversial. Although disruption of mTORC2 by RNA interference in cancer cell lines has a moderate effect on actin distribution, no effect of mTORC2 loss is noticed in mouse embryonic fibroblasts derived from either rictor or mLST8-knockout mice [26]. In human ECs, an earlier report indicated mTORC2 deficiency inhibited cell migration and Rac1 activity [27], and a subsequent study showed that mTORC2 activated Rac1 selectively through Akt [28]. In response to VEGF stimulation, we observe a reduction in angiogenic sprouting of primary human ECs, and a marked decrease in the length of sprout extension after inactivation of mTORC2. These effects were strikingly enhanced when mTORC2 inactivation was added to Akt knockdown, consistent with an independent contribution of mTORC2 signalling. Mechanistically, this correlates with impaired integrin-mediated adhesion to matrix, and formation of organized focal adhesion complexes that anchor actin stress fibers to enable cell contractility and movement.

In line with our findings that mTORC2 inhibition may hinder tumor escape, a recent study revealed mTORC2, but not mTORC1, is involved in a distinct pathway that encompass SDF-1α, CXCR4, and PI3K [29]. Tumor angiogenesis in mice was significantly reduced after mTORC2 inhibition only. An analysis of targets downstream of mTORC2 showed that 6-phosphofructo-2-kinase (PFKFB3), a key regulator of glycolytic flux and sprouting angiogenesis, was reduced when mTORC2 was targeted and when tumor angiogenesis was inhibited. This study supports our findings that mTORC2 is a key regulator of angiogenesis that is downstream of both receptor tyrosine kinases and G protein-coupled receptors[29].

We carried our investigations further and identified FAK as a novel downstream effector coupled to mTORC2, independent of Akt/mTORC1. Cellular adhesion to extra cellular matrix is mediated by transmembrane receptors called integrins [30]. Integrins have high affinity to extracellular matrix proteins. Once bond to ECM, integrins signal through their intracellular domain to FAK, which promotes actin polymerization and cellular migration [31,32]. Studies using FAK knock out mice provided direct evidence supporting the role of FAK in angiogenesis as FAK-deficiency was embryonically lethal due to severe cardiovascular defects [33]. Recent studies showed that FAK plays a significant role in tumor progression and that FAK inhibition attenuates tumor growth by reducing tumor neovascularization [34,35]. Consistently, our results confirms the role of FAK in VEGF-mediated angiogenesis and links the migration, adhesion and angiogenesis defects in mTORC 2 deficient HUVEC to FAK reduced activity independent of Akt. However, the mechanism by which mTORC 2 regulates FAK is still to be determined.

FGD5

In addition to mTORC2, Facio-Genital Dysplasia-5 (FGD5) represents a potential candidate to regulate unique EC functions [36]. FGD5 null mice did not survive beyond embryonic day12 [37]. Histological examination of E12 normal mice embryos showed a robust expression of FGD5 in aorta-gonad mesonephros, from which the aorta originates [37]. Taken together, FGD5 may have a pivotal role in vascular development and angiogenesis. Thus, in the current study we sought to investigate the role of FGD5 in VEGFA-guided angiogenesis. Indeed, genetic silencing of FGD5 in primary human EC reduced VEGFA-dependent angiogenic sprouting and lamellipodia formation. High-resolution confocal images showed a defect in both the number and the length of filopodia, which was confirmed by a decrease in the expression of specific tip cell markers. These defects were noticed as early as 10 minutes after VEGFA stimulation. At the molecular level, FGD5 was associated with VEGFR2, and localized to both the EC membrane ruffles and endosomes. Loss of function experiments, showed a decrease in VEGFR2 signaling to mTORC2, change in VEGFR2 trafficking, and increase in VEGFR2 lysosomal degradation in FGD5-deficinet EC. Our data suggest VEGFR2 shuttling to the lysosomes after FGD5 loss could be attributed to decrease in VEGFR2/p85 coupling.

We were the first to demonstrate the significance of FGD5 in tumor angiogenesis and VEGFA-dependent angiogenesis using a 3D in vitro model that relies on EC invasion of a physiological matrix (fibrin). Maryam et al investigated the effect of FGD5-loss on angiogenesis in a highly growth factors enriched media [38], whereas Kourgane et al used a 2D matrigel based angiogenesis assay [39], which is a less physiological culture system [40]. In 2D cultures, we showed that EC failed to upregulate specific tip cell genes in response to VEGFA, which implied incapability of tip cell

differentiation, an important component of angiogenesis. In line with literature, our data confirms that EC response to growth factors changes with the change in the environment [41,42].

Although FGD protein family consists of multiple members: FRG, FGD-1 [43], -2 [44], -3 [45] , -4 (Frabin) [46] and -5, studies have shown that some members share the same functions. For example, FGD2 was localized with EEA-1 positive early endosomes and regulated Rho GTPases dependent vesicular trafficking [47]. FGD2 has also been associated with membrane ruffles of Hela cells, which is controlled by Rac1 and cortactin [47]. FGD1 induced filopodia-like finger protrusions and FGD3 induced lamellipodia-like short microspikes in human tumor cell lines [48]. Moreover, when Frabin was over expressed in Swiss 3T3 cells, it similarly induced changes in cellular structure characterized by spikes-like protrusions [46]. These data are consistent with our findings that FGD5 regulates vesicular trafficking, filopodia and lamellipodia formation in human EC.

Despite the finding that FGD5- deficiency targeted VEGFR2 to lysosomal degradation, we did not notice any change in VEGFR2 plasma membrane expression after VEGF stimulation. The FGD5-regulated VEGFR2 trafficking could contribute to the late angiogenic defects after FGD5 loss. However, it could not explain the early protrusion defect that occurred within 10 minutes of VEGFA stimulation. Thus, we attribute the reduction in protrusions to a defect in VEGFR2 signaling to Akt and cortactin. In agreement with our conclusion, studies have shown that Akt signaling regulates lamellipodia localization of cortactin complexes in endothelial cells [49]. Further, the Akt downstream effector Akt-phosphorylation enhancer (APE), which is an actin binding protein, was also colocalized with cortactin at the EC leading edge [50].

Our findings that FGD5 regulated tip cell markers expression coincides with a previous report that showed up regulation of the Notch signaling pathway, including Notch1, Notch4, DLL4 after transgenic overexpression of FGD5 [36]. One explanation of the noticed transcriptional changes is the VEGFR2 downstream effector PI3Kβ isoform, a member of the PI3K IA class, which regulates the expression of the angiogenic tip cell markers apelin and Dll4, and in turn controls EC migration and angiogenesis [51]. Another explanation is the FOXO family of transcription factors, which are targets for phosphorylation by Akt. FOXO1 genetic silencing alters mRNA expression of angiogenic patterning genes that identify tip cell phenotypes, and significantly decreases most of the tip cell markers (ESM1, ANG2, PDGFB, Apelin, NRP1) in HUVECs [52]. Finally, the genetic up regulation of the tip cell genes could be induced after FGD5-mediated Cdc42 activation via the p38 mitogen-activated protein kinase-signaling pathway that potentiates the transcriptional activity [53].

For a long time, endocytosis has been considered primarily as a mean of extinguishing receptor signaling. Ligand binding to its particular receptor was thought to trigger internalization of the receptor-ligand complex into endosomes, with subsequent degradation in lysosomes. However, it is well established now that signalling continues in different endosomal compartments and that trafficking of endosomes containing activated receptors (RTKs and GPCRs) regulates receptor-signaling [54-56]. Thus the relocation of VEGFR2 to the degradation endosomes after FGD5 loss can affect VEGFR2/PI3K coupling, which may have a higher affinity to one endosome compared to another. On the other hand, accumulating evidence from literature supports that VEGFR2 trafficking is affected by the endosomal cargo [57,58,59]. Thus, a defect in VEGFR2/PI3K coupling might lead to the shift of VEGFR2 to degradation. Whether FGD5 potentiates

VEGFR2/PI3K coupling and in turn protects VEGFR2 from degradation, or it regulates trafficking and localizes VEGFR2 to the recycling endosomes, which could be the designated compartment for PI3K binding, is still to be determined.

Recently, pathways that regulate endocytosis and trafficking have emerged as significant contributors to tumorigenesis and angiogenesis [60,61]. FGD5 was previously localized in the early endosomes [39] and our finding that FGD5 is associated with VEGFR2 can explain its role in VEGFR2 trafficking. Of note, VEGFR2 exists in a wide array of complexes with other transmembrane proteins such as VEGFR3, Nrp1, VE-cadherin, Ephrin-B2 and thrombospondin receptor CD47 [62,63], which can affect its signalling and determine its fate after endocytosis. Initiation of VEGFR2 endocytosis requires the presence of Ephrin-B2 [64]. Further, Nrp1 targets endocytosed VEGFR2 to the Rab5/Rab11 recycling pathway then back to the plasma membrane. In contrast, when VE-cadherin is absent or not engaged at EC junctions, VEGFR-2 is internalized more rapidly and remains in the cytosol for a longer time [58]. In a recent study, pharmacological induction of VEGFR2 endocytosis promoted VEGF-mediated angiogenesis in vivo, and improved blood flow in models of hind limb ischemia, suggesting a role of VEGFR2 endocytosis in vascular repair after ischemic injury [65].

SDF1

Cancer angiogenesis is different from the developmental vasculogenesis in the variety of pro-angiogenic cues that initiate the process [66,67]. Further, in addition to cancer cells, stromal cells of the host were found to produce a significant amount of angiogenic cues [68-70]. Analysis of the angiogenic factors secreted by tumors in animal models and data from clinical studies identified a plethora of upregulated molecules other than VEGF. Of these, ANG1, FGF, PDGF, and other

ligands for endothelial receptor tyrosine kinases (RTK) [71-73]. Most important, stromal-derived factor (SDF1) significantly contributed to drive tumor neovascularization [74-78]. The initial response to VEGF-inhibition wanes as persistent tumour ischemia recruits new vessels via alternate pro-angiogenic cues including agonists for RTKs (e.g. ANG1/TIE2 [79,80]), and GPCRs (e.g. SDF1 [81-84]). Therefore, identifying targets that can control multiple angiogenesis pathways can represent a potential approach to hinder tumor escape.

The PI3Kinaseβ isoform uniquely signals downstream of both RTKs and GPCRs [51,85]. Additionally, PI3Kinaseβ is uniquely regulated by the RhoGTPase Cdc42, whereas the other isoforms are regulated by Ras [86]. The guanine exchange factor (GEF) that generates active Cdc42-GTP in the EC is unknown, but FGD5, a RhoGEF with EC-restricted expression in the adult [87-89] represents a good candidate. Hence, we sought to study the role of FGD5 in SDF1-mediated PI3Kinaseβ activity. In this study, we observed that PI3K signalling was blunted after FGD5 knockdown in response to VEGF, and more profoundly to SDF1; SDF1-stimulated PI3K activity was dependent on Cdc42 activation; and FGD5 loss markedly reduced angiogenic sprouting to VEGF, SDF1, and a mix of pro-angiogenic agonists. This is consistent with regulation of EC PI3Kinaseβ via FDG5 Cdc42 GEF activity, but FGD5 loss may have additional PI3Kinaseβ-independent effects.

Previously, we showed that EC PI3Kinaseβ played a critical role in angiogenesis [90]. We reported that PI3Kinaseβ loss or treatment with an inhibitor of PI3Kinaseβ in human primary ECs blocked both VEGF- and SDF1-driven angiogenic sprouting and sprout extension in 3D fibrin matrices [90]. Capillary formation and repair in vivo among mouse EC deficient in PI3Kinaseβ were markedly impaired [90,91], and in EC, PI3Kinaseβ critically mediated signaling to Akt after

GPCR stimulation [90]. Interestingly, a recent study demonstrated that SDF1 was indispensable for alveologenesis and vascular regeneration after pneumonectomy in mice [92,93] . SDF1 was found to bind to CXCR4 on the pulmonary endothelium, and primed the pulmonary vasculature for angiogenesis and subsequentially alveologenesis. Further, this effect was lost in endothelial-restricted CXCR4 deficient mice [92]. Taken together, FGD5 regulation of PI3Kβ down stream of SDF1/CXCR4 can potentially represent a novel AI target, or empower vascular repair.

Apelin and its receptor APJ exist in a variety of tissues, but play a significant role in the heart, lung and tumors. Accumulating evidence indicates that the expression of apelin and APJ is upregulated by hypoxia through the hypoxia-inducible factor-1 alpha (HIF-1α) signaling pathway [94]. Because hypoxia has long been considered as the key derivative of angiogenesis, apelin is being heavily investigated in conditions associated with ischemia and pathological angiogenesis as vascular injury and repair. Investigations highlighted an essential role of apelin in promoting the physiological and pathological angiogenesis [95-97]. Selectively targeting apelin or APJ in EC significantly reduced hypoxia-induced proliferation in vitro and hypoxia-induced regenerative angiogenesis [98-100]. In tumors, the over-expression of apelin accelerated angiogenesis and facilitated the formation of new vessels for tumor growth in vivo [96,101,102].

In this work we investigated the role of apelin in vascular repair. Apelin deficiency led to accelerated vascular injury in models of chronic allograft vasculopathy. The injury was characterized by intimal thickness and obliteration of vascular lumen of both major epicardial coronaries and the small intramyocardial coronary arteries. Consistently, ECG tracing showed concurrent changes in the cardiac electrical activity. In a very interesting experiment we studied the host immune response to the apelin deficient graft. Surprisingly, the rate of Tcell proliferation in the peripheral blood of the recipients was doubled after 6 weeks of hosting the

apelin deficient grafts. These findings indicate that apelin could have a protective role in vasculature that may involve keeping the immune system under surveillance and protecting the EC in the front line from severe immunological reactions. However, the underlying mechanism powering the apelin's vascular protective role is still to be determined.

Apelin may have a vascular protective role by inducing phosphorylation of endothelial nitric oxide synthase (eNOS) and nitric oxide (NO) release from endothelial cells thereby stimulating angiogenesis, while loss of apelin may sensitize endothelial cells to apoptosis [103]. Studies demonstrated that ischemia reperfusion injury is initiated by endothelial dysfunction due to decreased endothelial NO release and increased oxidative stress. NO deficiency-induced endothelial dysfunction was previously reported in many organ vascular beds such as the kidney [104], intestine [105], heart [106], and hind limb [107]. Further, this defect is now known to aggravate leukocyte-endothelial interactions [108]. In line with literature, our results showed that apelin is a potent eNOS activator by a mechanism that required FGD5 and PI3Kβ.

Another mechanism that may explain apelin deficiency-induced CAV is induction of vascular mural cells proliferation and migration. Accumulation of fibroblasts and vascular smooth muscle cells (VSMC) at the site of injury are hallmarks of CAV. Studies showed that knockdown of apelin worsens the hypoxia-induced pulmonary hypertension (PH) and resulted in muscularization of the alveolar wall arteries through a decrease in the AMPK/KLF2/eNOS signaling pathway [109]. The apelin/APJ signaling is a critical mediator of VSMC proliferation, which is associated with pulmonary vascular remodeling and PH [110]. Moreover, it has been shown that exogenous apelin inhibits the autophagy and reduces the proliferation of pulmonary artery SMC through the PI3K/Akt/mTOR signaling pathway [111].

The evidence that apelin protects against fibrosis emerged from studying models of renal fibrosis. Mice subjected to unilateral ureteral obstruction (UUO) surgery showed elevated levels of apelin, p-Akt and eNOS. Furthermore, losartan, an angiotensin II receptor antagonist that may reduce apelin degradation, alleviates UUO-induced renal fibrosis via the apelin/APJ/Akt/eNOS pathway [112].

Summary of results

- Chronic mTORC1 inhibition, but not mTORC 2, activates PI3kinase signalling to Akt in primary human ECs. mTORC2 regulates EC matrix adhesion, motility, and angiogenesis both *in vitro* and *in vivo* independent of downstream Akt-regulated events. These data indicate that mTORC2 in the endothelium is an attractive target to inhibit neoangiogenesis as adjuvant cancer therapy.

- FGD5 is a key regulator of early lamellipodia-, filopodia- and tip cell-formation in VEGF-guided sprouting angiogenesis. FGD5 regulates VEGFR2 trafficking to lysosomes (Figure I), VEGFR2 signalling to cortactin Y421 and PI3K coupling to VEGFR2. These data indicate that FGD5 is an attractive target to regulate pathological angiogenesis.

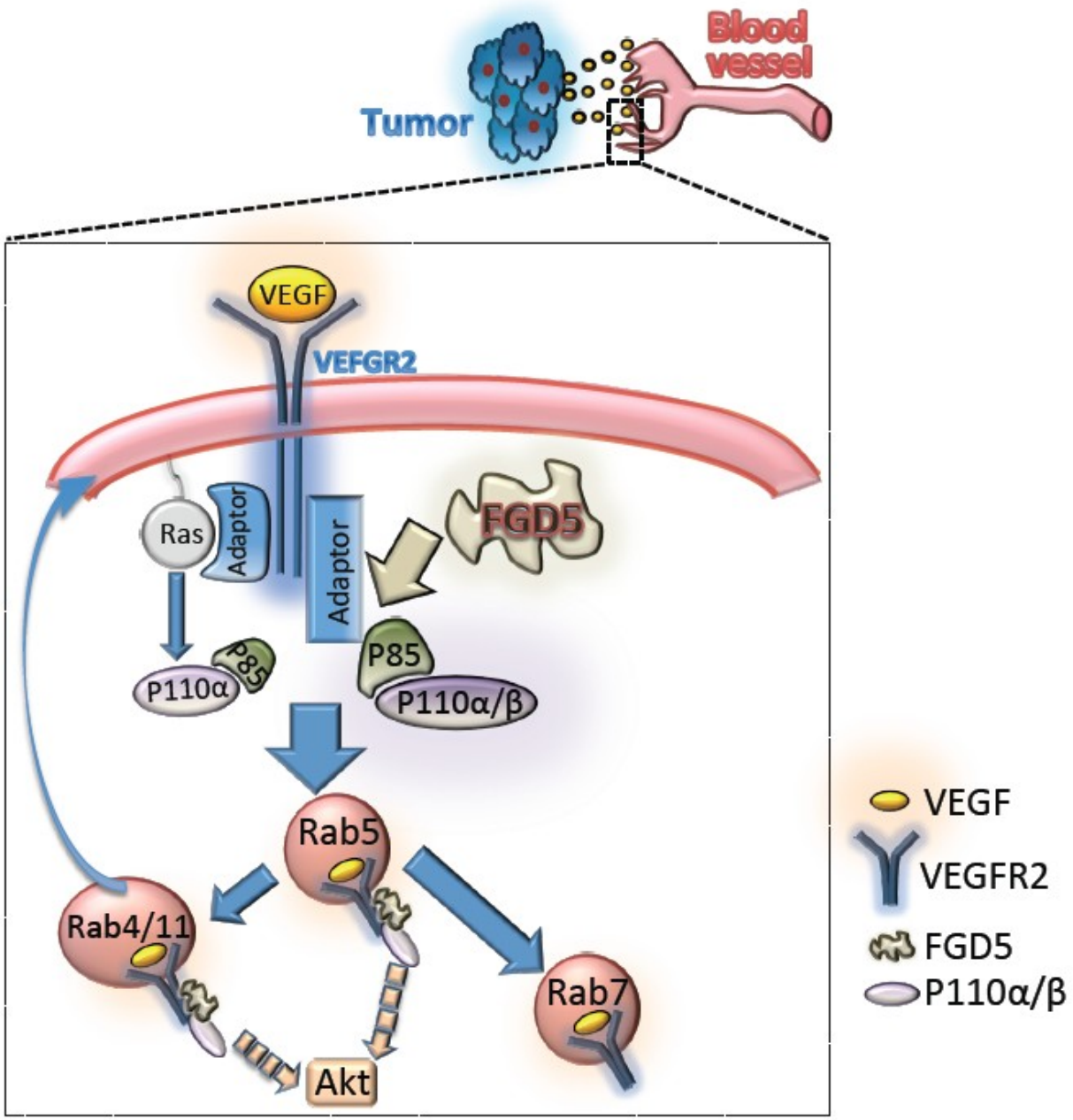

Figure I. FGD5 regulates VEGFR2 trafficking.

- FGD5 regulates SDF1-driven angiogenesis and SDF1 signalling to PI3Kinaseβ (Figure II). FGD5 regulates specific GPCRs signalling by a distinct mechanism different from endosomal trafficking and receptor upregulation. FGD5 may regulate PI3Kinaseβ via

Cdc42. These data indicate that FGD5 can serve as a convergence node on different angiogenic pathways; and can represent a potential candidate to prevent tumor escape.

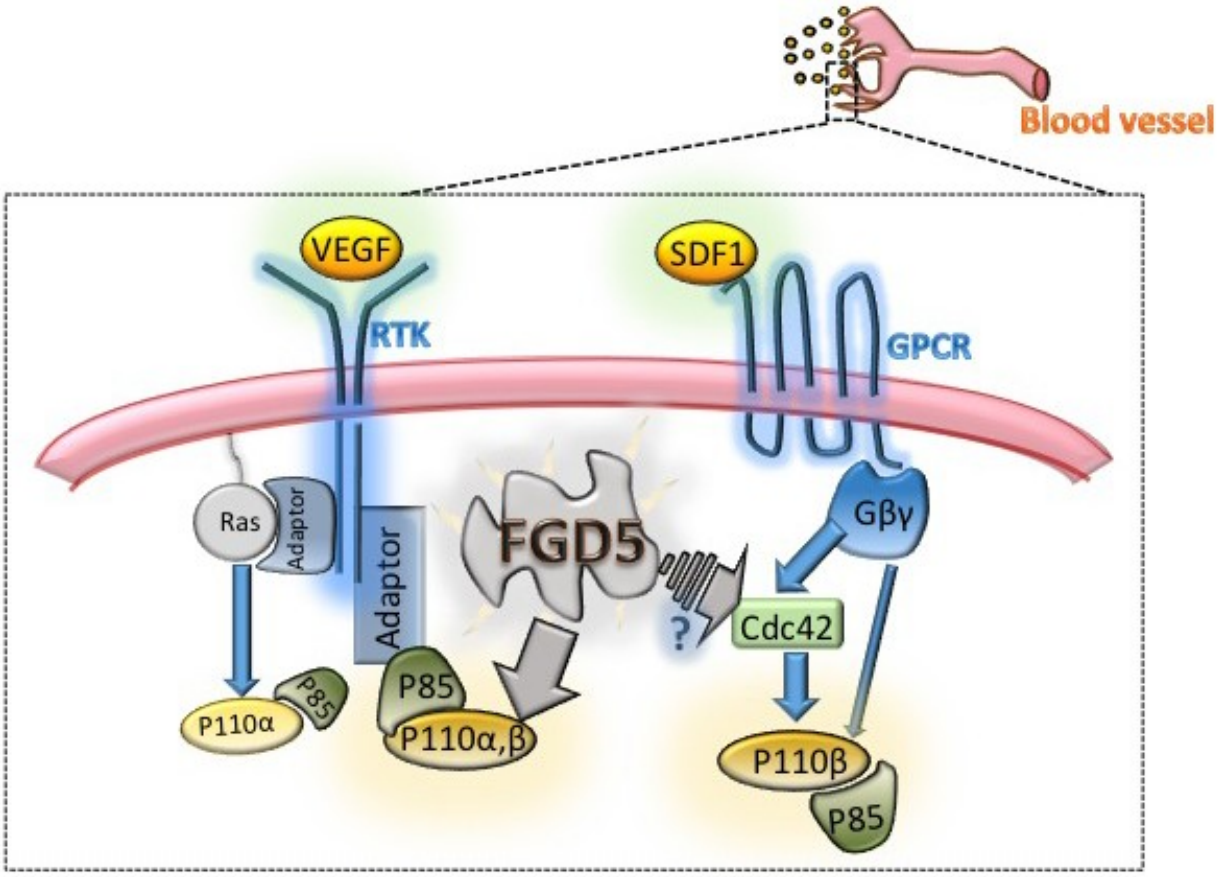

Figure II. FGD5 regulates SDF-mediated PI3Kinase signalling.

- Apelin loss aggravates chronic allograft vasculopathy (CAV). Apelin induces eNOS activity by a mechanism that requires FGD5 and PI3Kinaseβ. Apelin deficient cardiac allografts triggers the host immune response. These data indicate that apelin may have a protective a role against CAV development.

Future directions

1) **Determining the key functional domain in FGD5.** Althought the structure of FGD5 is well understood, little is known about the functions of the different domains in FGD5 peptide. We seek to study the siginficance of each domain separately.

2) **Determining the significance of FGD5 in pathological angiogenesis in vivo.** FGD5 homozygous deletion is lethal in mice but FGD5 heterozygous deficient mice are available. However, FGD5 deficiency has not been investigated in the context of tumor angiogenesis or in allograft vasculopathy. We seek to chracterize the vascular phenotype of FGD5 deficincy and its effect on tumor neovascularization, and vascular repair after EC injury.

3) **Determining if EC tip cell markers are upregulated in CAV.**
   Both inflamamtory and proangiogenic stimuli have been shown to inititae EC tip cell differentiation in vitro. Therfore, we seek to determine if PI3Kβ–dependent EC tip cell differentation contributes to vascular repair.

4) **To determine if exogenous apelin synthetic peptides can protect against CAV development.** Apelin peptide is identified as an EC product that mediates myocardial repair in ischemia reperfusion injury by direct effects on cardiomyocytes and angiogenesis in the heart. Therfore, we seek to investigate if synthetic apelin administration will delay the developmnet of CAV in mice.

References

1. Scheel C, Weinberg RA. Cancer stem cells and epithelial–mesenchymal transition: Concepts and molecular links. 2012;22(5):396-403.

2. Bindea G, Mlecnik B, Tosolini M, et al. Spatiotemporal dynamics of intratumoral immune cells reveal the immune landscape in human cancer. *Immunity*. 2013;39(4):782-795.

3. Gerber HP, Ferrara N. Pharmacology and pharmacodynamics of bevacizumab as monotherapy or in combination with cytotoxic therapy in preclinical studies. *Cancer Res*. 2005;65(3):671-680. doi: 65/3/671 [pii].

4. Macedo LT, da Costa Lima AB, Sasse AD. Addition of bevacizumab to first-line chemotherapy in advanced colorectal cancer: A systematic review and meta-analysis, with emphasis on chemotherapy subgroups. *BMC Cancer*. 2012;12:89-2407-12-89. doi: 10.1186/1471-2407-12-89 [doi].

5. Strickler JH, Hurwitz HI. Bevacizumab-based therapies in the first-line treatment of metastatic colorectal cancer. *Oncologist*. 2012;17(4):513-524. doi: 10.1634/theoncologist.2012-0003 [doi].

6. Patel M, Vogelbaum MA, Barnett GH, Jalali R, Ahluwalia MS. Molecular targeted therapy in recurrent glioblastoma: Current challenges and future directions. *Expert Opin Investig Drugs*. 2012;21(9):1247-1266.

7. De Bock K, Mazzone M, Carmeliet P. Antiangiogenic therapy, hypoxia, and metastasis: Risky liaisons, or not? *Nature reviews Clinical oncology*. 2011;8(7):393-404.

8. Bagri A, Berry L, Gunter B, et al. Effects of anti-VEGF treatment duration on tumor growth, tumor regrowth, and treatment efficacy. *Clin Cancer Res*. 2010;16(15):3887-3900. doi: 10.1158/1078-0432.CCR-09-3100 [doi].

9. Hudes G, Carducci M, Tomczak P, et al. Temsirolimus, interferon alfa, or both for advanced renal-cell carcinoma. *N Engl J Med*. 2007;356(22):2271-2281.

10. Foster DA, Toschi A. Targeting mTOR with rapamycin: One dose does not fit all. *Cell Cycle*. 2009;8(7):1026-1029.

11. Ballou LM, Lin RZ. Rapamycin and mTOR kinase inhibitors. *Journal of chemical biology*. 2008;1(1-4):27-36.

12. Feldman ME, Apsel B, Uotila A, et al. Active-site inhibitors of mTOR target rapamycin-resistant outputs of mTORC1 and mTORC2. *PLoS biology*. 2009;7(2):e1000038.

13. Sarbassov DD, Ali SM, Kim D, et al. Rictor, a novel binding partner of mTOR, defines a rapamycin-insensitive and raptor-independent pathway that regulates the cytoskeleton. *Current biology*. 2004;14(14):1296-1302.

14. Guba M, von Breitenbuch P, Steinbauer M, et al. Rapamycin inhibits primary and metastatic tumor growth by antiangiogenesis: Involvement of vascular endothelial growth factor. *Nat Med*. 2002;8(2):128-135.

15. Del Bufalo D, Ciuffreda L, Trisciuoglio D, et al. Antiangiogenic potential of the mammalian target of rapamycin inhibitor temsirolimus. *Cancer Res*. 2006;66(11):5549-5554.

16. Barilli A, Visigalli R, Sala R, et al. In human endothelial cells rapamycin causes mTORC2 inhibition and impairs cell viability and function. *Cardiovasc Res*. 2008;78(3):563-571.

17. Sarbassov DD, Ali SM, Sengupta S, et al. Prolonged rapamycin treatment inhibits mTORC2 assembly and akt/PKB. *Mol Cell*. 2006;22(2):159-168.

18. Phung TL, Ziv K, Dabydeen D, et al. Pathological angiogenesis is induced by sustained akt signaling and inhibited by rapamycin. *Cancer cell*. 2006;10(2):159-170.

19. Atkins MB, Hidalgo M, Stadler WM, et al. Randomized phase II study of multiple dose levels of CCI-779, a novel mammalian target of rapamycin kinase inhibitor, in patients with advanced refractory renal cell carcinoma. *Journal of Clinical Oncology*. 2004;22(5):909-918.

20. Kuhn JG, Chang SM, Wen PY, et al. Pharmacokinetic and tumor distribution characteristics of temsirolimus in patients with recurrent malignant glioma. *Clinical Cancer Research*. 2007;13(24):7401-7406.

21. O'Reilly KE, Rojo F, She Q, et al. mTOR inhibition induces upstream receptor tyrosine kinase signaling and activates akt. *Cancer Res*. 2006;66(3):1500-1508.

22. Chandarlapaty S, Sawai A, Scaltriti M, et al. AKT inhibition relieves feedback suppression of receptor tyrosine kinase expression and activity. *Cancer cell*. 2011;19(1):58-71.

23. Muranen T, Selfors LM, Worster DT, et al. Inhibition of PI3K/mTOR leads to adaptive resistance in matrix-attached cancer cells. *Cancer cell*. 2012;21(2):227-239.

24. Zhang Q, Nakhaei-Nejad M, Haddad G, Wang X, Loutzenhiser R, Murray AG. Glomerular endothelial PI3 kinase-α couples to VEGFR2, but is not required for

eNOS activation. *American Journal of Physiology-Renal Physiology*. 2011;301(6):F1242-F1250.

25. Jacinto E, Loewith R, Schmidt A, et al. Mammalian TOR complex 2 controls the actin cytoskeleton and is rapamycin insensitive. *Nat Cell Biol*. 2004;6(11):1122-1128.

26. Guertin D, Stevens D, Thoreen C, Burds A, Kalaany N. J. 1 moffat, M. brown, KJ fitzgerald, and DM sabatini. 2006. ablation in mice of 2 the mTORC components raptor, rictor, or mLST8 reveals that mTORC2 is required 3 for signaling to akt-FOXO and PKCalpha, but not S6K1. *Dev.Cell*. ;11:859-871.

27. Dada S, Demartines N, Dormond O. mTORC2 regulates PGE< sub> 2-mediated endothelial cell survival and migration. *Biochem Biophys Res Commun*. 2008;372(4):875-879.

28. Kim E, Yun S, Ha J, et al. Selective activation of Akt1 by mammalian target of rapamycin complex 2 regulates cancer cell migration, invasion, and metastasis. *Oncogene*. 2011;30(26):2954-2963.

29. Ziegler ME, Hatch MM, Hughes CC. mTORC2 mediates SDF-1α/CXCL12-induced angiogenesis. *Cancer Res*. 2015;75(15 Supplement):5228-5228.

30. Ramsay AG, Marshall JF, Hart IR. Integrin trafficking and its role in cancer metastasis. *Cancer Metastasis Rev*. 2007;26(3-4):567-578.

31. Zhao X, Guan J. Focal adhesion kinase and its signaling pathways in cell migration and angiogenesis. *Adv Drug Deliv Rev*. 2011;63(8):610-615.

32. Schaller MD, Otey CA, Hildebrand JD, Parsons JT. Focal adhesion kinase and paxillin bind to peptides mimicking beta integrin cytoplasmic domains. *J Cell Biol*. 1995;130(5):1181-1187.

33. Furuta Y, Kanazawa S, Takeda N, et al. Reduced cell motility and enhanced focal adhesion contact formation in cells from FAK-deficient mice. *Nature*. 1995;377(6549):539-544.

34. Liu S, Pu L, Huang Y, et al. Study on attenuating angiogenesis of pulmonary malignant tumor by targeting FAK both in vivo and in vitro. *CHEST Journal*. 2016;149(4_S):A311-A311.

35. Moen I, Gebre M, Alonso-Camino V, Chen D, Epstein D, McDonald DM. Anti-metastatic action of FAK inhibitor OXA-11 in combination with VEGFR-2 signaling blockade in pancreatic neuroendocrine tumors. *Clin Exp Metastasis*. 2015;32(8):799-817.

36. Cheng C, Haasdijk R, Tempel D, et al. Endothelial cell-specific FGD5 involvement in vascular pruning defines neovessel fate in mice. *Circulation*. 2012;125(25):3142-3158. doi: 10.1161/CIRCULATIONAHA.111.064030; 10.1161/CIRCULATIONAHA.111.064030.

37. Gazit R, Mandal PK, Ebina W, et al. Fgd5 identifies hematopoietic stem cells in the murine bone marrow. *J Exp Med*. 2014;211(7):1315-1331. doi: 10.1084/jem.20130428; 10.1084/jem.20130428.

38. Nakhaei-Nejad M, Haddad G, Zhang QX, Murray AG. Facio-genital dysplasia-5 regulates matrix adhesion and survival of human endothelial cells. *Arterioscler Thromb Vasc Biol*. 2012;32(11):2694-2701. doi: 10.1161/ATVBAHA.112.300074; 10.1161/ATVBAHA.112.300074.

39. Kurogane Y, Miyata M, Kubo Y, et al. FGD5 mediates proangiogenic action of vascular endothelial growth factor in human vascular endothelial cells. *Arterioscler Thromb Vasc Biol*. 2012;32(4):988-996. doi: 10.1161/ATVBAHA.111.244004; 10.1161/ATVBAHA.111.244004.

40. Staton CA, Reed MW, Brown NJ. A critical analysis of current in vitro and in vivo angiogenesis assays. *Int J Exp Pathol*. 2009;90(3):195-221. doi: 10.1111/j.1365-2613.2008.00633.x; 10.1111/j.1365-2613.2008.00633.x.

41. Fischbach C, Kong HJ, Hsiong SX, Evangelista MB, Yuen W, Mooney DJ. Cancer cell angiogenic capability is regulated by 3D culture and integrin engagement. *Proc Natl Acad Sci U S A*. 2009;106(2):399-404. doi: 10.1073/pnas.0808932106 [doi].

42. Baker BM, Chen CS. Deconstructing the third dimension: How 3D culture microenvironments alter cellular cues. *J Cell Sci*. 2012;125(Pt 13):3015-3024. doi: 10.1242/jcs.079509 [doi].

43. Olson MF, Pasteris N, Gorski JL, Hall A. Faciogenital dysplasia protein (FGD1) and vav, two related proteins required for normal embryonic development, are upstream regulators of rho GTPases. *Current Biology*. 1996;6(12):1628-1633.

44. Pasteris N, Gorski JL. Isolation, characterization, and mapping of the mouse and human< i> Fgd2 genes, faciogenital dysplasia (FGD1; aarskog syndrome) gene homologues. *Genomics*. 1999;60(1):57-66.

45. Pasteris N, Nagata K, Hall A, Gorski JL. Isolation, characterization, and mapping of the mouse< i> Fgd3 gene, a new faciogenital dysplasia (FGD1; aarskog syndrome) gene homologue. *Gene*. 2000;242(1):237-247.

46. Obaishi H, Nakanishi H, Mandai K, et al. Frabin, a novel FGD1-related actin filament-binding protein capable of changing cell shape and activating c-jun N-terminal kinase. *J Biol Chem*. 1998;273(30):18697-18700.

47. Huber C, Martensson A, Bokoch GM, Nemazee D, Gavin AL. FGD2, a CDC42-specific exchange factor expressed by antigen-presenting cells, localizes to early endosomes and active membrane ruffles. *J Biol Chem*. 2008;283(49):34002-34012. doi: 10.1074/jbc.M803957200; 10.1074/jbc.M803957200.

48. Hayakawa M, Matsushima M, Hagiwara H, et al. Novel insights into FGD3, a putative GEF for Cdc42, that undergoes SCFFWD1/β-TrCP-mediated proteasomal degradation analogous to that of its homologue FGD1 but regulates cell morphology and motility differently from FGD1. *Genes to Cells*. 2008;13(4):329-342.

49. Lee J, Ozaki H, Zhan X, Wang E, Hla T, Lee M. Sphingosine-1-phosphate signaling regulates lamellipodia localization of cortactin complexes in endothelial cells. *Histochem Cell Biol*. 2006;126(3):297-304.

50. Enomoto A, Murakami H, Asai N, et al. Akt/PKB regulates actin organization and cell motility via girdin/APE. *Developmental cell*. 2005;9(3):389-402.

51. Haddad G, Zhabyeyev P, Farhan M, et al. Phosphoinositide 3-kinase beta mediates microvascular endothelial repair of thrombotic microangiopathy. *Blood*. 2014;124(13):2142-2149. doi: 10.1182/blood-2014-02-557975; 10.1182/blood-2014-02-557975.

52. Dharaneeswaran H, Abid MR, Yuan L, et al. FOXO1-mediated activation of akt plays a critical role in vascular homeostasis. *Circ Res*. 2014;115(2):238-251. doi: 10.1161/CIRCRESAHA.115.303227; 10.1161/CIRCRESAHA.115.303227.

53. Kang JS, Bae GU, Yi MJ, et al. A cdo-bnip-2-Cdc42 signaling pathway regulates p38alpha/beta MAPK activity and myogenic differentiation. *J Cell Biol*. 2008;182(3):497-507. doi: 10.1083/jcb.200801119; 10.1083/jcb.200801119.

54. Dobrowolski R, De Robertis EM. Endocytic control of growth factor signalling: Multivesicular bodies as signalling organelles. *Nature reviews Molecular cell biology*. 2012;13(1):53-60.

55. Platta HW, Stenmark H. Endocytosis and signaling. *Curr Opin Cell Biol*. 2011;23(4):393-403.

56. Sorkin A, von Zastrow M. Endocytosis and signalling: Intertwining molecular networks. *Nature reviews Molecular cell biology*. 2009;10(9):609-622.

57. Ballmer-Hofer K, Andersson AE, Ratcliffe LE, Berger P. Neuropilin-1 promotes VEGFR-2 trafficking through Rab11 vesicles thereby specifying signal output. *Blood*. 2011;118(3):816-826. doi: 10.1182/blood-2011-01-328773; 10.1182/blood-2011-01-328773.

58. Lampugnani MG, Orsenigo F, Gagliani MC, Tacchetti C, Dejana E. Vascular endothelial cadherin controls VEGFR-2 internalization and signaling from intracellular compartments. *J Cell Biol*. 2006;174(4):593-604. doi: 10.1083/jcb.200602080.

59. Simons M. An inside view: VEGF receptor trafficking and signaling. *Physiology (Bethesda)*. 2012;27(4):213-222. doi: 10.1152/physiol.00016.2012 [doi].

60. Lanahan AA, Hermans K, Claes F, et al. VEGF receptor 2 endocytic trafficking regulates arterial morphogenesis. *Developmental cell*. 2010;18(5):713-724.

61. Parachoniak CA, Park M. Dynamics of receptor trafficking in tumorigenicity. *Trends Cell Biol*. 2012;22(5):231-240.

62. Sina K, Sonia T, Xiujuan L, Laura G, Lena C. Signal transduction by vascular endothelial growth factor receptors. *Biochem J*. 2011;437(2):169-183.

63. Kaur S, Martin-Manso G, Pendrak ML, Garfield SH, Isenberg JS, Roberts DD. Thrombospondin-1 inhibits VEGF receptor-2 signaling by disrupting its association with CD47. *J Biol Chem*. 2010;285(50):38923-38932. doi: 10.1074/jbc.M110.172304; 10.1074/jbc.M110.172304.

64. Sawamiphak S, Seidel S, Essmann CL, et al. Ephrin-B2 regulates VEGFR2 function in developmental and tumour angiogenesis. *Nature*. 2010;465(7297):487-491.

65. Zhao J, Niu H, Li A, Nie L. Acetylbritannilactone modulates vascular endothelial growth factor signaling and regulates angiogenesis in endothelial cells. *PloS one*. 2016;11(2):e0148968.

66. Lee RS, Yamada K, Houser SL, et al. Indirect recognition of allopeptides promotes the development of cardiac allograft vasculopathy. *Proc Natl Acad Sci U S A*. 2001;98(6):3276-3281. doi: 10.1073/pnas.051584498 [doi].

67. Russell PS, Chase CM, Madsen JC, et al. Coronary artery disease from isolated non-H2-determined incompatibilities in transplanted mouse hearts. *Transplantation*. 2011;91(8):847-852. doi: 10.1097/TP.0b013e3182122f82 [doi].

68. Colvin RB, Smith RN. Antibody-mediated organ-allograft rejection. *Nature Reviews Immunology*. 2005;5(10):807-817.

69. Sis B, Jhangri GS, Bunnag S, Allanach K, Kaplan B, Halloran PF. Endothelial gene expression in kidney transplants with alloantibody indicates Antibody-Mediated damage despite lack of C4d staining. *American Journal of Transplantation*. 2009;9(10):2312-2323.

70. Sis B, Jhangri G, Riopel J, et al. A new diagnostic algorithm for Antibody-Mediated microcirculation inflammation in kidney transplants. *American journal of transplantation*. 2012;12(5):1168-1179.

71. Weis M, Hartmann A, Olbrich HG, Hör G, Zeiher AM. Prognostic significance of coronary flow reserve on left ventricular ejection fraction in cardiac transplant recipients. *Transplantation*. 1998;65(1):103-108.

72. Amano H, Bickerstaff A, Orosz CG, Novick AC, Toma H, Fairchild RL. Absence of recipient CCR5 promotes early and increased allospecific antibody responses to cardiac allografts. *J Immunol*. 2005;174(10):6499-6508. doi: 174/10/6499 [pii].

73. Chow A, Pearcey J, Husain S, et al. A new model of pure acute antibody-mediated rejection shows concurrent complement-mediated injurious and anti-inflammatory effects of high titer anti-MHC IgG DSA. . 2014;98:383-384.

74. Libby P, Swanson SJ, Tanaka H, Murray A, Schoen FJ, Pober JS. Immunopathology of coronary arteriosclerosis in transplanted hearts. *J Heart Lung Transplant*. 1992;11(3 Pt 2):S5-6.

75. Shimizu K, Sugiyama S, Aikawa M, et al. Host bone-marrow cells are a source of donor intimal smooth-muscle–like cells in murine aortic transplant arteriopathy. *Nat Med*. 2001;7(6):738-741.

76. Li J, Han X, Jiang J, et al. Vascular smooth muscle cells of recipient origin mediate intimal expansion after aortic allotransplantation in mice. *The American journal of pathology*. 2001;158(6):1943-1947.

77. Hu Y, Davison F, Ludewig B, et al. Smooth muscle cells in transplant atherosclerotic lesions are originated from recipients, but not bone marrow progenitor cells. *Circulation*. 2002;106(14):1834-1839.

78. Wu GD, Tuan T, Bowdish ME, et al. Evidence for recipient derived fibroblast recruitment and activation during the development of chronic cardiac allograft rejection1. *Transplantation*. 2003;76(3):609-614.

79. Murray AG, Libby P, Pober JS. Human vascular smooth muscle cells poorly co-stimulate and actively inhibit allogeneic CD4+ T cell proliferation in vitro. *J Immunol*. 1995;154(1):151-161.

80. Zhang P, Manes TD, Pober JS, Tellides G. Human vascular smooth muscle cells lack essential costimulatory molecules to activate allogeneic memory T cells. *Arterioscler Thromb Vasc Biol*. 2010;30(9):1795-1801. doi: 10.1161/ATVBAHA.109.200758 [doi].

81. Raisanen-Sokolowski A, Mottram PL, Glysing-Jensen T, Satoskar A, Russell ME. Heart transplants in interferon-gamma, interleukin 4, and interleukin 10 knockout mice. recipient environment alters graft rejection. *J Clin Invest*. 1997;100(10):2449-2456. doi: 10.1172/JCI119787 [doi].

82. Suzuki J, Cole SE, Batirel S, et al. Tumor necrosis factor Receptor-1 and-2 double deficiency reduces graft arterial disease in murine cardiac allografts. *American Journal of Transplantation*. 2003;3(8):968-976.

83. Yu L, Qin L, Zhang H, et al. AIP1 prevents graft arteriosclerosis by inhibiting interferon-gamma-dependent smooth muscle cell proliferation and intimal expansion. *Circ Res*. 2011;109(4):418-427. doi: 10.1161/CIRCRESAHA.111.248245 [doi].

84. Bai Y, Ahmad U, Wang Y, et al. Interferon-gamma induces X-linked inhibitor of apoptosis-associated factor-1 and noxa expression and potentiates human

vascular smooth muscle cell apoptosis by STAT3 activation. *J Biol Chem*. 2008;283(11):6832-6842. doi: 10.1074/jbc.M706021200 [doi].

85. Mancuso MR, Davis R, Norberg SM, et al. Rapid vascular regrowth in tumors after reversal of VEGF inhibition. *J Clin Invest*. 2006;116(10):2610-2621. doi: 10.1172/JCI24612 [doi].

86. Warren CM, Iruela-Arispe ML. Signaling circuitry in vascular morphogenesis. *Curr Opin Hematol*. 2010;17(3):213-218. doi: 10.1097/MOH.0b013e32833865d1 [doi].

87. Sato TN, Tozawa Y, Deutsch U, et al. Distinct roles of the receptor tyrosine kinases tie-1 and tie-2 in blood vessel formation. *Nature*. 1995;376(6535):70-74. doi: 10.1038/376070a0 [doi].

88. Suri C, Jones PF, Patan S, et al. Requisite role of angiopoietin-1, a ligand for the TIE2 receptor, during embryonic angiogenesis. *Cell*. 1996;87(7):1171-1180.

89. Kono M, Mi Y, Liu Y, et al. The sphingosine-1-phosphate receptors S1P1, S1P2, and S1P3 function coordinately during embryonic angiogenesis. *J Biol Chem*. 2004;279(28):29367-29373. doi: 10.1074/jbc.M403937200 [doi].

90. Maekawa H, Oike Y, Kanda S, et al. Ephrin-B2 induces migration of endothelial cells through the phosphatidylinositol-3 kinase pathway and promotes

angiogenesis in adult vasculature. *Arterioscler Thromb Vasc Biol*. 2003;23(11):2008-2014. doi: 10.1161/01.ATV.0000096655.56262.56 [doi].

91. Gerhardt H, Golding M, Fruttiger M, et al. VEGF guides angiogenic sprouting utilizing endothelial tip cell filopodia. *J Cell Biol*. 2003;161(6):1163-1177. doi: 10.1083/jcb.200302047.

92. Rafii S, Cao Z, Lis R, et al. Platelet-derived SDF-1 primes the pulmonary capillary vascular niche to drive lung alveolar regeneration. *Nat Cell Biol*. 2015;17(2):123-136.

93. Vanhaesebroeck B, Waterfield M. Signaling by distinct classes of phosphoinositide 3-kinases. *Exp Cell Res*. 1999;253(1):239-254.

94. Ronkainen VP, Ronkainen JJ, Hanninen SL, et al. Hypoxia inducible factor regulates the cardiac expression and secretion of apelin. *FASEB J*. 2007;21(8):1821-1830. doi: fj.06-7294com [pii].

95. Cox CM, D'Agostino SL, Miller MK, Heimark RL, Krieg PA. Apelin, the ligand for the endothelial G-protein-coupled receptor, APJ, is a potent angiogenic factor required for normal vascular development of the frog embryo. *Dev Biol*. 2006;296(1):177-189.

96. Masri B, van den Berghe L, Sorli C, Knibiehler B, Audigier Y. Apelin signalisation and vascular physiopathology. *J Soc Biol*. 2009;203(2):171-179. doi: 10.1051/jbio/2009021 [doi].

97. Yang F, Bai Y, Jiang Y. Effects of apelin on RAW264. 7 cells under both normal and hypoxic conditions. *Peptides*. 2015;69:133-143.

98. Eyries M, Siegfried G, Ciumas M, et al. Hypoxia-induced apelin expression regulates endothelial cell proliferation and regenerative angiogenesis. *Circ Res*. 2008;103(4):432-440. doi: 10.1161/CIRCRESAHA.108.179333 [doi].

99. Zhang J, Liu Q, Hu X, et al. Apelin/APJ signaling promotes hypoxia-induced proliferation of endothelial progenitor cells via phosphoinositide-3 kinase/akt signaling. *Molecular medicine reports*. 2015;12(3):3829-3834.

100. Kunduzova O, Alet N, Delesque-Touchard N, et al. Apelin/APJ signaling system: A potential link between adipose tissue and endothelial angiogenic processes. *FASEB J*. 2008;22(12):4146-4153. doi: 10.1096/fj.07-104018 [doi].

101. Sorli SC, Le Gonidec S, Knibiehler B, Audigier Y. Apelin is a potent activator of tumour neoangiogenesis. *Oncogene*. 2007;26(55):7692-7699.

102. Heo K, Kim YH, Sung HJ, et al. Hypoxia-induced up-regulation of apelin is associated with a poor prognosis in oral squamous cell carcinoma patients. *Oral Oncol*. 2012;48(6):500-506.

103. Alastalo TP, Li M, Perez Vde J, et al. Disruption of PPARgamma/beta-catenin-mediated regulation of apelin impairs BMP-induced mouse and human pulmonary arterial EC survival. *J Clin Invest*. 2011;121(9):3735-3746. doi: 10.1172/JCI43382 [doi].

104. Noiri E, Nakao A, Uchida K, et al. Oxidative and nitrosative stress in acute renal ischemia. *Am J Physiol Renal Physiol*. 2001;281(5):F948-57.

105. Muià C, Mazzon E, Di Paola R, et al. Green tea polyphenol extract attenuates ischemia/reperfusion injury of the gut. *Naunyn Schmiedebergs Arch Pharmacol*. 2005;371(5):364-374.

106. Teng JC, Kay H, Chen Q, et al. Mechanisms related to the cardioprotective effects of protein kinase C epsilon (PKC ε) peptide activator or inhibitor in rat ischemia/reperfusion injury. *Naunyn Schmiedebergs Arch Pharmacol*. 2008;378(1):1-15.

107. Chen Q, Kim E, Elio K, et al. The role of tetrahydrobiopterin (BH4) and dihydrobiopterin (BH2) in ischemia/reperfusion (I/R) injury when given at reperfusion. *Advances in Phamacological Sciences*. 2010;2010.

108. Weyrich AS, Buerke M, Albertine KH, Lefer AM. Time course of coronary vascular endothelial adhesion molecule expression during reperfusion of the ischemic feline myocardium. *J Leukoc Biol*. 1995;57(1):45-55.

109. Chandra SM, Razavi H, Kim J, et al. Disruption of the apelin-APJ system worsens hypoxia-induced pulmonary hypertension. *Arterioscler Thromb Vasc Biol*. 2011;31(4):814-820. doi: 10.1161/ATVBAHA.110.219980 [doi].

110. Morrell NW, Adnot S, Archer SL, et al. Cellular and molecular basis of pulmonary arterial hypertension. *J Am Coll Cardiol*. 2009;54(1s1):S20-S31.

111. Zhang H, Gong Y, Wang Z, et al. Apelin inhibits the proliferation and migration of rat PASMCs via the activation of PI3K/akt/mTOR signal and the inhibition of autophagy under hypoxia. *J Cell Mol Med*. 2014;18(3):542-553.

112. Nishida M, Okumura Y, Oka T, et al. The role of apelin on the alleviative effect of angiotensin receptor blocker in unilateral ureteral obstruction-induced renal fibrosis. *Nephron Extra*. 2012;2(1):39-47. doi: 10.1159/000337091 [doi].